

# **ZEOLITE '06**

7th International Conference on the Occurrence,  
Properties, and Utilization of Natural Zeolites

## **Book of Abstracts**

**Edited by Robert S. Bowman and Susan E. Delap**

**16–21 July 2006  
Socorro, New Mexico, USA**

## Cover Credits

*Cover photograph:* The St. Cloud clinoptilolite deposit near Winston, New Mexico USA.

Patrick Freeman, president of St. Cloud Mining Company, stands at the lower left.

Photograph courtesy of St. Cloud Mining Company.

*Inset:* Scanning electron micrograph image of clinoptilolite. Image by Barbara Carlos courtesy of Los Alamos National Laboratory.

## Copy Editing

Lynn Deming, Head

Karen Bailey-Bowman

Tiffany Chisum

Paul Jacobo

George Kanesta

Linda Lambert

Tony Perreault

Melody Rapson

## Graphic Design

Susan E. Delap

Joby Elliott

The ***Book of Abstracts*** is available on the conference website:

<http://www.ees.nmt.edu/Zeolite06/>

Copyright © 2006 by the International Natural Zeolite Association (<http://icnz.lanl.gov/>)

Printed and bound in the United States of America.

## **Local Organizing Committee**

**R. S. Bowman** (Chair), New Mexico Tech, USA  
**G. S. Austin**, New Mexico Bureau of Geology and Mineral Resources, USA  
**J. M. Barker**, New Mexico Bureau of Geology and Mineral Resources, USA  
**W. X. Chavez, Jr.**, New Mexico Tech, USA  
**S. Chipera**, Los Alamos National Laboratory, USA  
**S. E. Delap**, New Mexico Tech, USA  
**V. W. Lueth**, New Mexico Bureau of Geology and Mineral Resources, USA  
**L. Majkowski-Taylor**, New Mexico Tech, USA  
**P. A. Mills**, New Mexico Tech, USA  
**J. Sullivan**, Los Alamos National Laboratory, USA

## **International Scientific Board**

**T. Armbruster**, University of Bern, Switzerland  
**D. L. Bish**, Indiana University, USA  
**R. S. Bowman**, New Mexico Tech, USA  
**P. Cappelletti**, Università di Napoli Federico II, Italy  
**C. Colella**, Università di Napoli Federico II, Italy  
**R. T. Cygan**, Sandia National Laboratories, USA  
**A. Langella**, Università del Sannio, Italy  
**P. J. Leggo**, University of Cambridge, UK  
**Z. Li**, University of Wisconsin—Parkside, USA  
**D. Ming**, NASA Johnson Space Center, USA  
**R. Pabalan**, Southwest Research Institute, USA  
**D. Vaniman**, Los Alamos National Laboratory, USA

## **Sponsors**

**Biolite, Inc.**, Winston, New Mexico, USA  
**Coyote Cliff, LLC**, Hobbs, New Mexico, USA  
**Cycletrol Industries**, Carson City, Nevada, USA  
**GSA Resources, Inc.**, Tucson, Arizona, USA  
**Los Alamos National Laboratory**, Los Alamos, New Mexico, USA  
**New Mexico Bureau of Geology & Mineral Resources**, Socorro, New Mexico, USA  
**New Mexico Tech**, Socorro, New Mexico, USA  
**St. Cloud Mining Company**, Truth or Consequences, New Mexico, USA  
**Steelhead Specialty Minerals**, Spokane, Washington, USA  
**Teague Mineral Products**, Adrian, Oregon, USA  
**Zeotech Corporation**, Fort Worth, Texas, USA



## Preface

This volume contains abstracts submitted for oral and poster presentations at Zeolite'06, the 7th International Conference on the Occurrence, Properties, and Utilization of Natural Zeolites. The conference was held 16–21 July 2006 at the New Mexico Institute of Mining and Technology in Socorro, New Mexico, USA.

Zeolite'06 is the latest in a series of conferences organized under the auspices of the International Natural Zeolite Association (INZA), formerly the International Committee on Natural Zeolites (ICNZ). The initial conference was held in Tucson, Arizona, USA in 1976 (Zeolite'76); subsequent conferences were held in Budapest, Hungary (Zeolite'85); Havana, Cuba (Zeolite'91); Boise, Idaho, USA (Zeolite'93); Ischia (Naples), Italy (Zeolite'97); and Thessaloniki, Greece (Zeolite'02).

The abstracts herein are organized alphabetically by first author in each of four separate sections:

- Symposium on 250 Years of Natural Zeolite Science
- Symposium on the Legacy of Fred Mumpton
- Invited Technical Presentations
- Contributed Technical Presentations

An author index at the end of the volume lists the page number of each author's abstract(s). Submitted abstracts were edited for English grammar and usage and adherence to a prescribed format. Authors were given the opportunity to approve the edited abstracts prior to publication.

This volume of Zeolite'06 abstracts is dedicated to the memory of Fred Mumpton, who did so much to further scientific and practical interest in natural zeolites.

*R. S. Bowman*  
*Socorro, New Mexico, USA*  
*July 2006*



# CONTENTS

<b><i>250 Years of Natural Zeolite Science</i></b>	<b><i>1</i></b>
Cronstedt's zeolite <i>C. Colella and A. F. Gualtieri</i>	3
Discovering the properties of natural zeolites: Ion exchange <i>R. T. Pabalan</i>	5
Discovering the properties of natural zeolites: Adsorption and molecular sieving <i>D. Tchernev</i>	6
Early discovery of zeolite minerals <i>W. S. Wise</i>	8
<b><i>Legacy of Fred Mumpton</i></b>	<b><i>9</i></b>
Cross-linking natural zeolite research and applications: A tribute to Fred A. Mumpton <i>T. Armbruster</i>	11
Fred Mumpton and "clinoptilolite redefined" <i>D. L. Bish and J. Boak</i>	13
Fred Mumpton and Italy: A reciprocated love <i>C. Colella</i>	15
Persnickety editor, founding father, mentor, and friend: The legacy of Fred Mumpton <i>D. W. Ming</i>	17
Memories about Dr. Mumpton <i>V. A. Nikashina</i>	19
How a thirty-year friendship with Fred Mumpton affected my life and my career as a scientist <i>D. Tchernev</i>	20
<b><i>Invited Papers</i></b>	<b><i>23</i></b>
Exploration guides for zeolite deposits in lacustrine tuffs, with reference to the Taupo Volcanic Zone, New Zealand <i>R. L. Brathwaite</i>	25
Ion-exchange studies on Italian natural zeolites: Experiments and data processing <i>D. Caputo</i>	27
The use of Biolite (a calcium clinoptilolite zeolite) in diets for natural beef production <i>K. S. Eng, R. Bechtel, and D. Hutcheson</i>	29
Does porous mean soft? The state of the art on the elastic behavior of microporous silicates <i>G. Diego Gatta</i>	31
Atomistic simulation of adsorption, diffusion, and ion exchange in zeolites <i>E. J. Maginn</i>	33
New clay barrier technology for waste sites and treatment of contaminated water outflow from waste sites through application of natural zeolites. <i>H. Minato and T. Morimoto</i>	34
Predicting adsorption and transport in zeolite thin film membranes for hydrogen separation using grand canonical Monte Carlo and molecular dynamics simulations <i>M. C. Mitchell</i>	36

Irradiation and thermal effects in zeolites for the sorption and release of radionuclides in the geosphere <i>L. M. Wang and R. C. Ewing</i>	37
<b>Contributed Papers</b>	<b>39</b>
The oxidative dehydrogenation of C <sub>1</sub> –C <sub>2</sub> alcohols on copper-contained zeolites and HTSC <i>L. Akhalbedashvili</i>	41
Cs <sup>+</sup> and Sr <sup>2+</sup> ion exchange properties of irradiated and chemically modified clinoptilolite <i>L. Akhalbedashvili, N. Kekelidze, M. Alapishvili, G. Maisuradze, Y. Keheyman, and G. Yertsyan</i>	43
Application of zeolite in oil refinery wastewater treatment <i>A. Al-Haddad and M. Al-Salem</i>	45
Application of surfactant-modified zeolite for oilfield- produced water treatment: Examining regeneration and long-term stability <i>C. R. Altare, R. S. Bowman, E. J. Sullivan, L. E. Katz, and K. A. Kinney</i>	46
Phenol and aniline sorption from water solution by Armenian natural zeolites and their further chemical conversion <i>Y. Amirbekyan, A. Isakov, D. Hovhannisyan, and G. Torosyan</i>	48
Reversible conversion of tetranatrolite to paranatrolite under ambient conditions <i>G. S. Atalan and P. S. Neuhoff</i>	50
Competitive adsorption of priority trace elements by surfactant-modified zeolite and its potential application to remediate hazardous leachable elements from fly ash <i>S. Bhattacharyya, R. J. Donahoe, and E. Y. Graham</i>	52
Spectroscopic study of the formation of hydroxyl groups during dehydration of natural zeolites <i>D. L. Bish, R. Milliken, and C. T. Johnston</i>	53
St. Cloud zeolite, a working model of sustainability <i>J. Bokich</i>	55
Relationship between total and external cation exchange capacities of zeolites from the western United States <i>R. S. Bowman</i>	56
Properties of zeolitized tuff/organic matter aggregates relevant for their use in pedotechnique. II: Thermal and microstructural characterization <i>A. Buondonno, A. Colella, E. Coppola, B. de'Gennaro, A. Langella, A. Letizia, and C. Colella</i>	58
Occurrence and utilization of mordenite-clinoptilolite deposits in lacustrine tuffs, Ngakuru, Taupo Volcanic Zone, New Zealand <i>R. L. Brathwaite and D. Hill</i>	60
Copper removal from aqueous solutions using clinoptilolite in fixed-bed reactors <i>V. Çağın, N. Morali, and İ. İmamoğlu</i>	62
Sorption kinetics of humic acids on zeolitic tuffs <i>S. Capasso, E. Coppola, P. Iovino, M. Lombardo, S. Salvestrini, and C. Colella</i>	64
Zeolitization processes in Roccamonfina ignimbrite (Southern Italy): A help in recording fossil human tracks? <i>P. Cappelletti, G. Rolandi, and M. de'Gennaro</i>	66



Authigenic mineralization in the largest Italian volcanoclastic deposit: The Campanian Ignimbrite <i>P. Cappelletti, G. Cerri, A. Colella, M. de Gennaro, A. Langella, A. Perrotta, and C. Scarpati</i>	69
Modeling of water and ethanol adsorption data on a commercial zeolite-rich tuff and prediction of the relevant binary isotherms <i>D. Caputo, F. Iucolano, F. Pepe, and C. Colella</i>	71
Lead release after different thermal treatments of a Pb-exchanged clinoptilolite-rich material <i>G. Cerri, A. Brundu, M. Biagioli, and A. Langella</i>	73
Zn-exchanged clinoptilolite-rich rock as carrier for erythromycin in anti-acne therapy: An in vitro evaluation <i>G. Cerri, M. de' Gennaro, M. C. Bonferoni, C. Caramella, and C. Juliano</i>	75
Features of formation of analcime in Perm copper sandstones <i>I. Chaikovski and O. Kropacheva</i>	77
A model for the impact of ferritized clinoptilolite on flooded soils <i>K. Chakalov, T. Popova, K. Mitov, O. Petrov, and E. Filcheva</i>	78
Investigation of Mongolian zeolites for heavy metal uptake <i>A. Chimedtsogzol, A. Dyer, C. D. Williams, and H. Poellmann</i>	80
Uptake of mercury solutes by natural zeolites from Mongolia <i>A. Chimedtsogzol, A. Dyer, L. Campbell, C.D. Williams, and H. Poellmann</i>	81
Zeolitization of intracaldera sediments and rhyolitic rocks of Valles caldera, New Mexico, USA <i>S. J. Chipera, F. Goff, C. J. Goff, and M. Fittipaldo</i>	82
Use of zeolites as selective sorbates for radiological decontamination applications <i>S. J. Chipera, M. E. Smith, D. Counce, D. Ehler, P. Longmire, and T. Taylor</i>	84
Experimental study of interfacial phenomena in some pollutants-enriched model solutions vs. surface engineered clinoptilolite <i>E. Chmielewska, L. Sabová, K. Gáplovská, F. Pepe, D. Caputo, and A. Wu</i>	86
Bactericidal action of Cuban natural clinoptilolite containing clusters and nanoparticles of silver <i>B. Concepción-Rosabal, N. Bogdanchikova, I. De la Rosa, M.T. Olguín, D. Alcántara, and G. Rodríguez-Fuentes</i>	88
Fumonisin B <sub>1</sub> adsorption on modified clinoptilolite rich zeolitic tuff <i>A. Daković, M. Tomašević-Čanović, G. E. Rottinghaus, and S. Matijašević</i>	90
Hydrothermal treatment of Sardinian clinoptilolite-bearing ignimbrites for increasing cation exchange capacity <i>A. De Fazio, P. Brotzu, M. R. Ghiara, L. M. Fercia, R. Lonis, and A. Sau</i>	92
Expanded lightweight aggregates production using Italian zeolitized volcanoclastic materials and industrial wastes <i>R. de Gennaro, P. Cappelletti, G. Cerri, M. de' Gennaro, M. Dondi, S.F. Graziano, and A. Langella</i>	94
Zeolite-feldspar epiclastic rocks as flux in ceramic tile manufacturing <i>R. de' Gennaro, M. Dondi, P. Cappelletti, G. Cerri, M. de' Gennaro, G. Guarini, A. Langella, L. Parlato, and C. Zanelli</i>	96

Modification of natural clinoptilolite for nitrogen and methane separation <i>S. Deng, D. Reiersen, and V. Viswanathan</i>	98
Purification of polluted water collected from Porsuk River, Eskişehir, by using clinoptilolite obtained from Gordes region, Turkey <i>Z. Dikmen and O. Orhun</i>	100
The application of the extended Freundlich adsorption isotherm model on zeolites <i>Z. Donmez and O.Orhun</i>	101
Chemical activation of clinoptilolite rich zeolite from central Mexico using microwave heating <i>E. B. Drąg and J. Krason</i>	102
Catalytic combustion of Cl-VOCs on the zeolitic matrix <i>E. B. Drąg, M. Kulażyński, and J. Krason</i>	103
Selective catalytic NO reduction by ammonia on clinoptilolite and mordenite zeolites <i>E. B. Drąg, M. Kulażyński, and J. Krason</i>	104
Removal of PAHs from n-paraffin by modified clinoptilolite <i>H. Faghihian and M. H. Mousazadeh</i>	105
Use of Cuban natural zeolites in Brazil: Fields of application <i>F. Farias, F. Borsatto, J. A. Febles, and M. Velázquez</i>	107
Agricultural results obtained in the use of the Cuban zeolites in some Latin American countries <i>J. A. Febles González and M. Velázquez</i>	108
Accessing real micropore volumes of zeolites <i>R. X. Fischer, W. H. Baur, C. C. Pavel, and W. Schmidt</i>	109
Utilization of zeolite for reducing sodium and salt concentrations in saline-sodic coalbed natural gas waters <i>G. K. Ganjgunte, G. F. Vance, R. W. Gregory, and R. C. Surdam</i>	111
Human urine treated by MgO and zeolite for efficient nutrient recovery and reuse in agriculture <i>Z. Ganrot and G. Dave</i>	113
New organo-zeolite fertilizer <i>T. A. Gasparyan, G. G. Karamyan, G. M. Aleksanyan, and L. R. Revazyan</i>	114
A comparative study of Cd <sup>2+</sup> removal from aqueous solutions using two different Turkish clinoptilolite samples <i>K. Gedik and I. Imamoglu</i>	115
Optimization of pretreatment for Cd <sup>2+</sup> removal and regeneration of metal loaded clinoptilolite in fixed bed columns <i>K. Gedik and I. Imamoglu</i>	117
Lateral and vertical zeolite grade variations in the Tufo Lionato ignimbrite unit (Colli Albani, Roma, central Italy) <i>C. Giampaolo, S. Lo Mastro, D. De Rita, and G. Giordano</i>	119
Zeolite characterization of Vico red tuff with black scoriae ignimbrite flow: The quarrying district of Civita Castellana (Viterbo, Italy) <i>C. Giampaolo, L. Mengarelli, E. Torracca, and C. Spencer</i>	121
Plant productivity and characterization of zeoponic substrates after three successive crops of radishes <i>J. E. Gruener, D. W. Ming, C. Galindo, Jr., and K. E. Henderson</i>	122

Crystal chemistry and genetic relationships of zeolites and associated minerals from Faeroe Islands <i>A. Guastoni and G. Artioli</i>	124
Effects of feeding clinoptilolite zeolite and acidogenic compounds to poultry <i>E. C. Hale III</i>	126
Iron-modified light expanded clay aggregates for the removal of arsenic from groundwater <i>M. N. Haque, G. M. Morrison, I. Cano-Aguilera, and J. L. Gardea-Torresdey</i>	128
Natural zeolite from southern Germany: Applications in concrete <i>F. Hauri</i>	130
Activated adsorption of chlorinated hydrocarbons on erionite <i>M. A. Hernández, F. Rojas, G. Rueda, R. Portillo, E. Campos Reales, and V. Petranoskii</i>	132
Thermodynamic properties of natrolite <i>G. L. Hovis and P. S. Neuhoﬀ</i>	134
Zeolites and associated clay minerals from the altered Sheinovets caldera ignimbrites (eastern Rhodopes, southern Bulgaria) <i>R. Ivanova and S. Gier</i>	136
Sorption of gases, cesium, and strontium by clinoptilolite-rich zeolites <i>J. M. Jabłonski, J. Krason, and A. Miecznikowski</i>	138
Removal of paraquat pesticide residue from pre-treated wastewater using activated faujasite tuff from Jordan <i>H. A. Jbara and K. M. Ibrahim</i>	140
Characterization of Mexican zeolitic rocks <i>M. J. Jiménez Cedillo, M. T. Olguín Gutiérrez, and M. J. Solache Ríos</i>	142
Adsorption of pesticides on functionalized zeolites <i>V. Jovanović, V. Dondur, L. Damjanović, G. Jordanov, and A. Daković</i>	144
The roles of zeolite in the nitrogen removal process and treatment of ammonium-rich wastewater using sequencing batch biofilm reactor (SBBR) <i>J. Y. Jung, D. H. Son, I. T. Yeom, and Y. C. Chung</i>	146
Hydrothermal synthesis of microporous titanosilicates <i>V. Kostov-Kytin, S. Ferdov, B. Mihailova and O. Petrov</i>	148
The influence of zeolite-containing material on the respiratory activity of a leached chernozem contaminated by hydrocarbons <i>A. Krivosheeva, N. Archipova, V. Breus, G. Khaidarova, and I. Breus</i>	150
Metal nanodots formed and supported on chabazite surfaces <i>S. M. Kuznicki, D. J. A. Kelly, J. Chen, J. Bian, C. Lin, Y. Liu, D. Mitlin, and Z. Xu</i>	152
Chemical upgrading of sedimentary Bowie, Arizona sodium chabazite <i>S. M. Kuznicki, C. Lin, D. J. A. Kelly, J. Bian, A. Koenig, J. Chen, Y. Liu, and Z. Xu</i>	153
Natural zeolite bitumen cracking and upgrading <i>S. M. Kuznicki, W. C. McCaffrey, J. Bian, E. Wangen, and A. Koenig</i>	155
A molecular modeling investigation of cation and water adsorption in crystalline titanosilicate materials. <i>J. P. Larentzos and E. J. Maginn</i>	157
Sustaining plant growth in conditions of extreme metal pollution <i>P. J. Leggo and B. Ledésert</i>	158

Competitive adsorption of polycyclic aromatic hydrocarbons on organo-zeolites <i>J. Lemić, M. Tomašević–Čanović, S. Milošević, M. Adamović, and S. Milićević</i>	159
Computational and experimental studies of the structure and dynamics of water in natural zeolites <i>D. W. Lewis, D. Salih, A. R. Ruiz-Salvador, H. Emerich, W. van Beek, C. L. I. M. White, and M. A. Green</i>	161
Grain size effect on chromate sorption and transport through surfactant-modified zeolite columns <i>Z. Li</i>	163
Natural zeolite occurrences in New Mexico <i>V. W. Lueth</i>	165
Quantitative mineralogy and genetic history of the natural zeolite deposits of coastal Ecuador <i>L. Machiels, F. Morante, R. Snellings, J. Elsen, and C. Paredes</i>	166
Structural investigation of $\text{Zn}^{2+}$ sorption on clinoptilolite tuff <i>K. Margeta, N. Zabukovec Logar, N. Novak Tusar, K. Maver, I. Arcon, V. Kaucic, and S. Cerjan-Stefanovic</i>	168
Peculiarities of sorption extraction of oil products from aquatic environment <i>T. Martynova</i>	170
Removal of <i>Giardia lamblia</i> and model organism <i>Saccharomyces cerevisiae</i> from contaminated waters through the use of surfactant-modified zeolite (SMZ) <i>D. Meier and R. S. Bowman</i>	172
Hydraulic-loading and NaCl concentration effect on regeneration of exhausted homoionic natural zeolite <i>Z. Milán, K. Ilangovan, C. de las Pozas, and O. Monroy</i>	174
Analysis of zeolite exchange capacity cations <i>W. J. Miles</i>	176
X-Ray diffraction identification of smectite clays associated with zeolite minerals <i>W. J. Miles</i>	177
The investigation of zeolite-containing material as a potential sorbent for petroleum hydrocarbons <i>A. Mishchenko, A. Krivosheeva, V. Breus, S. Neckludov, and I. Breus</i>	178
Sorption of lead by a Mexican heulandite-clinoptilolite- rich tuff <i>M. M. Llanes Monter, M. T. Olguín Gutiérrez, and M. J. Solache Ríos</i>	180
Time dependent $\text{Zn}^{2+}$ and $\text{Pb}^{2+}$ removal with clinoptilolite and release of exchangeable ions <i>N. Morali, V. Çağın, and İ. İmamoğlu</i>	182
Investigation of heavy metal ( $\text{Cu}^{2+}$ , $\text{Ni}^{2+}$ , $\text{Zn}^{2+}$ , $\text{Pb}^{2+}$ ) uptake by clinoptilolite and release of exchangeable ions <i>N. Morali, V. Çağın, and İ. İmamoğlu</i>	184
Study of the effects of natural zeolite from the Tsagaantsav deposit on dynamics of pH, volatile fatty acids, and ammonia of rumen contents of one-year-old sheep <i>D. Narmandakh, M. Zolzaya, and Sh. Demberel</i>	186
Direct measurement of partial molar heats of hydration in zeolites by differential scanning calorimetry <i>P. S. Neuhoff and J. Wang</i>	188

Isotope-geochemical evidence for uranium retardation in zeolitized tuffs at Yucca Mountain, Nevada, USA <i>L. A. Neymark, J. B. Paces, S. J. Chipera, and D. T. Vaniman</i>	190
About features of ion exchange, mathematical modeling, and calculation of dynamic ion-exchange processes on natural clinoptilolites <i>V. A. Nikashina</i>	192
Study of natural zeolites in Vernadsky Institute <i>V.A. Nikashina</i>	194
The role of interfacial water in the clinoptilolite-heulandite zeolite system <i>N. W. Ockwig, T. M. Nenoff, L. L. Daemen, M. T. Hartl, and R. T. Cygan</i>	195
Comparison of water quality improvement by natural mordenite and bamboo coal inside the biotope, Japan <i>M. Okamoto, T. Kobayashi, and E. Sakamoto</i>	196
Magnetic modified natural clinoptilolite from Bigadic region, Turkey. <i>Ö. Orhun and Z. Dikmen</i>	198
First reported occurrence of clinoptilolite-rich tuff deposits in the Mexican Volcanic Belt (state of Michoacan, southwestern Mexico) <i>M. Ostrooumov and I. Ostrooumova</i>	199
Analysis of physical and chemical properties of natural zeolite in the southeast region of Mongolia <i>J. Oyuntseteg and R. Lkhagvajav</i>	201
Experimental and thermodynamic modeling study of multicomponent ion-exchange of alkali and alkaline-earth metals in clinoptilolite <i>R.T. Pabalan and F.P. Bertetti</i>	202
Application of natural zeolites in the production of controlled-release fertilizers <i>A. Pawelczyk and A. Popowicz</i>	203
On the geology of the zeolite deposit Beli Plast in NE Rhodopes, Bulgaria <i>P. I. Petrov</i>	205
Magnetic and structural characterization of modified Romanian clinoptilolite <i>R. Pode, E. Popovici, V. Pode, and V. Georgescu</i>	206
Clinoptilolitized pyroclastic rocks from Oaxaca (south Mexico): A mineralogical and technological study <i>N. Popov, Y. Yanev, Tz. Iliev, and T. Popova</i>	208
Pedogenic origin of clinoptilolite and heulandite in magnesium-rich sedimentary deposits (Madrid Basin, Spain) <i>M. Pozo, J. Casas, J. A. Medina, M. I. Carretero, and J. A. Martín Rubí</i>	210
Characterization of zeolite modified with cation active polyelectrolyte and its effect on biological wastewater treatment <i>P. Princz, B. Koczka, K. Marthi, G. Pokol, and S. E. Smith</i>	212
Combustion treatment of $\text{Co}^{2+}$ and $\text{Cs}^{+}$ exchanged Mexican clinoptilolite <i>R. Rodríguez-Trejo, P. Bosch, and S. Bulbulian</i>	214
Removal of the human pathogen <i>Giardia intestinales</i> from groundwater <i>C. Rust, D. Schulze-Makuch, and R. Bowman</i>	216
Dehydration behavior in natural zeolite of the heulandite group: An in situ NIR study <i>K. Sadhana, K. Shiva Prasad, P. S. R. Prasad, and S. Ramana Murthy</i>	218

Zeolite facies metamorphism in the Hvalfjörður area, Iceland <i>R. S. Selbekk and T. Weisenberger</i>	220
Natural zeolites and bentonite characteristics affecting $K^+$ and $NH_4^+$ sorption and desorption behaviour <i>A. S. Sheta, A. M. Falatah, and M. Al-Sewailem</i>	221
Dehydration and rehydration mechanism in natural natrolite: An FTIR study <i>K. Shiva Prasad and P. S. R. Prasad</i>	222
Computational studies of the nucleation and growth of zeolites <i>B. Slater, D. Salih, M. Mora-Fonz, C. R. A. Catlow, and D. W. Lewis</i>	224
Studying the composition and properties of zeolite-containing rocks of Tatar-Shatrashane occurrence <i>V. I. Sukhareenko, S. I. Usenko, L. I. Borisova, T. V. Serova, and T. A. Morozova</i>	226
Selectivity of clinoptilolite for $Na^+$ , $Cu^{2+}$ , $Zn^{2+}$ , and $Pb^{2+}$ evaluated by a Margules empirical model coupled with a linear free energy correlation approach <i>J. C. Torres and J. C. Gubulin</i>	228
Mexican surfactant-modified natural zeolite as an adsorbent of azo dyes from aqueous solution <i>J. Torres Pérez, M. Solache Ríos and M. Olguín Gutiérrez</i>	230
Intraparticle diffusion of Pb, Cu, and Zn ions during exchange processes on the natural zeolite clinoptilolite <i>M. Trgo, N. Vukojević Medvidović, J. Perić</i>	232
Pollutant removal of stormwater from traffic areas using zeolite-containing substrates <i>M. Upmeyer</i>	234
Blended cements containing high volume of natural zeolites: Superplasticizer requirement and compressive strength of mortars <i>B. Uzal and L. Turanlı</i>	236
Ion exchange reactions of natural zeolites: adsorption, exchange kinetics, and desorption <i>G. F. Vance, G. K. Ganjegunte, and M.A. Urynowicz</i>	238
Investigation of sorption processes for uranium, plutonium, and americium using tuffs in thin section <i>D. T. Vaniman, J. J. Kitten, and S. J. Chipera</i>	240
Chabazite, Ca-K-Na phillipsite, analcime, and natrolite: alkaline zeolites filling amygdales in tertiary basalts in Patagonia, Argentina, South America <i>M. E. Vattuone, C. I. Martínez Dopico, Y. Berbeglia, E. Gallegos, and S. Crosta</i>	242
Results of the application of organo-mineral products from natural zeolites as substitutes of chemical fertilizers <i>M. Velázquez Garrido, J. A. Febles González, C. J. Louis, L. Gómez, B. Villavicencio, and J. Estrada</i>	244
Adsorption of arsenite and arsenate with pre-treated Chilean zeolites <i>C. Vidal Cruz, M. E. Torres, and M. A. Mardones</i>	245
Removal of lead ions by a fixed bed of clinoptilolite—the effect of the influent flow <i>N. Vukojević Medvidović, J. Perić, M. Trgo, and M. N. Mužek</i>	247
Dehydration/rehydration-induced structural phase transitions in natrolite <i>H.-W. Wang and D. L. Bish</i>	249
Temperature dependence of heat in hydration of natrolite and analcime <i>J. Wang and P. S. Neuhoff</i>	251

Zeolites on fissures of crystalline basement rocks in the Swiss Alps <i>T. Weisenberger and K. Bucher</i>	253
Electro-physical and optical properties of natural zeolites (clinoptilolite) from Armenia and USA (preliminary results) <i>H. N. Yeritsyan, S. K. Nickoghosyan, A. A. Sahakyan, V. V. Harutunyan, E. A. Hakhverdyan, and N. E. Grigoryan</i>	254
Clinoptilolite in volcanic neck structure near Kralevo deposit, Haskovo region (Bulgaria) <i>A. Yoleva, O. Petrov, S. Djambazov, O. Malinov, and D. Stoycheva</i>	256
The determination of immersion heats and investigation of amphoteric effect of some natural zeolites (Turkey) <i>E. Yörükoğulları, M. Sakızcı, and H. Özçelik</i>	258
Using natural zeolites as deicers on highways <i>E. Yörükoğulları and M. Sakızcı</i>	259
Adsorption of ethylene on natural and modified natural zeolites from Bigadic and Gördes, Turkey <i>E. Yörükoğulları and B. Erdoğan</i>	261
Perchlorate removal using surfactant-modified zeolite <i>P. Zhang, D. M. Avudzeaga, and G. Zikalala</i>	263
<b><i>Author Index</i></b>	<b>265</b>





# **250 Years of Natural Zeolite Science**



## Cronstedt's zeolite

C. Colella<sup>1</sup> and A. F. Gualtieri<sup>2</sup>

<sup>1</sup>*Università Federico II; Napoli; Italy; E-mail: carmine.colella@unina.it*

<sup>2</sup>*Università degli Studi di Modena e Reggio Emilia; Modena, Italy*

### Introduction

Zeolite was discovered exactly 250 years ago. Axel A. F. Cronstedt (1722-1765), the famous Swedish mineralogist, was the first scientist who described the distinctive property of this class of minerals, i.e., its peculiar frothing characteristics when heated before the blowpipe. Cronstedt examined two samples, one which was said to come generically from Iceland, the other coming from Svappavaara in northern Sweden. From Cronstedt's indications, the Swedish site has been located near Kiruna, where the first zeolite, a stilbite, was collected.

This work describes the structure and microstructure of the first discovered zeolite, the stilbite, from Svappavaara (northern Sweden).

### Experimental Methods

The stilbite sample was provided by Dennis Holmberg, a minerals collector, living in the area where the historical stilbite sample was found. The Svappavaara area is situated 42 km ESE of Kiruna in Norbotten County (northern Sweden). The main rock types in that area belong to the supracrustal and intrusive rocks of Archean age. The Svappavaara group is one of the two major supracrustal petrographic units and consists of tuffites, graphite-bearing schist, biotite-rich quartzite, scapolitefels, amphibole schist, limestone, and skarn. These rocks are partly banded and may host minerals of hydrothermal origin such as zeolites. Besides stilbite, the Svappavaara minefield contains minerals like apophyllite, chabazite, diopside, epidote, gypsum, hematite, calcite, chrysocolla, quartz, microcline, natrolite, and others.

For the Rietveld structure refinement of the stilbite sample, the pure crystals separated by optical microscopy were hand ground in an agate mortar; the powder, with an average particle size of about 5  $\mu\text{m}$ , was side loaded on a 2 mm-thick flat Al holder to minimize preferred orientation effects. Data collection was performed at ca. 25 °C with relative humidity of ca. 40%, using an X'Pert Pro Panalytical  $\theta$ - $\theta$  BB diffractometer (Cu radiation), equipped with an RTMS detector. The refinements were performed using the GSAS package (Larson and Von Dreele, 1999). Starting atomic coordinates for the structural model were taken from Cruciani et al. (1997) and refined in space group  $F2/m$ .

The chemical composition was obtained by the average of several microprobe point-analyses. Electron probe micro-analysis (EPMA) was performed using an ARL-SEMQ instrument operating in wavelength-dispersive mode with 15 kV and 20 nA beam current and a defocused beam of 30  $\mu\text{m}$  in diameter. Microprobe data were normalized to 100 wt% using the weight loss of the thermogravimetric (TG) analysis performed in air using a thermal analyzer Seiko SSC 5200 equipped with TG/DTA 320U Module.

A number of stilbite crystals were mounted on Al stubs and prepared for the SEM analysis. The stubs were gold-coated (5 nm thick film). Micrographs were collected using a Philips XL 40/604 equipped with an EDS detector.

### Results and Discussion

The chemical formula derived from the EPMA and TG analyses with  $(\text{Si} + \text{Al}) = 36$  was  $(\text{Ca}_{4.03}\text{Mg}_{0.01}\text{Na}_{0.03}\text{K}_{0.11})[\text{Si}_{27.81}\text{Al}_{8.19}\text{O}_{72}] \cdot 28.62\text{H}_2\text{O}$ .

The  $\text{H}_2\text{O}$  content corresponds to the weight loss of the sample at 800°C. The reliability of the chemical formula is supported by the very low (-0.4%) charge balance error (E).

The chemical composition is very close to that of stellerite. Despite the chemical composition, the results of the structure refinement clearly indicate that the investigated sample is actually stilbite. As a matter of fact, the refined  $\beta$  angle is 90.194(5)°. SEM pictures show twinned crystals of stilbite (Figure 1). Stilbite is invariably twinned and stilbite twins are pseudomorphed because of the pseudo-orthorhombicity of the structure. Commonly, stilbite twins appear as fourlings or eightlings.

Figure 2 displays a sketch of the refined structure of stilbite. In agreement with Cruciani et al. (1997), Ca has a 9-fold coordination with water molecules only at an average distance of 2.549 Å.

The large average cation-anion distance (3.179 Å) and a 9-fold coordination were found for the other extra framework site occupied by a small fraction of K (and Na) atoms.

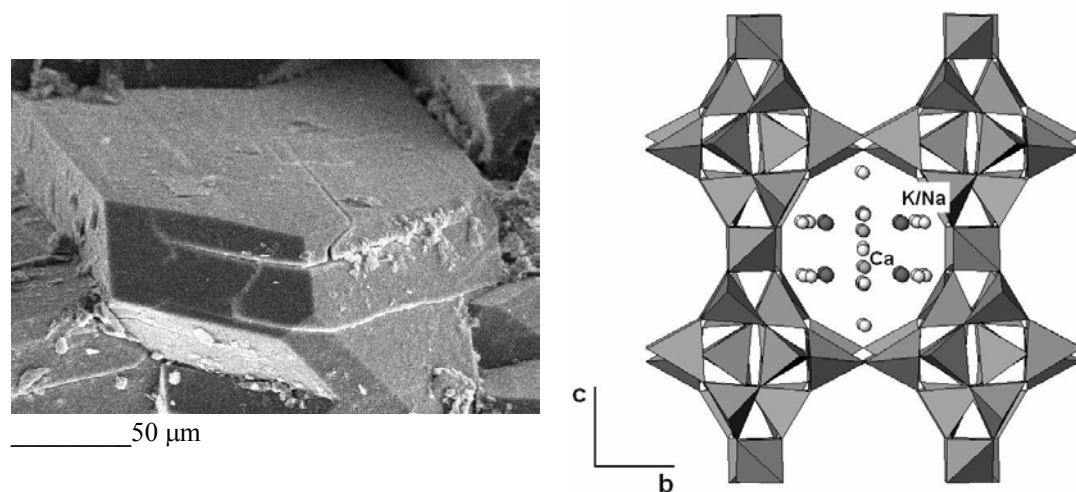


**Figure 1** (left). SEM micrograph of the Kiruna stilbite crystals

**Figure 2** (right). The structure of Kiruna stilbite along the a axis. The dark balls are the K/Na extraframework cations, the pale dark balls are the Ca extraframework cations, and the empty balls are the water molecules.

## References

- Cruciani G., Artioli G., Gualtieri A.F., Ståhl K. and Hanson, J.C. (1997) Dehydration dynamics of stilbite using synchrotron powder diffraction. *American Mineralogist*, **82**, 729-739.
- Larson, A.C. and Von Dreele, R.B. (1999): Generalized Structure Analysis System, Los Alamos, New Mexico, LAUR, pp. 179.

## **Discovering the properties of natural zeolites: Ion exchange**

**R. T. Pabalan**

*Southwest Research Institute<sup>®</sup>; San Antonio, Texas, USA; Email: [rpabalan@swri.org](mailto:rpabalan@swri.org)*

Zeolites are crystalline, hydrated aluminosilicates of alkali and alkaline earth cations characterized by an ability to hydrate/dehydrate reversibly and to exchange some of their constituent cations with dissolved cations in solution, both without a major change in structure. The ion-exchange property of these minerals has generated worldwide interest for use in diverse applications such as the treatment of nuclear, municipal, and industrial waste water. Although commercial applications of ion-exchange processes have used mainly synthetic zeolites, the earliest studies of ion-exchange phenomena were based on observations of natural materials, including natural zeolites. In this paper, a historical perspective is provided on early studies of ion-exchange phenomena and their theoretical description, with particular emphasis on natural zeolites.

## **Discovering the properties of natural zeolites: Adsorption and molecular sieving**

**D. Tchernev**

*The Zeopower Company; Chestnut Hill, Massachusetts, USA: Email: zeopower@usa.net*

### **Introduction**

Commercial adsorbents that exhibit ultra porosity include activated carbons, activated clays, inorganic gels, such as silica gel and activated alumina, and the crystalline aluminosilicate zeolite. Activated carbons, activated alumina, and silica gel do not possess an ordered crystal structure and consequently their pores are nonuniform. The distribution of the pore diameters within the adsorbent particles may vary widely from 20 to several thousand Angstroms, as is the case for some activated carbons. Hence, all molecular species, with the possible exception of high molecular weight polymers, may enter the pores. Zeolite molecular sieves, on the other hand, have pores of uniform size (3–10Å) which are uniquely determined by the unit structure of the crystal. These pores will completely exclude molecules that are larger than their diameter. J. W. McBain (1932) originated the term “molecular sieves” to define porous solid materials that exhibit the property of acting as sieves on a molecular scale.

### **Experimental Methods**

The first definite experiments on the separation of gaseous mixtures using the dehydrated natural zeolite mineral chabazite as a molecular sieve were performed by R. M. Barrer (1945). He classified zeolites in three groups based on their ability to adsorb or exclude molecular species of different sizes. His classification defined the approximate intra-channel dimension. In 1948, the first industrial research effort at the Union Carbide Corporation resulted in the synthesis and the manufacture of synthetic zeolite molecular sieves, which have never existed as natural minerals.

The most important molecular sieve effects are observed in dehydrated crystalline zeolites. These materials have a high internal surface area available for adsorption due to the channels and pores that uniformly penetrate the entire volume of the solid. The external surface of the adsorbent constitutes only a small fraction of the total available surface area. Molecular sieve action may be total or partial. If total, the diffusion of one species into the solid may be wholly prevented while the diffusion of a second species occurs. If partial, the components of a binary mixture of gases diffuse into the solid at different rates depending on the conditions, and the diffusion may be thermally activated with a specific activation energy. All adsorption processes involving physical adsorption are exothermic; that is, they evolve heat. For adsorption to take place, the free energy change of the adsorbent must be negative. The change in enthalpy is negative since the change in entropy is negative because the adsorbed molecules are in a more ordered state. At low levels of adsorption, the initial heat of adsorption has several component interaction energies that include dispersion and short-range repulsion energies, polarization energy, and electrostatic interactions of the local electrostatic field in the zeolite with the dipole and quadrupole moments of the adsorbed molecule. Barrer (1966) has emphasized that the total energy of interaction may be resolved into two types: (1) the type due to dispersion, repulsion, and polarization, and (2) the type due to the dipole and quadrupole interaction. At higher loading, the adsorbed molecules may interact with each other, thus, further complicating the thermal activation of the diffusion process.

### **Results and Discussion**

Once the selective adsorption and molecular sieving properties of natural zeolites were discovered and understood, their use in many practical applications followed rapidly. One of the major fields of application was the separation of gases. The removal of SO<sub>2</sub>, CO<sub>2</sub>, and NO<sub>x</sub> from power plant stack gases provided reduction of air-polluting gases. In the natural gas industry, the removal of H<sub>2</sub>S and H<sub>2</sub>O from well gas by chabazite before the gas is pumped through the pipeline, provided not only improved performance and lifetime of the compressors, but also permitted the purification and utilization of landfill methane gas. Oxygen production from air using mordenite, chabazite, or clinoptilolite was suggested by Barrer (1938) and described by Dominé and

Hay (1968) producing 95% pure oxygen. In Japan, Tamura (1970) described the industrial-size production (500 m<sup>3</sup>/hr) of 90% pure oxygen for the improved production of steel. In the USA, small oxygen generators for medical applications are readily available. The use of natural zeolites in agriculture as a soil additive for control of fertilizer, pesticide, and herbicide release and moisture retention is widely utilized. It is also used in animal nutrition and for ammonia removal from feed lots and in aquaculture.

The use of natural zeolites for adsorption cooling and refrigeration began in 1969 using solar energy and continued later using other sources of heat such as, natural gas or waste heat from internal combustion engines. Closed cycle adsorption cooling using natural zeolites is similar to the liquid absorption cycle using ammonia and water in some refrigerators powered by a flame. The solid adsorbents desorb, when heated, a refrigerant at high temperature and pressure and reabsorb it at low pressure when cooled, acting like a compressor. With solar energy as the source of heat, the zeolite cycles one time per day; the solar icebox was introduced in 1974, followed by the solar milk cooler in 1975, and heating/air conditioning panels in 1976. When using other sources of heat, the cycle time depends on the dynamics of the adsorption and desorption process. We established that desorption is heat-rate limited, while adsorption is mass-rate (diffusion) limited. Zeolite adsorption is inherently cyclic. In order to make the process continuous, the zeolite is divided into two parts: one in desorption while the other is adsorbing. This permits energy to be regenerated by removing heat from the zeolite being cooled during adsorption and using it to heat the zeolite in desorption. Up to 80% of the energy can be regenerated, significantly increasing the overall efficiency of the system. Research with other working fluids such as alcohols, freons, CO<sub>2</sub>, etc., shows promise in using natural zeolites to convert small temperature variations into large pressure differences, which can be used for waste heat to power conversion. Open-cycle systems utilize zeolite desiccant wheels as dehumidifiers to reduce the moisture content of the ambient air to very low dew points in special industrial processes.

## References

- Barrer, R.M. (1938) The sorption of polar and non-polar gases by zeolites. *Proceedings of the Royal Society of London, Series A, Mathematical and Physical Sciences*, **167**, 392–420.
- Barrer, R.M. (1945) Zeolites as molecular sieves. *Trans. Soc. Chem. Ind.*, **64**, 130.
- Barrer, R.M. (1966) Specificity in physical adsorption. *J. Colloid Interface Science*, **21**, 415.
- McBain, J.W. (1932) *The Sorption of Gases and Vapors by Solids*. Chapter 5. Rutledge and Son, London.
- Dominé, D. and Hay, L. (1968) Process for separating mixtures of gases by isothermal adsorption: possibilities and applications. *Molecular Sieve*, Soc. Chem. Industry, London, p. 204-216
- Tamura, T. (1970) Oxygen concentration process. U.S. Patent 3,533,221, Oct. 13, 1970, 10 pp.

## Early discovery of zeolite minerals

W. S. Wise

University of California; Santa Barbara, California, USA; Email: wise@geol.ucsb.edu

The discovery and description of zeolite minerals during the late 18th century depended on new concepts concurrently developed in crystallography, mineralogy, and chemistry. Of particular importance were the discoveries in chemistry and crystallography. Axel F. Cronstedt's invention of the blowpipe provided the means for melting a mineral sample and thereby providing a qualitative test for water within the sample. This was also the time when many chemical elements were discovered and the techniques of analytical chemistry were developed. Two notable chemists, Martin H. Klaproth and Louis N. Vauquelin, provided many useful analyses of minerals, but in some cases, especially with zeolites, missed some important elements. The only method of determining the quantitative proportion of individual components was by gravimetric analysis, meaning each component had to be chemically separated from the sample and weighed. If an element, such as sodium, could not be precipitated, there was no way to determine its abundance.

Several fundamental concepts of crystallography were developed during these years. Using the new Carangeot contact goniometer, Romé de l'Isle (1772) proposed his general law of constancy of interfacial angles and thereby established the science of crystallography. René-Just Haüy (1801) proposed a geometrical law of crystallization that gave crystallography a mathematical footing.

Using the available chemical analyses and crystallographic observations, Haüy (1801) organized information for eight minerals thought to be zeolites. The names he used are harmotome, stilbite, chabasie, analcime, mesotype, prehnite, lapis lazuli (lazurite), and zeolithe efflorescente (laumontite). During the next few decades, improvements in analytical methods and refined observations on crystals caused the number of known zeolite minerals to more than double. Heulandite was separated from stilbite, and mesotype was divided into natrolite, mesolite, and scolecite. Other zeolites discovered in the early 19th century are brewsterite, epistilbite, phillipsite, gismondine, gmelinite, levyne, and edingtonite.

The emergence of the polarizing microscope as a research tool early in the 19th century was a valuable tool in refining crystallographic observations on zeolites. It was (and remains) most useful in documenting the ubiquitous twinning of minerals, like stilbite and phillipsite.

Near the end of the 19th century Dana (1899) listed twenty two minerals in the zeolite group, of which all but two, ptilolite and laubanite, remain valid today. Members of the zeolite group were considered to be hydrated silicates of aluminum with sodium, potassium, calcium, and rarely, barium and strontium. All occurred in cavities of volcanic rocks, and less commonly in veins cutting granite, and all had the property of expelling water when heated.

### References

- Dana, J. D (1899) *A System of Mineralogy*, John Wiley, New York.  
Haüy, R. J. (1801) *Traité de mineralogie*, Chez Louis, Paris, France.  
Romé de l'Isle, J.B.L. (1772) *Essai de Crystallographie*, Chez Knapen & Delaguet, Paris, France.



# **Legacy of Fred Mumpton**



## Cross-linking natural zeolite research and applications: A tribute to Fred A. Mumpton

**T. Armbruster**

*Universität Bern; Bern, Switzerland; Email: Thomas.Armbruster@krist.unibe.ch*

Almost exactly 30 years ago, Fred Mumpton organized the first International Conference on the Occurrence, Properties and Utilization of Natural Zeolites, in Tucson, Arizona. Mumpton and L. B. Sand assembled the proceedings volume of the Zeolite '76 conference, which was published in 1978, and dedicated to their “better halves.” This book is still a key contribution to the understanding of natural zeolites and their applications.

As a crystallographer active in the field of small molecules trapped in the structural channels of cordierite, about ten years after this first conference, I became aware of the activity of Fred Mumpton in the area of natural zeolites. The general subject and particularly the outlook on potential applications of natural zeolites influenced my scientific view, and I started to reinterpret cordierite small-cavity research as a step towards understanding zeolites. The visit of my friend Mickey Gunter in 1990 at the crystallography laboratory in Bern, Switzerland, was the beginning of our crystallographic activity on natural zeolites focusing on the following problem: Which zeolite properties are related to the porous bulk structure and which to the nature of the large active surface? In particular single-crystal diffraction techniques seemed to be tailor-made to study bulk effects excluding surface contributions. Favorite research subjects were the minerals heulandite and clinoptilolite, their de- and rehydration behavior, and the bonding properties of various extraframework cations introduced by cation exchange.

On the occasion of Zeolite '93 at Boise, Idaho, I first met Fred Mumpton and became fascinated by his inspiring personality and profound sense of humor. Most admirable was his outstanding ability to link basic research and application technology. On the conference-accompanying field trips, we learned several showy experiments from Fred, such as how to identify a rock composed of fibrous zeolites in the field. Pictures of this unique and simple experiment demonstrated by Fred (Fig. 1) were subsequently shown to some hundred geology graduate students in North America and Europe during my Mineralogical Society of America lecture tour, entitled “Natural Zeolites, from Structure to Applications.” This lecture covered almost all aspects on natural zeolites, which I learned from Fred. During the more recent natural zeolite meetings, Fred became more and more concerned that the quality of research in his favorite field would not maintain the high standards established at the beginning of his natural zeolite activity. To demonstrate both research quality and progress since Zeolite '76, he was the impetus for the book *Natural Zeolites: Occurrence, Properties, Applications*, published in 2001 by the Mineralogical Society of America in the series *Reviews in Mineralogy and Geochemistry*. Mickey and I were proud that Fred asked us to write the chapter on crystal structures of natural zeolites.



**Figure 1.** Fred Mumpton demonstrates that a zeolite rock containing high concentrations of fibrous zeolites (mordenite and/or erionite), hit with a geological hammer, remains attached to the tip of the hammer whereas a rock composed of platy zeolites (e.g., clinoptilolite) will drop down. Some friends of the pioneer of natural zeolite research have engraved the initials F. M. into the soft zeolitic rock in the background. The photograph was taken during the field trip at the Zeolite '93 conference.

## Fred Mumpton and “clinoptilolite redefined”

D. L. Bish<sup>1</sup> and J. Boak<sup>2</sup>

<sup>1</sup>Indiana University; Bloomington, Indiana, USA; Email: bish@indiana.edu

<sup>2</sup>Colorado School of Mines; Golden, Colorado, USA

Fred Mumpton, through his seminal 1960 paper and subsequent work, played a pivotal role in enhancing our recognition that clinoptilolite (CPT) is probably the most important zeolite on the surface of the Earth. Although heulandite (HEU) was first recognized in the 1700s, CPT was not named until 1932 (Schaller, 1932) and has had a confusing history, as reviewed by Mumpton (1960). Mordenite, named after its type locality (Morden, Nova Scotia), was discovered by How (1864), who provided chemical data. Subsequently, Cross and Eakins (1886) described the orthorhombic mineral ptilolite, named from πτιλον, meaning “down,” an allusion to the light downy nature of the fibrous aggregates. Pirsson (1890) described a second occurrence of mordenite from Wyoming, based primarily on chemical analyses, even though this material had a platy habit. Adding confusion, Dana (1914) described mordenite as monoclinic, based on Pirsson (1890), although the type material was apparently the fibrous orthorhombic variety, also known as ptilolite. Based on new crystallographic data showing that Pirsson’s mordenite was monoclinic and had inclined optical extinction, Schaller (1932) proposed the name clinoptilolite for the platy mineral whose composition was close to ptilolite, thus the name clino, for monoclinic or inclined, and ptilolite.” Today, mordenite takes precedence over ptilolite for the orthorhombic fibrous mineral. Mumpton (1960) reviewed available data and suggested that CPT be redefined as the high-silica member of the HEU group. He argued “that clinoptilolite is a zeolite mineral closely related to, but distinct from, heulandite in composition, properties, stability and genesis.” He also commented that there does not appear to be complete solid solution between the two species. It is remarkable that the International Mineralogical Association subcommittee on zeolites (Coombs et al., 1997) made *one* exception to their Rule 3 (“zeolite mineral species shall not be distinguished solely on the basis of the framework Si:Al ratio”) and accepted both the names clinoptilolite and heulandite.

To this day, some uncertainty remains regarding the degree of solid solution between HEU and CPT. Although some derivative properties (e.g., thermal stability) differ considerably between the two, their basic framework topologies are identical (and many have remarked that derivative properties should not be used to define a distinct mineral). Some intermediate compositions show transitional thermal behavior, but this can be interpreted either as representing true compositional overlap *or* as an intergrowth of two phases. After Mumpton’s original study, additional data have been obtained that support the existence of distinct compositional ranges for each mineral. Bish and Boak (2001) described distinct chemical trends for both minerals, with CPT showing Ca/Ca+Na+K from 0.02–0.92 but restricted Si/(Si+Al) ratios (0.80–0.86); HEU shows restricted Ca/Ca+Na+K from 0.67–0.92, but a broader and lower Si/(Si+Al) ratio (0.74–0.85). Unlike natural samples, Ca, Na, and K can be almost completely exchanged in the laboratory, regardless of Si/Al ratio. Explanations for the apparently distinct compositional ranges of CPT and HEU include: 1) water chemistry controls variations; 2) phase equilibria limit variations; and 3) crystal structure limits variation. Explanation 1 is supported by a number of occurrences. Explanation 2 implies that low Si/Al compositions for CPT may be unstable with respect to another Na/K-mineral with limited Ca solid solution, such that low Si/Al HEU can form. Explanation 3 implies structural constraints, as documented by Ross et al. (1992) for some natrolite group minerals, in which covariation of alkali/alkaline-earth elements with Si/Al ratio reflects occupancy of extraframework channels. Fred Mumpton clarified the nature of CPT considerably with his 1960 work and was at least partially responsible for the later IMA nomenclature decision. Without more data, it may be difficult to distinguish among crystallographic, petrologic, and geochemical constraints on compositional ranges.

### References

- Bish, D.L. and Boak, J. (2001) Clinoptilolite-heulandite nomenclature. In Bish, D.L. and Ming, D.W., eds., *Natural Zeolites: Occurrence, Properties, Applications*. MSA Reviews in Mineralogy and Geochemistry, **45**, 207-216.

- Coombs, D.S. et al. (1997) Recommended nomenclature for zeolite minerals: Report of the subcommittee on zeolites of the IMA, Commission on New Minerals and Mineral Names, *Canadian Mineralogist*, **35**, 1571-1606.
- Cross, W. and Eakins, L.C. (1886) On ptilolite, a new mineral. *American Journal of Science*, **32**, 117.
- How, D.C.L. (1864) On mordenite, a new mineral from the trap of Nova Scotia. *Journal Chemical Society, London*, **17**, 100-104.
- Dana, E.S. (1914) *The System of Mineralogy of James Dwight Dana*. 6th Edition, John Wiley & Sons, Inc., London.
- Mumpton, F.A. (1960) Clinoptilolite redefined. *American Mineralogist*, **45**, 351-369.
- Pirsson, L.V. (1890) On mordenite. *American Journal of Science*, **40**, 232-237.
- Ross, M., Flohr, M.J.K., and Ross, D.R. (1992) Crystalline solution series and order-disorder within the natrolite mineral group. *American Mineralogist*, **77**, 685-703.
- Schaller, W.T. (1932) The mordenite-ptilolite group; clinoptilolite, a new species. *American Mineralogist*, **17**, 128-134.

## Fred Mumpton and Italy: A reciprocated love

C. Colella

*Università Federico II, Napoli, Italy; Email: carmine.colella@unina.it*

Fred Mumpton was a man with the gift of a great human drive, constantly displayed in his relations with people, but I feel that he had a particular propensity for Italians, especially for those of us living in south-central Italy. He perhaps loved our solar character, our optimistic way of life, our friendliness, but, I suspect, he particularly appreciated the fact that most of us live in the middle of, and sometimes on, his beloved sedimentary zeolite deposits. He had traveled more than once to Italy to visit the large phillipsite- and/or chabazite-rich formations cropping out over extended areas of Tuscany, Latium, Umbria, and Campania (including the Caserta Plain, the so-called Phlegraean Fields, Ischia, and Procida islands, among others), which represented a conspicuous exception with respect to the much more common clinoptilolite deposits he had encountered (and in some case discovered) in so many countries around the world. He was perhaps the first non-Italian man who read the papers (in Italian!) written by Riccardo Sersale in the fifties dealing with the discovery of the Italian sedimentary zeolite formations and the reconstruction in the laboratory of zeolite genesis in nature. He had, in fact, great respect for scientists who made, prior to American geologists, exploratory investigations of zeolite deposits in several volcanic areas around the world, e.g., the green tuff formation of Yokotemachi in Japan, the low-grade metamorphic rocks of Southland in New Zealand, and the Neapolitan yellow tuff around Naples, Italy.

Apart from Rosario Aiello, who possibly met him in 1974 while attending near Palo Alto (California) the 2nd Seminar of the U.S.-Japan Cooperative Science Program on Zeolite Occurrence, Mineralogy and Use, most of us first met Fred in 1976 during the memorable Tucson Conference—the initial, and probably unequalled, international meeting of the same series of the present conference. Our first experience was better than we had ever hoped: Fred welcomed us with a private drink in his hotel room, sharing with a few friends (among them the Italians!) a bottle of *saké* that some Japanese colleagues had brought to him from the Far East.

His peerless passion for natural zeolites surely affected my research and, consequently, to some extent, my life. Until 1976, my research interests were focused on zeolite synthesis, especially from low-cost raw materials such as natural rhyolitic and trachytic glass. I had worked also on natural zeolites, e.g., the use of zeolitic tuff as a desiccant, but I could not imagine that this would have become my main research field. Fred's fascinating lecture at the Tucson conference, followed by the exhaustive review published in the conference proceedings, and the trip to the Bowie zeolite deposit—the first I had ever visited (see Fig. 1)—were influential in causing me to focus my research efforts on the enormous deposits of sedimentary zeolites present in Italy, trying to find possible applications in environmental and industrial fields.

Let's pass now to the involvement of Fred Mumpton in the organization of international zeolite meetings in Italy. Unexpectedly, he played an important role in the selection of Naples as the site of the 5th IZA Conference and, of course, of Riccardo Sersale as the general organizer. The suggestion of Naples as the conference site came from the former IZA chairman and secretary-treasurer, Jan Uytterhoeven and Walter Meier, respectively, but Fred Mumpton and Leonard Sand sponsored this proposal with enthusiasm, believing this site would give new visibility to natural zeolites, neglected by the latest IZA conferences. They were right; in fact, the Naples conference had the highest number of presentations on natural zeolites ever reported (also in the future IZA conferences).

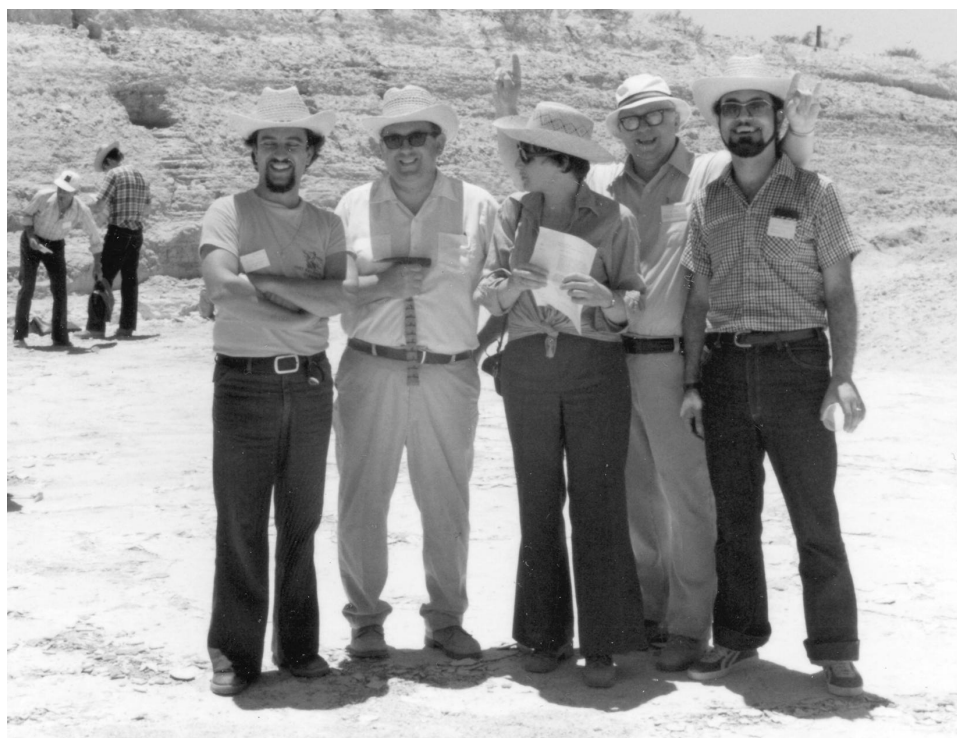


**Figure 1.** Visit to the Bowie zeolite deposit in June, 1976. From left to right: Rosario Aiello, Fred Mumpton, Iliana Galabova, Len Sand and Carmine Colella

But, no doubt, Fred was dominant especially in the success of the international events held in the island of Ischia in June 1997. We had there ten days (September 19–29, 1997) of intense scientific engagement in two consecutive meetings: the 4th FEZA Euroworkshop on “Occurrence, Properties, and Utilization of Natural Zeolites” and Zeolite '97, the 5th installment of this series of conferences. In the first event he presented an opening lecture titled: “Natural zeolites: where have we been, where are we going,” then published in the Proceedings of Zeolite '97, in which a series of considerations on his thirty-year experience in defending “the rights of natural zeolites” were reported, including historical facts and prospects, complaints and recommendations, proud defense of his views, and acknowledgment of deficiencies.

His involvement as unofficial supervisor in the organization of Zeolite '97 was, as usual, superb. When I presented in Boise the plan to organize the next conference in Ischia, he did not hide his enthusiasm for the site and encouraged me with advice and suggestions. He accepted with some reluctance the job of co-editor of the proceedings of the conference: it was really an act of friendship, as he had decided to close his active involvement in the vicissitudes of natural zeolites. The long period we spent in refereeing and editing the papers of the volume “Natural Zeolites for the Third Millennium,” although very tiring and exacting, was one of the most exciting of my life, really a great experience. I had the pleasure of frequently earning Fred’s approval of my work and the satisfaction of knowing that he had been very glad to work with me (actually I worked with him!), as we had the same rigorous approach in the refereeing process.

How we were both rigorous referees was the last thing he told me again when I met him, in Thessaloniki, at the time of Zeolite '02. In his mild look I noted a blend of esteem and affection, the same feelings I have now and will save in the future for my memory of him.



## **Persnickety editor, founding father, mentor, and friend: The legacy of Fred Mumpton**

**D. W. Ming**

*NASA Johnson Space Center; Houston, Texas, USA; Email: douglas.w.ming@nasa.gov*

I first met Fred Mumpton during my second year of Ph.D. research at Texas A&M University in 1982. I had just started a research program to survey and characterize zeolites in soils of south Texas. Fred was invited by my major professor, Dr. Joe Dixon, to visit the university and check out some of the local Texas zeolites, including clinoptilolite in the nearby Catahoula Formation. I had read many of the articles and books Fred had written and edited while I was preparing for my Ph.D. research; needless to say, as a student, I was in awe and thrilled to meet Fred Mumpton. That visit was the start of a long and close relationship with Fred. For the next 20+ years we had many interactions. It was an honor and privilege to have had the opportunity to interact with Fred. To us all, Fred wore many different hats. But to me, Fred was the persnickety editor, founding father, mentor, and most importantly, friend.

### **Persnickety Editor**

Anyone would tell you that one of Fred's outstanding talents was his ability to edit a paper into a sound scientific piece of work. I discovered this very early in my career when Fred and I wrote a zeolite chapter for a soil mineralogy textbook (Ming and Mumpton, 1989). Fred worked with me patiently to get the chapter into top-notch shape (a mandatory requirement for Fred). Over the next few years we edited a book together (Ming and Mumpton, 1995). It was a great learning experience as Fred taught me the tricks of the trade. I use to this day his "recipe" for a sound scientific paper (Mumpton, 1990). I think that if Fred could talk to me this minute, he would remind me that it would be a good idea to refresh everyone's memory on the recipe for writing a sound science paper. So, with Fred looking over my shoulder somewhere up there, here is that recipe. The format for the recipe consists of the following parts: 1) Title, 2) Authorship, 3) Abstract, 4) Introduction, 5) Experimental Methods (or Methods & Materials), 6) Results, 7) Discussion, 8) Conclusions (or Summary & Conclusions), 9) Acknowledgments, and 10) References Cited. I cannot go into the details for each of these sections, but I encourage readers to read Fred's comments. I will, however, state that the abstract may be the most important part of the paper because this may be the only section read by many. As Fred stated, "the abstract should be a fact-filled condensation of the entire paper." The abstract should convey the rationale for undertaking the study, a brief statement about the methods, the important findings (including specific data, and anyone who has had an article edited by Fred will attest to this), and the pertinent interpretations (conclusions) of those findings. Although Fred may have been a persnickety editor, his overarching goal was to *help* a writer clearly express his or her scientific findings to his or her colleagues.

### **Founding Father**

Perhaps Fred will be most remembered for his love of natural zeolites and his desire to bring scientists together from around the world to discuss their passion. For nearly 30 years, Fred led the International Committee on Natural Zeolites (ICNZ). His foresight to bring scientists and technologists together to discuss natural zeolites at the first conference in Tucson, Arizona, in 1976 led to seven international conferences (including this 7<sup>th</sup> conference in Socorro). I helped Fred organize the 4<sup>th</sup> International Conference on Natural Zeolites in Boise, Idaho, June 1993. It was hard work to organize the meeting, and I marveled at Fred's enthusiasm and energy in leading the effort. He reminded me from time to time (when I wanted to quit) why such conferences were important and that all of this hard work would pay off. Fred would tell me that the conference would provide the opportunity to highlight the latest information on the occurrence, structure, physical and chemical properties, and applications of natural zeolites. Most importantly, it would set the stage from which future researchers would launch even more intriguing investigations.

Fred stepped down as chair of ICNZ after the 5<sup>th</sup> international meeting on Ischia in 1997. I tried to persuade Fred not to step down, but as he put it, "It's time." I took over Fred's position as chair of ICNZ. I knew that it would be impossible to fill Fred's shoes, but what struck me the most was the amount of time Fred spent on

ICNZ. I was not an able substitute for Fred Mumpton; he devoted his life to the advancement of the science of natural zeolites. Fred was truly a pioneer in developing the natural zeolite discipline and the founding father of our organization.

### Mentor and Friend

Fred was not only my mentor, but my dear friend. He was always willing to help me out with a project or a problem. Back in 1982, he started out as my mentor. One of the first items that he taught me was how to correctly pronounce the names of natural zeolites. He told me that if I was going to get “into” the natural zeolite business that I better learn how to pronounce the names correctly. I wrote down those pronunciations and they are presented in Table 1.

I worked daily with Fred after I finished my Ph.D. We worked together writing papers, organizing meetings, and editing books. I felt at times that I was in way over my head, but Fred was always patient and willing to provide guidance to pull me through a tough situation. It was during this time that Fred and I became good friends. Ardeth (Fred’s better half) was always at his side, and I perhaps spent as much time on the phone talking to Ardeth as I did Fred. They were both my mentors and inspired me to continue my research in the arena of natural zeolites. Their support, guidance, and friendship helped me get to where I am today in the scientific world. Fred, you are dearly missed, but your legacy will live on because you took the time to mentor and build friendships with so many of us. Thanks Fred for your dedication, leadership, and most importantly, your friendship!

**Table 1.** Mumpton’s pronunciation of common zeolites as translated by D.W. Ming

Zeolite	Mumpton’s Pronunciation
analcime	ăn ăl sîm
chabazite	kăb à sît
clinoptilolite	klî nō tîl ô lîr
erionite	ēr ē ô nît
heulandite	hû lăn dît
mordenite	môr dē nît
phillipsite	fîl lîp sît

### References

- Ming, D.W. and F.A. Mumpton (1989) Zeolites in soils. Pp. 873-911 in: *Minerals in soil environments (2nd edition)* (J.B. Dixon and S.B. Weed, editors). Soil Science Society of America Journal, Madison, WI.
- Ming, D.W. and F.A. Mumpton (eds.) (1995) *Natural Zeolites '93: Occurrence, Properties, Use*. International Committee on Natural Zeolites, Brockport, NY, 622 pp.
- Mumpton, F.A. (1990) The universal recipe or how to get your manuscript accepted by persnickety editors. *Clays & Clay Minerals*, **38**, 631–636.

## **Memories about Dr. Mumpton**

**V. A. Nikashina**

*Russian Academy of Sciences; Moscow, Russia; Email: nikashina@geokhi.ru*

I became acquainted with Dr. Mumpton in 1993, in the beginning through correspondence before the Zeolite Conference of 1993 in Boise, Idaho (after submitting my thesis), then in person in Boise during the Conference. Up to 1993, Russian scientists had practically no opportunity to participate in the International Zeolite Conferences because we could not afford the expenses. In 1993, all my expenses and the expenses of my four colleagues from the former Soviet Union were paid by the organizing committee of the Zeolite Conference and the International Science Foundation because of the efforts and concern of Dr. Mumpton. I was notified by a fax with Dr. Mumpton's signature that I would receive my flight tickets at the Moscow office of the International Science Foundation. I was impressed and touched. I expressed my gratitude and appreciation to the organizing committee and to Dr. Mumpton personally during the meeting in Boise. The year 1993 was a milestone in terms of my further participation in the International Zeolite Conferences. We have participated in all Zeolite Conferences over the subsequent years.

Dr. Mumpton came to Moscow; I met him and always felt his enormous charm. Unfortunately, my poor English limited our relations. But I always felt his understanding and encouragement. Dr. Mumpton's positive energy was so powerful that I always felt that it gave me force and confidence, and each contact with him was so pleasant to me.

I was shocked by his courage when I saw in what heavy condition he arrived at the 2002 Conference in Thessaloniki. Mrs. Mumpton told me how hard the trip was to Thessaloniki for Dr. Mumpton. But he not only overcame all difficulties of the transcontinental flight, he also actively participated in that Conference. I admire the human force and courage of this person.

I am immensely grateful to him for the lessons I received during the editing phase while preparing the materials from the conferences in 1993 and 1997 for publication. Dr. Mumpton's requirements for writing the text and for the design of the report were always excellent. We had to meet all these requirements, and not all the authors could. It was a remarkable lesson for me, which I have acquired to my mind, and I shall use this experience in my further scientific work.

Scientific meetings at the International Zeolite Conferences are always very useful. For Russian scientists during our political reorganization (Perestroika), these international meetings were doubly valuable. In fact, in Russia since 1992, regular scientific meetings on natural zeolites were not simple at all. Financial opportunities did not allow us to organize such meetings during that time. The organization of a Russian zeolite meeting is also a problem now.

I bow down before Dr. Mumpton for his understanding, help, and efforts, which allowed Russian scientists to participate in the Zeolite Conferences. I appreciate so much Dr. Mumpton's activity, and I shall remember this person up to the end of my life.

## How a thirty-year friendship with Fred Mumpton affected my life and my career as a scientist

D. Tchernev

*The Zeopower Company; Chestnut Hill, Massachusetts, USA; Email: zeopower@usa.net*

In 1969, I was a materials scientist working in the field of magnetic materials and magnetic information storage at the University of Texas at Austin when, by accident, I came in contact with a neighbor and colleague at UT who was a crystallographer and had worked at Shell research lab in Houston. He taught me the basic properties of molecular sieve zeolites. My first experiments were performed with synthetic zeolites, as they were easy to obtain from lab supply houses. The results were disastrous: the refrigerant gases I was using (CFC) were catalyzed with the production of highly corrosive gases, such as HF and HCl, which destroyed my equipment. In 1974, I moved back to MIT and continued to experiment with synthetic zeolites and other refrigerants, such as alcohols, which were also dehydrated and decomposed by the catalytic action of the zeolites, and at the end with water vapor (which was finally stable). However, the heat of adsorption of water was very high (1800 to 2200 btu/lb) because those zeolites were especially designed to dry gases. As the heat of vaporization of water is only 1000 btu/lb, the efficiency of the system was very low. In 1975, I was contacted at MIT by Fred Mumpton, who suggested that I try natural zeolites, as their heat of adsorption is considerably less. He introduced me to Al Letcher of Lancaster, California, who was working some natural zeolite deposits, and I received my first clinoptilolite from Horseshoe Dam, Arizona, and chabazite/erionite from Bowie, Arizona. The chabazite proved to be the best material for my work because its heat of adsorption for water is only 1200 btu/lb, and it promises an efficiency of 80%.

Fred also encouraged me to present a paper at the 1976 zeolite conference in Tucson, Arizona, which I did. At the conference, he introduced me to Len Sand, R.A. Sheppard, and other zeolite dignitaries. The most unusual situation happened when Fred introduced me to Professor Tsitsishvili from Georgia. This was at the height of the cold war. I had escaped from behind the iron curtain and did not want to harm my family still there by advertising my being in the USA. Professor Tsitsishvili, on the other hand, wanted to have his picture taken with me, and Fred was eager to please him. It took long negotiations to convince me to pose for the picture, but Fred won. The field trip to the Bowie deposit cemented our friendship. Despite Fred's good planning and bringing three huge trash cans full of ice, beer, soft drinks, and water, the bus trip lasted longer than expected; Arizona is very hot in the summer, and we ran out of all liquids. At the last stop at a Bowie café, we discovered our mutual love for cold beer and all was right again.

At our next meeting, at the 5<sup>th</sup> IZA conference in Naples, Italy, in 1980, we all had a wonderful mid-week trip to the island of Ischia in the gulf of Naples. On the return trip on the boat, I was standing at the bar with Donald Breck, Fred, and Edith Flanigan, when Edie told me that she knew the secret of the Bowie zeolite deposit that makes it so good: it is its very low density. Fred already knew this as the deposit was sedimentary volcanic ash converted to zeolite, but I had to convince myself. Returning home, I measured the weight of a piece of rock from the Bowie deposit; the dehydrated sample had a density of 0.8 gr/cc—i.e., it will float in water. Considerable further testing of the dynamics of adsorption and desorption on this zeolite showed how the very low density, 40% of the crystal density of 2 gr/cc, results in a material superior to any other for my needs.

At the beginning of the field trip to the Italian zeolite deposits, another crisis occurred: while Ardeth and Fred were loading their luggage in their rented car, some young Italians on a motor scooter drove by and grabbed Ardeth's pocketbook, which was lying on top of the car, with all their money, passports, etc. We passed the hat for the Mumptons and got them sufficient funds, but for new passports they had to go to Rome.

At the '93 conference in Boise, Idaho, there was a large Bulgarian delegation, and Fred asked me to help him host them and translate for them when necessary. There I asked myself: Why did Fred like me? He always said it was my rolling RRRR, when I called him "FRRRRRed" across the room. Maybe it was my Bulgarian background and accent. He liked Bulgarian zeolites, Bulgarian food, and especially the "Shopska Salata," a salad with lots of white Bulgarian cheese on top. He tried to make it himself at home but could not find the right cheese. So we arranged with my Bulgarian zeolite friends to smuggle some of the cheese into the USA. By the time we had given him the cheese, he had found a local source somewhere in the upstate New York area. Our

discussions at the Boise conference convinced me to start serious studies of the dynamics of adsorption and desorption on zeolites.

At the '95 Sofia conference, Fred had a good time with the food and drinks, while I was surrounded and overwhelmed by relatives and barely had time to see him. At the '97 conference in Naples-Ischia, we had a long discussion, and Fred encouraged me to redirect my work, using waste heat from automotive engines rather than solar heat. He also asked me if I would be interested writing a chapter for the new Z-book, and I was. The '02 conference in Thessaloniki was the last conference that we attended together. I brought back cheese for Fred's salad, with the help of the Great Cheese Smuggling Conspiracy. We had long discussions and he convinced me to try to organize a conference on the medical application of zeolites, possibly under the sponsorship of NATO. He had already collected a good portion of papers on the subject and a list of people working in the field and possible candidates for conference participation. As always, when Fred heard of a new application of natural zeolites, he tried to foster it and publicize it for the whole world to know.

Fred taught me not only about natural zeolites, good beer and good food; he was a fantastic editor. His small pamphlet on how to write a good paper should be required reading for everyone planning to write articles in the future. He was firm but gentle: when I sent him my first draft of the chapter for the new Z-book, he mailed it back with a cover letter starting, "Dimiter, this is the best writing that you have ever done. However . . . ," and it was followed by a sea of red ink on every page of the manuscript. He was right of course, and after many more rewrites, the chapter definitely was greatly improved. It was typical of Fred to try to correct you without hurting your feelings or putting you down. I have learned so much from Fred Mumpton that I will be forever grateful and cherish the privilege of knowing him.



# Invited Papers





## **Exploration guides for zeolite deposits in lacustrine tuffs, with reference to the Taupo Volcanic Zone, New Zealand**

**R. L. Brathwaite**

*GNS Science; Lower Hutt, New Zealand; Email: b.brathwaite@gns.cri.nz*

Descriptive and genetic geological models are widely used in the exploration of many types of metallic and non-metallic mineral deposits, and they are based on the geological, geochemical, and geophysical attributes that are common to a number of similar mineral deposits that are presumed to have been formed by the same genetic process. The main attributes are geological setting, host rock lithology, form of the deposit, economic minerals, mineralogy of ore and host rocks, and geochemical and geophysical characteristics. Descriptive and genetic geological models of zeolite deposits hosted in lacustrine tuffs in the Ngakuru area of the Taupo Volcanic Zone (TVZ) have been developed as a guide to defining exploration targets in the region. This kind of approach can be also applied to exploration for zeolite deposits in other volcanic terranes.

The geological setting of the zeolite deposits in the TVZ is a continental margin volcano-tectonic zone along the Pacific-Australian plate boundary in the North Island of New Zealand. The TVZ contains voluminous rhyolitic tephra, ignimbrites, and lavas, with minor dacite and andesite. Extensive lake deposits are represented by intercalated tuffs, silts, diatomite, and pumice sands. In the TVZ, there are about twenty active and extinct geothermal fields that are associated with hydrothermal convection along faults.

The volcanic containers that host the zeolite deposits consist of sequences of thinly stratified vitric tuffs up to 50 m in thickness. The vitric tuffs unconformably overlie ignimbrite (~240 ka age by  $^{40}\text{Ar}$ - $^{39}\text{Ar}$ ) and rhyolite (~145 ka age by  $^{40}\text{Ar}$ - $^{39}\text{Ar}$ ), and are overlain by silts, pumice sands, and diatomite. The form of the deposits reflects the geometry of the host vitric tuffs in being flat-lying and stratiform. Some of the zeolite deposits are adjacent to sinters, and to hydrothermal eruption breccias, which are unsorted breccias with clasts of rhyolite, ignimbrite, and zeolitic tuffs in a matrix of smectite and opal-CT. Hydrothermal eruption breccias are interpreted as the products of steam-driven eruptions.

The primary components in the tuffs are glass shards, with minor pumice clasts and volcanic plagioclase, quartz, and biotite crystals. Glass shards in the vitric tuffs are replaced by zeolite minerals that, from X-ray diffraction analysis, consist of up to 80% mordenite  $\pm$  clinoptilolite (Brathwaite, 2003). Mordenite dominates over clinoptilolite in the lower part of the vitric tuff sequence. Amorphous silica (opal-A), opal-CT, and K-feldspar are also present as secondary minerals. Mordenite occurs as a mesh of crystals replacing glass shards, and as thin fibres coating platy crystals of clinoptilolite. Both the mordenite and clinoptilolite are very fine grained (1–10  $\mu\text{m}$ ). Mordenite and clinoptilolite, accompanied by K-feldspar, opal-A, and opal-CT, occur in lesser amounts in the adjacent underlying ignimbrite.

Chemically the zeolitic vitric tuffs are of rhyolitic composition (Brathwaite, 2003). Relative to unaltered vitric tuffs, the zeolitic tuffs are slightly enriched in K and depleted in Na. But this geochemical signature is quite subtle and is probably not useful as an exploration guide.

The zeolite deposits are associated with broad magnetic lows, within which there are coincident gravity and resistivity lows. The magnetic lows are due to the hydrothermal destruction of magnetite in the zeolitic tuffs relative to the presence of primary magnetite in the unaltered tuffs, ignimbrites, and rhyolite lavas that surround or underlie the zeolite deposits. Gravity lows are a result of the very low densities (0.66–1.12 g/cm<sup>3</sup>) of the zeolitic tuffs. The zeolitic tuffs have relatively low resistivities of 20–35  $\Omega$ , which is probably due to their high porosity (45–73%) and hence high water content.

The host rocks were produced by rhyolitic pyroclastic eruptions that deposited glass-rich vitric tuffs into a lake about 15–20 km from the likely eruptive source. The presence of sinters, hydrothermal eruption breccias, and/or quartz-adularia alteration in fault breccias in the vicinity of the zeolite deposits suggests that they are associated with geothermal activity similar to the active geothermal systems in the TVZ. The Wairakei geothermal system contains mordenite (Steiner, 1977) and clinoptilolite, which formed at temperatures of 60°–160°C, with mordenite forming at higher temperatures than clinoptilolite. The main fluid type at Wairakei, and similar geothermal systems, is a dilute alkali chloride water of near neutral pH. By analogy, mordenite and clinoptilolite in the Ngakuru deposits probably formed at similar temperatures as a result of interaction of alkali

chloride water, diluted with lake or groundwater, with glass shards, and with pumice in the vitric tuffs (Brathwaite, 2003). The occurrence of silica sinter above the zeolitic tuffs implies deposition of sinter at the ground surface from hot alkali-chloride water of near-neutral pH (Herdianita et al., 2000). The spatial association of the zeolite deposits with sinter indicates that the zeolites were formed at a shallow depth, i.e., 25 m to a maximum of 80 m below the paleosurface. The zeolite deposits are located on or close to faults, which indicates that the faults acted as feeders for heated alkali-chloride water that caused the deposition of the zeolite minerals.

Key features to look for in exploration for zeolite deposits of this type are

- Lacustrine vitric tuff host rocks, which provide large volumes of reactive volcanic glass.
- Diatomite, which may occur down or up stratigraphy from lacustrine tuffs.
- A spatial association with geothermal systems and faults to provide a source and conduit for heated alkali-chloride waters, which react with the vitric tuffs to form the zeolites. Hydrothermal eruption breccias, sinter overlying zeolitic tuffs, and hydrothermal adularia in permeable fault zones are indicators of hydrothermal activity that may have formed zeolites.
- Geophysical signatures that have coincident gravity and resistivity lows within broad magnetic lows that represent hydrothermal alteration zones.

## References

- Brathwaite, R.L. (2003) Geological and mineralogical characterization of zeolites in lacustrine tuffs, Ngakuru, Taupo Volcanic Zone, New Zealand. *Clays and Clay Minerals*, **51**, 589–598.
- Herdianita, N.R., Browne, P.R.L., Rodgers, K.A. and Campbell, K.A. (2000) Mineralogical and textural changes accompanying ageing of silica sinters. *Mineralium Deposita*, **35**, 48–62.
- Steiner, A. (1977) The Wairakei geothermal area North Island, New Zealand. *New Zealand Geological Survey Bulletin*, **90**, 135 p.

## **Ion-exchange studies on Italian natural zeolites: Experiments and data processing**

**D. Caputo**

*Università Federico II di Napoli; Napoli, Italy; Email: domenico.caputo@unina.it*

Ion-exchange properties of Italian natural zeolites coming from sedimentary deposits have been deeply investigated over the last decades in order to assess their potential use in several fields such as wastewater treatment, soil amendment, and soil-less substrate preparation. Many papers concerning thermodynamic, kinetic and/or fixed-bed dynamic studies of ion-exchange reactions in sedimentary phillipsite- and/or chabazite-rich tuffs, and more recently clinoptilolite-bearing rocks, have been published. This paper intends to review these studies.

Early evaluations of ion-exchange properties of Italian sedimentary zeolites were carried out by Sersale (1958) in the framework of his studies on the genesis and constitution of Neapolitan yellow tuff, a zeolitic rock occurring widely in the volcanic area of southern Italy and containing phillipsite as the main zeolitic phase.

The first studies on the potential applications of Italian zeolitic tuffs as ion exchangers started only in the 1970s, when some chabazite-rich tuffs were tested for both water softening and iron and manganese removal from water. Later on, in the early 1980s, preliminary investigations on the ability of phillipsite-rich tuff to remove ammonium from wastewaters were carried out by Colella et al. (1984). All these researches were essentially based on kinetic and/or dynamic studies, in which ion-exchange selectivity was evaluated in static experiments and/or testing fixed beds eluted by solutions of the examined cation, respectively. Kinetic and/or dynamic investigations in fixed-bed runs and modeling of obtained data were performed also using phillipsite- and/or chabazite-rich tuffs for  $\text{Pb}^{2+}$ ,  $\text{Cr}^{3+}$ ,  $\text{Cu}^{2+}$ ,  $\text{Zn}^{2+}$ ,  $\text{Ba}^{2+}$ , and  $\text{Co}^{2+}$  (see Refs. in Colella, 2002; de Gennaro and Colella, 2003).

A systematic study of basic thermodynamic aspects of ion-exchange reactions involving Italian natural zeolites started in the 1990s. Cation-exchange equilibria between its Na-exchanged form and various toxic and noxious cations, namely  $\text{Cr}^{3+}$ ,  $\text{Cd}^{2+}$ ,  $\text{Pb}^{2+}$ ,  $\text{Cu}^{2+}$ ,  $\text{Zn}^{2+}$ ,  $\text{Cs}^+$ ,  $\text{Sr}^{2+}$ ,  $\text{Ba}^{2+}$ ,  $\text{Co}^{2+}$ ,  $\text{NH}_4^+$ , and some alkaline and earth-alkaline cations, such as  $\text{K}^+$ ,  $\text{Ca}^{2+}$ , and  $\text{Mg}^{2+}$ , were investigated in order to evaluate the selectivity of the exchanger toward the above cations (Colella, 2002). An overall estimation of the ion-exchange selectivity was made from thermodynamic quantities, such as the equilibrium constant  $K_a$  and the standard Gibbs free energy  $\Delta G^\circ$  of the exchange reaction. These quantities were computed from equilibrium data by using a procedure set up by Caputo and co-workers (1995; 2005) and based on the method of evaluation of the activity coefficients of cations in solution proposed by Ciavatta (1980). A new thermodynamic model was recently proposed by Pepe et al. (2003) and used for the description of Na-Pb exchange equilibria on chabazite. This model, namely the “Double Selectivity Model,” is based on the hypothesis that zeolite can be modelled as composed by two different groups of cation sites available for ion-exchange reactions, each characterized by its own selectivity towards any given cation couple.

The  $K_a$  values computed from equilibrium data allowed the following selectivity series to be worked out:

phillipsite

(Si/Al = 2.4 – 2.7):  $\text{Ba}^{2+} > \text{Cs}^+ \approx \text{K}^+ > \text{Pb}^{2+} > \text{NH}_4^+ > \text{Ca}^{2+} > \text{Na}^+ > \text{Sr}^{2+} > \text{Zn}^{2+} > \text{Co}^{2+}$

chabazite

(Si/Al = 2.2 – 2.6):  $\text{Cs}^+ > \text{NH}_4^+ > \text{K}^+ > \text{Pb}^{2+} > \text{Na}^+ > \text{Ba}^{2+} > \text{Cd}^{2+} > \text{Sr}^{2+} > \text{Cu}^{2+} > \text{Zn}^{2+} > \text{Co}^{2+}$

clinoptilolite

(Si/Al = 4.2):  $\text{NH}_4^+ > \text{Pb}^{2+} > \text{Na}^+ > \text{Cd}^{2+} > \text{Cu}^{2+} \approx \text{Zn}^{2+}$ .

The good selectivities that Italian natural zeolites display for some toxic and noxious cations, such as  $\text{Ba}^{2+}$ ,  $\text{Cs}^+$ ,  $\text{Pb}^{2+}$ , and/or  $\text{NH}_4^+$ , fully confirm the possibilities of practical applications of these materials in decontaminating wastewaters and/or recovering contaminated soils.

## References

- Caputo, D., Dattilo, R. and Pansini, M. (1995) Computation of thermodynamic quantities of ion exchange reactions involving zeolites. Pp. 143–151 in: *Proceedings of III Convegno Nazionale di Scienza e Tecnologia delle Zeoliti, Italy* (R. Aiello, editor). De Rose Montalto (Cosenza).
- Caputo, D., de Gennaro, B., Aprea, P., Ferone, C., Pansini, M., and Colella, C. (2005) Data processing of cation exchange equilibria in zeolites: a modified approach. *Studies in Surface Science and Catalysis*, **155**, 129–140.
- Ciavatta, L. (1980) The specific interaction theory in evaluating ionic equilibria. *Annali di Chimica*, **70**, 551–567.
- Colella, C. (2002) Application of natural zeolites. Pp. 1156–1189 in: *Handbook of Porous Solids* (F. Schüth, K.S.W. Sing and J. Weitkamp, editors). Volume **2**, Wiley-VCH, Weinheim, Germany.
- Colella, C., Aiello, R. and Nastro, A. (1984) Evaluation of phillipsite tuff for the removal of ammonia from aquacultural wastewaters. Pp. 239–244 in: *Zeoagriculture. Use of Natural Zeolites in Agriculture and Aquaculture* (W.G. Pond and F.A. Mumpton, editors). Westview Press, Boulder.
- de Gennaro, B. and Colella, A. (2003) Ba and Co removal from water by elution through fixed beds of phillipsite- and/or chabazite-rich tuffs. *Separation Science and Technology*, **38**, 2221–2236.
- Pepe, F., Caputo, D. and Colella, C. (2003) The double selectivity model for the description of ion-exchange equilibria in zeolites. *Industrial Engineering & Chemistry Research*, **42**, 1093–1097.
- Sersale, R. (1958) Genesi e costituzione del Tufo Giallo Napoletano. *Rend. dell'Accademia di Scienze Fisiche e Matematiche della Società Nazionale di Scienze, Lettere ed Arti in Napoli, Serie 4, Vol. XXV*, 181–207.

## **The use of Biolite (a calcium clinoptilolite zeolite) in diets for natural beef production**

**K. S. Eng, R. Bechtel, and D. Hutcheson**

*San Antonio, Texas, USA; Email: engnm@hotmail.com*

Natural beef production requiring non-medicated (n-med) diets is becoming more popular in the United States. Conventional U.S. feedlot diets normally contain low levels of ionophores and other antibiotics. It is thought these additives improve performance, prevent subclinical acidosis and metabolic problems, and reduce liver abscesses. In recent years we have conducted a number of studies comparing various zeolites in med and n-med high concentrate finishing diets. These diets have been composed of corn silage for roughage, flaked corn, and a substantial amount of wet corn milling byproducts.

The feed additives used included Rumensin (R) and Tylan (T). Previous studies indicated a particular calcium clinoptilolite zeolite (Biolite) (B) gave the most favorable results when included in experimental diets at 1.2% (DMB) in place of an equivalent amount of corn. Our experiences would indicate the majority of other zeolites tested have limited value in feedlot rations.

Data collected included daily gain, consumption, feed efficiency, rumen pH, and observations on bloat and metabolic problems. Carcass data including liver abscess occurrence were collected. Also, the impact of B on the loss of ammonia from feedlot lagoons was measured. The information contained in this paper is a summary of data from seven separate experiments.

Table 1 shows the impact of the various treatments on rumen pH. Rumen samples were collected from cattle prior to the morning feeding using a Geishauser Probe. The results indicate that the addition of B to either med or n-med rations significantly increased rumen pH.

The incidence of total liver abscesses and A+ abscesses is shown in Table 2. There were no significant differences in total liver abscesses; however, RTB treatment tended to have the lowest total abscess level. The number of A+ abscesses with the RTB treatment had a significantly lower level of 2.2%. It is possible that these differences in A+ abscesses may relate to the rumen buffering effect of the B.

Ammonia air emission from confined feeding operations is a potential environmental problem throughout the world. It is estimated that 75% of the total ammonia emissions originate from confined feeding operations. Previous research has indicated that certain zeolites, including B, added to feedlot diets can reduce manure ammonia losses. In the following study, manure was collected from animals fed diets containing RT, RT + B, 0 additives, and 0 + B. Using experimental lagoons, ammonia emissions were measured over a 28-day period. The results are shown in Table 3. Treatments 2 and 4, which is manure from rations containing B, had significantly lower ammonia emissions compared to manure from rations without B.

Production of ethanol, fructose, etc., from corn has increased dramatically, and as a result, there is a tremendous amount of wet gluten and distillers available for the cattle-feeding industry. Because of the interest in feeding wet corn, byproducts, and natural beef production, we have conducted seven trials using a wet-corn byproduct diet and comparing medicated diets, med diets + B, and n-med diets + B. Initially, non-med diets without B were also tested, but because of frequent metabolic problems, this treatment was discontinued. Table 4 contains the average performance on cattle receiving 1) med diets, 2) med diets + B, and 3) non-med diets + B. There were seven separate trials, and in each individual trial there were significant performance differences. Biolite tended to improve the performance of cattle receiving med diets and non-med diets + B. Rumensin is known to decrease the incidence of subclinical acidosis in cattle fed high concentrate diets, and it would appear that B may serve the same function. The impact of B on rumen pH and liver abscesses would tend to confirm this.

In summary, the addition of B to rations (1.2% DMB) increases rumen pH, decreases the incidence of A+ liver abscesses, and improves performance—especially in non-med finish rations. Probably because of B's affinity for ammonia, manure from diets containing B reduced ammonia emissions from experimental feedlot lagoons.

**Table 1. Effect of Biolite treatment on rumen\*pH**

RT	6.42b	means with different super script letter differ, P <.05
R	6.43b	
O	6.46b	
RTB	6.63a	
RB	6.65a	
OB	6.66a	

\*Sample collected by Geishauser Probe

**Table 2. Effect of ration treatment on total liver abscesses**

<u>Total Liver Abscess</u>		<u>A + Liver Abscess</u>
RT	19.1%	8.6b%
RTB	16.1	2.2a
RB	20.8	5.7ab
OB	19.3	5.1ab
0	27.7	7.9ab

**Table 3. Feedlot lagoon ammonia emissions (PPM)**

<u>Treatment Day</u>	<u>RT</u>	<u>RTB</u>	<u>0</u>	<u>0 B</u>
1	0	0	0	0
7	7	2	9	4
14	161	93	127	101
18	200	146	200+	167
21	200	144	189	150
24	183	126	167	104
28	22	9	47	10

**Table 4. Feedlot performance**

<u>Treatment</u>	<u>1</u> RT	<u>2</u> RT + B	<u>3</u> B
ADG (kg/d)	1.53	1.61	1.69
Consumption (kg/d)	9.9	10.0	10.2
Feed/gain	6.33	6.09	6.02

## **Does porous mean soft? The state of the art on the elastic behavior of microporous silicates**

**G. Diego Gatta**

*Università degli Studi di Milano; Milano, Italy; Email: [diego.gatta@unimi.it](mailto:diego.gatta@unimi.it)*

### **Introduction**

The physical and chemical or physiochemical properties of open-framework materials, i.e., natural and synthetic micro- and mesoporous silicates, titanates, phosphates, sulfides, and selenides, make them materials of attention for their advanced technological applications. As a consequence, their temperature-induced transformations, catalytic properties, ionic conductivity, and photoluminescent features have largely been investigated in the last decades. In contrast, the elastic properties and the pressure-induced structural modifications of microporous materials are not well known. Only a few studies have been dedicated to zeolites under pressure; in addition, the majority of them have been devoted to the fibrous zeolite group.

### **Experimental Methods**

High-pressure (HP) experiments on zeolite-A (LTA), heulandite (HEU), natrolite (NAT), scolecite (NAT), mesolite (NAT), thomsonite (THO), edingtonite (EDI), bikitaite (BIK), yugawaralite (YUG), mordenite (MOR), levyne (LEV), and analcime (ANA) have been performed by several research groups in the last few years by means of in situ single-crystal X-ray diffraction or synchrotron powder diffraction with a diamond anvil cell (DAC) and by using penetrating or non-penetrating pressure transmitting media (Table 1). All the experiments have been conducted up to  $P < 7.5$  GPa. For the experiments performed by means of single-crystal X-ray diffraction, cell parameters and intensity data were collected at different pressure values in order to determine the elastic parameters (axial and volume compressibility, unit-strain ellipsoid orientation, and magnitude) and to refine the crystal structures. However, due to the low quality of the HP data, the majority of the HP experiments performed by means of in situ synchrotron powder diffraction provided only the HP cell parameters suitable for a description of the elastic parameters.

### **Results and Discussion**

Among the aforementioned zeolites, analcime shows a first-order phase transition from cubic to triclinic symmetry between 0.9-1.0 GPa. Such a transition is not influenced by the nature of the  $P$ -medium adopted. An anomalous elastic behavior with a change in the compressional mechanism was observed for levyne between 0.6-1.0 GPa, uninfluenced by the nature of the  $P$ -medium used. In contrast, zeolite-A shows normal or anomalous compressibility and volume discontinuities at HP as a function of the  $P$ -media used. Similarly, natrolite and mesolite showed a  $P$ -induced volume expansion between 0.8-1.5 GPa through the selective sorption of water molecules from the pressure fluid (methanol:ethanol:water), giving rise to an HP over-hydrated phase. All the other zeolites did not show any phase transition within the  $P$ -ranges investigated.

In order to describe the elastic parameters of the aforementioned zeolites, the volume compressibility has been calculated using a second- or third-order Birch-Murnaghan equation of state. The bulk modulus values ( $K_{T0} = -V_0(\partial P/\partial V)_{P=0} = 1/\beta$ ;  $\beta$  is the volume compressibility coefficient) for each given zeolite are reported in Table 1. Excluding natrolite, for which only data of the HP over-hydrated phase are available, the elastic parameters of all the other zeolites reported in Table 1 have been calculated on the basis of experiments performed using non-penetrating  $P$ -media (i.e., without interference between  $P$ -medium and HP structural behavior).

The elastic data of zeolites reported so far allow us a comparative study of their isothermal behavior and structural evolution under HP conditions: a) The peculiar characteristic of the zeolite structures, with large channels and a framework that is very flexible but has rigid units (e.g., the tetrahedra), implies that the main deformation mechanisms at HP are represented through tetrahedral tilting; b) The compressibility of zeolites appears not to be directly related to the microporosity, which can be represented by the framework density (FD). For example, the bulk moduli of the isomorphic fibrous zeolites (i.e., natrolite, scolecite, and thomsonite)

are different even though their FD is similar (Table 1); c) The elastic parameters available for natural zeolites allow us to infer that microporosity does not imply necessarily high compressibility. In fact, the majority of the zeolites mentioned here appear to be less compressible than a lot of rock-forming minerals like  $\alpha$ -quartz, Na-rich feldspars, Na-rich scapolites, some di-octahedral and tri-octahedral micas, some amphiboles, and some carbonates. A high compressibility is generally expected for open-framework structures due to the tetrahedral tilting, which produces inter-tetrahedral angle variations and accommodates the effect of pressure. However, the bonding between the host zeolitic framework and the stuffed guest species (cations and H<sub>2</sub>O molecules) affect the overall compression behavior, making this class of porous material unexpectedly less compressible than other silicates.

**Table 1.** Elastic parameters of zeolites

	FD (T/1000Å <sup>3</sup> )	$K_{T0}$ (GPa)	$(\partial K_{T0}/\partial P)$	Note	Ref.
Natrolite	17.8	43(2)	4.0 (fixed)	$P > 1$ GPa	Gatta (2005)
Scolecite	17.8	54.6(6)	4.0 (fixed)		Gatta (2005)
Thomsonite	17.7	49(1)	4.0 (fixed)		Gatta (2005)
Edingtonite	16.6	59.3(4)	4.0 (fixed)	Tetragonal Orthorhombic	Gatta (2005)
		59.3(2)	4.0 (fixed)		
Heulandite	17.1	27.5(2)	4.0 (fixed)		Comodi et al. (2001)
Zeolite-A	12.9	22.1(3)	4.0 (fixed)		Arletti et al. (2003)
		19.6(6)	5.1 (3)		
Analcime	18.5	56(3)	4.0 (fixed)	$P < 1$ GPa	Gatta et al. (2006)
		19(2)	6.8 (7)	$P > 1$ GPa	
Levyne	15.2	56(4)	4.0 (fixed)	$P < 1$ GPa	Gatta et al. (2005)
		48(1)	4.0 (fixed)	$P > 1$ GPa	
Yugawaralite	18.3	34(1)	4.0 (fixed)	$P < 4$ GPa	Arletti et al. (2003)
Mordenite	17.2	41(2)	4.0 (fixed)		Gatta and Lee (2006)

## References

- Arletti, R., Ferro, O., Quartieri, S., Sani, A., Tabacchi, G. and Vezzalini, G. (2003) Structural deformation mechanisms of zeolites under pressure. *American Mineralogist*, **88**, 1416-1422.
- Comodi, P., Gatta, G.D. and Zanazzi, P.F. (2001) High-pressure structural behaviour of heulandite. *European Journal of Mineralogy*, **13**, 497-505.
- Gatta, G.D. (2005) A comparative study of fibrous zeolites under pressure. *European Journal of Mineralogy*, **17**, 411-421.
- Gatta, G.D. and Lee, Y. (2006) On the elastic behaviour of zeolite mordenite: A synchrotron powder diffraction study. *Physics and Chemistry of Minerals*, **32**, 726 – 732.
- Gatta, G.D., Comodi, P., Zanazzi, P.F. and Boffa Ballaran, T. (2005) Anomalous elastic behavior and high-pressure structural evolution of zeolite levyne. *American Mineralogist*, **90**, 645-692.
- Gatta, G.D., Nestola, F. and Boffa Ballaran, T. (2006) Elastic behavior, phase transition and pressure induced structural evolution of analcime. *American Mineralogist* (in press).



## **Atomistic simulation of adsorption, diffusion, and ion exchange in zeolites**

**E. J. Maginn**

*University of Notre Dame; Notre Dame, Indiana, USA; Email: ed@nd.edu*

This talk will provide an overview of the development and application of atomistic-level simulation methods to the study of adsorption, diffusion, and ion exchange in zeolites. Atomistic simulation of these processes has been carried out by a large number of researchers over the past twenty or more years. These simulations are typically performed using classical potential models that represent the energetic interactions between the guest species and the host lattice. The parameters for these potential models are developed in one of three ways: by fitting the model to experimental data, by using first principles quantum calculations, or by a combination of both. Once the potential model is fixed, the thermodynamics and dynamics of the guest species can be studied by generating trajectories and applying statistical thermodynamics to analyze the results. The outcome of these simulations is an extremely detailed picture of the underlying molecular processes responsible for the performance characteristics of the material.

The most common method for studying adsorption is grand canonical Monte Carlo (GCMC) simulation. In this approach, an external chemical potential of the guest species is imposed upon the fixed volume lattice, and the number of guest species sorbing in the pores is computed. This approach enables direct calculation of adsorption isotherms, isosteric heats of adsorption, and the location of the guest species within the lattice. For multi-component simulations, thermodynamic selectivity may also be determined.

The dynamics of guest species is commonly examined using a technique called molecular dynamics (MD). In MD, the guest species are treated as classical particles, and atomic positions are advanced deterministically by integrating a variant of the Newtonian equations of motion. By tracking the position of the molecules as a function of time, dynamic properties such as self-diffusivities can be computed. Thermodynamic properties may also be computed by averaging over the positions of the molecules. Because MD is inherently a short-time technique, slow dynamics that occur on timescales of more than about 50 ns are beyond the practical limits of MD. To examine these slow processes, other techniques such as transition state theory and coarse-grained models are used.

Ion exchange in zeolites has been studied much less than adsorption and diffusion. The methods to examine this process involve the use of free energy simulation techniques such as thermodynamic integration or free energy perturbation. The dynamics of ions in zeolites is typically sluggish, so special techniques are required to obtain adequate sampling. This fact, combined with the inherent difficulty of simulating ionic systems, has made ion exchange simulations hard to carry out.

Examples will be given from the literature and the speaker's own work on each of these topical areas. The simulations will be compared against experiment to assess the relative strengths and weaknesses of the approaches. Some overall recommendations and some suggestions about the future direction of atomistic modeling in this field will be given.

## **New clay barrier technology for waste sites and treatment of contaminated water outflow from waste sites through application of natural zeolites.**

**H. Minato<sup>1</sup> and T. Morimoto<sup>2</sup>**

<sup>1</sup>*The University of Tokyo & Hyogo University of Teacher Education; Tokyo, Japan; E-mail: h.minato@astec-geo.co.jp*

<sup>2</sup>*Astec Co. Ltd.; Himeji, Japan*

### **Introduction**

New clay barrier materials and application systems have been proposed in recent years for protection of disposal sites containing harmful waste materials. Artificial liner materials, such as rubber or plastic sheets and/or cement walls containing clay (for example bentonite), are usually designated according to local administrative regulations. It is frequently reported that liner materials, such as organic sheets with clay barriers, are damaged easily by decomposition or mechanically and/or chemically, thus causing severe environmental problems in the surrounding area. Damage is caused by outflow of waste waters and gases in the area. In order to avoid such environmental damage, a new clay barrier material has been developed using a mixture of natural inorganic materials. Minerals such as weathered soils, i.e., volcanic loam *Masa-Do* (Japanese for weathered soil from granitic rocks), and natural zeolites with some carbonate minerals, dolomite, calcite, and their calcined equivalents have proved to be most effective. The clay barrier, a mineral aggregate named Sealing Soil, and the mechanism of its function is explained in the following paragraph. The method has already received two Japanese patents. Outflow of polluted wastewater from the sites are treated with mineral compounds of natural zeolites (TRP). After application of TRP-zeolites, wastewater is converted into harmless effluent.

### **Experimental Methods**

70–80 wt. % of the main clay barrier material, called Viscous Mud, is composed of surface-weathered soils containing clay minerals (low-grade-crystallinity halloysite, smectite, chlorite, etc.) in addition to sandy materials (quartz, opal, feldspar, mafic minerals, etc.). In addition there are low-crystalline and amorphous materials such as allophane, hydroxides of Si, Al, Fe, and others. 5 wt. % each of the natural zeolites mordenite (ZI) and clinoptilolite (ZN) are added. Their chemical analyses are shown in Table 1. Calcined carbonate materials, i.e. dolomite and calcite, are added at a rate of 5–10 wt. %. The reaction mechanism of the barrier materials to the discharged harmful elements of waste sites are cation-exchange-reactions with zeolites, adsorption and fixation. Fixation of minor elements in newly formed hydrous aluminosilicate crystals is permanent. The thickness of the barrier wall has to be designed according to its adsorption capacity and the mechanical strength required for the waste site.

### **Results and Discussion**

There are several sites in Japan (Tokyo and Osaka area) where the safety barrier system has been applied for about ten years. At waste sites with outflows of polluted water, treatment with TRP-zeolites according to the methods explained above are being applied successfully. The technique is shown in Figure 1.

**Table 1.** Chemical analysis and cation-exchange

Specimen	ZI	ZN
SiO <sub>2</sub>	65.86 Wt.%	61.8 Wt.%
Al <sub>2</sub> O <sub>3</sub>	11.99	12.6
Fe <sub>2</sub> O <sub>3</sub>	2.24	1.86
MgO	0.29	1.02
CaO	2.53	1.67
Na <sub>2</sub> O	1.49	2.20
K <sub>2</sub> O	1.69	3.01
LOI	----	8.8
CEC meq/100g	161	148

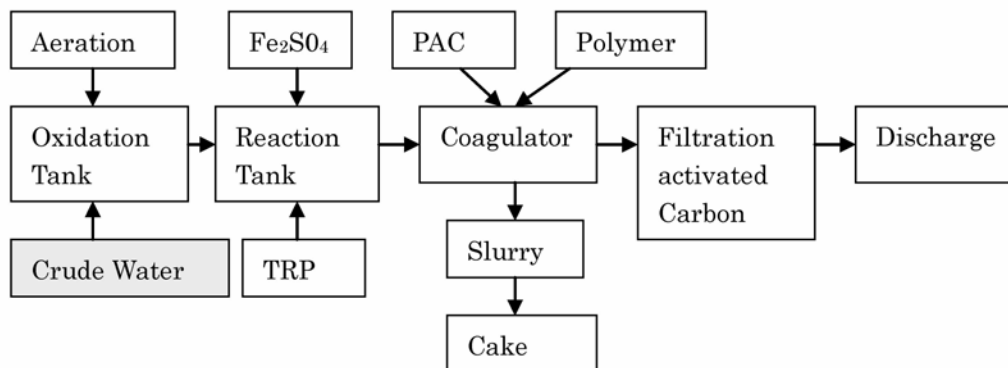


**Figure 1.** Schematic flow chart of the process for remediation of polluted water

## **Predicting adsorption and transport in zeolite thin film membranes for hydrogen separation using grand canonical Monte Carlo and molecular dynamics simulations**

**M. C. Mitchell**

*New Mexico State University; Las Cruces, New Mexico, USA; Email: martmitc@nmsu.edu*

Finding more economical and less energy-demanding ways of separating hydrogen from methane in refinery waste streams and from the output streams of steam reforming is very important. Separation of hydrogen from other gas phase species can be carried out using inorganic molecular sieve membranes made from zeolites. Computer simulations provide a cost-effective and important complement to experimental separation studies. We have used computer simulation techniques to predict adsorption and transport of a reformat mixture of hydrogen, methane, carbon dioxide, and carbon monoxide in the presence and in the absence of water in a silicalite membrane. We have also studied the effect of temperature on the separation capability. Adsorption isotherms were determined using grand canonical Monte Carlo (GCMC) simulations. Molecular dynamics (MD) simulations were also carried out for single components, binary mixtures of hydrogen/methane, hydrogen/carbon dioxide, a quaternary mixture of hydrogen/methane/carbon dioxide/carbon monoxide, and a five-species mixture including water. These simulations were used to determine self-diffusion coefficients. The results of the simulations indicate that silicalite is an effective material for separating hydrogen from other gas phase species.

## **Irradiation and thermal effects in zeolites for the sorption and release of radionuclides in the geosphere**

**L. M. Wang and R. C. Ewing**

*University of Michigan; Ann Arbor, Michigan; Email: lmwang@umich.edu*

### **Introduction**

Site restoration activities at DOE facilities and the permanent disposal of nuclear waste generated at DOE facilities involve working with and within various types and levels of radiation fields. The radiation exposure due to the release and sorption of long-lived actinides (e.g.,  $^{237}\text{Np}$ ) and fission products (e.g.,  $^{137}\text{Cs}$  and  $^{90}\text{Sr}$ ) may cause changes in important properties of geological materials along transport pathways of radionuclides through the geosphere. Through a comprehensive study of microstructure and ion exchange capacity under varying types of irradiation (electrons, ions, and neutrons), dose rate, temperature, and ion exchange conditions, we have developed a basic understanding of radiation effects on the ion exchange and retention capacity of zeolites and clays for Cs and Sr. The results provide an essential database for the long-term effectiveness of zeolites and other porous or layer structured materials in radionuclide retention, as well as the mobility of radionuclides in contaminated sites.

### **Experimental Methods**

Thermal and radiation effects on the microstructures of zeolites (analcime, natrolite and zeolite-NaY) as well as a group of other porous or layer structured materials have been investigated by X-ray diffraction (XRD) and transmission electron microscopy (TEM) after electron, ion beam, and neutron irradiations. The electron irradiation was carried out in electron microscopes with electron energies of 200, 300, and 400keV or by in situ TEM, so that microstructural evolution under irradiation could be observed continuously at various temperatures. Using this method, critical irradiation doses for complete amorphization of the zeolite structure at various temperatures has been determined. Larger amounts of partially or completely amorphized zeolite samples have also been obtained by thermal annealing at temperatures between 900–1000°C. Results from Cs and Sr ion exchange and adsorption experiments on zeolite of various degrees of amorphization have been compared to determine the effects of amorphization on the ion exchange capacity of and ion release rate from these samples. The data were finally validated with partially amorphized samples obtained by neutron irradiation conducted in the Ford Nuclear Reactor at the University of Michigan.

### **Results and Discussion**

The results have demonstrated that zeolites of various types are extremely susceptible to irradiation-induced solid-state amorphization. Amorphization can either be induced by ionization processes (as occurs with  $\beta$ - or  $\gamma$ -irradiation) or by direct displacement damage processes (as by  $\alpha$ -recoil). The critical doses for complete amorphization of these phases can be as low as  $< 0.1$  displacement per atom (dpa) or  $10^8$  Gy in ionization energy deposition (a dose equivalent to that expected in a zeolite with 10 wt.% loading of  $^{137}\text{Cs}$  in 400 years). The progressive process of amorphization of these materials under electron irradiation is clearly demonstrated by electron diffraction and by high resolution transmission electron microscopy (HRTEM) recorded during in situ TEM. The progressive amorphization process was quickly evident by the gradual fading of Bragg-diffracted beam intensities and the appearance of an amorphous halo in the electron diffraction patterns. Amorphization was considered complete when all the Bragg-diffracted beam intensities had completely disappeared at the critical amorphization dose. Bubbles or cavities were also observed in zeolite phases during the course of the radiation damage. In some of the zeolites the bubbles are believed to be filled with structural water. For different structures of zeolites, bubbles may or may not form during the course of irradiation. In natrolite, bubble formation was concurrent with the damage process, whereas in analcime, bubbles formed after the material was fully amorphized. No bubble formation was observed in NaY-zeolite. TEM observation has shown that zeolites with larger aperture size are less likely to form bubbles due to a higher release rate of structural water upon radiation.

The ion-exchange and desorption experiments of zeolite-NaY have shown that thermally amorphized zeolite-NaY lost approximately 95% of its ion exchange capacity for Cs and Sr due to the loss of exchangeable cation species and/or the blockage of access to exchangeable cation sites. Meanwhile, the rate of desorption or dissolution of Sr and Na from zeolite-NaY pre-loaded with Sr was greatly reduced after amorphization. Results with the same trend have also been obtained from the neutron-irradiated samples. The lower desorption rate of Na and Sr from the amorphized zeolite indicates that amorphization of zeolite may reduce the desorption of exchangeable cations owing to the blockage of access to structural channels. Because near-field or chemical processing materials will receive a substantial radiation dose only after they have incorporated radionuclides, these results suggest that radiation effects may in fact retard the release rate of adsorbed or ion-exchanged radionuclides. However, long-term leaching studies are needed to test the long-term stability of these amorphous phases, since amorphous phases are in general believed to be thermodynamically unstable.

# Contributed Papers





## **The oxidative dehydrogenation of C<sub>1</sub>–C<sub>2</sub> alcohols on copper-contained zeolites and HTSC**

**L. Akhalbedashvili**

*Tbilisi State University; Tbilisi, Georgia; E-mail: alkali@yahoo.com*

### **Introduction**

Previous studies have shown that the activity of initial synthetic and natural zeolites in ethanol and methanol oxidation is caused by the presence of active molecular oxygen near alcohol, adsorbed on alkali cations; however, the introduction of transition metals ions changes the character of catalytic action (Akhalbedashvili et al., 2001, 2002).

### **Experimental Methods**

In recent work, a comparison of the activity of copper-containing catalytic agents on various carriers in the conversion of C<sub>1</sub>–C<sub>2</sub> to alcohols was carried out. In particular, as a matrix, the synthetic zeolites X, Y, mordenite, ZSM-5 and natural zeolite clinoptilolite (CL) were applied; the oxidic form high-temperature superconductors (HTSC) Y<sub>1</sub>Ba<sub>2</sub>Cu<sub>3</sub>O<sub>x</sub> and Bi<sub>2</sub>Sr<sub>2</sub>CaCu<sub>3</sub>O<sub>x</sub> were also used. Zeolite catalysts were prepared by an ion-exchange method from solutions of copper-ammonia complexes and copper nitrate; HTSC samples were synthesized by the traditional ceramic technique from the corresponding metal oxides. The catalytic experiments were carried out by the microflow method with varying of temperature, the size of catalyst grain, and gas flow rate. The composition of the initial mixture and yields was analyzed chromatographically.

### **Results and Discussion**

On copper-exchanged zeolites, such as X and Y, the main products of the conversion to alcohols are CO<sub>2</sub> and H<sub>2</sub>O in the investigated temperature range. Other byproducts of the conversion—C<sub>2</sub>H<sub>4</sub>, CO, the ethoxy ethane—were not detected. It must be noted that the conditions of ion exchange (pH=5 and pH=10) has an influence on the state of copper cations. It is found that samples obtained at pH=5 are more active in a deep oxidation than samples obtained at pH=10, and CuNaY(10) exhibits major activity in a partial oxidation up to aldehyde. Practically, the complete oxidation of methanol and ethanol was observed on CuNaY(5).

The catalytic activity of initial mordenite, and especially of ZSM-5, is extremely low up to 773 K; the introduction of Cu<sup>2+</sup> in their structure and the formation of coordinative-unsaturated isolated Cu (II) ions with the symmetry of plane square result in the appearance of high activity and selectivity in deep oxidation of alcohols.

The reactions, as complete and partial oxidation, to intermolecular dehydration of methanol and ethanol up to dimethyl ether and C<sub>2</sub>H<sub>4</sub> accordingly, occurred on CuCl under 493 K. The dehydration of ethanol prevails up to 553 K, and the degree of conversion up to CH<sub>3</sub>CHO does not exceed 10% in all temperature ranges. The conversion of ethanol occurs under two parallel and consecutive paths: CH<sub>3</sub>CH<sub>2</sub>OH → C<sub>2</sub>H<sub>4</sub> → CO<sub>2</sub> (I) and CH<sub>3</sub>CH<sub>2</sub>OH → CO<sub>2</sub> (II). However, the second path prevails.

The major reaction products from HTSC in the conversion of alcohols were aldehydes, CO<sub>2</sub>, and CO. Neither ethers, nor C<sub>2</sub>H<sub>4</sub> and H<sub>2</sub>, were detected. The catalytic activity of Bi<sub>2</sub>Sr<sub>2</sub>CaCu<sub>3</sub>O<sub>x</sub> in oxidative dehydrogenation and deep oxidation was much lower than of Y<sub>1</sub>Ba<sub>2</sub>Cu<sub>3</sub>O<sub>x</sub>. It may be suggested that the observed difference in activity and in the mechanism of alcohol conversion can be caused by the structural differences between Y<sub>1</sub>Ba<sub>2</sub>Cu<sub>3</sub>O<sub>x</sub> and Bi<sub>2</sub>Sr<sub>2</sub>CaCu<sub>3</sub>O<sub>x</sub>—the difference in the number of CuO-CuO<sub>2</sub> layers per unit cell, or in the number of active centers as well as the different coordination environments of these centers and their different accessibilities to reagent molecules.

From the above data, it follows that copper-exchanged Y zeolites are characterized by the greatest total activity and selectivity. They differ by the lowest temperatures of conversion to alcohols and high oxidative ability. In an example of CuNaY samples, it is clear that not only the nature and the amount of a substituting cation, but also its state in a zeolite matrix (which, in turn, depends on conditions of heat treatment and ion exchange), substantially define a direction and depth of catalytic process. The influence of conditions of

modification on a state of a cation is proved both with our catalytic and EPR data. It is known that at pH=5, the formation of cluster structures as a result of hydrolysis using salt, is carried out with participation of OH-groups. The heat treatment causes formation of clusters of copper ions, which exchange interaction, causing the weakening of EPR-signal strength. The identical clusters, which include non-lattice oxygen, determine high catalytic activity in deep oxidation of alcohols. The mobility and reactivity of copper clusters is also incremented by additional coordination of copper ions with reagent molecules. The sample prepared at pH=10 contains the copper ions, which are coordinated with ammonia molecules at the expense of the greater coordination ability of  $\text{NH}_3$ , in comparison with OH-groups. Such complexes interfere with the formation of cluster structures. The heat treatment of this sample causes the transference of isolated copper cations on SII and SI prime sites. It is confirmed with an increase of the signal strength of isolated ions  $\text{Cu}^{2+}$ , which are more strongly interlinked to a zeolite lattice in comparison with cluster structures.  $\text{Cu}^{2+}$  ions localized in sodalite cavities in SII', under the influence of molecules of alcohol at reaction temperatures, migrate in large cavities — sites SIII and complete coordination up to octahedral at the expense of molecules of alcohol.

So, the catalytic activity of the zeolites and HTSC-materials in the reaction of the oxidative dehydrogenation of  $\text{C}_1$ - $\text{C}_2$  alcohols is determined by the presence of the identical active sites—the associates of copper ions with oxygen; for zeolites they are migratory in to the big cavities, copper ions with extra coordination by oxygen, and for superconductive cuprates they are the fixed O – Cu – O chains or  $\text{CuO}_2$  planes, which are capable of changing their coordination at a loss of oxygen.

## References

- Akhalbedashvili, L., Mskhiladze, A., Sidamonidze, Sh. (2001) In *Studies in Surface Science and Catalysis*, **135**, 231.  
Akhalbedashvili L., Maisuradze G., Mskhiladze A., Sidamonidze Sh. (2002) *2<sup>nd</sup> FEZA Conference. Book of Abstracts and Recent Research Reports*.

## **Cs<sup>+</sup> and Sr<sup>2+</sup> ion exchange properties of irradiated and chemically modified clinoptilolite**

**L. Akhalbedashvili<sup>1</sup>, N. Kekelidze<sup>1</sup>, M. Alapishvili<sup>1</sup>, G. Maisuradze<sup>1</sup>, Y. Keheyan<sup>2</sup>, and G.Yertsyan<sup>3</sup>**

<sup>1</sup>*Tbilisi State University, Georgia; Email: aklali@yahoo.com*

<sup>2</sup>*Roma State University, Italy*

<sup>3</sup>*Yerevan Institute of Physics, Armenia*

### **Introduction**

The peculiar properties of zeolites are related to their crystal structure and to the distribution of exchangeable cations in the different possible positions of the channels and cavities of the crystal lattice. Ion exchange capacity is one of the main parameters that characterizes sorption and technological properties of high-silica natural zeolites. Cation exchange on zeolites is easily carried out by treating zeolite crystals with solutions of the corresponding salts, and thus the special kind of selectivity based on the ion sieving action of entrance cavities of elementary cells can be observed. The most common natural zeolite is clinoptilolite (CL), a member of the heulandite family of zeolites. It has important applications in ion exchange, molecular sieving, and catalysis. It is well known that CL is extensively used in wastewater purification for the removal of heavy metals (Collela, 1995), toxic and radioactive elements (Breck, 1974), and especially radionuclides of cesium and strontium from low-level waste streams of nuclear power plants (Akhalbedashvili et al., 2003).

### **Experimental Methods**

The goal of the present work is to study the ion exchange sorption of cesium and strontium on a CL specimen taken from a deposit in Armenia. The experiments used various forms of CL: (i) unmodified specimen, (ii) modified by e- and  $\gamma$ -irradiation, (iii) hydronium-exchanged with hydrochloric acid, and (iv) cation-exchanged forms. The following parameters were determined: exchange capacity, E, for Sr<sup>2+</sup> and Cs<sup>+</sup>, distribution factor, K<sub>d</sub>, and sorption factor, K<sub>s</sub>. From the data, the changes in chemical potential,  $\Delta\mu$ , were calculated for cesium and strontium in the investigated systems. The corresponding values are listed in Table 1.

### **Results and Discussion**

Irradiation reduced the sorption characteristics of the samples by almost a factor of two, and weak dependence on radiation flux was observed. The exchange capacity of Sr<sup>2+</sup> on the samples irradiated with a flux from 10<sup>12</sup> up to 10<sup>14</sup> e/cm<sup>2</sup> is lower compared to the non-irradiated samples, whereas the sample irradiated with a flux of 10<sup>15</sup> e/cm<sup>2</sup> showed a small increase in exchange capacity. The exchange capacity for Cs<sup>+</sup> did not show a significant dependence on irradiation flux and the measured values were in the range of 0.419–0.430 meq/g. Irradiation with  $\gamma$ -ray (20 and 70 Mrad) also decreased the ion exchange capacity of zeolite.

It is possible to assume that the e-irradiation excites the aluminum-silicon-oxygen skeleton, increasing the electron density and promoting the formation of the peroxide ion, O<sub>2</sub><sup>2-</sup>. As a result of metastable equilibrium, the cations in zeolite regroup, which is why accessing strontium ions is difficult.

The ion exchange activity of calcium-exchanged CL differs most in relation to strontium, whose E (Sr<sup>2+</sup>) is twice the value for the unmodified zeolite and whose sorption coefficient K<sub>s</sub> reaches 100%. The calcium in the zeolite is completely exchanged with strontium in the aqueous solution.

**Table 1.** Calculated values of exchange capacity  $E$ , distribution coefficient  $K_d$  and change of standard chemical potential  $\Delta\mu^0$  for some studied samples

Sample	$\text{Cs}^+$			$\text{Sr}^{2+}$		
	$E, \text{meq}\cdot\text{g}^{-1}$	$K_d\cdot 10^2, \text{mL}\cdot\text{g}^{-1}$	$\Delta\mu, \text{kJ}\cdot\text{mol}^{-1}\cdot\text{K}^{-1}$	$E, \text{meq}\cdot\text{g}^{-1}$	$K_d\cdot 10^2, \text{mL}\cdot\text{g}^{-1}$	$\Delta\mu, \text{kJ}\cdot\text{mol}^{-1}\cdot\text{K}^{-1}$
CL(Ar)	0.50	2.71	−7.03	0.70	2.07	−8.44
CL(Ar)H	0.88	2.87	−7.24	0.72	3.04	−8.29
CL(Ar) <sup>12</sup> *	0.42	1.12	−4.31	0.36	1.74	−5.85
CL(Ar) <sup>15</sup> *	0.43	1.42	−4.66	0.38	1.13	−5.84
CL(Ar)Ba <sup>12</sup> *	0.34	2.04	−5.29	0.52	2.23	−5.44
CL(Ar)H( $\gamma$ ) **	0.26	0.89	−2.32	0.35	1.06	−1.63
CL(Ar)HCa	1.11		−12.79			−10.11

\* - e-irradiated; \*\* -  $\gamma$ -irradiated

Other results were obtained for ion exchange capacity on cesium: neither  $\gamma$ -irradiation, e-irradiation nor chemical modification influenced the ion exchange sorption of cesium. A possible explanation is that the size of  $\text{Cs}^+$  ions (radius of 0.165 nm) allows them to penetrate into the large  $\underline{A}$  channels of CL only.

The samples modified through chemical means—hydronium-exchange and calcium-exchange—are the most effective ion exchange sorbents for strontium. The complete sorption of strontium on Ca-CL is consistent with existing data that show strontium exchanges effectively with calcium and magnesium in the zeolite (about 84% of sorbed strontium), less so (~15%) with sodium, and almost not at all with potassium. The sorption process for this sample is characterized by comparing the results for the various CL forms with those for the unmodified CL and the hydronium-exchange CL.  $K_s$  for the unmodified CL(Ar) is equal to 49%, but only 26% from the sum of calcium, magnesium, sodium, and potassium cations are replaced by strontium; the rest—either physical adsorption or replacement of  $\text{H}^+$ —is less probable. It may be concluded, on the basis of calculated values of  $\Delta\mu$ , that the ion exchange process is thermodynamically more favored on samples modified by a chemical method than on samples modified by e- and especially  $\gamma$ -irradiation. The e-irradiation excites the Al-Si-O skeleton and increases the electron density so that some of the cations from narrow channels move and partly block the big, open  $\underline{A}$  channels, causing a decrease in  $\text{Sr}^{2+}$  adsorption. Our experiments show that untreated CL(Ar) and hydronium-exchanged CL(Ar)H forms are characterized by high ion exchange activity on strontium and cesium in comparison with irradiated samples; the most effective ion exchange sorbents for these ions are CL samples modified by a chemical method.

## Application of zeolite in oil refinery wastewater treatment

**A. Al-Haddad and M. Al-Salem**

*Kuwait University; Kuwait City, Kuwait; Email: hadad@kuc01.kuniv.edu.kw*

Kuwait is an oil-producing country. Two million barrels of oil are being produced daily. Seventy percent (70%) of the oil production is being treated in three refinery plants. Oil refineries are located on the gulf. Large amounts of treated wastewater are being dumped in the sea. Presently, wastewater is treated by a skimming process and an aeration ditch, followed by a dilution process. This treatment is to match KUEPA requirements shown partially in Table 1.

The purpose of the present project is to test the efficiency and viability of using natural zeolite in oil refinery wastewater treatment versus the present technology applied in this area. Two different types of natural zeolite (carbonized and ODA) from Slovakia were used to determine the impact on the water treated in refineries. Initial results from tests performed on controlled samples indicated a better quality of treatment for the removal of the dissolved hydrocarbons. The second step is to measure the performance of zeolite on real samples from the refinery.

Flow and design parameters affecting pollutants removal will be studied. Adsorption parameters will be evaluated to optimize operating conditions for pollutants removal. Tests are done using IR-Spectrometer (Perkin) and UV-Spectrometer (Phillips).

**Table 1.** A sample of KUEPA requirements for industrial wastewater from oil refineries

Parameter	Required Value
pH	6–8
Temperature	10 degrees difference
BOD5	30 mg/L
COD	2.5 mg/L
Salinity	33–42%
TSS	10 mg/L
Total Soluble Solids	1500 mg/L
Hydrocarbons	5 PPM
Cd	0.7 µg/L

## **Application of surfactant-modified zeolite for oilfield- produced water treatment: Examining regeneration and long-term stability**

**C. R. Altare<sup>1</sup>, R. S. Bowman<sup>1</sup>, E. J. Sullivan<sup>2</sup>, L. E. Katz<sup>3</sup>, and K. A. Kinney<sup>3</sup>**

<sup>1</sup>*New Mexico Tech; Socorro, New Mexico, USA; Email: caltare@nmt.edu*

<sup>2</sup>*Los Alamos National Laboratory; Los Alamos, New Mexico, USA*

<sup>3</sup>*University of Texas at Austin; Austin, Texas, USA;*

Oilfield-produced water represents a large waste stream in the United States. The majority of this water is reinjected into the subsurface, at considerable cost to producers. Surfactant-modified zeolite (SMZ) presents a low-cost, easily regenerable treatment option that can remove organic contaminants, such as benzene, toluene, ethylbenzene, and the xylenes (BTEX), from produced water. SMZ treatment coupled with additional treatment processes, such as reverse osmosis, can yield water that is suitable for surface discharge and/or beneficial use.

Previous work by Ranck et al. (2005) has shown that zeolite aggregate modified with hexadecyltrimethylammonium (HDTMA) is an effective sorptive medium for BTEX. Produced water is pumped through a packed SMZ column and BTEX is partitioned into the hydrophobic regions of the sorbed surfactant. Benzene, the most water-soluble BTEX compound, is the first to elute from the column. Once the column becomes saturated with BTEX, air is blown through the column. The volatile organic compounds desorb from the SMZ and enter the vapor phase. This vapor stream can then be directed into a vapor phase bioreactor (VPB), which degrades BTEX into innocuous compounds.

This work has two main goals, the first of which is to examine the regeneration of a BTEX-saturated SMZ column. We examine how varying the air flow rate during regeneration impacts BTEX removal. Knowledge of this process is critical for coupling the SMZ treatment system with the VPB. Four columns of virgin SMZ were fully saturated with BTEX and regenerated using different flow rates. Analysis of the effluent vapor stream shows that for each BTEX compound removal is achieved in roughly the same number of pore volumes regardless of flow rate. Figures 1 and 2 show the sorption and regeneration results, respectively, for toluene. This information can be used to aid in prediction of BTEX removal rates for different flow rates.

The second goal of our research is to examine the long-term chemical and physical stability of SMZ for produced water treatment. Two columns were packed with 14–40 mesh size SMZ, the same size used in pilot scale treatment columns. Fifty sorption and regeneration cycles were performed on each column using produced water obtained from Burlington Resources in Farmington, New Mexico. Sorption cycles were run for 100 pore volumes, enough for benzene to reach full breakthrough. In order to monitor changes in the physical properties of the SMZ, tritium tracer tests were conducted on the virgin SMZ after the 25<sup>th</sup> and 50<sup>th</sup> regeneration cycles. Additionally, measurements of column hydraulic conductivities were made after every 5<sup>th</sup> cycle using a constant-head permeameter. Chemical stability of the SMZ was monitored by noting changes in the sorptive capacity of the SMZ. After each cycle was complete, the effluent water was analyzed for HDTMA to determine surfactant washoff.

Results from these laboratory studies will be used to design field-scale produced-water treatment systems and predict their long-term performance.

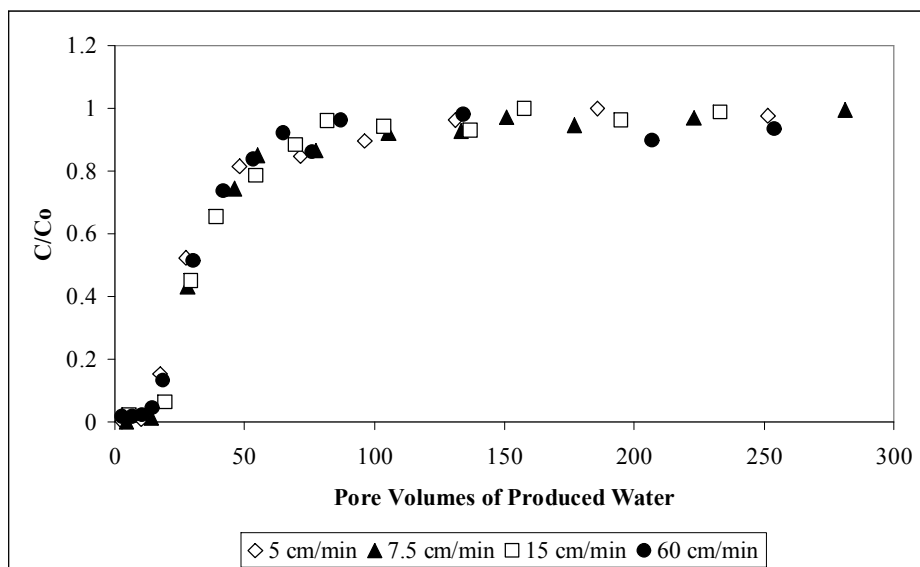


**Figure 1.** Laboratory results for toluene sorption on virgin SMZ. Sorption conditions were the same for all columns; the symbols represent the air flow rates used for subsequent regeneration shown in Figure 2.

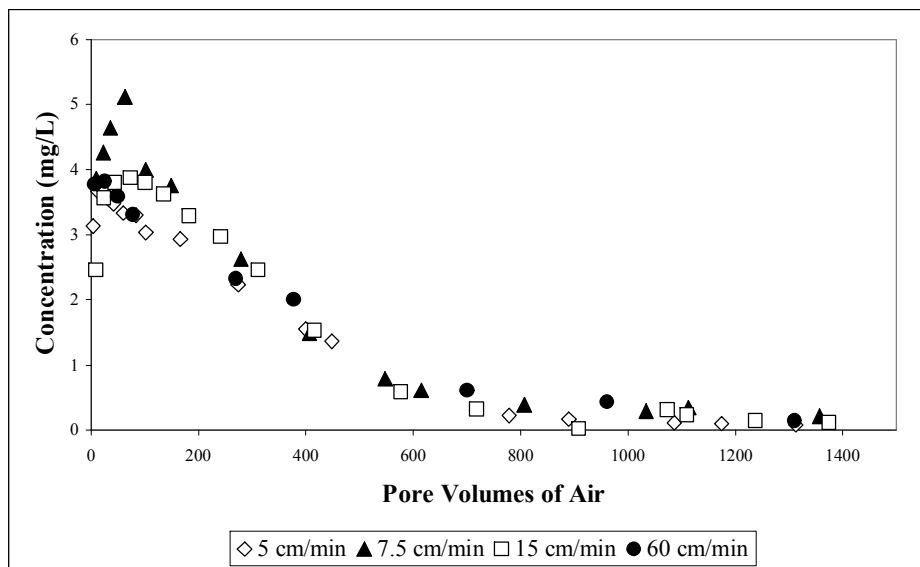


**Figure 2.** Laboratory results for toluene removal from SMZ at varying air flow rates.

## References

- Ranck, J., Bowman, R., Weeber, J., Katz, L., and Sullivan, E. (2005) BTEX removal from produced water using surfactant-modified zeolite. *Journal of Environmental Engineering*, **131**, 434-442.

## Phenol and aniline sorption from water solution by Armenian natural zeolites and their further chemical conversion

Y. Amirbekyan<sup>1</sup>, A. Isakov<sup>2</sup>, D. Hovhannisyan<sup>3</sup>, and G. Torosyan<sup>2</sup>

<sup>1</sup>Rescue Service of Ministry of Territorial Management; Yerevan, Republic of Armenia; Email: ocee@seua.am

<sup>2</sup>State Engineering University of Armenia; Yerevan, Republic of Armenia

<sup>3</sup>Yerevan University of Construction & Architecture; Yerevan, Republic of Armenia

### Introduction

In this paper, the results of research on the application of processed and synthesized zeolites as sorbents of phenol and aniline are presented.

The adsorptive activities of zeolites for the removal of phenol and aniline from tetrachloromethyl solution (CCl<sub>4</sub>) were investigated previously by Torosyan (2000). It appears that phenol removal is better on H-mordenite. We investigated the sorption possibilities of Armenian zeolites from natural deposits of sedimentary origin, which are widespread in the Idjevan (clinoptilolite) and Shirak (mordenite) regions of Armenia.

### Experimental Methods

The measurements were carried out on aqueous solutions of phenol and aniline in concentration limits from 0.1 up to 0.45 mol/L. Earlier, it was established that the sorption in these limits grows and has linear dependence on the factor of refraction in correction with the results of UV spectrum (Torosyan 2000).

All experiments were performed at room temperature. Solutions were constantly stirred for one hour. The removal of organic substances was carried out as follows: The precisely weighed portions of sorbents were added to certain volumes of organic substances in water, where the initial concentrations vary. The mix is carefully shaken up during the eighth hour. The mix is then allowed to settle. The quantity of the besieged substance on zeolites is determined by the precipitated organic fraction in the filtered solution using the methods of UV spectroscopy, highly effective liquid chromatography (HELCh), and refractometry. The amounts of sorped pollutants were calculated from the differences between the amount of pollutants added and that remaining in the final equilibrium solution.

The alkylation of sorbed phenol on zeolites with alcohols (methanol and ethanol) has been investigated. Methyl-phenols (cresols) and ethyl-phenols have important commercial use as intermediates in the chemical industry. The industrial method of ethyl-phenol synthesis is technologically combined, as the synthesis is carried out in a sulfuric acid medium. Such a strong, aggressive medium requires the use of non-corrosive, expensive equipment, and the process creates an opportunity for acid wastewater to result. Also widely applied in practice is methyl-phenyl ether, more commonly known under the name anisole. The practical application of ethyl-phenyl ether is known also as phenethol (Halgeri, 2000).

### Results and Discussion

During this study, it was found that the best adsorption of phenol was achieved on zeolites which have H-sites. The hydrogen bond is the reason for association in water solutions. Such bonding is shown during the sorption on adsorbents containing surface hydroxilic groups. Such effects take place during the adsorption of water, alcohols, amines, ammonia, and other compounds with active, mobile hydrogen on hydroxilic surfaces of alumina-silicate catalysts. Such a surface is formed in H-zeolites. Moreover, in zeolites are available to provide cations, which in turn promote phenol and aniline sorption.

Molecules of benzene cannot penetrate in a cavity of zeolites such as 5Å (a cavity makes approximately 4–5Å°), but will freely penetrate zeolites such as ZSM (a cavity makes approximately 7.5Å° and more). Adsorption of the small molecules of water depends on the sizes of the pore, and consequently is proportional to a specific surface hydroxyl group in zeolites, up to the rather thin porous silica KSK.

It is known, that sorption of hydrocarbons having p-electronic bonds—aromatic and unsaturated (alkenes)—decreases at a transition from naphthalene to benzene and alkenes. At last, the sorption of cyclanes, whose



molecules have no p-electronic bonds, becomes, first, very small, and, secondly, changes after passing an adsorptive level -azeotrope point.

On the H-surface of silica an especially strong adsorption occurs in solutions of weak adsorptive solvents whose molecules can form hydrogen bonds with hydroxyl groups:—phenols, alcohols, water, amines.

In the conversion of phenol and alcohols, carried out on zeolite at a temperature of 250–300°C, it was earlier supposed that the process takes place as an O-alkylation reaction with the formation of alkyl-phenyl ether; for example, in the case of anisole at high temperatures, will be rearranged in cresol, or as a direct high-temperature C-alkylation of benzene to phenol. The heating of anisole in alkylation reaction conditions results in the formation of p-cresol, with a low output. Heating ethyl-ether of phenol in the same conditions does not have a similar result, i.e., the formation ethyl-phenol. More than that, the O-alkylated products—alkyl-phenyl ethers—are not found. The output of C-alkylated phenol products is increased in the presence of water.

On the basis of these observations, it is possible to assume that C-alkylation takes place in the nucleus. The change of a phenol:ethanol ratio to 1:2 increases the output of alkylated products 20–22%.

Thus, the present research indicates an opportunity to adsorb phenol and aniline on natural zeolites surfaces. Thus the recycling of harmful phenolic waste can be accomplished.

## References

- Halgeri, A.B. ( 2000 ) Selective synthesis of para-ethylphenol over pore size tailored zeolite. *Applied Catalysis A*, **194-195**, 359-363.
- Sargsyan S.N., Grigoryan A.Sh., Harutjunyan S.A., and Torosyan G.H. (2000) Phenol removal from wastewater. *The Bulletin of Armenian Constructors*, **2**, 30-32.

## **Reversible conversion of tetranatrolite to paranatrolite under ambient conditions**

**G. S. Atalan and P. S. Neuhoff**

*University of Florida; Gainesville, Florida; Email: gokce@ufl.edu*

### **Introduction**

Disordered NAT topology zeolites (gonnardite, including the discredited species tetranatrolite and paranatrolite) are common rock-forming minerals in silica-undersaturated environments such as olivine-phyric metabasalts and alkaline intrusions (Ross et al., 2006, Neuhoff et al., 2002). Although it is clear that tetranatrolite collected under wet conditions from alkaline intrusions occurs as a hyperhydrated form commonly called paranatrolite that dehydrates in air to a tetranatrolite stoichiometry (e.g., Chao, 1980), the relative stabilities of these forms are unknown. Recently Lee et al. (2006) demonstrated that tetranatrolite can be reversibly converted to paranatrolite above 0.2 GPa. Here we report experimental evidence that this transition occurs reversibly under laboratory temperature and pressure conditions as a function of water vapor pressure.

### **Experimental Methods**

Tetranatrolite from Ilímaussaq, Greenland, was sampled with a hand drill and ground in an agate mortar. Three aliquots (several hundred mg each) of this sample were loaded into pre-weighed 0.5 mL Eppendorf tubes and equilibrated at room temperature over a saturated LiBr solution (5.5% relative humidity; RH) for 12 hours. Subsequently, these samples were equilibrated (for three to four hours) sequentially over a series of saturated salt solutions (LiBr, LiI, MgCl<sub>2</sub>, NaI, MgNO<sub>3</sub>, CoCl<sub>2</sub>, KI, NaNO<sub>3</sub>, NaCl, KCl, K<sub>2</sub>SO<sub>4</sub>) that buffered the water vapor pressure to relative humidities ranging from 5.5 to 95.8 % (precision better than 0.12 % RH). The mass of the sample plus Eppendorf tube was weighed after each equilibration (measurement precision  $\pm 0.05$  mg). The samples were allowed to equilibrate with the buffered atmospheres for three to four hours. After equilibration under the highest humidity conditions, the procedure was reversed to study the dehydration behavior of the sample. In addition, these aliquots were repeatedly hydrated and dehydrated by alternate equilibration over LiBr (5.5% RH) and K<sub>2</sub>SO<sub>4</sub> (95.8% RH) to test for reversibility.

### **Results and Discussion**

Figure 1 shows the variation in sample mass with relative humidity. Sample mass increases continuously with increasing humidity during the hydration process. The total mass change observed in these experiments (1.86%) is consistent with previous observations of the relative masses of tetranatrolite and paranatrolite (e.g., Chao, 1980). With decreasing humidity the sample loses water continuously, resulting in the initial mass of tetranatrolite at low humidity (5.5 %). Sample masses observed during dehydration are generally higher than those achieved during hydration. This hysteretic behavior is reversible, but may in part be due to kinetic effects. The total mass change between 5.5 and 95.8 % RH was reversed several times, indicating that the overall reaction is reversible. The topology of the curve in Figure 1 is not consistent with a Langmuir isotherm or an ideal site-mixing model for this reaction, suggesting non-ideal properties of mixing between tetranatrolite and paranatrolite.

The results of this study are consistent with the occurrence of paranatrolite in miaralitic cavities and pegmatite dykes at pressures and temperatures existing at Earth's surface. This observation is seemingly in conflict with the experimental results of Lee et al., (2006) that indicate stabilization of paranatrolite above 0.2 GPa. This discrepancy might be explained by low activities of water in the alcohol-water pressure medium employed by Lee et al., (2006).

Hydration under ambient temperature and pressure conditions over the range of water vapor pressures shown in Figure 1 implies a small Gibbs energy change for the dehydration of paranatrolite to tetranatrolite of  $\sim 1$ -2 kJ/mol H<sub>2</sub>O. This behavior is similar to that of the W1 water site in laumontite (Fridriksson et al., 2003). As with laumontite, paranatrolite probably forms initially as tetranatrolite in situ and undergoes retrograde hyperhydration during cooling.

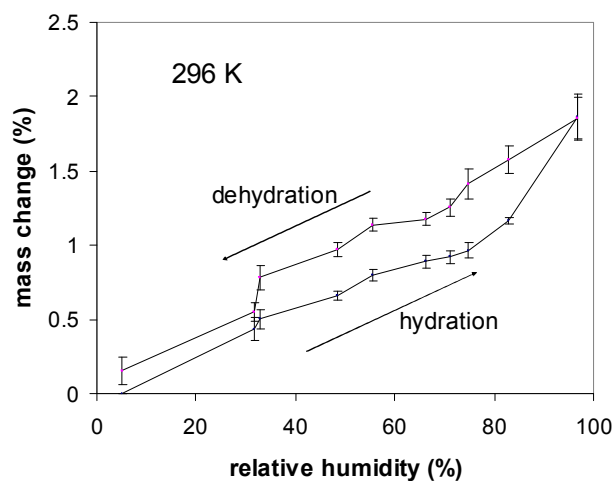


**Figure 1.** Mass change of Ilímaussaq tetranatrolite relative to the sample mass at 5.5% relative humidity as a function of % humidity at 296 K. Individual data points are the average of three observations, with error bars denoting one standard deviation.

## References

- Chao, G.Y. (1980) Paranatrolite, a New Zeolite from Mont St. Hilaire, Québec. *Canadian Mineralogist*, **18**, 8588.
- Fridriksson T., Carey W., Bish D.L., Bird D.K. (2003) Hydrogen-bonded water in laumontite II: Experimental determination of site-specific thermodynamic properties of hydration of the W1 and W5 sites. *American Mineralogist*, **88**, 1060-1072.
- Lee, Y., Hriljac, J.A., Parise, J.B. (2006) Pressure-induced hydration in zeolite tetranatrolite. *American Mineralogist*, **91**, 247-251.
- Neuhoff, P.S., Kroeker, S., Du, L.S. (2002) Order/disorder in natrolite group zeolites: A  $^{29}\text{Si}$  and  $^{27}\text{Al}$  MAS NMR study. *American Mineralogist*, **87**, 1307-1320.
- Ross, M., Flohr, M.J.K., and Ross, D.R. (1992) Crystalline solution series and order-disorder within the natrolite mineral group. *American Mineralogist*, **77**, 685-703.

## **Competitive adsorption of priority trace elements by surfactant-modified zeolite and its potential application to remediate hazardous leachable elements from fly ash**

**S. Bhattacharyya, R. J. Donahoe, and E. Y. Graham**

*University of Alabama; Tuscaloosa, Alabama, USA; Email: bhatt001@bama.ua.edu*

Fly ash contains hazardous leachable oxyanions of arsenic, boron, chromium, molybdenum, selenium, and vanadium. These element species are negatively charged and are generally mobile in the environment. Conventional treatment processes are ineffective in the removal of these anionic species from the environment. Fly ash also contains high concentrations of leachable cations such as nickel and strontium. Large amounts of fly ash are produced in the US from coal-fired electric power plants and disposed in surface impoundments and landfills. Due to the volume of fly ash produced and its leachable trace element content, the potential release of these toxic elements into the environment due to leaching is of concern. Simple and effective treatment processes are necessary to generate a coal combustion byproduct residue that is stable and to remediate existing ash disposal facilities.

Studies have shown that the use of surfactant-modified zeolite (SMZ) in permeable reactive barriers (PRBs) appears to offer unique advantages over conventional treatment processes in the removal of anionic metals from solution. Zeolites are hydrated aluminosilicate minerals characterized by cage-like structures, high internal and external surface areas, and high cation exchange capacities. Natural zeolites have a high affinity for cationic metals, but have little affinity for oxyanions. However, it has been shown that treatment of natural zeolites with surfactants such as hexadecyltrimethylammonium (HDTMA) enable them to sorb oxyanions. Clinoptilolite, a natural zeolite, is ideal for this purpose due to its low cost and high abundance in the US.

The objective of this study is to evaluate the competitive adsorption of toxic priority elements arsenic, boron, chromium, molybdenum, nickel, selenium, strontium, and vanadium from synthetic ash leachate solutions by SMZ. The results of these adsorption experiments will enable us to evaluate the potential use of SMZ as a permeable reactive barrier material installed at closed fly ash disposal facilities to intercept trace element leachate plumes or as an additive to ash slurries piped from the power plant to the disposal pond. Preliminary batch adsorption experiment data show that SMZ effectively removes oxyanions of chromium, molybdenum, and vanadium from the solution, but fails to remove oxyanions of arsenic, boron, and selenium. Unmodified zeolite is more effective in removing the cations of nickel and strontium from solution than is surfactant-modified zeolite.

## **Spectroscopic study of the formation of hydroxyl groups during dehydration of natural zeolites**

**D. L. Bish<sup>1</sup>, R. Milliken<sup>2</sup>, and C. T. Johnston<sup>3</sup>**

<sup>1</sup>*Indiana University; Bloomington, Indiana; USA; Email: bish@indiana.edu*

<sup>2</sup>*Brown University; Providence, Rhode Island; USA*

<sup>3</sup>*Purdue University; West Lafayette, Indiana; USA*

Many crystal structural and adsorption experiments on natural zeolites provide evidence of irreversible structural changes accompanying dehydration. Rinne (1923) first showed the existence of heulandite B, which forms after heating heulandite to 350°C, and Alberti and Vezzalini (1983) later demonstrated that this structural transition resulted from statistical breakage of T-O-T bridges. Some have speculated that Al-O-Si bridges are broken by H atoms, locally creating an OH group. To determine whether OH groups were formed during thermally induced structural transitions in barrerite (stilbite-type framework), Alberti et al. (1983) measured near-infrared diffuse reflectance spectra on several heated specimens. Their spectra verified the existence of OH groups in heat-collapsed phases, consistent with an OH tetrahedral vertex resulting from the breakage of tetrahedral oxygen bridges. In addition, H<sub>2</sub>O adsorption studies on some natural zeolites show evidence for irreversible dehydration occurring, for example, above ~300°C in chabazite (Fialips et al., 2005). In contrast, adsorption studies on clinoptilolite (e.g., Carey and Bish, 1996) showed no evidence of irreversibility, even at the highest temperatures of measurement (248°C).

We conducted in situ (to 200°C) transmission and ex situ (to 850°C) diffuse reflectance infrared spectroscopic measurements of clinoptilolite, heulandite, chabazite, and mordenite to study the structural changes taking place on heating. In situ measurements used thin deposits on IR-transparent windows in a tubular furnace, and ex situ measurements were done in a dry-air atmosphere on samples that had been heated externally. These experiments were well suited to detect the formation of structural OH groups in the tetrahedral frameworks. Clinoptilolite and heulandite showed a 2.2 µm metal-OH band (likely Al-O-H) in diffuse reflectance spectra after heating to ~250°C (400°C for chabazite), and this band increased at higher temperatures (Fig. 1). This band was much stronger in heulandite spectra than in clinoptilolite and chabazite spectra, consistent with the lower thermal stability of heulandite. An OH band near 2.7–2.75 µm was also visible once the samples became partially dehydrated. Reflectance spectra for clinoptilolite, heulandite, and chabazite also showed a “crossover” or change in slope near 3.3–3.6 µm from 300–600°C, which may represent the occurrence of a structural change related to the formation of the metal-OH bonds. Spectra of these three minerals were qualitatively distinct, with chabazite showing a much more pronounced band near 2.7–2.75 µm than clinoptilolite or heulandite. The mordenite sample did not exhibit this behavior and the spectra did not show any metal-OH bands to the highest experimental temperature of 900°C. These spectra are consistent with the formation of OH groups in chabazite, heulandite, and clinoptilolite at relatively low temperatures during dehydration, probably associated with disruption of the tetrahedral framework.

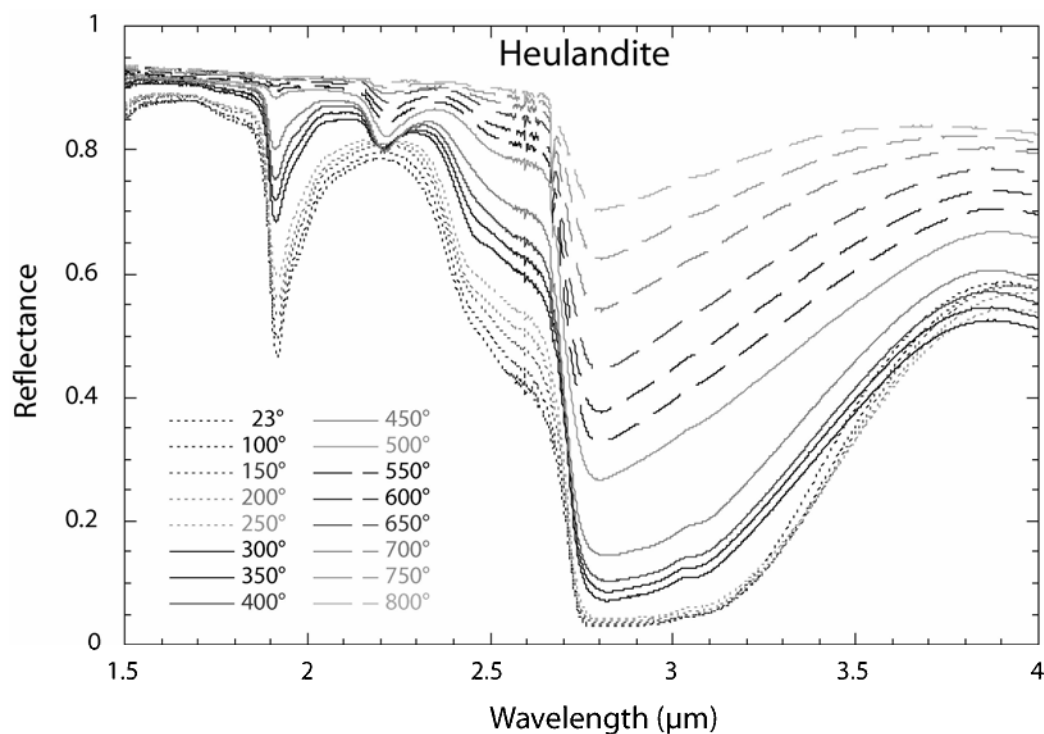


**Figure 1.** Diffuse-reflectance spectra of heulandite heated from 23°C to 800°C

## References

- Alberti, A. and Vezzalini, G. (1983) The thermal behaviour of heulandites: A structural study of the dehydration of Nadap heulandite. *Tschermaks Min. Petr. Mitt.*, **31**, 259–270.
- Alberti, A., Cariatì, F., Erre, L., Piu, P., and Vezzalini, G. (1983) Spectroscopic investigation on the presence of OH in natural barrerite and in its collapsed phases. *Physics and Chemistry of Minerals*, **9**, 189–191.
- Carey, J.W. and Bish, D.L. (1996) Equilibrium in the clinoptilolite-H<sub>2</sub>O system. *American Mineralogist*, **81**, 952–962.
- Fialips, C.I., Carey, J.W., and Bish, D.L. (2005) Hydration-dehydration behavior and thermodynamics of chabazite. *Geochimica et Cosmochimica Acta*, **69**, 2293–2308.
- Rinne, F. (1923) Bemerkungen und röntgenographische Erfahrungen über die Umgestaltung und den Zerfall von Kristallstrukturen. *Zeitschrift für Kristallographie*, **59**, 230–248.

## **St. Cloud zeolite, a working model of sustainability**

**J. Bokich**

*St. Cloud Mining Company; Truth or Consequences, New Mexico; Email: [jbokich@stcloudzeolite.com](mailto:jbokich@stcloudzeolite.com)*

St. Cloud Mining Company was born from a silver mining operation in central New Mexico, USA, in the early 1980's. When silver prices fell in the early 1990's, the company metamorphosed into an industrial minerals operation, utilizing much of the equipment and personnel that had been employed for the precious metals operations. During the establishment and evolution of the company, it continued to be one of the largest providers of non-government employment in Sierra County, New Mexico, sustaining not only direct jobs but the resulting tax benefits and support to local infrastructure.

In addition, continued research and development has continually grown the uses of St. Cloud zeolite, many of which contribute to increased sustainability through agricultural, industrial and environmental applications.

St. Cloud Mining Company began an underground silver mining and flotation processing operation in 1981 in Sierra County, New Mexico, near the present day St. Cloud zeolite operation. Sierra County was listed as the 15th poorest county in the United States in 2005.

Silver mining at St. Cloud ended in 1993, and the company converted to a surface mining and processing operation for clinoptilolite zeolite from a deposit located about 1.5 miles east of the silver processing plant.

Conversion from an underground silver mining and processing operation to an industrial minerals operation, mining and processing clinoptilolite zeolite, allowed the continuation of employment of local residents, sustaining employment and tax benefits and support to local infrastructure. St. Cloud retrained underground silver miners to conduct surface mining operations of the zeolite deposit, and retained the crushing circuit of the silver flotation processing plant, added drying and tertiary crushing and screening facilities as well as zeolite packaging and shipping facilities.

Through this metamorphosis to an industrial minerals operation, the company increased sustainability to Sierra County through the development of long-term economic resources that would have otherwise vanished with declining silver prices by the early 1990s.

In addition, continued development of new technologies and applications of St. Cloud zeolite has led to increasingly sustainable practices in agricultural, industrial and environmental applications. Use of zeolite as soil amendments has increased water retention and conservation and decreased nitrogen leaching into ground water systems, improving sustainable agricultural practices.

St. Cloud zeolite is also utilized as an animal feed supplement, reducing ammonia emissions to air and water resources while increasing the fertilizer value of manure, also consistent with sustainable agricultural practices.

Water and air filtration, paint, adhesives and household environmental applications all benefit sustainability of systems, functionally, environmentally and economically helping to conserve and protect resources that are increasingly limited or in demand.

## **Relationship between total and external cation exchange capacities of zeolites from the western United States**

**R. S. Bowman**

*New Mexico Tech; Socorro, New Mexico, USA; Email: bowman@nmt.edu*

Natural zeolites are characterized by high cation exchange capacities (CECs) and high specific surface areas. Most of the CEC and surface area is associated with Ångstrom-sized channels within the zeolite crystal structure. This internal surface area and internal CEC are accessible only to small molecules and ions such as water, Na<sup>+</sup>, or NH<sub>4</sub><sup>+</sup>. A fraction of the total CEC is associated with the external surfaces of zeolite crystals and is in theory accessible to all molecules and ions regardless of size. The external cation exchange capacity (ECEC) is thus an important zeolite characteristic, for it controls the reactivity of zeolites with many solution species. In addition, the ECEC is the most kinetically active portion of the exchange complex since access is less limited by diffusion.

In this study we determined the sorption of hexadecyltrimethylammonium (HDTMA<sup>+</sup>), a large organic cation, by 11 different natural clinoptilolite samples from the western United States. The HDTMA<sup>+</sup> is too large to enter the zeolitic channels, and its sorption provides an estimate of the ECEC. For each clinoptilolite the HDTMA<sup>+</sup> sorption was well described by the Langmuir isotherm equation and showed a clear sorption maximum (Fig. 1).

$$S = \frac{K_L S_m C}{1 + K_L C} \quad (1)$$

where  $S$  is the HDTMA<sup>+</sup> sorbed on the zeolite at equilibrium (mmol/kg),  $C$  is the equilibrium HDTMA<sup>+</sup> solution concentration (mmol/L),  $S_m$  is the sorption capacity or sorption maximum (mmol/kg), and  $K_L$  is the sorption intensity or Langmuir coefficient (L/mmol).

The HDTMA<sup>+</sup> sorption maxima for the 11 zeolites ranged from 58 to 266 mmol/kg, while the total cation exchange capacities ranged from 1200 to 2000 mmol/kg. There was no clear relationship between the magnitude of a sample's HDTMA<sup>+</sup> sorption maximum and its total CEC. The HDTMA<sup>+</sup> sorption maximum and the ECEC appear to be controlled by clinoptilolite crystal size, aggregate size, and aggregate porosity, rather than by the total CEC.



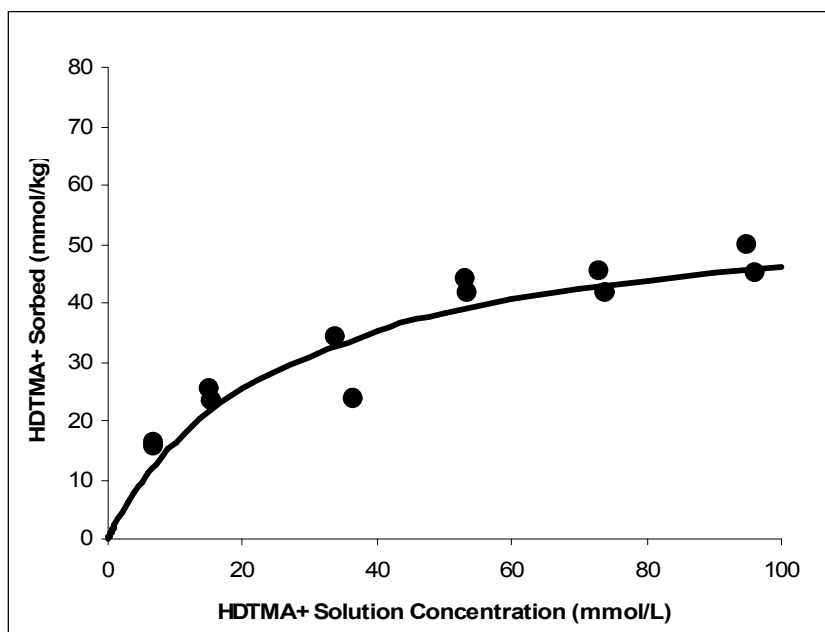


**Figure 1.** Sorption of HDTMA<sup>+</sup> by Mud Hills clinoptilolite (Barstow, California USA)

## Properties of zeolitized tuff/organic matter aggregates relevant for their use in pedotechnique. II: Thermal and microstructural characterization

A. Buondonno<sup>1</sup>, A. Colella<sup>2</sup>, E. Coppola<sup>3</sup>, B. de'Gennaro<sup>4</sup>, A. Langella<sup>5</sup>, A. Letizia<sup>3</sup>, and C. Colella<sup>4</sup>

<sup>1</sup> CRA-Istituto Sperimentale Agronomico; Bari, Italy; E-mail: andrea.buondonno@entecra.it

<sup>2</sup> Università di Napoli Federico II; Napoli, Italy

<sup>3</sup> Seconda Università degli Studi di Napoli, Caserta; Italy

<sup>4</sup> Università di Napoli Federico II; Napoli, Italy

<sup>5</sup> Università del Sannio; Benevento, Italy

### Introduction

Pedotechnique is an innovative branch of soil science, defined as “the design and realization of very specific soil (and substrate) volumes and profiles through very intensive use of advanced technology and very intensive soil manipulation” (Koolen and Rossignol, 1998). With this benchmark, a research program was started that was aimed at evaluating the possible use of organo-zeolite mixtures in pedotechnical strategies for soil restoration. In particular, the ability of natural zeolites in reacting with organic matter to form ped-like stable aggregates is under investigation.

Previous investigations (Buondonno et al., 2002) showed that organo-zeolite mixtures can evolve towards reorganized systems that are stable against spontaneous air-oxidation. Further studies (Bucci et al., 2005) showed that the interaction in an alkaline media between a zeolitized tuff, viz. Neapolitan Yellow Tuff (NYT), Ca ions, and tannic acid (AT), a polyphenol representative of low-molecular weight humic substances, led to the formation of aggregates that were resistant to chemical degradative treatments. Furthermore, both infrared and radiometry spectra clearly indicated that solid mineral (NYT), soluble species (Ca ions), and colloidal organic phases (AT) intimately interacted involving chemical and physical-chemical reactions.

This paper presents a closer examination of the thermal and structural properties of NYT-Ca-AT aggregates.

### Experimental Methods

Starting materials were: i) NYT, with the following chemical composition (wt %): SiO<sub>2</sub> = 52.15, Al<sub>2</sub>O<sub>3</sub> = 18.56, Fe<sub>2</sub>O<sub>3</sub> = 0.20, MgO = 0.20, CaO = 2.35, K<sub>2</sub>O = 7.54, Na<sub>2</sub>O = 3.30, P<sub>2</sub>O<sub>5</sub> = 0.11, and H<sub>2</sub>O = 15.73; cation exchange capacity (CEC) = 2.12 meq g<sup>-1</sup>; zeolite content = 58%, with phillipsite = 44%, chabazite = 4%, and analcime = 10% (10% of smectite was also present); ii) AT, C<sub>76</sub>H<sub>52</sub>O<sub>46</sub>; and iii) Ca, 0.5 M Ca(OH)<sub>2</sub> suspension.

Three aggregate models, with different NYT/AT weight ratios, i.e., 0.5, 1, or 2 w/w, but with a constant Ca/AT molar ratios, i.e., 3.2 mol/mol to obtain a neutral-subalkaline reaction environment (7.2 ≤ pH ≤ 7.5), were prepared. Such models will be referred to as NYT-Ca-AT5, NYT-Ca-AT10, and NYT-Ca-AT20, respectively. Reference models made by single or coupled starting materials were also prepared. Aggregates and reference models were characterized by XRD, SEM, thermal analysis, and porosimetry. The degree of polymerization of the organic component in the aggregates was estimated on the basis of the E4/E6 index. This was calculated as the ratio between the absorbance of water-extracts read at 465 nm and 620 nm.

### Results and Discussion

XRD patterns and SEM observations revealed the following: i) the absence of perceptible alteration of mineral phases, crystalline or noncrystalline, ii) the formation of secondary calcitic phases in Ca and NYT-Ca models, and iii) the possible inhibition of calcite crystallization in the presence of AT. Table 1 shows the distribution and variability of endothermic or exothermic DTA peaks of reference models and ternary aggregates. The observed and the expected weight losses are also reported.

**Table 1.** DTA endothermic or exothermic peaks (°C), and observed weight loss (owl) by TG or expected weight loss (ewl) weight loss (%) of reference models and standard aggregates.

Sample	DTA-exothermic	DTA-endothermic	TG-owl	TG-ewl	ews-owl
NYT		110°, 230°, 710°	10.4		
AT	330°, 550°	130°	94.0		
Ca		495°, 890°	42.0		
NYT-AT	340°, 645°	130°	44.2	52.2	8.0
AT-Ca	280°	140°, 670°, 840°, 910°	70.8	85.6	14.8
NYT-Ca-AT5	360°, 480°	130°, 310°, 720°	29.2	38.5	9.3
NYT-Ca-AT10	340°, 645°	130°, 760°	47.0	51.3	4.3
NYT-Ca-AT20	350°, 830°	140°, 310°	61.0	63.4	2.4

It is quite evident that in ternary aggregates the second exothermic peaks shift towards higher temperatures according to the organic matter content. Furthermore, for the same samples, the observed weight loss is always lower than the expected value, and the difference ewl-owl increases as the AT content decreases. It has also been ascertained that the degree of polymerization of the organic component is inversely dependent on its proportion in aggregates. Porosimetry measurements are still in progress.

On the whole, the present results strengthen previous findings that showed intimate interaction occurred between zeolitized materials and organic matter, especially in models with the lowest organic matter/tuff ratio, thus leading to the formation of stable aggregates. From this standpoint, such kinds of interactions resemble a fundamental process in early-stage pedogenesis, and they support the concept of the suitability of natural zeolitized materials in pedotechnical activities for soil rebuilding.

## References

- Buondonno, A., Coppola, E., Bucci, M., Battaglia G., Colella A., Langella, A. and Colella, C. (2002) Zeolitized tuffs as pedogenic substrate for soil re-building. Early evolution of zeolite/organic matter proto-horizons. *Studies in Surface Science and Catalysis*, **142**, 1751-1758.
- Bucci, M., Buondonno, A., Colella, C., Coppola, E., Leone, A.P., and Mammucari, M. (2005). Properties of zeolitized tuff/organic matter aggregates relevant for their use in pedotechnique. I: Chemical and physical-chemical properties. *Studies in Surface Science and Catalysis*, **155**, 103-116.
- Koolen, A.J. and Rossignol, J.P. (1998) Construction and use of artificial soils. *Soil Tillage Res.*, **47**, 151-155.

## Occurrence and utilization of mordenite-clinoptilolite deposits in lacustrine tuffs, Ngakuru, Taupo Volcanic Zone, New Zealand

R. L. Brathwaite<sup>1</sup> and D. Hill<sup>2</sup>

<sup>1</sup>GNS Science; Lower Hutt, New Zealand; Email: b.brathwaite@gns.cri.nz

<sup>2</sup>Blue Pacific Minerals; Matamata, New Zealand

Zeolites (mordenite, clinoptilolite, laumontite, and wairakite) have been known since the 1950s-1960s in the lower temperature parts of geothermal systems, such as Wairakei in the Taupo Volcanic Zone (TVZ). More recently, extensive mordenite-clinoptilolite deposits have been discovered within late Quaternary lake sediments in the Ngakuru area in the TVZ. The first deposit was found in 1992 at Mangatete Road, and commercial production followed soon after. Other zeolite deposits were subsequently discovered by Blue Pacific Minerals, who currently quarry and process zeolites from the Mangatete and Twist Road deposits.

The Ngakuru area lies within a NE-trending belt of active extension on the western side of the TVZ. The TVZ contains calc-alkaline volcanic rocks less than 2 Myr old, with voluminous tephra, ignimbrites, and rhyolites, and minor dacite and andesite lavas. Within the TVZ there are extensive lake sediments, as indicated from the occurrence of diatomaceous silts, pumice sands, and tuffs over an area of 110 by 40 km, including the Ngakuru area. The TVZ is a region of elevated heat flow through thin crust (15 km) intruded by magma. Much of the heat flow is manifested by high-temperature geothermal fields, including a small geothermal field at Horohoro in the northern part of the Ngakuru area.

Most of the Ngakuru area is underlain by the Ohakuri Ignimbrite, mainly consisting of non-welded pumice lapilli tuff dated by <sup>40</sup>Ar–<sup>39</sup>Ar at c. 240 ka. Several domes of the Kapenga Rhyolites, dated by <sup>40</sup>Ar–<sup>39</sup>Ar at c. 145 ka, crop out in the north of the area. The Ohakuri Ignimbrite is overlain by the Ngakuru Formation, a 100–300 m-thick sequence of lake sediments containing vitric tuff, pumiceous tuff, silts, diatomite, and pumice sands. The Ngakuru Formation is overlain by the c. 64 ka Earthquake Flat Pyroclastics and alluvial sands and gravels of the Hinurera Formation, which are overlain by tephra (< 24 ka).

Vitric tuff beds in the Ngakuru Formation are the main host rocks for the zeolite deposits, some of which are localized adjacent to faults. Individual zeolite deposits contain 50–80% zeolite over thicknesses of up to 45 m in thinly stratified vitric tuffs. The zeolitic tuffs are white, with iron staining along joints.

The primary components in the tuffs are glass shards, with minor pumice clasts and volcanic plagioclase, quartz, and biotite crystals. Glass shards in the vitric tuffs are replaced by zeolite minerals which, from X-ray diffraction analysis, consist of up to 80% mordenite ± clinoptilolite (Brathwaite, 2003). Mordenite occurs as a mesh of crystals replacing glass shards, and as thin fibres coating platy crystals of clinoptilolite. Mordenite dominates over clinoptilolite in the lower part of the vitric tuff sequence. Amorphous silica (opal-A), opal-CT, and K-feldspar are also present as secondary minerals. The zeolites and other minerals are very fine grained (<10 µm), with open meshes of crystals that result in low densities (0.66–1.12 g/cm<sup>3</sup>) and high porosities (52–70%) in mordenite-rich tuffs. Zeolitic tuff samples typically have cation exchange capacities of 80–110 meq/100 g and internal surface areas of 25–58 m<sup>2</sup>/g, which combine to give high liquid and odour absorption capacities (Mowatt, 2002). Mordenite and clinoptilolite, accompanied by K-feldspar, opal-A, and opal-CT, occur in lesser amounts in the adjacent underlying ignimbrite. Chemically the vitric tuffs are of rhyolitic composition (Brathwaite, 2003).

The presence of sinter, hydrothermal eruption breccia, and/or silicified fault breccia in the vicinity of the zeolite deposits suggests that they are associated with geothermal activity similar to active geothermal systems in the TVZ, such as Wairakei where mordenite and clinoptilolite formed at temperatures of 60–160°C. The main fluid type at Wairakei is a dilute alkali-chloride water of near neutral pH. By analogy, mordenite and clinoptilolite in the Ngakuru deposits probably formed at similar temperatures as a result of interaction of alkali-chloride water, diluted with ground or lake water, with glass in the vitric tuffs (Brathwaite, 2003).

Following acquisition of the Mangatete quarry and an associated processing plant in 1998, Blue Pacific Minerals has expanded their operations and made significant improvements to the processing plant. Additional occurrences of zeolitic tuffs, including the Twist Road deposit, were discovered by Blue Pacific Minerals. A quarry and covered drying pad have been developed at Twist Road. The quarries are worked by benching with

hydraulic excavators on a campaign basis, mainly in the summer to facilitate drying of the zeolitic tuff. The raw material is crushed and screened on site and placed in stockpiles ( $\sim 40\,000\text{ m}^3$ ) for drying in the open air, or on the covered  $5000\text{ m}^2$  drying pad during wet months, before carting to the secondary processing plant at Tokoroa, 25 km away. Secondary processing involves gas-fired kiln drying of the zeolite followed by a crushing and screening to produce a range of products of different particle size ranges and densities. Further processing by nutrient loading onto granular zeolite for the animal feed and fertilizer industries is carried out at Blue Pacific Minerals Waharoa facility, 105 km north of Ngakuru (Hill, 2005).

The high cation exchange and open pore structure with high internal surface areas of the Ngakuru zeolite make it very effective in applications such as ammonium removal from waste water, and in animal feeds and fertilizers by providing an ideal host for loading with beneficial organic or inorganic liquids. The same characteristics provide for an extremely efficient mechanism for the absorption of liquids and odours (predominantly ammonia) for the pet-litter and oil-spill markets. The sports-turf market also makes use of these two main attributes, but also requires a material that is resilient to mechanical breakdown to allow it to be blended with sand. The Twist Road deposit provides these characteristics, and several recently constructed major sports stadiums include  $\sim 8\%$  zeolite in the turf root zone to aid nutrient and moisture retention.

## References

- Brathwaite, R.L. (2003) Geological and mineralogical characterization of zeolites in lacustrine tuffs, Ngakuru, Taupo Volcanic Zone, New Zealand. *Clays and Clay Minerals*, **51**, 589-598.
- Hill, D. (2005) Australasian zeolites clean up. *Industrial Minerals*, March 2005: 50-53.
- Mowatt, C. (2002) An overview of the characteristics and potential uses for the Ngakuru zeolites. In: Misaelides, P. (ed.) *Zeolite '02, 6<sup>th</sup> International Conference on the Occurrence, Properties and Utilization of Natural Zeolites*, Thessaloniki, Greece, pp. 247-248.

## Copper removal from aqueous solutions using clinoptilolite in fixed-bed reactors

V. Çağın, N. Moralı, and İ. İmamoğlu

Middle East Technical University; Ankara, Turkey; Email: vcagin@metu.edu.tr

### Introduction

Natural zeolites, particularly clinoptilolite, have relatively innocuous exchangeable ions in their structure and exhibit high selectivity for certain cations. Therefore, in recent years, clinoptilolite has gained significant interest as a low-cost ion-exchanger in studies examining removal of heavy metal cations from wastewaters. The objective of the current investigation was to 1) examine the potential of Turkish clinoptilolite (from Bigadiç reserve) to remove copper from aqueous solutions, and 2) determine the prevailing mechanisms in an upflow fixed-bed column arrangement.

### Experimental Methods

Scanning electron microscopy/energy dispersive spectroscopy (SEM/EDS) and X-ray diffraction (XRD) were used to analyze the chemical and mineralogical composition of the clinoptilolite samples respectively. Glass columns with internal diameter of 2.5 cm and bed height of 26.5 cm were used in the experiments.

Prior to the exhaustion studies, samples were pretreated in two steps. Firstly, samples were rinsed with deionized water several times until a clear supernatant was achieved, and rinsed samples were dried for 24 hours at 105<sup>0</sup> C. This way, fine particles from clinoptilolite grains were removed to avoid clogging during operation (Abadzic and Ryan, 2001). Secondly, samples were conditioned with 1 M NaCl at 2 BV/h for 20 hours. Conditioning of the samples would enhance the ion exchange capacity of the material, and NaCl was selected as the pretreatment agent since sodium ions are the most weakly bound ions on clinoptilolite and thus are the most easily exchanged with other cations (Inglezakis, 2005).

Following pretreatment, fixed beds of clinoptilolite having 0.833–1.180 mm particle size were exhausted with 2, 4, and 8 BV/h of 200 mg Cu<sup>2+</sup>/L to determine the effect of different flow rates on copper removal capacity. Additionally, the effect of particle size was examined using 1.180–1.400 mm clinoptilolite at 4 BV/h. For all test runs, pH and temperature of the feed solution were kept at 5±0.1 and 29±2 °C, respectively.

Samples were collected at the exit of the column at various time intervals and analyzed for concentrations of Cu(II), Mg(II), Ca(II), Na(I), K(I), and Si(IV). The pH and temperature also were measured. All runs were carried out in duplicate.

### Results and discussion

XRD analysis revealed the Bigadiç sample to be approximately 50% clinoptilolite, with quartz, illite, and biotite as the main impurities. The chemical composition of raw material is (in %wt) SiO<sub>2</sub>—78.31, Al<sub>2</sub>O<sub>3</sub>—11.44, Fe<sub>2</sub>O<sub>3</sub>—1.93, Na<sub>2</sub>O—0.26, K<sub>2</sub>O—3.37, CaO—4.23, and MgO—0.48. After pretreatment, the chemical composition was changed as follows: SiO<sub>2</sub>—76.37, Al<sub>2</sub>O<sub>3</sub>—12.68, Fe<sub>2</sub>O<sub>3</sub>—1.64, Na<sub>2</sub>O—3.09, K<sub>2</sub>O—2.90, CaO—2.20, and MgO—1.13. SEM/EDS results indicate that the sodium content increased considerably (approximately twelve times) after conditioning.

According to the results of exhaustion experiments, 2 and 4 BV/h runs exhibited almost identical trends and capacities utilized at breakthrough. However, as the flow rate was increased to 8 BV/h, a decrease in capacity was observed due to decreased residence time of copper in the column. It is well known that zeolites require relatively long residence times due to their slow loading kinetics (Inglezakis and Grigoropoulou, 2004).

Increase in the particle size of clinoptilolite resulted in lower capacity, which is consistent with the literature (Inglezakis and Grigoropoulou, 2004). Contact times in column studies are theoretically inadequate for heavy metal ions to overcome the pore diffusion resistance, particularly in higher size fractions of clinoptilolite (Malliou et al., 1994), leading to a decrease in metal removal capacity.

Trends of the exchangeable cations and silica with time revealed that sodium is the primary cation released in all test runs. There seemed to be almost no calcium, potassium, and magnesium until copper ions were first

detected in the effluent. At this time, sodium concentration in the effluent began to decrease corresponding to an increase in copper concentration in the effluent. However, magnesium concentration exhibited a sharp increase right after the first detection of copper ions in the effluent and was followed by a gradual decrease. Calcium concentration in the effluent also exhibited a peak at this point, although not as sharp as that of magnesium. However, in contrast to magnesium, another gradual increase for calcium was observed starting from the breakthrough point up to a time when the beds began to be exhausted. This second peak of calcium was more significant than the single peak of magnesium. Although release of magnesium, calcium, and sodium was also observed at later stages of the runs, almost no potassium was detected in the effluent at any time.

The results demonstrated a good charge balance between sorbed copper and the total amount of released exchangeable cations from the clinoptilolite structure, indicating ion-exchange as the predominant mechanism.

On the other hand, silica measurements demonstrated that dissolution of the clinoptilolite structure may also be important, particularly in the earlier phase of the runs where the effluent exhibited a basic character (~9.5). Silica release from clinoptilolite structure is said to take place mainly at high or low pH values (Doula et al., 2002). Furthermore, since some portion of the total amount of exchangeable cations in the aqueous phase is attributed to dissolution, some portion of copper uptake is considered to be due to adsorption.

This study identified the potential of Turkish clinoptilolite as a promising sorbent for continuous removal of copper ions. Analysis of exchangeable cations revealed quite interesting results with respect to their release priority. Ion-exchange is identified as the main mechanism in copper solution-clinoptilolite interaction for the specific conditions of this study.

## References

- Abadzic, S.D. and Ryan, J.N. (2001) Particle release and permeability reduction in a natural zeolite (clinoptilolite) and sand porous medium. *Environmental Science and Technology*, **35**, 4501–4508.
- Doula, M., Ioanou, A. and Dimirkou, A. (2002) Copper adsorption and Si, Al, Ca, Mg and Si release from clinoptilolite. *Journal of Colloid and Interface Science*, **245**, 237–250.
- Inglezakis, V.J. (2005) The concept of capacity in zeolite ion-exchange systems. *Journal of Colloid and Interface Science*, **281**, 68–79.
- Inglezakis, V.J. and Grigoropoulou, H. (2004) Effects of operating conditions on the removal of heavy metals by zeolite in fixed bed reactors. *Journal of Hazardous Materials*, **112**(1–2), 37–43.
- Malliou, E., Loizidou, M., Spyrellis, N. (1994) “Uptake of lead and cadmium”, *The Science of the Total Environment*, **149**, 139–144.

## Sorption kinetics of humic acids on zeolitic tuffs

S. Capasso<sup>1</sup>, E. Coppola<sup>1</sup>, P. Iovino<sup>1</sup>, M. Lombardo<sup>1</sup>, S. Salvestrini<sup>1</sup>, and C. Colella<sup>2</sup>

<sup>1</sup>Second University of Naples; Caserta, Italy; Email: sante.capasso@unina2.it

<sup>2</sup>Federico II University; Naples, Italy

### Introduction

Humic substances (HS) arise from the decay of plants and animals and represent about 50–80% of the organic matter in water coming from terrestrial sources, lakes, and rivers. They are natural polymers containing aromatic blocks, characterized by a broad molecular weight distribution and high chemical heterogeneity with acidic character due to carboxylic and phenolic groups. Humic acids (HA) are the fraction of HS soluble in water at neutral and basic pH.

In a previous study, we showed that natural zeolites, namely zeolitic tuffs, are able to bind HA through the action of the surface extraframework cations and that this ability was markedly enhanced if the zeolitic material was enriched by divalent cations, especially  $\text{Ca}^{2+}$  (Capasso et al., 2005). Accordingly, in a very recent paper, we proposed to use pre-exchanged  $\text{Ca}^{2+}$ -rich tuffs to remove HA from water (Capasso et al., 2006).

The aim of this investigation was to analyze the time dependence of HA sorption isotherms on a phillipsite-rich Neapolitan yellow tuff (NYT) and on a clinoptilolite-rich tuff (CLT), both of them previously  $\text{Ca}^{2+}$ -enriched by cation exchange.

### Experimental Methods

NYT (phillipsite 44%, chabazite 4%, smectite 11%, analcime 10%, plus some other non-exchanging phases, CEC 2.12 meq/g) and CLP (clinoptilolite 79%, opal and feldspar as ancillary phases, CEC 1.97 meq/g), both with different amounts of exchangeable calcium ion, were used in this study. Sorption experiments were conducted using batch methods.

Tuff samples were mixed with HA solution, pH 7.2, 0.01 M Tris buffer, and stored at room temperature on a shaker, one oscillation per second. Periodically, the supernatant was centrifuged and analysed by VIS-spectrometry.

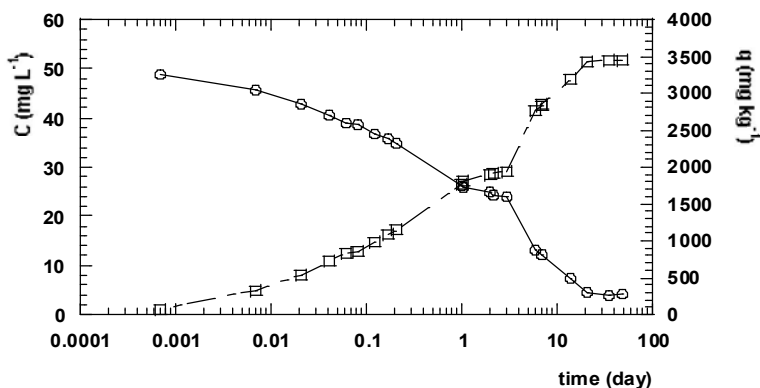


**Figure 1.** Dependence of HA adsorbate per unit mass ( $q$ , right axis) and of the concentration in solution ( $C$ , left axis) on the time. Experimental conditions: 0.4 g  $\text{Ca}^{2+}$ -enriched NYT, 30 mL of 50  $\text{mg L}^{-1}$  HA solution, room temperature.

### Results and Discussion

Figure 1 shows a typical time dependence of the adsorption of HA on zeolitic tuff. As can be seen, there is initially a fast sorption of HA on the tuff leading to a pseudo-equilibrium state in a few days. Afterwards, the amount of sorbate increased again, until it reached an equilibrium state.

Figure 2 reports the sorption isotherms for NYT enriched in calcium ion (exchangeable calcium 41.3 %) and in the native form (exchangeable calcium 25.4 %) recorded at various times.



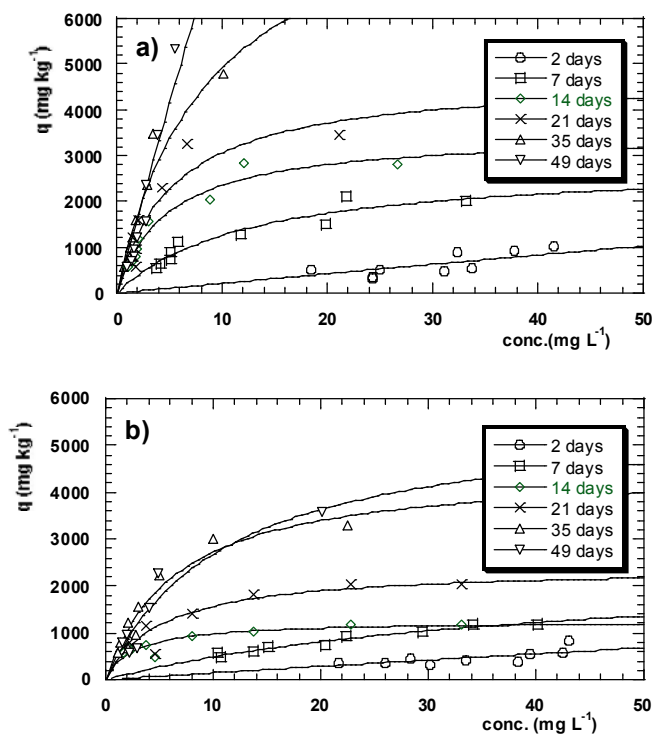


**Figure 2.** Sorption isotherms of humic acids on  $\text{Ca}^{2+}$ -enriched (a) and on natural NYT (b) at the times indicated in the figures.

The Langmuir sorption curve fitted the experimental data well, allowing the calculation of the maximum HA sorbable amount ( $Q$ ) and the affinity constant between the sorbate and the sorbent ( $k$ ). For both samples,  $Q$  value increased with the time, while  $k$  values were constant within the experimental error. Similar behavior was obtained with CLT, both in the native form and in the  $\text{Ca}^{2+}$ -enriched form (exchangeable calcium 40.2% and 91.8%). However, for the latter tuff, although characterised by higher content of zeolite and of exchangeable calcium, the  $Q$  values are lower.

## References

- Capasso, S., Salvestrini, S., Coppola, E., Buondonno, A. and Colella, C. (2005) Sorption of humic acid on zeolitic tuff: A preliminary investigation. *Applied Clay Science*, **28**, 159–165.  
 Capasso, S., Colella, C., Coppola, E., Iovino, P. and Salvestrini, S. (2006) Removal of humic substances from water by means of  $\text{Ca}^{2+}$ -enriched natural zeolites. *Water Environment Research*, in press.

## **Zeolitization processes in Roccamonfina ignimbrite (Southern Italy): A help in recording fossil human tracks?**

**P. Cappelletti, G. Rolandi, and M. de'Gennaro**

*Università Federico II; Napoli, Italy; Email: piergiulio.cappelletti@unina.it*

### **Introduction**

This paper reports on the mineralogical characterization of a zeolite-bearing pyroclastic flows deposit from Roccamonfina Volcano (Central-Southern Italy) and the Brown Leucitic Tuff; the studied outcrop is located in *Tora e Piccilli* locality. This locality is also known as *Ciampate del Diavolo* (Devil's footsteps) because three fossilized trackways of human footprints on the deposit were recognised and described in a previous report (Mietto et al., 2003). The research focused attention on the mineralogical composition of the deposit, aiming to clarify the role of the secondary mineralization process that gave rise to the zeolite (mainly chabazite) formation in the recording of those fully bipedal tracks.

### **Experimental Methods**

Five samples were collected from the top to the bottom of the outcrop; mineralogical composition of bulk samples was obtained by means of XRPD (Panalytical X'Pert Pro apparatus equipped with an X'Celerator RTMS detector, CuK $\alpha$  radiation, 40 kV, 40 mA). Powders with a grain size < 10  $\mu$ m were obtained by means of a McCrone micronising mill, and  $\alpha$ -Al<sub>2</sub>O<sub>3</sub> (1 mm, Buehler Micropolish) was added to each sample in the amount of 20 wt% as an internal standard for quantitative determination. Thermal analyses (Netzsch STA-409 multiple thermoanalyzer) were also performed to obtain information on the cationic composition of the zeolitic phase. Scanning electron microscopy was carried out with a Jeol JSM-5310 apparatus. Accurate handpicking of feldspars was also performed to obtain suitable amounts of sample for radiometric dating.

### **Results and Discussion**

The Brown Leucitic Tuff (BLT) is a compositionally zoned poorly-to-strongly lithified pyroclastic deposit from the Roccamonfina Volcano, dated about 385.000 y.b.p., and constituted by three main facies (white, brown, and orange). This latter facies (accounting for about 40% vol. of the whole BLT) crops out in the northeast sector of the volcano and was reported by a previous author as containing zeolites (Luhr & Giannetti, 1987). Investigated samples belong to this facies and come from the *Ciampate del Diavolo* outcrop. In this outcrop, a steep slope (up to 80°) on the surface of a single ignimbritic unit is present. On this inclined surface three trackways are recognised: 1) Trackway A, about 13 m long and Z-shaped, consisting of 27 footprints on a 4.26 m of elevation difference; 2) Trackway B, about 8.60 m long, consisting of 19 footprints with occasional handprints (probably due to attempts of maintaining balance) and evidences of slipping; 3) Trackway C, about 10 m long, consisting of 10 regular footprints (Mietto et al., 2003).

From the macroscopic view, all samples can be described as lithoid tuffs, brown-yellowish in colour, with rounded yellow pumice ( $\phi$ = 0.2-1 cm) and lithic scoriae. Occasionally lava fragments are present where whitish leucite crystals are visible. Sample CdD3 (1.5 m from the top) contains small accretionary lapilli.

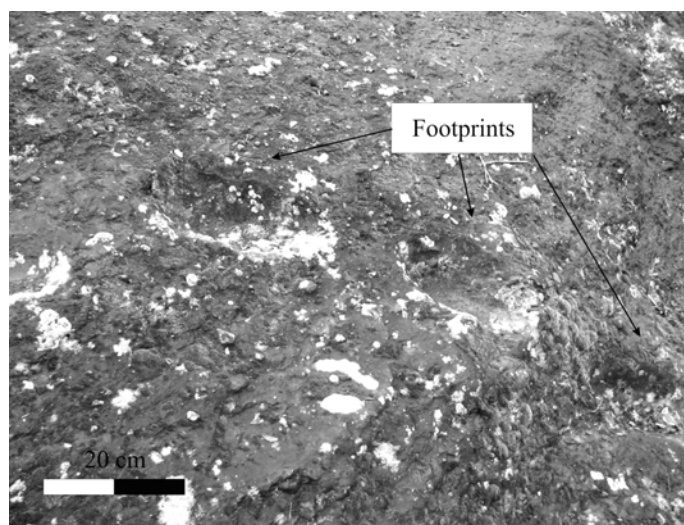


**Figure 1.** Footprints from Trackway B, Ciampate del Diavolo outcrop

Mineralogical composition of the investigated samples shows that chabazite (up to 50% wt) is the main authigenic phase, along with minor phillipsite; pyrogenic minerals are K-feldspars, plagioclase, augite, and biotite. Unreacted glass is also reported. Analcime is detected in two out of five samples, and its presence could be related both to analcimization of leucite (from lava fragments) or early steps of the authigenic process. Noteworthy is the fact that analcime presence seems to prevent phillipsite formation. Thermal behaviour of investigated samples provides useful information on the chabazite cationic composition: a typical broad endothermic effect is present at about 200°C, but each curve also shows a distinctive shoulder around 300°C, this latter being related to K-rich chabazites (de' Gennaro & Franco, 1976). A weak endothermic effect is also present in two samples at about 500°C and could be ascribed to the presence of a small quantity of halloysite. SEM observation allowed us to observe the typical rhomboedral chabazite crystals, along with prismatic phillipsite crystals.

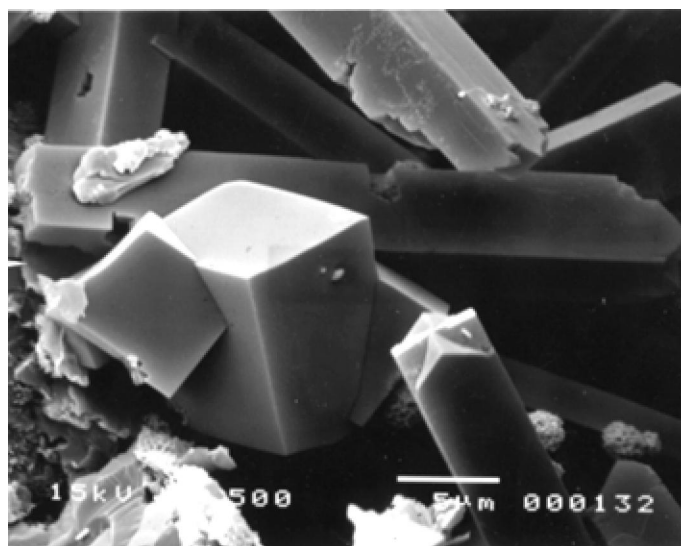


**Figure 2.** Rhomboedral chabazite and prismatic phillipsite from CdD4 sample (SEM image)

Zeolitization processes, at expense of the glassy precursor, likely occurred in the volcanoclastic deposit after the trackways were produced in the still soft cineritic deposit, thus allowing the fossilized pathways to be recorded in a nowadays lithoid tuff. It can also be inferred that the zeolitization-lithification process developed in relatively short times, thus preventing erosive processes from damaging the fossil trackways.

## **References**

- Mietto, P., Avanzini, M. and Rolandi, G. (2003) Human footprints in Pleistocene volcanic ash. *Nature*, **422**, 133.
- de Gennaro, M. and Franco, E. (1976) La K-Cabasite di alcuni tufi del Vesuvio. *Rend. Acc. Naz. Lincei*, **60**, 490 - 497.

## **Authigenic mineralization in the largest Italian volcanoclastic deposit: The Campanian Ignimbrite**

**P. Cappelletti<sup>1</sup>, G. Cerri<sup>2</sup>, A. Colella<sup>1</sup>, M. de Gennaro<sup>1</sup>, A. Langella<sup>3</sup>, A. Perrotta<sup>3</sup>, and C. Scarpati<sup>3</sup>**

*1Università Federico II; Napoli, Italy; Email: piergiulio.cappelletti@unina.it*

*2Università di Sassari; Sassari, Italy*

*3Università del Sannio di Benevento; Benevento, Italy*

### **Introduction**

This paper deals with the mineralogical features of the most important and widespread pyroclastic formation of southern Italy: the Campanian Ignimbrite (CI). The research defines the mineralogical composition throughout the sequence studied and aims to clarify the role of primary (volcanic) and secondary (authigenic) processes leading to the formation of two lithified facies; a grey feldspathized one (WGI) and the overlying yellow unit (LYT) affected by zeolitization processes. This latter facies is deeply zeolitized and thus of relevant technological interest.

### **Experimental Methods**

Detailed volcanological and mineralogical investigations were carried out on the Campanian Ignimbrite formation by means of sampling in several different outcrops all over the Campania region.

The following laboratory tests were performed: quantitative X-ray powder diffraction analyses using the reference intensity ratio (RIR) technique, whole rock chemical analyses by ICP and X-ray fluorescence spectroscopy (XRF), and chemical composition of single crystal phases by energy dispersive spectrometry (EDS) and wavelength dispersive Spectrometry (WDS) analysis on polished thin sections; optical microscopy observations and SEM observations were also carried out.

### **Results and Discussion**

The Campanian Ignimbrite eruption is the most widespread event that occurred at Campi Flegrei (Italy) 39 ka ago. Investigations of groundmass and crystals compositions were performed to assess the secondary minerogenetic processes that affected the products of this eruption. The Campanian Ignimbrite is characterized by a basal, stratified pumice lapilli deposit, emplaced during the early phase of the eruption. These products fell from a sustained column in a wide region east of the source area, reaching the Aegean Sea. The column collapse produced a huge pyroclastic density current that buried an area > 30,000 km<sup>2</sup> under a thick ashy to pumiceous or scoriaceous block ignimbrite. Based on sedimentary structures and textures, four stratigraphical units have been identified throughout the flow deposit sequence (Cappelletti et al., 2003). The lowermost unit is a stratified and incoherent ash to sandy deposit (Unconsolidated Stratified Ash Flow (USAF)) that changes in color from whitish at the base to reddish at the top. A welded grey ash deposit (welded grey ignimbrite (WGI)) overlays the USAF unit. WGI is made up of reverse graded black scoriae embedded in an ashy matrix with subordinate lithics and crystals. Columnar jointing and fumarolic pipes are locally observed. The WGI is overlaid by a yellow lithified tuff (LYT) made up by an ashy matrix with dispersed rounded lapilli to block pumice clasts. The uppermost unit is incoherent and is made up by coarse pumice clasts within an ashy matrix (coarse pumice flow [CPF]). Vertical contacts between the different units are completely gradational. Single units are not ubiquitously dispersed over all the studied area. Because stratigraphic details of the pyroclastic current sequence differ azimuthally and also change with the distance from the source, it is possible to reconstruct a complete stratigraphic sequence only in a few outcrops where all the distinguished units overlap. The area investigated, with the aim to find a large number of exposures representative of the lateral distribution of the different facies of the Campanian Ignimbrite, is a wide region that extends from the Roccamonfina volcano in the north, to Benevento in the east, to the Sele Plain in the south. The investigated samples were collected in twenty-six different outcrops of the Campanian Ignimbrite formation.

The zeolitization processes that involved this volcanic formation accounted for the emplacement of a volcanic succession from a single sustained pyroclastic current, characterized by a different thermal evolution. The welded portion (WGI unit) affected by the highest temperatures is generally found between incoherent units. The upper unit, mainly constituted by a still-hot glassy fraction, aroused interest due to percolation of water that progressively leached the amorphous portion. The increase of the pH of the solution downwards enhanced the zeolitization and the consequent lithification of the LYT unit. The zeolitization of the deposit went on as long as temperatures consistent with the invoked process were preserved.

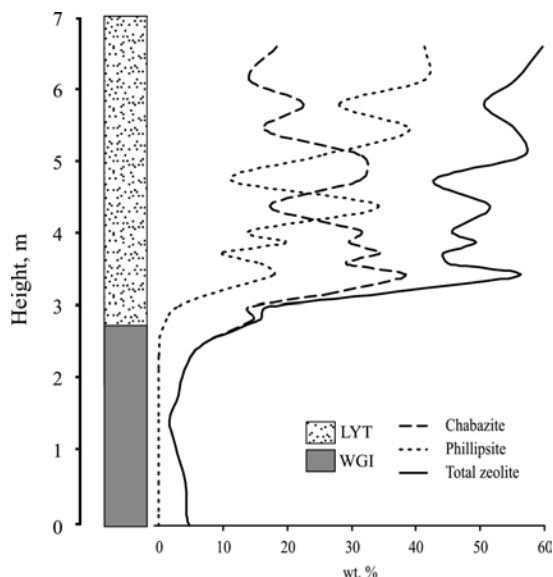


**Figure 1** Typical stratigraphic sequence of Campanian Ignimbrite; chabazite, phillipsite and total zeolite content (XRPD) are also reported.

The present paper details the zeolitization process considering some specific stratigraphic sections that show the transition between the WGI and LYT units. In particular, detailed chemical analyses were carried out on the authigenic phases in order to explain a peculiar behaviour of the two main zeolites (phillipsite and chabazite) in terms of mutual abundance. A typical section of the LYT unit (Fig. 1) evidences downwards a progressive increase of the total zeolite content that fits well with the model previously reported. However, as far as the two zeolites are considered, a continuous inversion of the reciprocal abundance recorded is likely related to physio-chemical variations of the solutions in an open hydrologic system characterized by particular thermal conditions.

## References

- Cappelletti, P., Cerri G., Colella, A., de' Gennaro, M., Langella, A., Perrotta, A., and Scarpati, C. (2003) Authigenic mineralization processes in the Campanian Ignimbrite. *Mineral Petrol*, **79**, 79–97.

## **Modeling of water and ethanol adsorption data on a commercial zeolite-rich tuff and prediction of the relevant binary isotherms**

**D. Caputo<sup>1</sup>, F. Iucolano<sup>1</sup>, F. Pepe<sup>2</sup>, and C. Colella<sup>1</sup>**

<sup>1</sup>*Università Federico II; Napoli, Italy; E-mail: domenico.caputo@unina.it*

<sup>2</sup>*Università del Sannio; Benevento, Italy*

Anhydrous ethanol is a very important renewable fuel that can be produced, among other possible alternative routes, by fermentation of biomass. Among the alternative techniques to dehydrate ethanol, adsorption processes appear particularly interesting because it is easy to individuate an adsorbing material characterized by a high selectivity towards water, and, therefore, capable of leading to high separation factors. In the present paper, a zeolitic tuff from Campania, Italy, containing both phillipsite and chabazite was considered as a potential adsorbent for the production of anhydrous ethanol from gas phase water–ethanol mixtures.

The zeolite sample used was an ignimbrite from Tufino (Naples, Italy), commercially named CAB 70, with a zeolite (phillipsite+chabazite) content of 58%. Three different grain size fractions of the original tuff were used (<0.125 mm, +0.125–0.250 mm, and +0.250–0.500 mm). The different size fractions have different zeolite contents (from 68% for the finest fraction to 18% for the coarsest). The adsorption properties of such samples were investigated by determining the equilibrium isotherms for pure water and ethanol vapors at different temperatures, using a gravimetric technique based on a McBain–type balance.

Selected experimental results are reported as adsorption isotherms in Figures 1 and 2. Both figures are relative to the medium-sized fraction of the tuff (+0.125–0.250 mm) and to temperatures ranging between 20–80°C. Figure 1 refers to water, whereas Figure 2 is relative to ethanol. The isotherms show that the selected material has a good adsorption capacity towards water (almost 4 mol/kg at the lowest temperature considered), and that this capacity, while it obviously decreases as temperature increases, is still close to 3 mol/kg at 80°C. The results obtained for ethanol qualitatively agreed with those relative to water. In particular, the adsorption capacity on the intermediate fraction ranged between 1.2 mol/kg at 20°C and about 0.8 mol/kg at 80°C. In general, the experimental results showed that the tuff samples considered have a good capacity towards water, with a molar water/ethanol ratio in the order of 3 (or a mass ratio of 1.2) in the whole temperature range considered.

With the aim of having a clearer description of the adsorption phenomena studied, the Dubinin–Astakhov (DA) isotherm (Dubinin, 1975) was used to model the experimental data. According to the DA model, the following expression can be used to describe the adsorption isotherms on a microporous material:

$$q = \frac{W}{v_{mol}} = \frac{W_o}{v_{mol}} \exp\left[-(A/E)^n\right] \quad A = -RT \ln(p/p^o)$$

where  $W$  is the volume occupied by the adsorbent within the available micropores,  $v_{mol}$  is the molar liquid volume of the adsorbate (which is assumed to behave as an ordinary liquid within the micropores),  $A$  is the adsorption potential, defined as the molar energy required for the isoentropic compression of the adsorbed species to the saturation pressure,  $R$  is the gas constant, and  $p^o$  is the saturation pressure of the adsorbate.

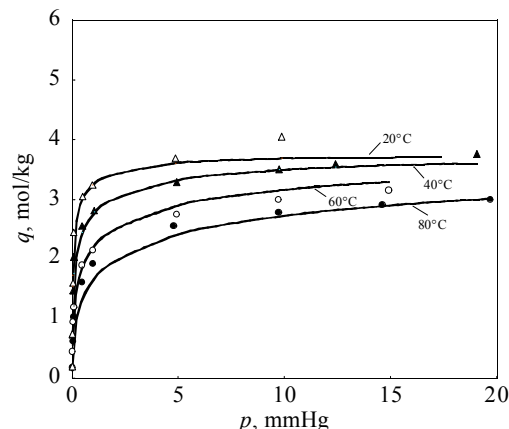


**Figure 1.** Water adsorption isotherms on intermediate fraction of the tuff.  $\Delta$ : 20°C;  $\blacktriangle$ : 40°C;  $\circ$ : 60°C;  $\bullet$ : 80°C; continuous lines: DA model.

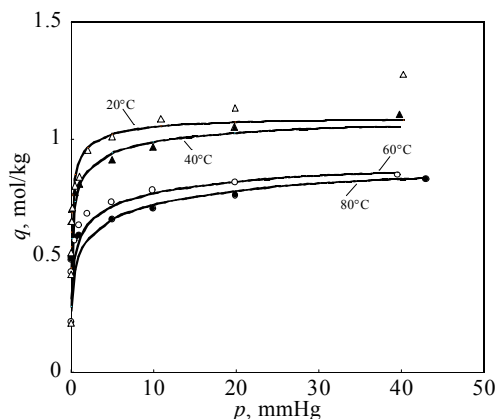


**Figure 2.** Ethanol adsorption isotherms on intermediate fraction of the tuff.  $\Delta$ : 20°C;  $\blacktriangle$ : 40°C;  $\circ$ : 60°C;  $\bullet$ : 80°C; continuous lines: DA model.

In order to estimate the most likely values of  $W_o$  and  $E$  for the available isotherms ( $n$  is often taken equal to 2: see Do, 1998), a non-linear regression was carried out. The parameters obtained by the regression are reported in Table 1. Inspection of this table shows that there is a strong correlation between the phillipsite+chabazite content of the tuff and the estimated values of the micropore volume  $W_o$ . This indicates that, as expected, phillipsite and chabazite play a predominant role in the adsorption process, clearly overshadowing the contributions by the other components of the tuff. Furthermore, it appears that the estimated values of the characteristic energies  $E$  are fairly close (even though the one relative to water is about 20% lower than the one relative to ethanol).

**Table 1.** Parameters of the DA model for the three grain size fractions considered.

Fraction used	Zeolite content (phill. + chab.)	$W_o$ (ml/kg)	$E_{H_2O}$ (kJ/mol)	$E_{EtOH}$ (kJ/mol)
Fines	68%	121 $\pm$ 11	-20 $\pm$ 1	-25 $\pm$ 2
intermediate	40%	64 $\pm$ 4		
Coarse	18%	35 $\pm$ 3		

Using the Dubinin-Astakhov model, the isosteric heat was evaluated for adsorption of each species, and it turned out that adsorption of 1 mole of water releases 60–90 kJ, while the isosteric heat is in the order of 50–90 kJ for ethanol. Eventually, once again using the Dubinin-Astakhov model, the binary water–ethanol adsorption isotherms were predicted. The model results, not reported here for the sake of brevity, showed that the selected tuff is very selective towards water, and in particular it showed that, if the azeotropic mixture is considered, a very satisfactory molar separation factor in the order of 6–7 can be achieved.

## References

- Do, D.D. (1998) *Adsorption Analysis: Equilibria and Kinetics*, Imperial College Press, London.  
Dubinin, M.M. (1975) Physical adsorption of gases and vapors in micropores. *Progr. in Surf. Membr. Sci.*, **9**, 1–70.



## **Lead release after different thermal treatments of a Pb-exchanged clinoptilolite-rich material**

**G. Cerri<sup>1</sup>, A. Brundu<sup>1</sup>, M. Biagioli<sup>2</sup>, and A. Langella<sup>3</sup>**

<sup>1</sup> *Università degli Studi di Sassari; Sassari, Italy; Email: gcerri@uniss.it*

<sup>2</sup> *Università degli Studi di Sassari; Nuoro, Italy*

<sup>3</sup> *Università del Sannio; Benevento, Italy*

### **Introduction**

Lead removal from polluted water using clinoptilolite-rich materials has been well investigated and is a well-known process (Semmens & Seyfarth, 1978). Generally, the complete regeneration of a heavy-metal-loaded exchanger is not profitable (particularly when decontamination has not been performed in exchange columns); hence, the used material may become a new potential source of lead pollution.

Using a clinoptilolite-rich material partially exchanged into Pb-form, this work evaluated how the concentration of contacted solutions and two-hour thermal treatments of the material at 450, 600, and 900°C affected the kinetics and the amount of lead released.

### **Experimental Methods**

The sample used for the present investigation (Sardinian clinoptilolite-rich rock “LacBen”) was previously characterized (Cerri et al., 2002). The material was ground and sieved to increase the zeolite content. The mineral composition after beneficiation process was determined by XRPD analysis (reference intensity ratio method).

Using a batch exchange method modified from that used by Cerri et al. (2002), the material was pre-exchanged into Na-form, then contacted with a 0.5 M solution of  $\text{Pb}(\text{CH}_3\text{COO})_2$ . All the tests were performed twice, and the eluted solutions were analyzed by AAS. The release of lead was evaluated after interaction at 20°C with  $\text{NaNO}_2$  solutions having 0.5 and 0.05 total normalities (7 exchange cycles, 2 h each; solid/liquid ratio = 1 g/25 ml).

Three different Pb-loaded materials were heated for two hours at 450, 600, and 900°C. Lead release as a function of each thermal treatment was tested after contact with a 0.5 N sodium solution at the same conditions described above.

### **Results and Discussion**

The mineral content (wt.%) after zeolite enrichment was determined as follows: clinoptilolite 83%; feldspar 9%; opal-CT 4%; quartz 2%; smectite  $\leq 1\%$ ; biotite  $\leq 1\%$ .

The final  $\text{Pb}^{2+}$  content in the material was 0.90 meq/g, corresponding to half of the CEC available (1.81 meq/g). Lead release in 0.5 and 0.05 N solutions is reported in Figure 1. After the last exchange cycle, 88% of the metal loaded was released by contact with the 0.5 N solutions, and 41% was released by contact with the 0.05 N solutions. Release kinetics were significantly different only during the first cycle of exchange (3.3 times higher in the 0.5 N solution), then release rates became similar.

Lead release from heated and unheated materials in 0.5 N solution is reported in Figure 2.

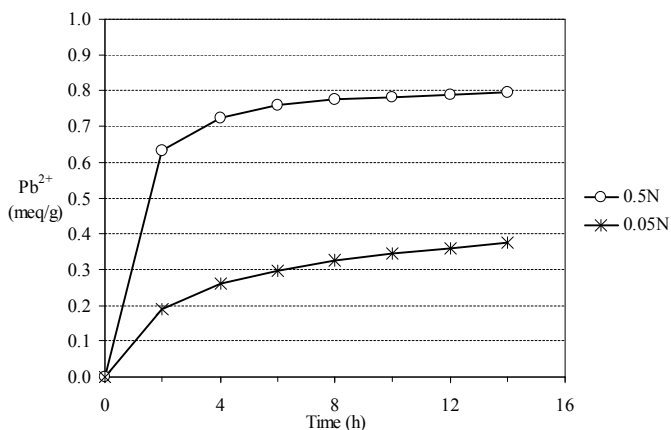


**Figure 1.** Pb<sup>2+</sup> released at 20 °C from untreated material in 0.5 and 0.05 N NaNO<sub>2</sub> solutions.

A progressive decrease of lead release was recorded after 2 hours of thermal treatments at increasing temperatures. Powders treated at 450 and 600°C released respectively about 63% and 33% of the initial lead content. Thermal treatments at 900°C prevented any lead release.

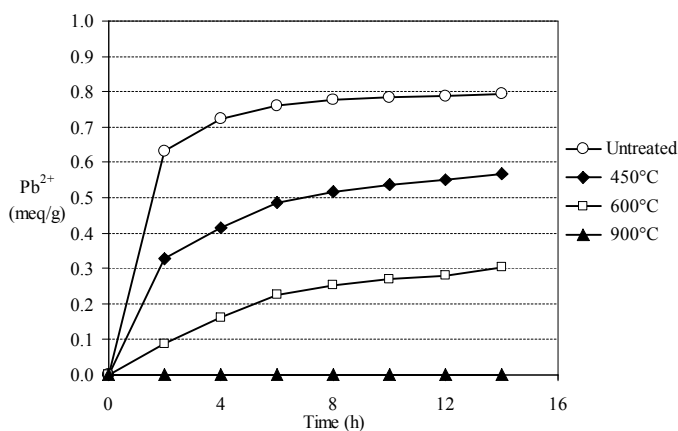


**Figure 2.** Pb<sup>2+</sup> released in 0.5 N NaNO<sub>2</sub> solutions reacted with thermally treated and untreated materials.

Release at the end of the first exchange cycle also decreased as a function of treatment temperatures. Powders treated at 450 and 600°C released respectively 52% and 14% with respect to the corresponding value for unheated material. During the subsequent six cycles, release kinetics from powders treated at 450 and 600°C are quite similar and slightly faster than from untreated material.

## References

- Cerri, G., Langella, A., Pansini, M. and Cappelletti, P. (2002) Methods of determining cation exchange capacity for clinoptilolite-rich rocks of the Logudoro Region in Northern Sardinia, Italy. *Clays & Clay Minerals*, **50**, 127-135.
- Semmens, M.J. and Seyfarth, M. (1978) The selectivity of clinoptilolite for certain heavy metals. pp. 517–526 in: *Natural Zeolites: Occurrence, Properties, Use* (L.B. Sand and F.A. Mumpton, editors). Pergamon Press, Oxford.

## Zn-exchanged clinoptilolite-rich rock as carrier for erythromycin in anti-acne therapy: An in vitro evaluation

G. Cerri<sup>1</sup>, M. de' Gennaro<sup>2</sup>, M. C. Bonferoni<sup>3</sup>, C. Caramella<sup>3</sup>, and C. Juliano<sup>4</sup>

<sup>1</sup>Università di Sassari; Sassari, Italy; Email: gcerri@uniss.it

<sup>2</sup>Università Federico II; Napoli, Italy

<sup>3</sup>Università di Pavia; Pavia Italy

<sup>4</sup>Università di Sassari; Sassari, Italy

### Introduction

Acne is a common pathology of the skin. The role played by the *Propionibacterium acnes* is generally recognized, and a topical treatment with antibiotics is widely accepted. A problem of increasing relevance is the development of antibiotic resistance. A reduced development of resistant *P. acnes* strains can be achieved by combining antibiotics, like erythromycin, with zinc (Bojar et al., 1994). The adsorption of erythromycin on a carrier capable of releasing zinc for ionic exchange after contact with the skin allows a stable and easy-to-handle system. Given this premise, by employing a clinoptilolite-rich rock, a Zn-exchanged carrier for erythromycin to be used in the topical treatment of acne was already prepared and optimized (Cerri et al., 2004). Clinoptilolite was chosen for its low selectivity towards zinc ions, to favor a prompt zinc release in the physiologic environment. It was also verified that erythromycin cannot be completely introduced into the clinoptilolite channels. This situation is favorable for its fast release. The aim of the present work was to check the antimicrobial efficacy of the Zn-carrier-erythromycin system (ZCE system) against *P. acnes*.

### Experimental Methods

Phosphate buffered saline (PBS Dulbecco A, pH 7.3), brain heart infusion (BHI) broth, brain heart infusion agar (BHA), and defibrinated horse blood were supplied by Oxoid (Basingstoke, England). Erythromycin was purchased from Sigma-Aldrich, and *Propionibacterium acnes* ATCC 6919 from LGC Promochem (Middelsex, U.K). Anaerobic conditions of growth of this microorganism were obtained in the Anaerobic Plus System with gas-generating kit H<sub>2</sub>/CO<sub>2</sub> (Oxoid). The zeolitized rock used to prepare the carrier was an ash-rich epiclastite, Oligo-Aquitania in age. It was sampled at the Bortivule locality, Sassari province, Sardinia Island, Italy. The ZCE system was obtained with a procedure described in Cerri et al. (2004). Briefly, the material (clinoptilolite content: 66±4 wt.%) was first Na- and subsequently Zn-conditioned. Erythromycin was loaded onto the micronized rock by vacuum drying. Drug content was quantified by the HPLC method (Perkin Elmer - Series 200). The antimicrobial activities of both erythromycin and ZCE system against *P. acnes* were determined by evaluating their minimum inhibitory concentration (MIC) and by measuring the exposure time required to kill a standard bacterial inoculum. MIC values were evaluated in 96-well round-bottom microtiter plates by a broth microdilution technique. Twofold serial dilutions of the drugs were prepared in triplicate in BHI broth, and each well was inoculated with 10<sup>4</sup> colony forming units (c.f.u.) of *Propionibacterium acnes*, obtaining final drug concentrations ranging from 12.5 to 0.012 µg/ml for erythromycin and from 54.1 to 0.05 µg/ml for the ZCE system. After 72 h incubation at 35°C in anaerobic conditions, the microplates were visually checked for bacterial growth and MICs were defined as the lowest concentrations that completely inhibited bacterial growth. *P. acnes* in the logarithmic phase of growth were suspended at a density of 1-5 × 10<sup>5</sup> c.f.u./ml in 10 ml of PBS containing 50 µg/ml of erythromycin or 216 µg/ml of drug-loaded Zn-carrier (corresponding to 50 µg/ml of erythromycin). A control tube (bacteria suspended in PBS alone at the same density) was included in each experiment. At time zero and at regular intervals, 0.5 ml of each suspension were removed, subjected to serial tenfold dilutions in PBS, and seeded onto blood agar (BHA + 10% blood) plates. The number of viable bacteria at each time was evaluated counting colonies on plates after anaerobic incubation for 72 h at 35 °C.

### Results and Discussion

Pure erythromycin showed against *P. acnes* an MIC value of 0.024 µg/ml, in agreement with the literature (Atkinson, 1986). The MIC of the ZCE system, under the same conditions, resulted in 0.10 µg/ml,

corresponding to 0.024 µg/ml, of erythromycin on the basis of the drug content of the system. These data demonstrate that the process of adsorption of erythromycin onto the clinoptilolite-rich carrier does not affect the antimicrobial activity of the antibiotic. The results of the contact time tests (Figure 1) demonstrated that viability of *P. acnes* suspended in the ZCE system strongly decreased after 2 and 3 hours of contact, with respectively 26.0% and 0.5% of surviving bacteria. After the same exposure times, bacterial viability in PBS and in erythromycin solution was slightly affected in a similar and not specific way. At the short test times (not long enough to allow erythromycin to carry out its specific mechanism of action), the effect of the ZCE system might be related to a direct action of the zinc carrier, suggesting an important synergism with the antibiotic molecule.

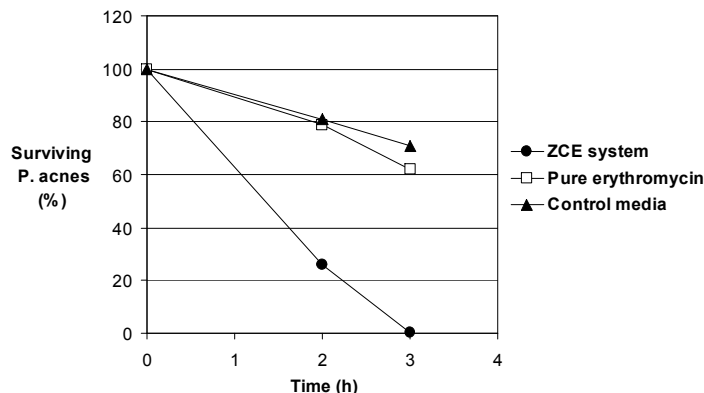


Figure 1. Contact time test

## References

- Atkinson, M.A. (1986) Species incidence and trend of susceptibility to antibiotics in the United States and other countries: MIC and MBC. In: *Antibiotics in Laboratory Medicine* (Lorian, V., editor). 2<sup>nd</sup> Ed., Williams & Wilkins, Baltimore.
- Bojar, R.A., Eady, E.A., Jones, C.E., Cunliffe, W.J. and Holland, K.T. (1994) Inhibition of erythromycin-resistant propionibacteria on the skin of acne patients by topical erythromycin with and without zinc. *Brit. J. Dermatol.*, **130**, 329–336.
- Cerri, G., de'Gennaro, M., Bonferoni, M.C. and Caramella, C. (2004) Zeolites in biomedical application: Zn-exchanged clinoptilolite-rich rock as active carrier for antibiotics in anti-acne topical therapy. *Appl. Clay Sci.*, **27**, 141–150.

## **Features of formation of analcime in Perm copper sandstones**

**I. Chaikovski and O. Kropacheva**

*Perm State University; Perm, Bukireva, Russia; Email: infj@psu.ru*

The copper sandstones formation of preUral that extends from Orenburg up to Solikamsk, until the middle of the 18th century, was the main source of copper extracted in Russia. Samples of copper sandstones from the Usovsky, Bogoslovski, and Risevski mines and from the collection of the mineralogical museum at Perm State University were used for the present research. Chemical analyses and morphological features of the investigated samples were carried out with a JSM-6400 scanning electron microscope, with energy dispersion prefix Link, located at the Institute of Geology at Komi NC (Russian Academy of Science).

The morphology of minerals and their textural relationship allow us to distinguish between primary and secondary associations. The secondary copper mineralization is related to the transformation of primary minerals. It is possible to determine some conditions of their formation. The mineralization in gravel prolayers is formed both in cavities and by replacement of chemically active fragments. The cement of gravelstones and conglomerates is composed of analcime, analcime with calcite, or calcite alone.

Analcime is characterized by a rather high silicon-to-aluminum ratio. The values we obtained varied within the limits of 2.12–2.7, suggesting a primary rather than secondary formation of analcime in copper sandstones. Analcime is the typomorphic mineral in epigenic zones within sedimentary formations containing altered pyroclastics. It is presumed to be indicative of zeolite formation in Perm red rocks from earlier easily altered aluminosilicate-bearing pyroclastics. All the investigated zeolite-bearing samples from the Bogoslovski, Usovski, and Risevski mines showed the occurrence of clay fragments. Surface boundaries between these fragments and neighboring pebbles are concave, reflecting the plasticity of the clays. Analcime is apparently growing into them from their periphery inward.

## A model for the impact of ferritized clinoptilolite on flooded soils

K. Chakalov<sup>1</sup>, T. Popova<sup>1</sup>, K. Mitov<sup>1</sup>, O. Petrov<sup>2</sup>, and E. Filcheva<sup>3</sup>

<sup>1</sup>NIPRORUDA JSCo; Sofia, Bulgaria; Email: konstantinchakalov@yahoo.com

<sup>2</sup>Bulgarian Academy of Sciences; Sofia, Bulgaria

<sup>3</sup>N. Poushkaarov Institute of Soil Science; Sofia, Bulgaria

### Introduction

Reduction of soil is the most important chemical change connected with flooding. The potentials Eh and Hr are both quantitative measures of the intensity of this change. As all reduction profoundly influences the growth of rice through the effects on pH, the availability of nutrients, or the production of toxins, a quantitative study of the Eh equilibrium in flooded soils is needed. Soil reduction is a direct consequence of the exclusion of oxygen by flooding. Within a few hours aerobic organisms use up the trapped oxygen and become quiescent or die. Facultative anaerobes follow the strict anaerobes as proliferates and use the same oxidized soil components as nitrate, MnO<sub>2</sub>, hydrate oxides of Fe (III), sulfate, and even their own metabolites as electron acceptors in their respiration. Also, products of the anaerobic metabolism of bacteria may reduce these substances by intrinsically chemical pathways. Because nitrate rapidly disappears in flooded soils, and because soils normally contain much more iron than manganese, the dominant redox systems in reduced soils are the iron hydroxide systems (Ponnamperuma, 1967). Soil moisture, organic carbon, oxygen concentration, and NO<sub>3</sub><sup>−</sup>–NO<sub>2</sub><sup>−</sup> content in the field affect the rate of nitrification (Parkin, 1990). The soil Eh could be managed using zeolite materials (Chakalov, 2001). The aim of this study is to describe a model for the impact of natural and ferritized zeolites on the storage of soil carbon and nitrogen in flooded soils.

### Experimental Methods

The studied clinoptilolite samples are from the Beli Plast deposit, Eastern Rhodopes, Bulgaria (size 0.8–2.5 mm; CEC 125 meq/100 g.). The ferritization of the zeolite was achieved by mechanically dressing K<sub>2</sub>HPO<sub>4</sub>-modified zeolite grains (P-z) with a film of ferrite (magnetite ~ 9 wt. %) – (Fe-P-z). The ammonium form is obtained by saturation and flushing of the sample with a saturated solution of NH<sub>4</sub>NO<sub>3</sub> and distilled water to reach a mineral nitrogen content of 1%. Fe-zeolite (modified with FeSO<sub>4</sub>) was prepared after the ammonium saturation. The model and vegetation pot experiment was carried out with soil from the Plovdiv region (horizon Ap, clay 40 wt.%) that was flooded twice under t = 30–31°C, in control conditions, for a period of 30 days under aerobic conditions and a period of 30 days under restoration (FC of 65%). Experiments with flooded soil and test plant rice were carried out in pots of 3dm<sup>3</sup> volume for each of 3 replications. Two vegetation series were performed with 10 days of flooding. Rice seedlings (15 days after germination) grown on peat mixture were used for pot tests. The pH and Eh values were measured in the pots periodically. Fresh soil samples were collected for analysis of pH, total N, N-NH<sub>4</sub>, N-NO<sub>3</sub>, mobile forms of K and P in Morgan solution buffered in pH 4.8, content of Fe<sup>2+</sup> and Fe<sup>3+</sup> determined in extraction with 0.1 N H<sub>2</sub>SO<sub>4</sub>, organic carbon, humic composition, and microbial and enzyme activity.

### Results and Discussion

Modified zeolite Fe-P-z maintains Eh of the media in the natural frontier for NO<sub>3</sub><sup>−</sup> reduction to NO<sub>2</sub><sup>−</sup>. It leads to 8–10% N sequestration. It is established that the control soil loses about 19% total N, while the treated soil loses 10–14% because of improved enzyme activity. The data from the vegetation experiment show that the test plant developed better in soil meliorated with the composition of NH<sub>4</sub>-Z and Fe-P-z. Total biomass was high in the variants with composition of NH<sub>4</sub>-Z and Fe-P-z, and Fe-P-z maintains relatively high soil productivity. Theoretical values of Eh show increasing iron activity in zeolite-amended soils, and Eh passes the critical value of 200 mV. The ratio Fe<sup>3+</sup>/Fe<sup>2+</sup> increased in all studied variants, while the composition NH<sub>4</sub>-Z and Fe-P-z strongly influenced this ratio. Dehydrogenase activity was highly increased in the soils treated with iron-containing materials. Ferrireductase activity decreased, and at the end of the experiment the activity increased in the variants with NH<sub>4</sub>-Z and magnetite. The studied amendments increased the bioproductivity of the flooded soil by up to 19–35%. The treatment of flooded soils with zeolite materials led to better storage of nitrogen and

carbon and stopped gleyization. The limitation of the mobility of  $\text{Fe}^{3+} \leftrightarrow \text{Fe}^{2+}$  improved the availability of phosphates for plant uptake.

Natural zeolites, ammonium-saturated forms, ferritized P-zeolites, and their combinations destroy the enzyme translocation of  $\text{H}^+$  due to anaerobic conditions in the media and e- between the organic and metal hydroxide phase of soil colloids. Zeolite ameliorants are competitors in sorption of  $\text{H}^+$ ,  $\text{NH}_4^+$ , and  $\text{Fe}^{2+}$ . Brushite membrane provides  $\text{HPO}_4^{2-}$ , which precipitates  $\text{Fe}^{3+} \leftrightarrow \text{Fe}^{2+}$ . Magnetite membrane is a source for electrons and oxygen and it competes with nitrate. In this way a relatively higher Eh potential is maintained in a natural frontier of  $\text{NO}_3^-$  reduction to  $\text{NO}_2^-$ . Accumulation of  $\text{H}^+$  in the zeolite component and the higher Eh values preserve condensation of organic matter in case of  $\text{NH}_4\text{-Z} + \text{P-Fe-z}$  amended flooded soils. Bioproductivity increases in flooded soils treated with a composition of  $\text{NH}_4$  zeolites and Fe-P-zeolites.

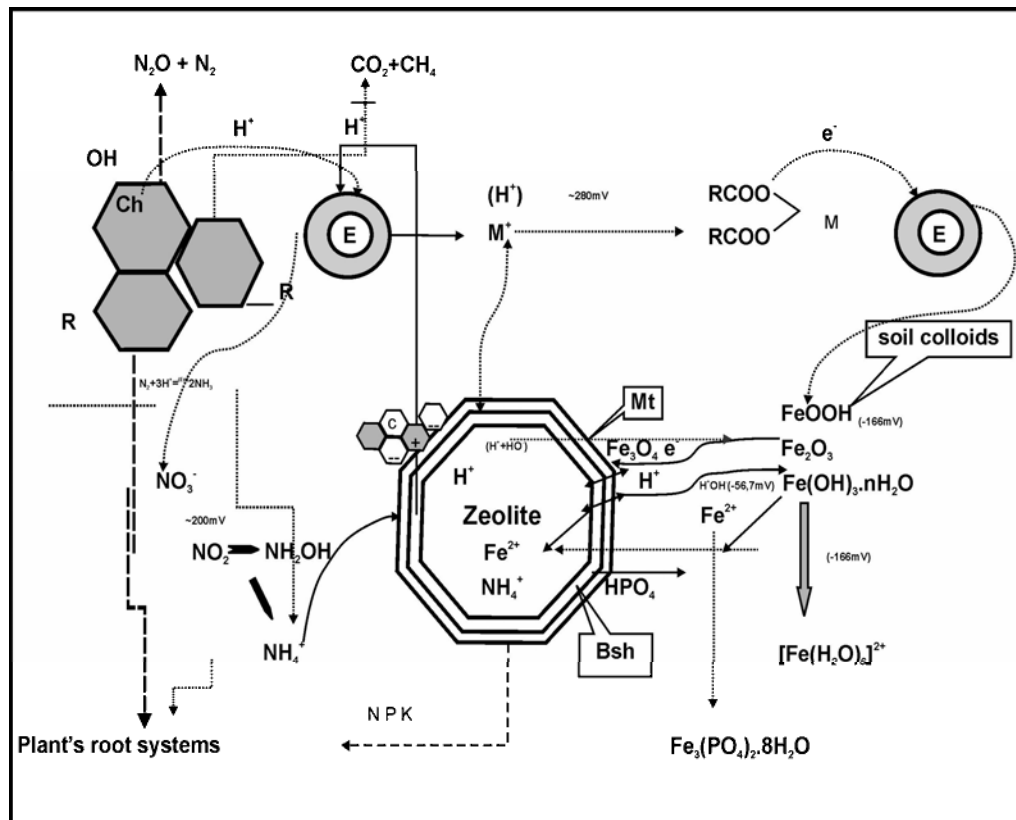


Figure 1. Hypothetical model

## References

- Chakalov, K., Popova, T., Filcheva, E. and Mitov, K. (2002) Improvement of zeolite effect on polluted soils for better nitrogen and carbon storage. I. Influence of zeolite amendments on oxidation-reduction charges (Eh) on heavy metal and AS polluted soils. Pp. 52–54 in: *Zeolite '02 Book of Abstracts: 6th International Conference on the Occurrence, Properties and Utilization of Natural Zeolites* (P. Misaelides, editor). Thessaloniki, Greece.
- Ponnamperuma, F.N., Tianco, E.M., and Loy, T. (1967) Redox equilibrium in flooded soils: I. The iron hydroxide systems. *Soil Science*, **103**, 374–382.
- Parkin T. S. (1990) Characterizing the variability of soil denitrification. Pp. 213–228 In: *Revabech. Denitrification in soil and sediment*. (N.P. Revsbech and Sorensen, Editors). Plemun Press. New York.

## **Investigation of Mongolian zeolites for heavy metal uptake**

**A. Chimedtsogzol<sup>1,2</sup>, A. Dyer<sup>1</sup>, C. D. Williams<sup>3</sup>, and H. Poellmann<sup>2</sup>**

<sup>1</sup>*University of Salford, Salford, UK; Email: [anaad.chimedtsogzol@geo.uni-halle.de](mailto:anaad.chimedtsogzol@geo.uni-halle.de)*

<sup>2</sup>*Martin Luther University, Halle-Wittenberg, Germany*

<sup>3</sup>*University of Wolverhampton, Wolverhampton, UK.*

Three clinoptilolites obtained from different locations in Mongolia and their cation exchanged forms have been investigated for the uptake of  $\text{Pb}^{2+}$ ,  $\text{Zn}^{2+}$ ,  $\text{Cd}^{2+}$ ,  $\text{Cu}^{2+}$ ,  $\text{Sr}^{2+}$ , and  $\text{Cs}^{+}$  cations from aqueous solutions using a batch method with radioactive tracer ( $^{22}\text{Na}$ ). The zeolite samples were examined using X-ray powder diffraction, crystal structure, X-ray fluorescence, and grain size analysis.

The zeolitic tuffs from the Tsagaantsav, Ergene, and Tushleg deposits are rich in clinoptilolite. The selectivity sequence for ions entering the natural zeolites was  $\text{Cs}^{+} > \text{Pb}^{2+} > \text{Cd}^{2+} > \text{Cu}^{2+} > \text{Zn}^{2+} > \text{Sr}^{2+}$  as indicated by values of  $K_d$ . An improvement in uptake ability for the metals was observed for the sodium homoionic form for all the metals investigated—especially for lead.

The results are discussed in the light of literature data, and the contrasting performances of the various clinoptilolites are ascribed to different cationic compositions of the minerals, arising from their two different minerogenetic conditions, which are proven to affect both cation exchange capacity and selectivity.



## **Uptake of mercury solutes by natural zeolites from Mongolia**

**A. Chimedtsogzol<sup>1,4</sup>, A. Dyer<sup>1</sup>, L. Campbell<sup>2</sup>, C.D. Williams<sup>3</sup>, and H. Poellmann<sup>4</sup>**

<sup>1</sup>*University of Salford; Salford, UK; Email: anaad.chimedtsogzol@geo.uni-halle.de*

<sup>2</sup>*University of Salford; Salford, UK*

<sup>3</sup>*University of Wolverhampton; Wolverhampton, UK*

<sup>4</sup>*Martin Luther University; Halle-Wittenberg, Germany*

The variation in toxicity of different Hg species is well known, with methylmercury being the most toxic to living organisms. In consideration of their potential use in remediation, zeolite minerals were tested for their sorption responses to two different solute species of mercury, methyl mercury CH<sub>3</sub>HgCl, and mercuric nitrate Hg(NO<sub>3</sub>)<sub>2</sub>.

The uptake of inorganic Hg<sup>2+</sup> and organic CH<sub>3</sub>Hg<sup>+</sup> from aqueous solutions by 3 natural zeolites from Mongolia have been investigated using the batch distribution coefficient (K<sub>d</sub>) method. Selectivity factors were estimated by determining batch distribution coefficients as a function of contact time, mercury and methylmercury concentration, and batch factor.

The Tsagaantsav deposit (TSA) was the most effective with a K<sub>d</sub> of 3284 mL/g for mercury (II) and 3748 mL/g for methylmercury. This zeolite (clinoptilolite) was selected for further study using homoionic forms and acid modified forms. For the homoionic forms, optimal sorption was found as follows: Na > NH<sub>4</sub> > Mg > K > Ca for the mercury, and Na > Mg > Ca > NH<sub>4</sub> > K for methylmercury. The sodium form was superior with a K<sub>d</sub> of 7539 mL/g for methylmercury. Acid modified zeolites resulted in reduced K<sub>d</sub>'s for nitric and sulphuric acid modifications with the highest methylmercury uptakes with a K<sub>d</sub> of 8618 mL/g, but no difference was found for the phosphoric acid modifications.

The modified Mongolian clinoptilolites were further assessed for methylmercury uptake in the presence of acid and alkaline solutions.

## **Zeolitization of intracaldera sediments and rhyolitic rocks of Valles caldera, New Mexico, USA**

**S. J. Chipera<sup>1</sup>, F. Goff<sup>2</sup>, C. J. Goff<sup>3</sup>, and M. Fittipaldo<sup>1</sup>**

<sup>1</sup>*Los Alamos National Laboratory; Los Alamos, New Mexico, USA; Email: chipera@lanl.gov*

<sup>2</sup>*University of New Mexico; Albuquerque, New Mexico, USA*

<sup>3</sup>*Rio Grande Research; Los Alamos, New Mexico, USA*

### **Introduction**

Valles caldera, located in north-central New Mexico, USA, formed during eruption of the upper Bandelier Tuff (ca. 1.25 Ma) and is well known as the type resurgent caldera (Smith and Bailey, 1968). Valles is also a host for a long-lived, high-temperature geothermal system. The 20-km-diameter Valles caldera is part of the youngest major episode of volcanism to occur in the Jemez volcanic field. As the caldera formed, roughly 300 km<sup>3</sup> of high-silica rhyolitic ignimbrite (upper Bandelier Tuff) filled the resulting caldera depression and radiated outward to cover surrounding topography. Immediately after the Valles caldera was created, three simultaneous events occurred: a lake developed, depositing laminated to bedded sediments; small volumes of rhyolite lava and tuff were erupted near the caldera center; and the central floor of the caldera began to rise, forming the resurgent dome of Redondo Peak. In this paper, we present data on recently recognized zeolitic alteration that is related to the formation of Valles caldera.

### **Experimental Methods**

Roughly 80 samples of altered and relatively fresh rock were collected, primarily from the middle to lower flanks of the resurgent dome and from various locations in the caldera moat. Quantitative XRD analyses were conducted with a Siemens D500 X-ray powder diffractometer using CuK $\alpha$  radiation, 2–70°2 $\theta$ , using 0.02° steps, and counting for at least 4s/step. Mineral abundances were determined using the FULLPAT QXRD program and method (Chipera and Bish, 2002). Scanning electron microscopy (Philips XL20 SEM) was used to study the morphology and textures of the samples and electron microprobe analyses of representative Valles zeolites were conducted using a Cameca SX50 electron microprobe.

### **Results and Discussion**

The alteration assemblages consist primarily of smectite-clinoptilolite-mordenite-silica, which replace groundmass and fill voids, especially in the tuffs and lacustrine rocks. Original rock textures are routinely preserved. Mineralization typically extends to depths of only a few tens of meters and resembles shallow “caldera-type zeolitization” as defined by Utada et al. (1999).

Alteration of the Bandelier Tuff and other resurgent dome rhyolites tends to be dominated by clinoptilolite and mordenite, although elevated smectite contents have been observed in altered pumice in these rocks. In contrast, resurgent dome sediments, many of which are lacustrine in origin, altered to clinoptilolite and smectite but very little, if any, mordenite. Often, lithic fragments dominated by dark green opal-CT are seen as inclusions in the altered volcanic tuffs. Opal-CT is ubiquitous throughout resurgent dome samples although opal-A is also observed in the lacustrine samples. In other regions of the Valles caldera, extensive acid-sulfate alteration has occurred, producing significant deposits of kaolin minerals, opal, and alunite with jarosite and goethite frequently observed as fracture coatings.

Clinoptilolite and mordenite abundances in the altered volcanics were found to be quite variable, even within the same outcrop. SEM analyses show the morphology of mordenite in these samples to be both fibrous and bladed and that the mordenite is often found as glass shard replacement. Clinoptilolite was found to form sharp prismatic crystals and is often surrounded by more fibrous mordenite and larger blebs of opal. Although inferences can be made locally as to the relative order of formation of the alteration minerals, it is rather difficult to state unequivocally which of the phases were first to form, as it appears that the minerals all formed simultaneously with only local variations affecting the order of crystallization of phases. Chemical analyses of the clinoptilolite and mordenite show them to be extremely calcic with the Valles mordenite plotting on the

calcic edge when compared to published chemical data. Heating tests have shown that most of the heulandite-group zeolite is clinoptilolite, although limited heulandite was also observed.

The geochemical conditions that result in zeolite formation have been outlined in numerous studies. Aqueous silica activity, cation concentrations and ratios, and pH are important fluid parameters that determine which zeolites will form or if they form at all. The presence or absence of minerals and assemblages can lead to certain inferences on conditions and environment of formation. Silica activity was high as inferred from the ubiquitous opal-CT. The presence of mordenite can further constrain the environmental conditions. Mordenite is favored over clinoptilolite by elevated temperature and Na content. Mordenite is not a common zeolite in saline-alkaline lake environments but is found in burial-diagenetic and hydrothermal type deposits and is found in the Yellowstone National Park samples at measured down-hole temperatures of 60 to 200°C. Mordenite commonly coexists with clinoptilolite/heulandite, suggesting similar conditions of formation. However, mordenite tends to form initially at higher temperatures than clinoptilolite and will persist to higher temperatures in diagenetic settings.

Geology and Ar<sup>40/39</sup> dates limit the period of extensive zeolite growth to roughly the first 30 kyr after the current caldera formed (ca. 1.25 to 1.22 Ma). Zeolitic alteration was promoted by saturation of shallow rocks with alkaline lake water (a mixture of meteoric waters and degassed hydrothermal fluids) and by high thermal gradients caused by cooling of the underlying Bandelier pluton and earliest post-caldera rhyolite eruptions. Zeolitic alteration of this type is not found in later volcanic and lacustrine rocks of the caldera moat ( $\leq 0.8$  Ma). In caldera settings, the floor of the collapse depression is underlain by a large subadjacent magma body, which generates a high geothermal gradient. The basin environment is subjected to multiple depositional events associated with resurgence, ongoing volcanism, and formation of intracaldera lakes. Zeolitization may display features apparent in burial diagenesis, saline-alkaline lake environments, and contact metamorphism, as well as hydrothermal alteration. Elevated heat flow due to magmatism and hydrothermal activity rapidly brings rock temperatures up to those attained more slowly in diagenetic deposits due to burial depth. The similarities of these authigenic environments have created confusion, causing Utada et al. (1999) to coin the term “caldera-type zeolitization” to describe the multiple environmental features observed in caldera-hosted zeolite deposits.

## References

- Chipera, S.J. and Bish, D.L. (2002) FULLPAT: A full-pattern quantitative analysis program for X-ray powder diffraction using measured and calculated patterns. *J. Appl. Cryst.* **35**, 744-749.
- Smith, R.L. and Bailey, R.A. (1968) Resurgent cauldrons. *Geol. Soc. Amer. Memoir* **116**, 613-662.
- Utada, M., Shimizu, M., Ito, T. and Inoue, A. (1999) Alteration of caldera-forming rocks related to the Sanzugawa volcanotectonic depression, northeast Honshu, Japan – With special reference to “caldera-type zeolitization.” *Resource Geol. Spec. Issue* No. 20, 129-140.

## **Use of zeolites as selective sorbates for radiological decontamination applications**

**S. J. Chipera, M. E. Smith, D. Counce, D. Ehler, P. Longmire, and T. Taylor**

*Los Alamos National Laboratory, Los Alamos, New Mexico, USA; Email: chipera@lanl.gov*

### **Introduction**

We are currently studying and developing decontamination technologies for mitigation and cleanup in the event of dispersal of radiological materials. Contamination can result from the accidental release of materials associated with industrial applications, of medical devices, or of materials related to the sterilization of foods and other products. Recently, attention has been given to the possibility that terrorists could release radiological materials in urban settings as a method to invoke fear and unrest in the general population. To clean up radiological contamination or spills, cleanup technologies that are efficient, rapid, cost-effective, and produce minimal waste are highly desirable. One of the decontamination methods that we are developing incorporates a novel strippable polymeric coating that can be applied to vertical building surfaces, structures, equipment, or other objects that will be accessible to the public. After allowing the coating to dry, it can then be removed as a strippable film with the radionuclides embedded into the stripped coating, which can then be disposed of or destroyed as a radiological waste material. One of the novel features of the decontamination technology is the use of cation selective, non-toxic, biodegradable oligopeptide chelators to attract and selectively bind the radionuclides of concern.

For the initial applications and experiments,  $^{60}\text{Co}$  and  $^{137}\text{Cs}$  (common isotopes used in medical treatments and food sterilization) were chosen as the radionuclides to study. Careful screening identified oligopeptides that will readily sorb Co. However, no oligopeptides have been identified thus far that demonstrate very high selectivity for Cs. To assist in the early proof of concept experiments, clinoptilolite, which has long been recognized as a stable phase with high selectivity for metal ions such as Cs, was incorporated into the coating. Clinoptilolite has already proven itself in numerous applications to remove Cs from waste waters and other sources.

### **Experimental Methods**

A natural clinoptilolite from Fish Creek Mountains, Nevada (#27054), which is of known high purity, was chosen to assist in the removal of Cs in these experiments. As zeolites are frequently used as fillers and thickeners in materials such as paints and agricultural products, there would be no detrimental effects on the polymeric coating material. Like many fillers, its concentration may be used to help tailor the coating's functional properties in terms of viscosity and drying properties. Typical concentrations of clinoptilolite added to the polymer were 0.1 to 1.0 wt%. Incorporation of zeolite in the polymeric film has an additional benefit in that zeolite serves as a repository for the radionuclides within the film, thus freeing peptide chelators to attract and complex more radionuclides from the surfaces being decontaminated.

To test the effectiveness of the coatings for the decontamination of materials used in construction in urban settings such as buildings, bridges, roadways, etc., 6 x 6 in<sup>2</sup> coupons of concrete, polished marble, and rough-surface granite were cut as surrogate building surfaces. Radioactive Cs and Co were applied to the sample coupons in low concentrations as a dry powder and dissolved in a liquid media. Counting of radioactive disintegrations on both the stripped films with entrained contaminants and the coupons allowed measurement of the very low concentrations of contaminants to access the effectiveness of the decontamination technology.

Although clinoptilolite was initially selected due to the well-established high selectivity for Cs, other zeolites may work as well or better in terms of selectivity for various radionuclides in the presence of competing cations or under different pH conditions such as would be present in a real decontamination scenario. To assess this, a selection of zeolites including clinoptilolite, mordenite, chabazite (SAPO-34), and several synthetic zeolites (Beta, Type Y, ZSM-5) were placed in solution containing 0.1 and 10 ppm Cs and Co to determine uptake. To make the experiments more realistic in complexity, two different solutions containing competing ions were used (Solution 1 = Al, Co, Mg, Na, and Ir in equal molar concentration with Cs; Solution 2 = Ca, Fe,

K, Sr, and Mn in equal molar concentration with Cs). The solutions were kept fairly acidic to keep solutes in solution.

## **Results and Discussion**

The polymeric coating proved to be extremely effective when the contaminant was applied as dry powder; in these conditions extremely high removal rates were obtained. Lesser quantities were removed when the contaminant was applied in liquid media although the technology still proved effective at greatly reducing the residual contamination. When radionuclides are dissolved in liquid media, it was found that the solution, along with the entrained radionuclides, became imbibed into the materials themselves via capillary wicking. The effect was more pronounced with the more porous materials such as the concrete.

In the experiments to assess whether other zeolites work as well or better than clinoptilolite, it was found that all zeolites had a strong affinity for Cs (90–100% uptake), which is the cation for which we have not yet found a sorptive peptide. It was confirmed that Cs uptake for the naturally occurring zeolites at 98–100% (clinoptilolite, mordenite, chabazite) was higher than with the synthetic zeolites. An additional benefit was the strong affinity for Co (95–100% uptake), which should complement sorption by the peptides. Again the natural zeolites outperformed the synthetic zeolites used in this study.

X-ray powder diffraction (XRD) analyses were conducted on the before and after sorption samples to determine if any degradation of the zeolites occurred due to the acidic conditions of the exchange solutions. XRD data showed all the zeolites to have been unaffected by the Cs exchange and high acid conditions except for the case of SAPO-34 (synthetic chabazite), which showed significant degradation. It should be noted, however, that the SAPO-34 zeolite appears to be a poorly crystalline material to begin with. A fully Cs-exchanged clinoptilolite has a significantly different XRD pattern compared to normal clinoptilolite, in terms of intensity ratios, which does not appear in the pattern from the Cs-exchange experiment. This implies that there is a significant amount of exchange capacity left in this sample for Cs. Natural clinoptilolite typically has a cation exchange capacity (CEC) of around 2.2 milliequivalents per gram (meq/g), as does natural mordenite.

Zeolites have long been known to have high sorptive capability for Cs and other radionuclides and have been used quite successfully in the cleanup and processing of radioactive waste streams. Zeolites have also been shown to be effective for decontamination of Cs and Co using the strippable polymeric film decontamination technology that Los Alamos National Laboratory is developing and will continue to play a roll in future development of this process and other decontamination technologies as well.

## **Experimental study of interfacial phenomena in some pollutants-enriched model solutions vs. surface engineered clinoptilolite**

**E. Chmielewská<sup>1</sup>, L. Sabová<sup>1</sup>, K. Gáplovská<sup>1</sup>, F. Pepe<sup>2</sup>, D. Caputo<sup>3</sup>, and A. Wu<sup>4</sup>**

<sup>1</sup>*Comenius University; Bratislava, Slovak Republic; Email: chmielewska@fns.uniba.sk*

<sup>2</sup>*University of Sannio; Benevento, Italy*

<sup>3</sup>*University of Naples Federico II; Naples, Italy*

<sup>4</sup>*University of Aveiro; Aveiro, Portugal*

### **Introduction**

The worldwide interest in renewable resources, reduction of greenhouse gas emissions, and more efficient and effective management of waste has created renewed interest in the fabrication of environmental adsorbents. Recently, numerous approaches have been studied for the development of cost-effective, sustainable adsorbents containing natural polymers like polysaccharides; in particular modified biopolymers derived from chitin, chitosan, starch, and cyclodextrin (Crini, 2005). Natural fibers, biopolymers, and biocomposites integrate the principles of sustainability, industrial ecology, eco-efficiency, green chemistry, and engineering in the development of the new generation of materials, products, and processes. Starch is an inexpensive, annually renewable material derived from corn and other crops. It is suitable for chemical modification. Research on starch-based materials has been widespread in recent years (Gross, 2003). The current research was focused on the fabrication of carbonized and hydrophobized clinoptilolite-rich tuffs using organic carbon-rich substances, particularly starch and waste vegetables, which were pyrolytically combusted to cover the external zeolite surface in carbon (Chmielewská, 2006). Hydrophobization of the zeolite surface was performed by octadecylammonium (ODA) surfactant. Modified clinoptilolite-rich tuffs were examined and compared with each other with regard to the removal of selected pollutants using model aqueous solutions. Moreover, some alternative advanced polysaccharide-based natural clinoptilolite was described and its advantages for the removal of specific pollutants discussed.

### **Experimental Methods**

Natural clinoptilolite-dominated zeolite, crushed and ground to between 0.4–1 mm, was supplied by Zeocem Company, which is mining at the East-Slovakian repository Nižný Hrabovec. The mineralogical and chemical composition of the raw zeolitic material is published elsewhere (Chmielewská, 2003).

Carbonization of the specific C-rich waste substratum took place inside a middle-range temperature pilot combustion chamber (plasmachemical reactor) installed at the laboratory that used direct heating by exhaust gas flow in an oxygen-free atmosphere. Hydrophobization of clinoptilolite with ODA-surfactant was thoroughly described in a paper (Chmielewská, 2006).

Equilibrium adsorption and isotherm measurements at the laboratory were done with aqueous model solutions of specific salts, including surface modified (hydrophobized, carbonized, and immobilized polysaccharide) vs. natural clinoptilolite with the solid-to-liquid ratio 1g/100 mL at  $T = 23 \pm 0.1^\circ\text{C}$ . All experiments were run in triplicate (batchwise mode).

For structural investigation of the synthesized zeolite-based hybrids and material characterization, the following methods have been used: external surface area and porosity of composed zeolite samples were determined at liquid nitrogen temperature (76 K) using a Micromeritics ASAP 2400 Apparatus, the differential thermal analysis (DTA) was performed with PerkinElmer DTA 1700 Derivatograph, scanning electron microscopy (SEM) was accomplished with Electron Probe Microanalyser JEOL-JXA 840A, microtopography of surface-modified zeolite was done with Atomic Force Microscope using the NanoScope Tapping Mode<sup>TM</sup>, and infrared spectra of the samples were made on FT-IR system and PerkinElmer Spectrometer. Aqueous model solutions were analyzed by means of Diode Array Spectrophotometer Hewlett Packard 8452A and by isotachopheresis using the Analyser ZKI 02 (Villa Labeco).

## Results and Discussion

The recent state-of-the-art nanotechnology is making enormous changes in adsorbent mass properties and resulting in numerous economic benefits. The cost-effective repositories of zeolite, bentonite, dolomite, and magnezite commodities have forced Slovakia to the forefront of the EU countries, focusing on further research and prospective activities and fabrication of new, innovative, and sustainable zeolite products. The synthesis, characterization, and application of hydrophobized grain-sized zeolite particles have been the subject of numerous studies showing that these materials exhibit superior hydrodynamic properties. However, carbonization and biopolymers coating on the surface of natural zeolites has not been published so far. Our research has focused on the processing and design of the porous carbon composite-zeolite system, similar to a conventional activated charcoal, to enhance and universalize the adsorption properties of natural clinoptilolite resulting in surface-area enlargement. Another type of zeolite surface modification is immobilization of biomolecules, like calcium alginate or starch, which may form various associates on the zeolite surface to acquire a reaction or adsorption bridging, electrostatic patch, or gelatinous model of aggregation. Surface-induced removal of specific pollutants on siliceous sand and gravel, or simple addition of starch or cellulose into flocculation process, has been applied in water treatment processes for many years. Both ways improve or intensify specific pollutant removal from treated waters. Biomimetics and biotectonics is one of the most dynamically developing sciences; therefore, our intention will be focused on the effective synthesis of novel biocompatible zeolite-composed adsorbents that are both suitable and economically feasible for water treatment processes.

## Acknowledgments

The authors acknowledge partial support of the research by the National Science Council GAV under contract Nos.: 1/1373/04 and 1/1385/04. Also bilateral Slovak-Italian project under the No. 09105 was devoted to the discussed research.

## References

- Chmielewská, E., Tylus, W. and Morvová, M. (2006) Supplementary research of clinoptilolite-rich tuff composites after adsorption trials using the XPS technique. *Central European Journal of Chemistry*, **4**, 1–12.
- Chmielewská, E., Jesenak, K. and Gaplovská, K. (2003) Arsenate and chromate removal on cationic surfactant-loaded and cation-exchanged clinoptilolite rich tuff vs. montmorillonite. *Collection of Czechoslovak Chemical Communications*, **68**, 823–836.
- Crini, G. (2005) Recent developments in polysaccharide-based materials used as adsorbents in wastewater treatment. *Progress in Polymer Science*, **30**, 38–70.
- Gross, R.A. and Kalra, B. (2003) Biopolymers and the environment. *Science*, **299**, 822–825.

## Bactericidal action of Cuban natural clinoptilolite containing clusters and nanoparticles of silver

B. Concepción-Rosabal<sup>1</sup>, N. Bogdanchikova<sup>2</sup>, I. De la Rosa<sup>3,4</sup>, M.T. Olguín<sup>3</sup>, D. Alcántara<sup>3</sup>, and G. Rodríguez-Fuentes<sup>1</sup>

<sup>1</sup>Universidad de La Habana-IMRE; La Habana, Cuba; Email: beatriz@fisica.uh.cu

<sup>2</sup>Universidad Nacional Autonoma de Mexico-CCMC; Ensenada, Mexico;

<sup>3</sup>Instituto Nacional de Investigaciones Nucleares; Mexico D.F., Mexico;

<sup>4</sup>Instituto Tecnológico de Toluca, Metepec, Mexico.

### Introduction

Zeolites are used in various high-tech areas, but recently they have been widely used in the area of water treatment. The bactericide effect of natural zeolites containing silver cations has been described in literature (Rivera-Garza et al., 2000). In our research, we aim to use the Cuban natural clinoptilolite (Ag-NC) containing silver in different states: ions, clusters, and nanoparticles in water purification. The Ag-NC was prepared by an ion-exchange method followed by H<sub>2</sub> reduction at high temperatures. The well-documented facts that this Cuban natural zeolite is innocuous to the human organism (Rodríguez-Fuentes *et al.*, 1997) and the natural abundance of the raw material are both essential when considering Ag-NC composites as an antibacterial material.

### Experimental Methods

Natural clinoptilolite (NZ) is the purified zeolite material obtained from the zeolitic rock of the Tasajeras deposit (Cuba). NZ is a mixture of about 78% clinoptilolite, 5% mordenite, and 17% other minority minerals. Samples of silver incorporated into Cuban natural clinoptilolite were prepared using AgNO<sub>3</sub> ion-exchange method as reported in previous work (Bogdanchikova et al., 2002). The Ag-NC samples were reduced in hydrogen flow at different temperatures. The samples were designed as Ag-NC100, where the number indicates reduction temperature. The results obtained by the combined use of XRD, UV-visible diffuse reflectance spectroscopy (UV-VIS), TEM, and SAXS analysis were carried out in previous work (Concepción-Rosabal et al., 2005) to determine the state of silver in the zeolitic structure and to study the particle-size distribution of the Ag agglomerates produced in the reduced samples. For microbiological experiments, *Escherichia coli* ATCC 8739 was selected as an indicator of fecal contamination of water. Luria Bertani (LB) was used as a growing medium for *E. coli* bacteria.

### Results and Discussion

From the analysis of UV-VIS spectra, we studied the state of silver in each sample and reported the influence of the reduction temperature on the state of silver in the clinoptilolite structure. For Ag-NC samples after ion exchange and, before temperature reduction, a peak at < 250 nm assigned to Ag<sup>+</sup> cations was observed in the spectra of all samples. Reduction at 100°C (Ag-NC100) caused an intensified peak at 320 nm, which is attributed to neutral and partially charged Ag<sub>8</sub><sup>σ+</sup> and Ag<sub>8</sub><sup>0</sup> clusters. The appearance of a very intense peak at 380 nm is attributed to quasi-colloidal particles with a diameter ca. 1 nm. After reduction at 500°C (Ag-NC500), two broad peaks at 300 and 410 nm is attributed to plasma resonance of small silver particles. Hence, reduction at 100°C leads to domination of quasi-colloidal particles and Ag<sub>8</sub> clusters. Reduction at 500°C results in spectra typical of large silver particles

In Figure 1 microbiological experiments are plotted. The cells of *E. coli* in watery solution exist after 75 min, possibly due to the exhaustion of nutrients. When *E. coli* is in contact with Na-NC, an increase in their colony-forming ability is observed. That is, the zeolitic mineral acts as food for these bacteria.



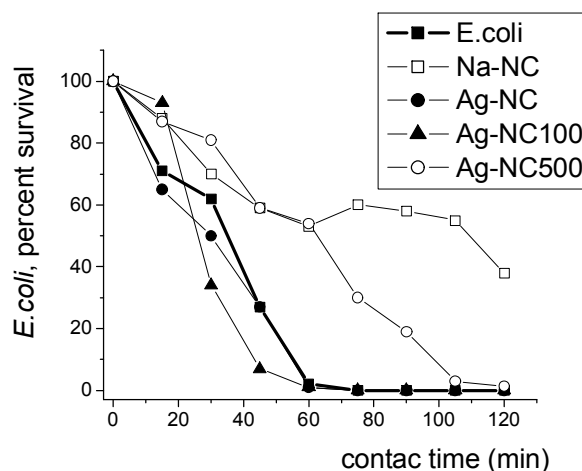


Figure 1. *E. coli* percent survival after being in contact with Ag-natural Cuban clinoptilolite samples

On the other hand, when *E. coli* is in contact with Ag-NC, the bacterial colonies are completely killed after 60 min. This bactericidal effect of Ag-NC is caused by the rapid release of silver ions in the water. In the case of Ag-NC100, the silver clusters are less accessible than ions, and its liberation happens more slowly. In the graph, Ag-NC100 begins to be bactericidal after only 30 min, but its bactericidal action is more durable than Ag-NC. The Ag-NC500 does not have bactericidal effect under these experimental conditions. Thus, the results of the present work demonstrated that the bactericidal effect of Ag-NC and Ag-CN100 zeolitic materials are the most promising for the application for water purification.

## References

- Bogdanchikova, N., Concepción-Rosabal, B., Petranoskii, V., Avalos, M., and Rodríguez-Fuentes, G. (2001) Different silver states stabilized in natural clinoptilolites. *Studies in Surface Science and Catalysis*, **135**, 243-251.
- Concepción-Rosabal, B., Rodríguez-Fuentes, G., Bogdanchikova, N., Bosch, P., Avalos, M., and Lara, V.H. (2005) Comparative study of natural and synthetic clinoptilolites containing silver in different states. *Microporous and Mesoporous Materials*, **86**, 249–255.
- Rivera-Garza, M., Olguín, M.T., García-Sosa, I., Alcántara D., and Rodríguez-Fuentes, G. (2000) Silver supported on natural Mexican zeolite as an antibacterial material. *Microporous and Mesoporous Materials*, **39**, 431–444.
- Rodríguez-Fuentes, G., Barrios, M.A., Iraizoz, A., Perdomo, I., and Cedre, B. (1997) Enterex: Anti-diarrheic drug based on purified natural clinoptilolite. *Zeolites*, **19**(8), 441–448.

## Fumonisin B<sub>1</sub> adsorption on modified clinoptilolite rich zeolitic tuff

A. Daković<sup>1</sup>, M. Tomašević-Čanović<sup>1</sup>, G. E. Rottinghaus<sup>2</sup>, and S. Matijašević<sup>1</sup>

<sup>1</sup>*Institute for Technology of Nuclear and Other Mineral Raw Materials; Belgrade, Serbia and Montenegro;  
Email: a.dakovic@itnms.ac.yu*

<sup>2</sup>*University of Missouri; Columbia, Missouri, USA*

### Introduction

Fumonisin, a group of mycotoxins produced by several *Fusarium* species, are known to cause diseases in horses and swine, as well as cancer in humans. A number of fumonisins have been characterized. They include fumonisin B<sub>1</sub> (FB<sub>1</sub>), FB<sub>2</sub>, FB<sub>3</sub>, and FB<sub>4</sub>. The primary fumonisin of concern in terms of toxicity is FB<sub>1</sub>, which is a common contaminant of corn worldwide (IARC Monographs, 1993).

The most promising and economical approach for detoxifying mycotoxin-contaminated animal feed is the addition of nutritionally inert mineral adsorbents to the diet to decrease the bioavailability of mycotoxins during absorption in the gastrointestinal tract. Aluminosilicates (natural zeolite-clinoptilolite and natural bentonite-montmorillonite) are the most widely utilized adsorbents. The unmodified surfaces of montmorillonite and clinoptilolite are effective in adsorbing aflatoxin *in vitro* and *in vivo*; however, their negatively charged surfaces are ineffective in binding other mycotoxins containing fairly nonpolar functional groups. The binding efficacy of adsorbents for mycotoxins is dependent on the crystal structure and physical properties of the mineral adsorbent as well as on the physio-chemical properties of the mycotoxins.

The objective of this paper is to evaluate the *in vitro* binding affinity of clinoptilolite-rich zeolitic tuff, modified with different amounts of octadecydimethylbenzyl ammonium ions (ODMBA), for FB<sub>1</sub>.

### Experimental Methods

A sample of natural zeolitic-rich tuff from the Zlatokop deposit (Vranje, Serbia, and Montenegro) was used as starting material. The mineralogical composition of the natural zeolitic-rich tuff, determined by X-ray powder diffraction analysis, was primarily clinoptilolite (minimum 85%) with trace amounts of feldspar, quartz and pyrite. The predominant cation associated with the zeolitic-rich tuff was calcium, the minimum cation exchange capacity (CEC) was 139 mmol/100 g and the external cation exchange capacity (ECEC) was 10 mmol/100 g.

The zeolitic tuffs were modified with ODMBA equivalent to 20, 50, and 100% of its ECEC (2, 5, and 10 mmolM<sup>+</sup>/100 g). The zeolitic tuff (5 g) was mixed with 100 mL of each of the three ODMBA solutions in a mixer at 9,000 rpm for 3 min at 50°C, centrifuged, rinsed with distilled water, and dried at 60°C. The samples were denoted as OZ-2, OZ-5, and OZ-10.

FB<sub>1</sub> was obtained from Sigma-Aldrich. A primary FB<sub>1</sub> stock solution (1,000 ppm) was prepared in acetonitrile:water (1:1); test solutions for adsorption studies were prepared by adding FB<sub>1</sub> stock solution to 0.1 M phosphate buffer adjusted to pH 3, 7, and 9 to give a final FB<sub>1</sub> concentration of 2 ppm. In order to investigate FB<sub>1</sub> adsorption, duplicate aliquots of 10 mL of the FB<sub>1</sub> buffer solution were added to 15 mL screw cap polypropylene tubes to which had been added 10, 20, 40, or 100 mg of each adsorbent. Samples were placed on a rotator shaker for 30 minutes at room temperature, centrifuged at 3,000 rpm for 10 minutes, and 2 mL of the aqueous supernatant removed for FB<sub>1</sub> analysis. An aliquot of the original buffered FB<sub>1</sub> solution was used as the HPLC standard. Samples were derivatized with *ortho*-phthalaldehyde (OPA) and examined by HPLC with fluorescence detection.

### Results and Discussion

Preliminary results of FB<sub>1</sub> adsorption (C<sub>0</sub> = 2 ppm, and solid/liquid ratio = 10 g/L) showed that the FB<sub>1</sub> adsorption index on unmodified clinoptilolite rich zeolitic tuff was 90.3%, 2.0%, and 6.2% at pH 3, 7, and 9, respectively (Daković et al., 2004). FB<sub>1</sub> is a hydrophobic molecule, but does contain carboxylic and hydroxyl functional groups (IARC, 1993) which suggests that FB<sub>1</sub> may exist in solution in different forms at different pHs. Since the unmodified surface of the zeolitic tuff has no affinity for anionic species, the results suggest FB<sub>1</sub>

may exist in the anionic form at pH 7 and 9. Because FB<sub>1</sub> is a hydrophobic molecule, it is adsorbed on zeolitic samples modified with long chain organic cations (ODMBA). The results of FB<sub>1</sub> adsorption on zeolitic samples modified with different amounts of ODMBA (OZ-2, OZ-5, and OZ-10), at different solid/liquid ratios, and at different pHs are presented in Table 1.

**Table 1.** FB<sub>1</sub> adsorption on zeolitic samples modified with different amounts of ODMBA

Table 1. <i>FB</i> <sub>1</sub> adsorption on zeolite samples modified with different amounts of <i>S. N. 1</i>									
Solid/liquid ratio (g/L)	OZ-2			OZ-5			OZ-10		
	<i>FB</i> <sub>1</sub> adsorption index, %								
	pH 3	pH 7	pH 9	pH 3	pH 7	pH 9	pH 3	pH 7	pH 9
10	97.5	82.4	82.8	97.5	95.0	96.6	98.0	95.2	95.7
4	74.9	65.6	46.4	92.8	95.3	91.4	92.8	96.4	97.3
2	72.2	37.4	32.4	84.9	76.6	74.2	87.6	85.0	90.2
1	69.3	28.1	16.6	75.5	63.3	56.1	72.7	80.0	75.0

As can be seen in Table 1, the presence of ODMBA ions at the zeolitic surface greatly improved adsorption of FB<sub>1</sub>, especially at pH 7 and 9. All three modified zeolitic tuffs followed a general trend of increasing adsorption of FB<sub>1</sub> with increasing solid/liquid ratio. Also, at the same solid/liquid ratio, FB<sub>1</sub> adsorption indexes increased with increasing percentage of ODMBA at the zeolitic surface. Thus, the highest FB<sub>1</sub> adsorption was achieved with the modified zeolitic tuff OZ-10, in which all inorganic cations at the surface were replaced with ODMBA. At the lower solid/liquid ratios for OZ-2, significant differences occurred in FB<sub>1</sub> adsorption over the three pHs with the highest adsorption indexes observed at pH 3. Since OZ-2 only has 20% of the inorganic cations replaced with ODMBA, the negatively charged uncovered surface of the modified zeolitic tuff may prevent the adsorption of the anionic form of FB<sub>1</sub> at pH 7 and 9. When ODMBA covers a higher percentage of the zeolitic tuff surface (samples OZ-5 and OZ-10), FB<sub>1</sub> adsorption was practically pH independent. Because FB<sub>1</sub> adsorption is higher on the modified zeolitic tuffs than the starting material, this suggests that hydrophobic interactions may play an important role in FB<sub>1</sub> adsorption by the modified zeolitic tuffs.

## References

- Daković, A., Tomašević-Čanović, M., Rottinghaus, G.E., Matijašević, S. and Radosavljević-Mihajlović, A. (2004) Adsorption of Fumonisin B1 on organozeolites. *Proceedings of the 7<sup>th</sup> International Conference on Fundamental and Applied Aspects of Physical Chemistry*. Physical Chemistry 2004 (Belgrade, 21-23 September) **2**, 727–729.
- International Agency for Research on Cancer (1993) Some Naturally Occurring Substances: Food Items and Constituents, Heterocyclic Aromatic Amines and Mycotoxins (1993) *IARC Monographs on the Evaluation of Carcinogenic Risk to Humans*, **56**, 445.

## Hydrothermal treatment of Sardinian clinoptilolite-bearing ignimbrites for increasing cation exchange capacity

A. De Fazio<sup>1</sup>, P. Brotzu<sup>1</sup>, M. R. Ghiara<sup>1</sup>, L. M. Fercia<sup>2</sup>, R. Lonis<sup>2</sup>, and A. Sau<sup>2</sup>

<sup>1</sup>Università Federico II; Napoli, Italy; Email: adefazio@unina.it

<sup>2</sup>PROGEMISA S.p.A. Società Sarda Valorizzazione Georisorse; Cagliari, Italy

Hydrothermal treatment with alkaline solution is a suitable process to enhance the cation-exchange capacity (CEC) of natural zeolite-bearing rocks (Kang and Egashira, 1997). Two clinoptilolite-bearing ignimbrites belonging to Tertiary Sardinian (Italy) volcanism, outcropping near the Bonorva and Romana villages (northern Sardinia), have been treated with 2 M NaOH, 3 M NaOH and 2 M NaOH + Al(OH)<sub>3</sub> at 100, 80 and 70 °C. Bronze Teflon-lined autoclaves and a reactor equipped with a magnetic stirrer were used for hydrothermal interactions. The interaction times ranged from ½ to 36 hours. Clinoptilolite contents (Morbidelli et al., 2001) of starting material ranged from 53±3 wt.% to 58±3 wt.%. The aims of this study were to identify newly-formed minerals and to define CEC of synthetic products in order to highlight the potential use of Sardinian natural clinoptilolite-bearing ignimbrites for agricultural applications and water purification.

The overall data set of hydrothermal experiments indicated that clinoptilolite progressively dissolved and that at higher interaction times a Na-P zeolite started to crystallize. Notably, the hydrothermal experiments performed with a 4560 Parr reactor equipped with magnetic stirrer and 2M NaOH+Al(OH)<sub>3</sub> solutions showed a sharp drop in the interaction times both for Na-P appearance and clinoptilolite dissolution. In particular, less than six hours were required for complete clinoptilolite dissolution and Na-P crystallization at 80°C. The best interacting solution was 2 M NaOH + Al(OH)<sub>3</sub>.

SEM observations on synthesized products showed that the early Na-P products were metastable, changing from typical ball-shaped morphology to star-shaped aggregates (Fig. 1) with increasing interaction, without any change of the XRD patterns.

In order to evaluate CEC of the synthesized products several samples with high interaction times and containing bladed or star-shaped Na-P aggregates were analysed following the technique described by Minato (1997). The CEC of the synthesized products was up to 2.5 times higher than that of the starting materials, ranging from 185 to 268 meq/100 gr.

Our results agree with those obtained by Kang and Esagashira (1997) on Korean natural zeolites. In particular, the data set clearly indicates the following:

- the clinoptilolite-bearing ignimbrites from Tertiary Sardinian volcanism can be used to produce high-power zeolites through hydrothermal treatment with alkaline solutions;
- the best interacting solution investigated is 2 M NaOH + Al(OH)<sub>3</sub>; likely due to the different Si/Al ratio of clinoptilolite and Na-P zeolite;
- using 2 and 3 M NaOH solutions quartz and feldspars are not altered;
- the early Na-P products are metastable and change in morphology with increasing interaction time, likely due to an increase in the crystallinity index.

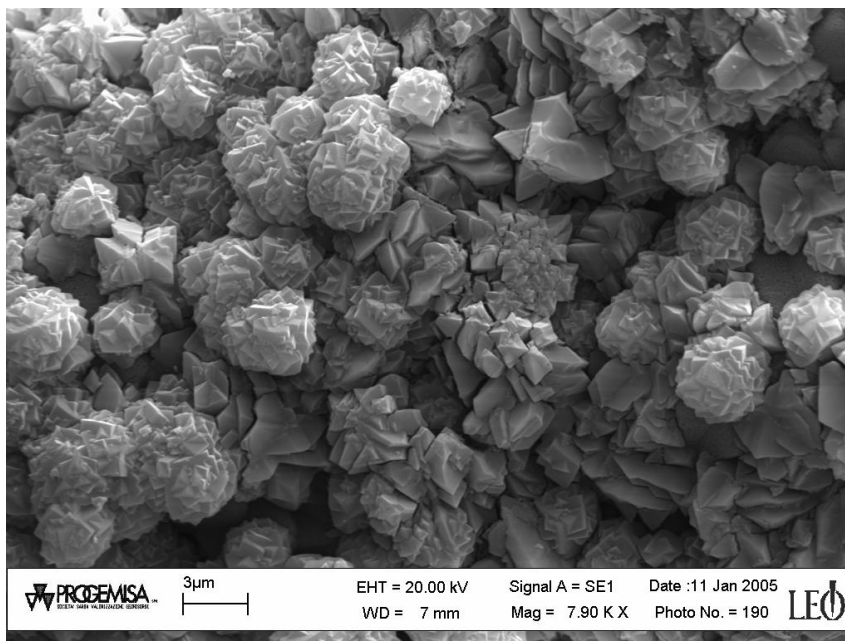


Fig. 1. Hydrothermal experiments with the 4560 Parr reactor.  
 Clusters of star-shaped Na-P zeolite at 6h. of interaction.

## References

- Kang, S.-J. and Egashira, K. (1997) Modification of different grades of Korean natural zeolites for increasing cation exchange capacity. *Applied Clay Science*, **12**, 131–144.
- Minato, H. (1997) Standardization of methods for zeolites determination and techniques for zeolite resources utilization. *Natural Zeolites*, Sofia '95.
- Morbidelli, P., Ghiara, M.R., Lonis, R. and Petti C. (2001) Quantitative distribution and chemical composition of authigenic minerals in clinoptilolite-bearing ignimbrites from northern Sardinia (Italy): influences for minerogenic models. *Periodico Mineralogia*, **70**, 71–97.

## Expanded lightweight aggregates production using Italian zeolitized volcanoclastic materials and industrial wastes

R. de' Gennaro<sup>1</sup>, P. Cappelletti<sup>2</sup>, G. Cerri<sup>3</sup>, M. de' Gennaro<sup>2</sup>, M. Dondi<sup>4</sup>, S.F. Graziano<sup>5</sup>, and A. Langella<sup>5</sup>

<sup>1</sup>Università Federico II; Napoli, Italy; Email: robdegen@unina.it

<sup>2</sup>Terra Università Federico II; Napoli, Italy.

<sup>3</sup>Università di Sassa; Italy

<sup>4</sup>Istituto di Scienza e Tecnologia dei Materiali Ceramici; Faenza, Italy

<sup>5</sup>Università del Sannio; Benevento, Italy

### Introduction

Aggregates are natural or artificial cohesionless materials constituted by elements with different grain size. According to the UNI EN 13055-1 definition, “lightweight aggregates” must have a mass/volume ratio not higher than 2000 kg/m<sup>3</sup> and a bulk unit weight not higher than 1200 kg/m<sup>3</sup>.

Lightweight expanded aggregates (LEA) can be formed by quick heating at high temperatures of some rocks that are able to bloat, like clay or shale. This research is aimed at 1) evaluating a zeolitized byproduct (Cab70), derived from wastes of the granulate production for zootechnical and agricultural uses, as unconventional raw material in LEA production, and taking advantage of its availability and low cost; 2) testing the use of mud from porcelain stoneware tile polishing (DPM) as a bloating agent for Cab70 in LEA production.

### Experimental Methods

Mineralogy of raw materials was investigated by X-ray powder diffraction analyses (XRPD). The reference intensity ratio (RIR) method provided a quantitative estimation of phase components. Chemical analyses were carried out by ICP-OES and XRF.

Both bulk materials and three different mixtures (Mix1 = 85% Cab70 + 15% DPM; Mix2 = 70% Cab70 + 30% DPM; Mix3 = 50% Cab70 + 50% DPM) were characterized by optical thermodilatometry (heating microscope) which allowed us to evaluate the maximum bloating temperature (mbt), the temperature of maximum expansion rate (tmer), and expansion after 20 min and 30 min. Afterwards, aggregates ( $\phi$  = 3–8 mm) obtained from grinding and sieving compacted powders of Cab70, DPM, and from the above three reported mixtures were heated at different temperatures both in a static kiln and a rotating kiln. The produced LEAs were characterized in terms of bulk unit weight and compressive strength. Finally, the rotating kiln allowed us to produce two sets 5 lt each of LEAs (Cab70 heated at 1380°C; Mix2 at 1300°C). On these LEAs the following physical properties were measured: grain size analyses (UNI 7549); grain size; bulk unit weight, also called loose weight; water absorption coefficient; and compressive strength of particles. The internal structure of LEAs was investigated under SEM at “Centro Interdipartimentale di Servizio per le Analisi Geomineralogiche” (C.I.S.A.G.).

### Results and Discussion

It is well known that a material that expands upon heating must be characterized by a suitable chemical composition—that influences the “softening” at high temperatures—and by the presence of substances able to develop gases (such as water, carbon dioxide, oxygen, etc.) (Riley, 1969). According to the Riley's diagram, both Cab70 and DPM have a chemical composition corresponding to expanding materials (Fig. 1). Notwithstanding that Cab70 shows quite a high water content (LOI. > 12% wt.) released upon heating, it exhibits a moderate bloating, which produces high unit weight LEAs (about 1 g/cm<sup>3</sup>). In comparison, the density of LEAs produced using clays is in the 0.5–0.7 g/cm<sup>3</sup> range.

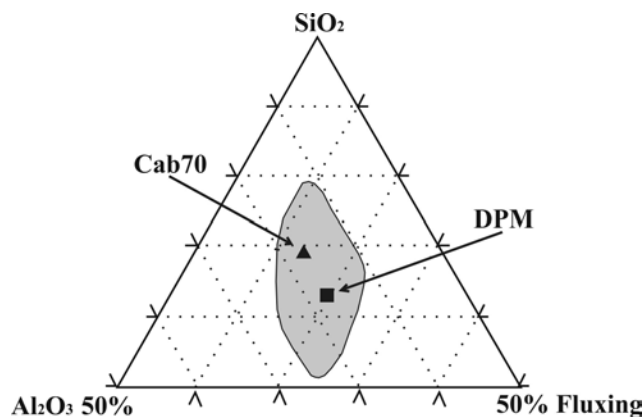


**Figure 1.** Riley diagram for Cab70 and DPM. Shaded area refers to bloating materials

Similar values can be achieved by using DPM starting from temperatures even lower than 1300°C. Development of gas in DPM is due to the presence of about 2% of SiC, occurring as an abrasive agent in porcelain stoneware tile polishing. It can be maintained that water release in Cab70 begins well before the material reaches a pyroplastic state, whereas SiC decomposition in DPM — requiring a higher temperature than water evolution — occurs when the material is in, or close to, the pyroplastic state. All these factors determine a more effective action of gas developed in DPM than in Cab70. Therefore, a better bloating of Cab70 can be achieved by adding DPM. Tests on the three mixtures gave evidence that the Cab70/DPM ratio in Mix2 gave rise to LEAs with unit weights close to those of commercial expanded clays. Table 1 reports the technical features of the two sets of LEAs produced using Cab70 and Mix2 as well as those of commercial Leca® products. Best results were obtained with Mix2, which has the highest strength/density ratio. Furthermore, Mix2 exhibits a very low water-absorption coefficient, comparable to “Lecapiù®”, a commercial product specifically employed to create barriers against humidity. On the contrary, technical parameters of Cab70<sub>LEA</sub> are the worst among the considered materials. In particular, the compressive strength/density ratio attains a very low value.

**Table 1.** Technical features of Cab70 and Mix2 LEAs compared to some commercial expanded clays (Leca® - Lightweight expanded clay aggregates, manufactured in Italy by Laterlite S.p.A., Milan)

Technical feature		Cab70 <sub>L</sub>	Mix2 <sub>L</sub>	Leca®	Lecapiù®	Leca Strutturale®
Grain size range	mm	3 ÷ 10	3 ÷ 10	3 ÷ 8	3 ÷ 8	3 ÷ 15
Loose weight	kg/m <sup>3</sup>	565	460	380	360	770
Bulk unit weight (single grain)	g/cm <sup>3</sup>	1.01	0.81	0.65	0.65	1.3
H <sub>2</sub> O absorption coefficient after 30m	%	3.3	0.7	7	< 1	> 4
H <sub>2</sub> O absorption coefficient after 24h	%	5.7	1.4	11	-	> 7
Compressive strength (single grain)	MPa	0.6	2.9	1.5	1.5	4.5
Compressive strength/density	kJ/kg	0.59	3.58	2.31	2.31	3.46

## References

Riley, C. M. (1969) Relation of chemical properties to the bloating of clays. *J. of Amer. Ceramic Soc.*, **34**, 121-128.

## Zeolite-feldspar epiclastic rocks as flux in ceramic tile manufacturing

R. de' Gennaro<sup>1</sup>, M. Dondi<sup>2</sup>, P. Cappelletti<sup>1</sup>, G. Cerri<sup>3</sup>, M. de' Gennaro<sup>1</sup>, G. Guarini<sup>2</sup>, A. Langella<sup>4</sup>, L. Parlato<sup>1</sup>, and C. Zanelli<sup>2</sup>

<sup>1</sup>Università Federico II, Napoli, Italy; Email: robdegen@unina.it

<sup>2</sup>CNR-ISTEC; Faenza, Italy

<sup>3</sup>Università di Sassari; Italy

<sup>4</sup>Università del Sannio; Benevento, Italy

### Introduction

In a previous work (de' Gennaro et al., 2003) naturally occurring zeolite-feldspar mixtures were found to be promising substitutes for conventional quartz-feldspathic fluxes, widely used in the ceramic industry, due to their enhanced fusibility and grindability.

Epiclastic rocks, outcropping extensively in western Sardinia, Italy, consist mainly of clinoptilolite+sanidine with minor smectite and belong to a volcanic-sedimentary succession resting on the Paleozoic basement and linked to a calcalkaline eruptive activity.

The present study is aimed at assessing the technological behavior of these raw materials during the tile-making process and their effect on the product performance.

### Experimental Methods

Mineralogy of raw materials was investigated by X-ray powder diffraction analyses (XRPD). The reference intensity ratio (RIR) method provided a quantitative estimation of phase components. Chemical analyses were carried out by ICP-OES and XRF.

An average composition of industrial stoneware bodies is characterized by ball clays (40 wt.%), sodic feldspar (25 wt.%), quartz-feldspathic sand (15 wt.%) and granitic aplite and rhyolite (20 wt.%). These last components have been replaced by the investigated epiclastic rock. The stoneware body underwent a laboratory simulation of a ceramic tile process mainly consisting in wet grinding, dry pressing, fast drying, and fast firing. The technological behavior was appraised determining slip properties and particle size distribution (ASTM C 958), as well as shrinkage, bulk density, porosity, and mechanical strength of both unfired and fired tiles (ASTM C 326, ISO 10545-3/4). Moreover, the phase composition was quantified by XRPD Rietveld-RIR.

### Results and Discussion

Each epiclastite has its peculiar features of mineralogical composition: prevailing clinoptilolite (>50%) in sample R2, comparable amount of clinoptilolite and feldspar in sample R3 (46% vs. 34%), and the highest contents of feldspar (> 50%) and smectite (> 30%) in sample R5 (Table 1).

Addition of epiclastic rocks bestowed a better grindability on stoneware bodies, inferred by the finer particle size. On the other side, the high amount of smectite caused an increased slip viscosity, especially in <sub>body</sub>R5, that needed a larger amount of water. Also, zeolite-bearing bodies improved the mechanical strength of the unfired tiles, as already remarked by de' Gennaro et al. (2003), despite their worse compressibility denoted by lower dry bulk density values (Table 2).

**Table 1.** Mineralogical composition of epiclastic rocks. tr = traces, abs = absent.

Epiclastite	Clinoptilolite	Feldspar	Smectite	Opal	Glass	Biotite	Quartz
R2	51	18	19	12	abs	tr	abs
R3	46	34	10	10	abs	tr	tr
R5	abs	55	33	abs	12	tr	abs

The finer particle size and lower bulk density explain the increased firing shrinkage and the faster sintering kinetics, leading to lower firing temperatures to achieve the target of water absorption <1%. It is important to highlight that the presence of epiclastites led to lower total porosity and higher bulk density values, in contrast



with previous observations on zeolitic tuffs into porcelain stoneware bodies (de Gennaro et al., 2003). Epiclastites have a limited effect on stoneware microstructure and phase composition, determining an increase of feldspar content at expense of quartz, with almost steady amounts of mullite and vitreous phase, and little changes of mechanical strength. The main drawback is the relatively high iron content that caused a dark color of stoneware bodies (Table 2).

**Table 2.** Ceramic properties and phase composition of stoneware bodies. *body*R0 stands for the reference sample with no epiclastite

Property	<i>body</i> R0	<i>body</i> R2	<i>body</i> R3	<i>body</i> R5
Slip water content (wt.%)	35.2	37.1	36.3	43.7
Slip median particle size ( $\mu\text{m}$ )	4.8	3.4	3.8	3.6
Dry bulk density ( $\text{g}\cdot\text{cm}^{-3}$ )	1.997	1.903	1.967	1.942
Drying shrinkage ( $\text{cm}\cdot\text{m}^{-1}$ )	0.05	0.05	0.14	0.09
Dry modulus of rupture (MPa)	3.3	3.3	4.3	3.4
Firing temperature ( $^{\circ}\text{C}$ )	1240	1220	1220	1220
Firing shrinkage ( $\text{cm}\cdot\text{m}^{-1}$ )	4.8	6.5	5.6	6.1
Water absorption (wt.%)	0.5	0.7	0.9	0.5
Total porosity (vol.%)	9.3	7.8	8.4	7.0
Bulk density ( $\text{g}\cdot\text{cm}^{-3}$ )	2.290	2.307	2.317	2.333
Modulus of rupture (MPa)	37.4	38.0	36.9	42.2
CIE-Lab ( $L^*$ )	67.6	58.1	57.7	52.7
Quartz (wt.%)	23	18	19	20
Plagioclase (wt.%)	1	6	12	7
Mullite (wt.%)	7	7	7	8
Vitreous phase (wt.%)	69	69	62	65

Epiclastic rocks, consisting of clinoptilolite+feldspar mixtures, can be actually used in the production of stoneware tiles in replacement of conventional quartz-feldspathic fluxes.

The advantages are better grindability, lower firing temperature, improved mechanical strength, and lower porosity. The disadvantages are higher slip viscosity and worse powder compressibility resulting in larger firing shrinkage and darker color due to relatively high iron oxide amounts.

## References

- de' Gennaro, R., Cappelletti, P., Cerri, G., de' Gennaro, M., Dondi, M., Guarini, G., Langella, A. and Naimo, D. (2003) Influence of zeolites on sintering and technological properties of porcelain stoneware tiles. *Journal of the European Ceramic Society*, **23**, 2237–2245.

## Modification of natural clinoptilolite for nitrogen and methane separation

S. Deng, D. Reiersen, and V. Viswanathan

New Mexico State University; Las Cruces, New Mexico; USA; Email: sdeng@nmsu.edu

Natural clinoptilolite zeolite was modified by purification and ion-exchange to improve its adsorption equilibrium and kinetic separation selectivity of nitrogen over methane. The adsorption equilibrium and kinetics data of both nitrogen and methane on several modified clinoptilolite zeolite samples were obtained in a volumetric adsorption apparatus (ASAP 2020, Micromeritics, USA). The adsorption equilibrium and kinetics selectivity were then determined from the experimental data. It was observed that a combined selectivity of 6.5 was obtained on a Mg-exchanged clinoptilolite that may be used as adsorbent for nitrogen and methane separation.

### Introduction

Of the more than 48 natural zeolites species known today, clinoptilolite is the most abundant in soils and sediments. Clinoptilolite is a member of the heulandite group of natural zeolites and has a Si/Al ratio between 4.25 and 5.25. Clinoptilolites have the general zeolite formula of  $\text{Na}_6\text{Al}_6\text{Si}_{30}\text{O}_{72} \cdot 24\text{H}_2\text{O}$ , assuming that  $\text{Na}^+$  is the only charge balancing ion (in all but the rarest cases there is a variety of cations balancing the negative charge). The unit cell is monoclinic, meaning that each edge of the unit cell has a different length, and it is usually characterized on the basis of 72 O atoms and 24 water molecules (Jayaraman et al., 2004).

Clinoptilolite has a unique pore structure that allows smaller molecules such as  $\text{CO}_2$  and  $\text{N}_2$  to diffuse in quickly while hindering the diffusion of slightly larger molecules such as  $\text{CH}_4$ . The clinoptilolite has a series of intersecting channels by which gas penetrates the crystalline structure. The blocking of pores by the exchangeable ions is responsible for the different pore sizes and selectivity of the clinoptilolite. The unique locations of the specific cations, rather than cation size, determine the resulting pore structure and the available pore sizes. At higher pressures and temperatures the cations from a salt solution can be exchanged for those present in a zeolite sample.

The removal of nitrogen from methane gas to meet the pipeline quality of greater than 90% is becoming important in the field of natural gas and enhanced oil recovery processes. The typical US pipeline specifications for natural gas is 950 BTU/ft<sup>3</sup> of < 4% inert contaminants. Methane removed from coal mines, natural gas reserves, and aging gas wells have a naturally occurring concentration of nitrogen; and the process of nitrogen injection for the removal of the methane further increases the level of nitrogen contamination. Nitrogen is typically removed in an adsorption process. Most known sorbents, such as activated carbon, large-pore zeolites and molecular sieves, silica gel, and activated alumina have an equilibrium selectivity that favors methane over nitrogen. Consequently, the search has focused on the modifications of sorbents and the kinetic separation, based on differences in diffusivities in the micropores because of the small but workable difference in the kinetic diameters of these two molecules (3.8 Å for methane and 3.64 Å for nitrogen). Clinoptilolites, a particular class of zeolites, are the current type of adsorbent being investigated because of its properties and cost effectiveness. The current samples tested are being supplied from the St. Cloud Mining Company in New Mexico. Selected natural clinoptilolite zeolites were modified by purification and ion-exchange to improve their adsorption selectivity and adsorption capacity in favor of nitrogen.

### Results and Discussion

It was observed from the adsorption studies that the separation of nitrogen and methane are based on difference of both equilibrium and kinetics. The combined effect of equilibrium and kinetics can be expressed by the following equation (Aguilar-Armenta et al, 2001):

$$\alpha_{\text{N}_2/\text{CH}_4} = \frac{K_{\text{N}_2}}{K_{\text{CH}_4}} \sqrt{\frac{D_{\text{N}_2}}{D_{\text{CH}_4}}} \quad (1)$$

The adsorption isotherms shown in the following figure can be used to calculate the equilibrium selectivity from the ratio of Henry's constants. The kinetic selectivity is calculated from the square root diffusivity ratio. The highest combined selectivity of 6.5 was obtained on an Mg-exchanged sample. These data can be used to evaluate the feasibility of using a pressure swing adsorption process for nitrogen and methane separation.

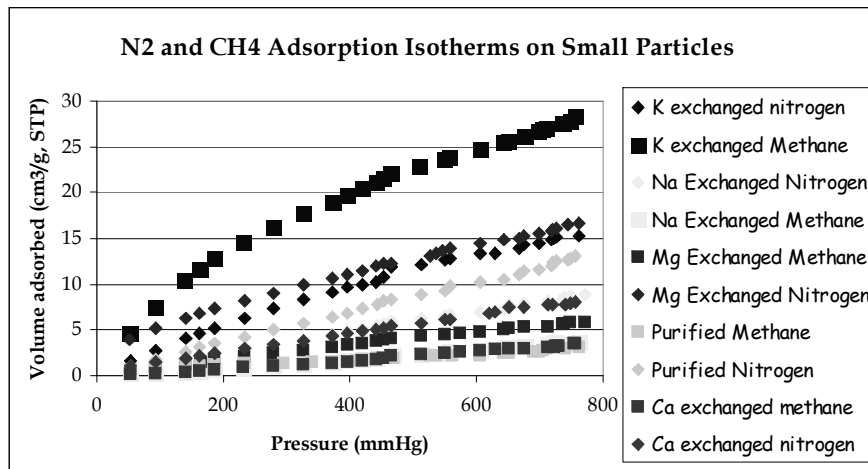


**Figure 1.** Adsorption isotherms of nitrogen and methane on clinoptilolite zeolite adsorbents

## References

- Aguilar-Armenta G., Hernandez-Ramirez G., Flores-Loyola E., Ugarte-Castaneda A., Silva-Gonzalez R., Tabares-Munoz C., Jimenez-Lopez A. and Rodriguez-Castellon E. (2001) Adsorption Kinetics of CO<sub>2</sub>, O<sub>2</sub>, N<sub>2</sub>, and CH<sub>4</sub> in Cation-Exchanged Clinoptilolite, *J. of Phy. Chem. B*, **105**, 1313–1319.
- Jayaraman A., Hernandez-Maldonado A. J., Yang R.T., Chinn D, Munson C. L. and Mohr D. H. (2004) Clinoptilolites for nitrogen/methane separation, *Chem. Eng. Sci.*, **59**, 2407 – 2417.

## **Purification of polluted water collected from Porsuk River, Eskişehir, by using clinoptilolite obtained from Gordes region, Turkey**

**Z. Dikmen and O. Orhun**

*Anadolu University; Eskişehir, Turkey; E-mail: zdikmen@anadolu.edu.tr*

One of the most common environmental applications of natural zeolites is the purification of waste water (Ören A. H. et al, 2006). The aim of this study is to investigate the usability of natural zeolites, clinoptilolite, obtained from Bigadic region, in the purification process of polluted water collected from Porsuk River, Eskişehir. The natural zeolite, clinoptilolite, used in this study has been selected among 2–4 mm dimensional particles by sieving. Then these clinoptilolite particles have been put into a column system prepared by us. Water samples taken from certain points of Porsuk River and at certain hours of the day have been passed through a column system filled with clinoptilolite. During this process, water samples leaving the column have been taken, once every ten minutes for the first hour and then once every twenty minutes after that. For the ions in the water samples, the curves of concentrations for various ions versus time have been obtained. The same process has been repeated for Na, Ca, and Mg ionic forms of clinoptilolite (Dyer A. et al, 1999).

The method used in the preparation of ionic forms, which is called column method, could be expressed as follows: The clinoptilolite samples among 2–4 mm have been put into the column. 1N-NaCl, CaCl<sub>2</sub>, and MgCl<sub>2</sub> solutions have been passed through the column. After the ion exchange processes through the column, clinoptilolite samples taken from column have been dried in the furnace for sixteen hours at 110°C. The obtained ionic forms have been located into the column in order to use in the purification of waste water.

Finally, the obtained results for the natural zeolite, clinoptilolite, have been compared to the results for ionic forms of clinoptilolite.

### **References**

- Dyer, A. and White, K. J. (1999) Cation diffusion in the natural zeolite clinoptilolite. *Thermochimica Acta*, 340-341, 341-348.
- Ören, A. H. and Kaya, A. (2006) Factors affecting adsorption characteristics of Zn<sup>2+</sup> on two natural zeolites, *Journal of Hazardous Materials*, **131**, 1-3, 59-65.

## The application of the extended Freundlich adsorption isotherm model on zeolites

Z. Donmez and O.Orhun

University of Anadolu; Eskişehir, Turkey; Email: zdonmez@anadolu.edu.tr

The statistical mechanical derivations of adsorption isotherms provide detailed information about adsorption of various gases on zeolites. The extended Freundlich adsorption isotherm equation was derived using the basic integral equation of adsorption. It was shown that the adsorption isotherm of CO<sub>2</sub> on BPL activated carbon was fitted to the extended Freundlich adsorption isotherm equation (Silva da Rocha et al, 1997).

In our study, we applied the extended Freundlich adsorption isotherm equation to the adsorption isotherm of nitrogen on clinoptilolite obtained from Gordes region in Turkey. As shown in Figure 1, the isotherms we obtained that had only one term in the equation were fitted to the extended Freundlich adsorption isotherm equation, but having considered terms until the fifteenth term showed a deviation between theoretical and experimental data occurring at a high pressure region. When we made this consideration, the adsorption isotherms were not fitted to the extended Freundlich adsorption isotherm equation.

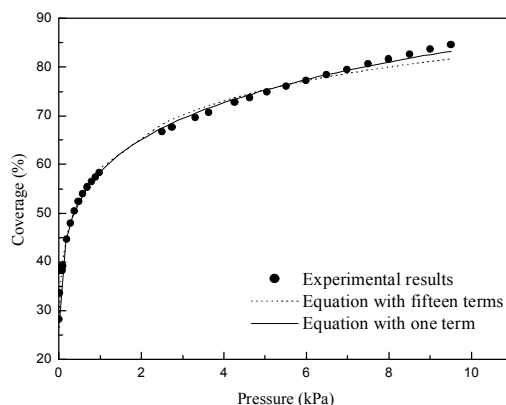


**Figure 1:** Experimental and theoretical isotherm-curves of clinoptilolite obtained from Gordes region, Turkey.

In addition to these experiments, we plan to do more experiments to test the results using different gases as adsorbates and different adsorbents.

### References

Silva da Rocha, M., Iha, K., Corat, E. J., Faleiros, A. C. and Suarez-Iha, M. E.V. (1997) *Journal of Colloid and Interface Science*, **185**, 493.

## Chemical activation of clinoptilolite rich zeolite from central Mexico using microwave heating

E. B. Drag<sup>1</sup> and J. Krasoń<sup>2</sup>

<sup>1</sup>Wrocław University of Technology; Wrocław, Poland; Email: edwarda.drag@pwr.wroc.pl

<sup>2</sup>Geoexplorers International, Inc; Denver, Colorado, USA

Large zeolite deposits recently discovered in central Mexico occur as pervasively zeolitized strata or irregular bodies within Oligocene age rhyolitic tuff and lava flow sequence. These deposits are confined to various size sedimentary basins or half-grabens. Zeolitized strata are usually clean, composed almost exclusively of clinoptilolite. Within the same region and volcanogenic sequence, zeolite mineralization also occurs as a matrix in conglomeratic layers. Clinoptilolite is often a main component of fine-grained material strata containing unaltered volcanic rock fragments. Neither of the latter two types of zeolite mineralization are suitable for mining and commercial consideration. Nevertheless, thickness of the strata and sequence with irregular bodies, composed of clean clinoptilolite, ranges from some ten centimeters up to 100 m.

Considering mining conditions, practical applications, and economic aspects of anticipated research results, only clean, clinoptilolite-rich strata were sampled. Samples used for this research were collected from the Angelica Concession, zeolite-based *OdorBond*<sup>TM</sup> (powdered into irregular <0.85 mm grains), from the Villa de Reyes area in the State of San Luis Potosi, in central Mexico

The purpose of this research has been to determine the possibility of enlarging the sorption capacity of the above-mentioned zeolites. The chemical activation—of acid and alkaline with HCl and NaOH solution—was attempted. The activation process was carried out with a reactive mixture exposed to microwaves and with the traditional method of heating analogous reactive sets at a temperature of 100°C. Various conditions of calcination of clinoptilolite with stable sodium hydroxide at a temperature of 500°C in a microwave oven were also investigated. The influence of various concentrations of reagents and the effect of the time of heating (calcination) of the samples with both methods on the quality of the resulting preparates was investigated. The sorption capacity of such adsorbates as water vapour, carbon dioxide, methanol, benzene, and iodine number were also investigated.

In the selective samples, clinoptilolite activates and the distribution of pores volume were determined and microscopic observations were made. A considerable increase of the volumetric sorption with reference to the investigated adsorbents was observed.

## Catalytic combustion of Cl-VOCs on the zeolitic matrix

E. B. Drag<sup>1</sup>, M. Kułażyński<sup>1</sup>, and J. Krasoń<sup>2</sup>

<sup>1</sup>*Wroclaw University of Technology; Wroclaw, Poland; Email: edwarda.drag@pwr.wroc.pl*

<sup>2</sup>*Geoexplorers International, Inc; Denver, Colorado, USA*

Increasing air pollution has become a serious problem in many countries. The manufacturing and consumption of chlorinated volatile organic compounds (Cl-VOCs) causes a growing concern for proper disposal and destruction of these hazardous wastes. Several control strategies, such as thermal and catalytic oxidation as well as adsorption, are applied to the emission control of these gases.

Because catalytic combustion operates at significantly lower temperatures and with considerably lower residence times than the thermal incineration, it offers many advantages over thermal destruction, resulting from lower combustion temperatures, smaller reactors made of less expensive materials, and higher efficiencies.

In the case of Cl-VOC combustion, the desired reaction is their total oxidation to carbon dioxide, water, and hydrogen chloride without formation of by-products.

Catalysts, which are used for total oxidation of Cl-VOCs, can be classified according to the active component in four groups: Pt-Pd based, vanadium on titanium, chromium based, and others. Noble metal-containing catalysts are the most effective for the catalytic combustion of VOCs. Less data have been published on their performance for destruction of Cl-VOCs and their performance seems to be inferior to chromium-based catalysts because they are severely inhibited by the reaction products (chlorine/hydrogen chloride).

Catalytic combustion of Cl-VOCs demands high resistance of the support material against chemical destruction by reaction products. For this reason, chemical resistance to HCl is one of the essential features of the support of catalyst for Cl-VOC combustion. In most cases, alumina serves as the support of the above-mentioned catalysts. However, a disadvantage is its low resistance against hydrogen chloride and chlorine. This is a reason to search for new carriers more resistant against this aggressive reaction medium. The objective of the presented study was to compare the behavior of different catalytically active components supported on natural zeolites. Combustion of trichloroethylene (TCE) was the model reaction for determination of catalytic activity of those catalysts. Effects of active phase type and reaction parameters on the activity and stability of catalysts supported on clinoptilolite and mordenite zeolites were examined.

Catalysts containing Cu, Cu-Mn, Fe and Pt supported on clinoptilolite and mordenite as well as alumina carriers were investigated. Catalytic activity of the prepared catalysts was determined in the reaction of TCE combustion. The measurements were carried out in a stainless steel fixed bed reactor. The reactor was loaded with 300 mg of the catalyst (particle size: 0.3–0.5 mm). The reaction mixture was composed of two streams mixed before the reactor inlet and carefully measured: air stream (in some experiments saturated with water vapor) and nitrogen stream saturated with TCE vapor in temperature-controlled saturator. The final composition of the feed entered the reactor was 12% O<sub>2</sub>, 88% N<sub>2</sub>, 600–2400 ppm of TCE and it was analyzed before and after it passed through the reactor. A GC equipped with FID was used for analysis.

Activity tests were carried out under normal pressure, at 10,000–75,000 h<sup>-1</sup> and at temperatures of 523–823 K. The activities reported were obtained after a period of 0.5 h operation under the stabilized conditions.

The studied materials are stable supports of catalysts for TCE combustion. Catalysts supported on clinoptilolite and mordenite zeolites differ in activity according to the type of active phase and conditions of reaction.

## **Selective catalytic NO reduction by ammonia on clinoptilolite and mordenite zeolites**

**E. B. Drag<sup>1</sup>, M. Kulażyński<sup>1</sup>, and J. Krason<sup>2</sup>**

<sup>1</sup>*Wrocław University of Technology; Wrocław, Poland; Email: edwarda.drag@pwr.wroc.pl*

<sup>2</sup>*Geoexplorers International, Inc; Denver, Colorado, USA*

The selective catalytic reduction (SCR) of nitric oxides using ammonia is a proven, long-used, and effective process of eliminating nitric oxides from waste gases. Vanadium catalysts carried on titanium dioxide as well as active carbons for nitric oxides reduction are applied. On the catalyst nitric oxides are converted to nitrogen and water.

The efficiency of converting nitric oxides into neutral constituents of the atmosphere depends on the process temperature, concentration of nitric oxides, and the presence of oxygen in the waste gas as well as the ammonia/nitric oxides molar ratio. The catalyst's type and shape, its activity, life period, and work load largely influence its efficiency. The presence of other impurities in the waste gas, e.g., SO<sub>2</sub>, determines the operational conditions of the process. The classic SCR technology process is conducted in the temperature range of 350–450°C.

In this research, as catalyst carriers for selective catalytic reduction of NO by ammonia, the natural zeolites clinoptilolite and mordenite were used. As the active face of the prepared catalyst, copper oxide was used. Two methods of preparation of catalysts were applied: ion exchange and impregnation from the solution of copper salts.

The research was conducted with laboratory flow equipment, using model gas of a determined chemical composition corresponding to a waste gas from power plant. The apparatus consisted of a model gas feeding system and dosage system, catalytic reactor, and analyzer for determining the content of nitric oxide in the gas. The conditions of the process were: temperature range from 100°C to 200°C, GHSV 3000 h<sup>-1</sup> and 5000 h<sup>-1</sup>, oxygen content in the model gas 6%, NO content within the range 400–600 ppm, ratio NH<sub>3</sub>/NO equal to 1, and water vapor content in the model gas ~1 %. Model gas and gas leaving the reactor were analyzed using the MSI 2500 analyzer.

The influence of quantity of copper (1 up to 10 wt.% Cu) on catalyst surface, temperature of SCR reaction, and gas flow space velocity were determined.

Additionally, the zeolite matrix was covered by a carbonaceous material mixture of propane and butane vapor. The samples were carbonized at 600°C in an argon atmosphere. The zeolite-carbon-based catalysts were prepared by a method analogous to that of the zeolite-based catalysts.

The investigated catalyst were high activity in SCR reaction tests. In selected catalysts porosity and sorption capacity as well as the bulk density were determined.

The ion exchange method of preparation of catalysts was most effective for both mordenite and clinoptilolite.

Activities of the prepared catalysts in laboratory tests of NO reduction by ammonia in the range 300–500 °C were 97 and 93%, respectively.



## Removal of PAHs from n-paraffin by modified clinoptilolite

H. Faghihian and M. H. Mousazadeh

University of Isfahan; Isfahan, Iran; Email: h.faghih@sci.ui.ac.ir

### Introduction

Polycyclic aromatic hydrocarbons (PAHs) are a complex class of organic compounds containing two or more fused aromatic rings. PAHs are widespread contaminants of the environment and a number of them are either known or suspected carcinogens. These compounds accompany n-paraffin and must be removed when n-paraffin is used in food and pharmaceutical production.

In this research the use of clinoptilolite and its modified forms for removal of PAHs from n-paraffin was studied. Modification was performed either by replacement of surface cations of zeolite by hexadecyltrimethylammonium ion or by introduction of cations into zeolite channels through ion exchange. Adsorption of PAHs by natural clinoptilolite was negligible, whereas the exchanged forms of zeolite removed between 14.88 to 18.64% of the initial PAH content of n-paraffin. The structure of zeolite did not change upon modification. Regeneration of zeolite was performed by washing with chloroform.

The removal of PAHs and other impurities from n-paraffins is accomplished by different methods. In the conventional method paraffin is treated with oleum (sulfuric acid and sulfur trioxide). The acid tar which is produced in this method is difficult to separate. Solvent extraction is also used for paraffin purification. The impurity level of this method exceeds 0.3% by weight and is higher than the desired level. The current method for removal of PAHs is catalytic hydrogenation. The main disadvantage of this method is conversion of some naphthenic compounds to aromatics. Purification of n-paraffin by adsorbents such as aluminosilicate or activated charcoal has also been studied. Surfactant-modified zeolites (SMZ) have been used as effective sorbents for removal of inorganic cations, inorganic anions, and neutral organic materials. SMZ prepared with hexadecyltrimethylammonium (HDTMA) is stable in high ionic strength solutions and over a wide range of pH. More than 90% of HDTMA remains bound to the zeolite surface after regeneration.

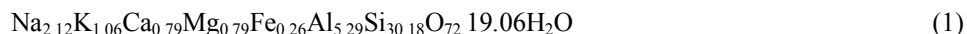
### Experimental Methods

Clinoptilolite was obtained from deposits of the Semnan region in northeastern Iran. The raw material was ground and screened ( $>250\mu\text{m}$ – $<420\mu\text{m}$ ). After removal of magnetic impurities by a magnetic bar, the ground sample was refluxed with deionized water in order to remove soluble impurities. The purified sample was characterized by wet chemical analysis, X-ray diffraction (XRD), and thermal methods (derivative thermogravimetry, DTG). To study the effect of cations on PAH removal, different cations including  $\text{Fe}^{3+}$ ,  $\text{Ag}^+$ ,  $\text{H}^+$ ,  $\text{NH}_4^+$  were introduced into the zeolite by ion exchange. Surfactant-modified zeolite was also prepared by contacting the purified zeolite with a solution of HDTMA. The samples are assigned as NZ for natural zeolite, NH4Z (treated with 0.1 M  $\text{NH}_4$ ), FeZ (treated with 0.1 M  $\text{FeCl}_3$ ), AgZ (treated with 0.1 M  $\text{AgNO}_3$ ) and SMZ (treated with 0.1 M HDTMA).

The cation content of the exchanged samples was estimated by atomic adsorption spectrometry using a Varian model 500 spectrometer. The surfactant content of the modified zeolite was determined by a CHN analyzer (Leco 300 model). DTG curves of the samples taken by a Mettler TA 4000 thermal analyzer were used to study thermal behavior of the samples. Adsorption of PAHs by natural and modified samples was studied under different experimental conditions. The amount of adsorbed PAHs was evaluated by a spectrophotometric method using a Varian UV-VIS spectrophotometer model CARY-500. Naphthalene was used as standard material and chloroform as solvent. The absorbance was measured at 269 nm. The standard addition method was used to prepare the calibration curve. IR spectra of the samples were taken by a Buck-500 Scientific Co. spectrometer to confirm the adsorption of PAHs by zeolite. Regeneration of samples was performed by treating the zeolite with chloroform by Soxhlet method.

### Results and Discussion

Based on the chemical analysis data, the unit cell formula of the mineral was calculated as:



The X-ray pattern of the sample was compared to the standard in the library of the instrument and had similar characteristic lines. Introduction of new cations into zeolite framework altered both water content and dehydration temperature. In  $\text{NH}_4\text{Z}$  sample the weight loss occurred between 340–550 K. This can be attributed to the slow release of  $\text{NH}_3$  molecules. Due to the thermal decomposition of surfactant, a weight loss peak was observed between 425–580 K in SMZ sample.

Impure paraffin was prepared from the Isfahan Refinery Complex. It contains 2.32% aromatic, 73.84% paraffin, 23.47% naphthenic and 0.37% olefin compounds. Adsorption of PAHs by natural clinoptilolite was negligible, whereas the exchanged forms of zeolite removed between 14.88 to 18.64% of the initial PAH content of n-paraffin. The structure of zeolite did not change upon modification.

## **Use of Cuban natural zeolites in Brazil: Fields of application**

**F. Farias, F. Borsatto, J. A. Febles, and M. Velázquez**

*Celta Brasil; Sao Paulo, Brasil; Email: fernandofaria@celtabrasil.com.br*

From the beginning of 2004, commercialization of Cuban natural zeolites began in Brazil. First, we analyzed the international trends for the market of this mineral. Then, we analyzed the main sectors of the market according to the characteristics of the southern region of Brazil. This was the most effective way to develop the first stage of commercialization. As a result of this investigation, we learned that the agricultural sector demands large volumes of the product. We conducted a series of introductory studies and validated the results obtained in Cuba and in other parts of the world on the fertilizer industry: Cuban natural zeolites improve substrates and soils for the cultivation of different crops, and improve the environmental conditions for pigs, birds, cattle raising, and so forth.

A second field of potential demand for this mineral is the industry of powdered detergents. Cuban natural zeolites are substituted to a certain percent for polluting products such as tripolyphosphates, which are widely used in this industry.

Another field in which intense work has been done is the introduction of Cuban natural zeolites in technologies for water treatment—treatments for potable water, residential water, and swimming pools.

In addition, Cuban natural zeolites are used in pet litter and to treat domestic animal waste (e.g., cattle manure).

To provide technological support for the research of Cuban natural zeolites and its wide range of uses, our company has developed an area that has a laboratory, a group of specialists, specialized technical consultants, and a show room that was inaugurated in April, 2006, where people can appreciate in a permanent way the different uses of this versatile mineral. Known as the Latin American Center of Reference of Zeolites, it includes live exhibits with plants and animals.

Our current work with Cuban natural zeolites shows the most outstanding results obtained so far, as well as indicates objectives to reach in the future.

## **Agricultural results obtained in the use of the Cuban zeolites in some Latin American countries**

**J. A. Febles González and M. Velázquez**

*Research Center for Mining and Metallurgy; Havana City, Cuba; Email: febles@cipimm.cu*

Since mid 1980s the study of the use of natural zeolites in a different application fields—agriculture — has attracted great attention in our country. The shortage of chemical fertilizers in the 1990s stimulated a quick utilization of the different investigative results that had been obtained since the mid-80s in the application of natural zeolites in the fertilizer industry, and in agriculture in general. As a result, natural zeolites were used as an economic alternative for fertilizers; they were produced in different combinations with minerals such as phosphoric rocks, organic sources, etc. A wide range of products of organo-mineral character were substituted to a great extent for the nutrients that the different cultivations required. At this moment in Cuba, almost all chemical fertilizers used in agriculture contain 15–25% natural zeolites. This has not only allowed us to increase the volumes of fertilizing products, but has also contributed to an increase in agricultural yields and the quality of crops, the improvement of soils, and the gradual improvement of the environment.

All these results have favorably contributed to an increase of interest in zeolites by agricultural producers of the region, and to the export of Cuban natural zeolites to Mexico, Colombia, Brazil, Guatemala, Martinique, and other countries.

Present work shows some of the agricultural results obtained from the use of Cuban natural zeolites in our country, as well as results obtained from more than 10 years of applications of Cuban natural zeolites through commercialization in different countries of the region. These results demonstrate the quality of Cuban natural zeolites and their effectiveness in different agricultural applications, as well as the different technologies that have been developed to increase the efficiency of the fertilizers in zeoponic, organoponic, and other types of cultivations and in different edaphoclimatic conditions.

## Accessing real micropore volumes of zeolites

R. X. Fischer<sup>1</sup>, W. H. Baur<sup>2</sup>, C. C. Pavel<sup>3</sup>, and W. Schmidt<sup>3</sup>

<sup>1</sup>Universität Bremen; Bremen, Germany; Email: rfischer@uni-bremen.de

<sup>2</sup>Northwestern University; Evanston, Illinois, USA

<sup>3</sup>Max-Planck-Institut für Kohlenforschung; Mülheim an der Ruhr, Germany

An outstanding property of zeolites is their ability to selectively adsorb molecules and gases. The adsorption capacity depends on the accessible free space in the zeolite pores. Access is limited by the size of the adsorbed molecule, the aperture of the pores, and the fillings of the cavities by cations and/or neutral species. Exact knowledge of the crystal structure theoretically provides all information to calculate the accessible void volume. However, such a calculation requires precise data on the volumes of the individual ions and assumptions on the interactions between probe molecules and the zeolite host material. Küppers and Liebau (2004) applied a method to microporous materials introduced by Spek (2002) to determine the geometry of pores. They calculate an envelope of the atoms building the inside wall of zeolite cavities at a distance  $\Delta$  (default is  $\Delta = 1.2 \text{ \AA}$ ) to the atoms' surfaces and then determine the free void space by superimposing a narrow grid and counting the grid points falling within the envelope. We have implemented this algorithm in the program package *BRASS* (Bremen Rietveld Analysis and Structure Suite; Birkenstock, Fischer, and Messner, 2006) calculating the void volume from refined or prescribed atomic parameters.

It is our aim to evaluate this method by comparing the theoretical calculations with sorption experiments on zeolite A. This zeolite contains both big (*grc*  $4^{12}6^88^6$  units, often called  $\alpha$ -cage) and small (*toc*  $4^66^8$  units, often named  $\beta$ -cage) pores with 4-ring, 6-ring, and 8-ring windows and therefore is an appropriate candidate for this study (Fischer and Baur, 2006).

The volumes of micropores of zeolitic materials are typically measured using gas adsorption methods using either nitrogen (at 77K) or argon (at 87K or 77K) as adsorptives. The volumes that are probed with such gases are the volumes being accessible by the adsorptives. Pores with pore openings smaller than the size of the gas molecules or atoms are thus not accessible (Fig. 1a) and the micropore volumes calculated on the basis of such measurements obviously do not report the real micropore volumes. For very small pores of sizes smaller than double the size of the probe molecules, the situation is even more complex because the molecules cannot fill such pores completely due to sterical hindrance (Figure 1b). In this case, the full micropore volume is not measured either. The effect of both problems could be reduced by using very small probe molecules which are able to pass the narrow windows and fill the micropores more or less completely (Fig. 1c).

The smallest probe molecules/atoms available are hydrogen molecules or helium atoms. Unfortunately, adsorption of these gases would require extremely low temperatures. In order to probe the true micropore volumes of zeolites, we investigated two alternative approaches. In a first attempt, we used water adsorption to evaluate the micropore sizes of a model zeolite. Water molecules are also small enough to pass even 6-rings in frameworks, and water adsorption can be measured at moderate temperatures. However, water adsorption is rather time consuming so we also investigated water desorption experiments on fully hydrated zeolites by measuring the amount of desorbing water upon heating on a thermobalance. These results were compared to those obtained by water adsorption experiments. In a second attempt, we tested helium pycnometry as a tool to obtain the specific densities of the zeolite framework (+ cations). Helium should be able to penetrate the complete pore system of a given dehydrated zeolite and should result in the volume of the zeolite framework according to Figure 1c.

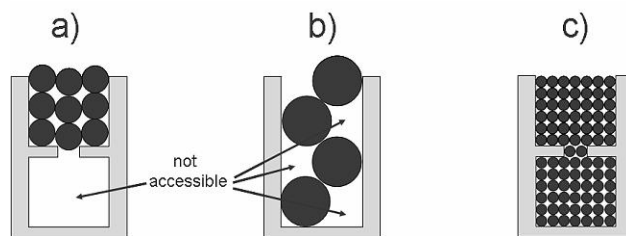


**Figure 1.** Accessibility of micropores by probe molecules

The Na-LTA zeolite was exchanged by Li, K, Rb, and Cs cations to obtain materials with different pore volumes due to the different sizes of the respective cations. The volumes determined by the adsorption experiments were compared with the volumes calculated by the method after Küppers and Liebau (2004).

The comparison of the experimental data with calculated data yields detailed information on the applicability of various probe molecules to zeolite sorption studies as well as on the crystallographic parameters determining the accessible void volume.

## References

- Birkenstock, J., Fischer, R.X. and Messner, T. (2006) BRASS: The Bremen Rietveld Analysis and Structure Suite. University of Bremen. [www.brass.uni-bremen.de](http://www.brass.uni-bremen.de).
- Fischer, R.X. and Baur, W.H. (2006) *Zeolite-type crystal structures and their chemistry. Framework Type Codes LTA to RHO*. Subvolume D in Landolt-Börnstein, *Numerical data and functional relationships in science and technology*, New Series, Group IV: Physical Chemistry, Volume 14, *Microporous and other framework materials with zeolite-type structures*, (R.X. Fischer and W.H. Baur, editors), Springer, Berlin, in press.
- Küppers, H. and Liebau, F. (2004) On the determination of volumes and shapes of micropores in inorganic crystals. *Zeitschrift für Kristallographie. Supplement Issue*, **21**, 120.
- Spek, A.L. (2002) PLATON. A multipurpose crystallographic tool. Utrecht University, NL.

## Utilization of zeolite for reducing sodium and salt concentrations in saline-sodic coalbed natural gas waters

G. K. Ganjegunte<sup>1</sup>, G. F. Vance<sup>2</sup>, R. W. Gregory<sup>3</sup>, and R. C. Surdam<sup>3</sup>

<sup>1</sup>Texas A&M University System; El Paso, Texas, USA; Email: gkganjegunte@ag.tamu.edu

<sup>2</sup>University of Wyoming; Laramie, Wyoming, USA

<sup>3</sup>Wyoming State Geological Survey; Laramie, Wyoming, USA

Coalbed natural gas (CBNG) production involves pumping water (e.g., CBNG water) from coal seams to reduce hydrostatic pressure in order to allow gas release. Unfortunately, CBNG water is dominated by sodium ( $\text{Na}^+$ ) and bicarbonate ( $\text{HCO}_3^-$ ) ions, with sodium adsorption ratios (SAR) that can exceed generally acceptable levels for surface disposal. Therefore, management of CBNG water is a major environmental challenge because of its quantity and quality. We evaluated the use of Ca-rich natural zeolites (80–90% clinoptilolite with a cation exchange capacity (CEC) of  $\sim 110$  meq/g) for removing  $\text{Na}^+$ , reducing SARs, and enhancing the beneficial use of the treated waters. A column study was performed using two CBNG waters with different SARs (19 and  $107 \text{ mmol}^{1/2} \text{ L}^{-1/2}$ ) and four zeolite size fractions. Results indicated initial leachate SARs of both CBNG waters decreased to  $<1.0$  after passing through zeolite columns. Exchange reactions involving high  $\text{Na}^+$  conditions suggested 1 tonne of zeolite, depending upon size, can be used to treat 50,000 to 85,000 liters of CBNG water to reduce SAR from  $34 \text{ mmol}^{1/2} \text{ L}^{-1/2}$  (typical SAR values in the Powder River Basin (PRB)) to an acceptable level of  $10 \text{ mmol}^{1/2} \text{ L}^{-1/2}$ . The use of zeolite technology appears to be an efficient, effective, and possibly affordable water treatment alternative that can maximize the beneficial use of CBNG water. These laboratory studies are being used to design an economically viable and efficient water treatment process for CBNG waters in the PRB.

### Introduction

Natural gas from coal deposits is considered an important source of energy and its production is a fast-growing industry in the western U.S. Within the PRB, there are about 24,000 CBNG wells permitted with another 50,000 wells scheduled to be drilled in the near future. CBNG production is accomplished by pumping water from coal seams to reduce hydraulic pressure in order to facilitate gas migration; cumulative CBNG-water over 15 years from PRB wells is estimated to be 366,000 ha-m (BLM, 2003). The quality of CBNG water is highly variable in the PRB and can be of poor quality (pH from 7.0 to 9.9, SAR as high as  $70 \text{ mmol}^{1/2} \text{ L}^{-1/2}$  and EC ranging from 0.4 to  $4.8 \text{ dS m}^{-1}$ ) (Rice et al., 2002). Use of CBNG waters for irrigation is becoming a popular option; however, there can be serious impacts to soil properties if not managed properly (Ganjegunte et al., 2005). Therefore, finding cost effective ways of improving CBNG water quality is the key to managing this enormous amount of potentially poor-quality water.

This study evaluated a Ca-rich zeolite for its possible improvement of CBNG water chemistry that would enable the beneficial use of treated CBNG waters by the industry, land owners, and for downstream users. Objectives of this study were to characterize the quality of 2 different CBNG waters, evaluate different size fractions of a Ca-rich zeolite from the St. Cloud deposit in New Mexico, evaluate the potential of these zeolite materials to improve poor-quality CBNG water, and to project how effective the zeolite would be for removing  $\text{Na}^+$  and reducing the SAR of the treated CBNG waters.

### Experimental Methods

Zeolite used in this study has a relatively high Ca content and was obtained from the St. Cloud zeolite mine near Winston, NM (Austin and Bowman 2002). Column experiments were conducted with 2 different qualities of CBNG water with different  $\text{Na}^+$  levels (Table 1) and 4 zeolites sizes (4x6, 6x8, 6x14 and 14x40) to determine cation exchange dynamics under low and high SAR conditions. Triplicates of each zeolite size (50 g) were loaded into each column (total of 24). Columns were leached 40 times with 50 ml volumes of the 2 CBNG waters. Leachates were analyzed for pH, EC, and concentrations of soluble cations  $\text{Na}^+$ ,  $\text{Ca}^{2+}$  and  $\text{Mg}^{2+}$ , with SAR determined from these cations.

**Table 1.** Selected chemical properties of CBNG water

Parameter	Low SAR	High SAR
pH	9.10	9.85
EC (dS/m)	0.69	4.76
Ca (mg/L)	4	4
Mg (mg/L)	1	1
Na (mg/L)	159	1129
SAR ( $\text{mmol}^{1/2}/\text{L}^{1/2}$ )	19	107

## Results and Discussion

The Ca-rich zeolite materials removed significant amounts of  $\text{Na}^+$  from CBNG waters both at low and high SAR conditions (Fig. 1). After first leaching, zeolites reduced SAR values of high Na and low Na waters from 104 to <1 and 19 to 0.6  $\text{mmol}^{1/2} \text{L}^{-1/2}$ , respectively. Based on column exchange reactions using high  $\text{Na}^+$  conditions, a tonne of zeolite can be used to treat 750 barrels CBNG water to reduce SAR from 34 (typical of PRB) to 10  $\text{mmol}^{1/2} \text{L}^{-1/2}$  (acceptable to most crops). Zeolite technology is potentially an efficient, effective, and affordable water treatment alternative that could maximize the beneficial use of CBNG water.

Zeolite technology is a novel approach that is efficient and cost-effective for improving the quality of large volumes of saline-sodic water being produced by the CBNG industry in the PRB of Wyoming & Montana. Using zeolites to treat CBNG water is a win-win strategy, which will promote the CBNG industry, federal, and state revenue, and agricultural production in addition to providing an environmentally friendly CBNG water management practice.

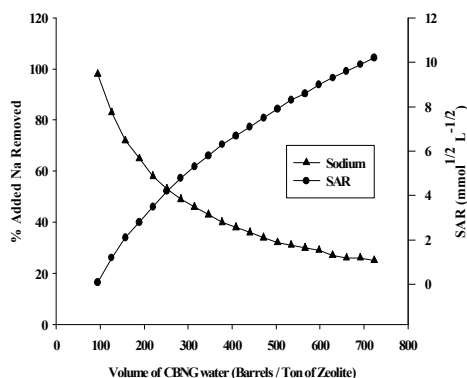


**Figure 1.** Reduction in cumulative CBNG water Na vs. change in SAR using zeolite ion-exchange columns



## Human urine treated by MgO and zeolite for efficient nutrient recovery and reuse in agriculture

Z. Ganrot and G. Dave

Göteborg University; Göteborg, Sweden; Email: zsofia.ganrot@miljo.gu.se

Recycling of nutrients between urban areas and farmland is a critical step toward an ecologically sustainable development. Human urine is the most nutrient-abundant part among domestic waste components, and urine separation has been proposed to achieve maximum recovery and recirculation of nutrients in Sweden. Several types of toilets and small-scale separation systems have been installed and tested. Storage and transportation of large amounts of urine, as well as spreading and hygiene, are the main obstacles in achieving system efficiency. The biggest problem today is reuse of anthropogenic nutrients on arable land.

This paper presents two different urine-processing techniques:

- Recovery of nutrients from urine as solid minerals, mainly as struvite.
- Use of of zeolite as an efficient nutrient adsorbent material in urine. A short presentation of the test results of plant availability of nutrient made on the obtained fertilizers in short-term pot trials on wheat under climate chamber conditions will be given.

Testing nutrient recovery from urine and testing the fertilizer value provided the following results:

- With the addition of small amounts of MgO to human urine, struvite was obtained and identified as the main component. With struvite precipitation, 98–100% of P, 22–64% of K, and 2–5.6 % of Ca were recovered. A 25% of the N recovery can also be achieved due to struvite crystallization.
- Natural zeolites (especially clinoptilolite) adsorb ammonium rapidly; the quality of the zeolite, its grain size, and the ion strength of the urine are important for the adsorption. Zeolite adsorption used in combination with struvite precipitation could recover 64–80% of the N in laboratory tests. Optimum combined recovery of N and P occurred at added concentrations of 0.1 g of MgO and 15–30 g of zeolite per liter of urine. The optimal additions are dependent on the initial N and P concentrations of the urine.

In the tests on wheat (*Triticum aestivum* L.), the struvite/zeolite mixtures showed better nutrient availability than the struvite alone, probably due to a synergistic effect between the struvite dissolution and zeolite ion exchange. Both struvite and struvite/zeolite mixtures acted as slow-release fertilizers. In tests with five substrates and five nutrient sources (two of them commercial fertilizers), the struvite/zeolite mixture from urine was similar to DAP and CaP as slow-release P-fertilizer.

## **New organo-zeolite fertilizer**

**T. A. Gasparyan, G. G. Karamyan, G. M. Aleksanyan, and L. R. Revazyan**

*Yerevan State University; Yerevan, Republic of Armenia; Email: gurgenal@ysu.am*

Modern technologies in agriculture are directed on the use of natural bio-fertilizers and other products aimed to enhance crop yieldss, improve soil quality, and kill plant pests, etc.

The average quantity of applied chemical fertilizers composed of nitrogen, phosphorous, and potassium is 100–120 kg/he. Often, common methods of fertilizer application are unsuccessful because the useful ingredients are washed out from the soil before entering the plant. These components will enter rivers, lakes, seas, causing to environment pollution.

On the other hand, the excess addition of fertilizers has some disadvantages; for example, nitrogen-based compounds can result in formation of very toxic nitrites and nitrosamines which may lead to various human illnesses.

The method of gradual addition of necessary components (potassium, phosphorus, nitrogen, microelements) into the soil may be carried out by using porous substrates, similar to inexpensive natural zeolites. Such fertilizer has prolonged effect on slow releasing the useful components and accumulation of water. It is used for conditioning and improving acidic, sandy, flood, volcanic, and turf-podzol soils.

Recently, there are widely used zeolites containing various nutrient additives. The distinctive feature of our fertilizer is that it contains humic acid, which has very beneficial influence on the quality and quantity of a crop and the treated soil. Our procedure also includes using a method of optimal saturation of zeolites with necessary components and humics extracted from raw natural materials.

New organo-zeolite fertilizer (NOZF) is a mixture of Armenian natural zeolite-clinoptilolite with humic and fulvic acids extracted from various organic and natural mineral materials (biohumus, peat, bituminous shale, lignite, etc.). The fertilizer is a quaggy, granulated mass, easily introduced into the soil. Preliminarily, the humic and fulvic acids are prepared by a special technique, and then ground zeolite (up to 1 mm) is impregnated with these acids. Such fertilizer contains all nutritious elements (macro and micro) in an easily assimilated (for plant) form; slowly and in an optimal way, it gives back to the plant these nutritions together with moisture. It is long lasting, does not require additional top-dressing, and has no unpleasant odor.

The addition of organo-zeolite fertilizer to dehumized acidic, neutral, and, particularly, high sandy soils leads to an increased yield of vegetables, gourds, and flowers, mainly cucumbers, tomatoes, cabbage, potatoes, etc., while simultaneously improving the soil quality (physical-chemical characteristics, fertility). NOZF can be successfully used in outdoor as well as indoor conditions.

Among other advantages of NOZF is the prevention of an accumulation of nitrates and heavy metals. Moreover, this fertilizer increases the content of sugar, ascorbic acid (Vitamin C), carotene, and other useful compounds in the plants and soil.

## A comparative study of $\text{Cd}^{2+}$ removal from aqueous solutions using two different Turkish clinoptilolite samples

K. Gedik and I. Imamoglu

Middle East Technical University; Ankara, Turkey; Email: kgedik@metu.edu.tr

### Introduction

Low-cost technologies that result in no further waste production and are applicable to metal-contaminated wastewaters are becoming popular. Zeolites, meanwhile, are widely used in pollution control applications as sorbents, especially during metal removal studies, owing to their high reserves, advantageous ion exchange capacities, and low cost.

In this study, clinoptilolite samples from two important reserves in Turkey were tested for their efficacy in removing  $\text{Cd}^{2+}$  ions from synthetic wastewaters. The effect of pH, particle size, temperature, prewashing of as-received samples, and metal concentration on metal removal were investigated in batch-type reactors. Both as-received and conditioned forms of clinoptilolite were used in the study.

### Experimental Methods

Zeolite samples were taken from two different sedimentary deposits in western Anatolia, namely Gördes (CLIN-1) in Manisa and Bigadiç (CLIN-2) in Balıkesir. They were ground and sieved to 0.17–0.83 mm, 0.83–1.18 mm, and 1.18–1.40 mm fractions. Characterization was done using XRD, XRF, and SEM analysis.

Analytical grade chemicals were used in experiments. Conditioning was performed by shaking flasks containing 10 g clinoptilolite in 250 mL of 2M NaCl solution at 150 rpm and 30°C for 24 hrs. Batch experiments were conducted at 1/100 w/v solid to liquid ratio, 125 rpm, and 25°C until equilibrium is reached. Equilibrium studies were carried out to determine the  $\text{Cd}^{2+}$  ion removal capacity of both clinoptilolite samples using 5–10000 mg/L  $\text{Cd}^{2+}$  ion concentration at specified conditions given above in their as-received (CLIN-1a, CLIN-2a) and conditioned (CLIN-1b, CLIN-2b) forms. The effects of prewashing as-received clinoptilolite and temperature (25°C and 50°C) on metal uptake capacity of samples at 750 mg/L and 3000 mg/L  $\text{Cd}^{2+}$  concentration for CLIN-1a and CLIN-2a, and CLIN-1b and CLIN-2b, respectively, were investigated under the same initial experimental conditions given above. All tests were run in duplicate.

### Results and Discussion

The chemical composition of CLIN-1a and CLIN-2a were as follows (% wt):  $\text{SiO}_2 = 74.36$ ,  $\text{Al}_2\text{O}_3 = 11.87$ ,  $\text{Fe}_2\text{O}_3 = 1.03$ ,  $\text{MgO} = 0.85$ ,  $\text{CaO} = 1.95$ ,  $\text{Na}_2\text{O} = 0.59$ ,  $\text{K}_2\text{O} = 4.07$ ,  $\text{MnO} = 0.02$ ,  $\text{TiO}_2 = 0.07$ ,  $\text{P}_2\text{O}_5 = 0.01$ , and  $\text{H}_2\text{O} = 6.50$  and  $\text{SiO}_2 = 72.76$ ,  $\text{Al}_2\text{O}_3 = 11.93$ ,  $\text{Fe}_2\text{O}_3 = 1.26$ ,  $\text{MgO} = 1.26$ ,  $\text{CaO} = 4.16$ ,  $\text{Na}_2\text{O} = 0.10$ ,  $\text{K}_2\text{O} = 3.13$ ,  $\text{MnO} = 0.03$ ,  $\text{TiO}_2 = 0.09$ ,  $\text{P}_2\text{O}_5 = 0.01$ , and  $\text{H}_2\text{O} = 1.40$ , respectively. The two samples differ from each other, especially in the composition of exchangeable cations. Analysis has revealed that CLIN-1 contains coarse grained clinoptilolite (80%) particles, whereas CLIN-2 has fine grained clinoptilolite (50%) particles. Quartz, biotite, and illite were identified as the main impurities. The electron micrographs verified that the surface property of the two clinoptilolite samples, being initially the same, turned to well formed plate crystals for CLIN-1 and flat crystals for CLIN-2 after conditioning.

Initial experimental results demonstrated pH 4 as the optimum initial pH for  $\text{Cd}^{2+}$  removal for both clinoptilolite samples. However, the time needed to reach equilibrium was 6 hrs for CLIN-1 and 24 hrs for CLIN-2. This is interpreted as the effect of diverse removal mechanisms of  $\text{Cd}^{2+}$  removal for the two clinoptilolite samples. Particle size was found to have no effect on metal removal efficiency. The  $\text{Cd}^{2+}$  removal efficiency of CLIN-1 and CLIN-2 remained around 85% and 60%, respectively, for all three particle sizes for the initial  $\text{Cd}^{2+}$  concentration of 30 mg/L. This indicates that  $\text{Cd}^{2+}$  removal occurs mainly via exchangeable cations found in the structure rather than on the surface of clinoptilolite. For the rest of the experiments, 0.83–1.11 mm particle sizes were used. Additionally, prewashing the as-received samples had no effect on  $\text{Cd}^{2+}$  removal.

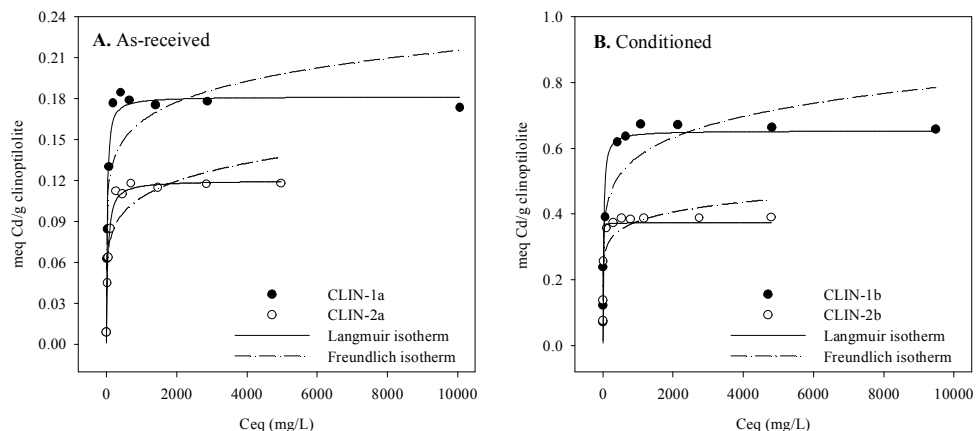


**Figure 1.** Equilibrium Cd<sup>2+</sup> removal for **A.** CLIN-1a and CLIN-2a, **B.** CLIN-1b and CLIN-2b

Equilibrium data obtained from Cd<sup>2+</sup> removal experiments revealed a better fit to the Langmuir isotherm model when compared to the Freundlich model, with maximum capacities of 0.18 meq/g for CLIN-1a and 0.11 meq/g for CLIN-2a. Conversion of the samples into their near-homoionic (Na<sup>+</sup>) forms were found to increase the metal removal capacity considerably with 0.65 meq/g and 0.37 meq/g obtained for CLIN-1b and CLIN-2b, respectively (Figure 1). The low Cd<sup>2+</sup> uptake capacity of CLIN-2a and CLIN-2b can be explained by the low clinoptilolite and correspondingly high impurity contents. Furthermore, Si<sup>4+</sup> ions were detected in considerable concentrations (0.09 meq/g) in solutions, which indicate dissolution of the CLIN-2 samples under low pH (4) values. On the other hand, CLIN-1 did not exhibit such behavior.

Cd<sup>2+</sup> removal capacities were increased under high temperature by 39% and 27% for CLIN-1a and CLIN-2a whereas the capacity increase was almost the same (15% and 18%) for CLIN-1b and CLIN-2b. Investigation of exchangeable cations yielded interesting results: Temperature enhanced the release of strongly bound K<sup>+</sup> and Ca<sup>2+</sup>, especially from CLIN-1a, while Ca<sup>2+</sup> was released more dominantly from CLIN-2a structure.

## Optimization of pretreatment for $\text{Cd}^{2+}$ removal and regeneration of metal loaded clinoptilolite in fixed bed columns

K. Gedik and I. Imamoglu

Middle East Technical University; Ankara, Turkey; Email: kgedik@metu.edu.tr

### Introduction

Natural zeolites, especially clinoptilolite, with their unique ion exchange properties are commonly used materials in metal removal applications. While the as-received forms are being used in studies successfully, the treatment of zeolites favors their ability to remove metal cations by increasing the content of a single cation. The so-called conditioning process should be optimized for effective pretreatment, time, and cost saving in ion exchange studies. Also, the regeneration of metal loaded clinoptilolite beds for further use is important for both recovery of metals and the sorbent.

In this study, the pretreatment of column-packed clinoptilolite was optimized under different initial conditions by changing the flow rate, pH, and quality of water used for the preparation of pretreatment solution. Metal solution was then passed through the columns at various flow rates and particle sizes. The regeneration of exhausted clinoptilolite beds under the optimized conditions was tested for their use in further cycles.

### Experimental Methods

A zeolite sample was taken from Manisa-Gördes sedimentary deposits located in Western Anatolia, Turkey. The sample was ground and sieved to 0.35–0.50 and 0.83–1.18 mm fractions. Samples were washed using distilled water and dried and stored in desiccators. Characterization was carried out via XRD and XRF analyses.

Analytical grade chemicals were used in all experiments. Optimization of pretreatment was carried out in parallel glass columns of 26.5 cm height and 2.5 cm internal diameter in upflow mode. Columns were packed with about 110 g of as-received clinoptilolite with 0.83–1.18 mm particle size. The pretreatment conditions tested in columns were: 1) total conditioner volume: 10, 20, and 40 BV; 2) initial pH: 5.5, 7.0; and 3) water quality: deionized, tap water. Concentration of NaCl solution and the volumetric flow rate were kept constant at 1M and 2BV/h, respectively. Batch experiments were then conducted using column conditioned samples at 125 rpm, 1g/100mL solid-to-liquid ratio, 200 mg/L  $\text{Cd}^{2+}$  concentration, pH of 4, and 25°C to determine the optimum pretreatment conditions.

Following batch experiments, the effect of volumetric flow rate (5, 10, 15 BV/h) and particle size were investigated at 200 mg/L  $\text{Cd}^{2+}$  concentration and pH of 4 at 25°C. Repetitive cycles of  $\text{Cd}^{2+}$  removal was carried out by regeneration of the bed using 1M NaCl with 20 BV at 2BV/h.

### Results and Discussion

The effect of total pretreatment solution volume on  $\text{Cd}^{2+}$  removal efficiency was found not to be considerable. A slight enhancement in  $\text{Cd}^{2+}$  uptake capacity by increasing solution volume from 10 to 40 BV was noticed (%5). An increase in the pH of the NaCl solution from 5.5 to 7 was observed to have no effect on metal removal capacity. Likewise, water quality was also found not to be an important factor in pretreatment despite the diverse ion content of tap water when compared to deionized water for the preparation of the NaCl solution. Consequently, the following pretreatment conditions were adopted: the median volume of 20 BV, pH of 5.5, and deionized water.

Following the determination of optimum pretreatment conditions, the change in  $\text{Cd}^{2+}$  uptake capacity using the pretreated samples was investigated at different volumetric flow rates. Results indicated similar metal removal capacities and breakthrough curves. Decreasing the particle size from 0.83–1.18 mm to 0.35–0.50 mm did not enhance the metal removal capacity detectably. This indicates that pore diffusion resistance is not the rate limiting factor in the columns.  $\text{Cd}^{2+}$  uptake capacity at exhaustion was calculated to be approximately 48.3 mg/g clinoptilolite for all conditions tested. Figure 1 shows the  $\text{Cd}^{2+}$  exhaustion-regeneration cycles. Breakthrough point was set at 5% and at about 1% of the feed solution for the first exhaustion cycle and for the rest of the cycles, respectively. The  $\text{Cd}^{2+}$ -loaded clinoptilolite was eluted successfully in progressing steps as

can be understood from the increase of the metal removal capacity at breakthrough point (31.3 and 37.2 mg/g clinoptilolite for first and second cycles, 47.4 mg/g for the last three cycles). This increase may be attributed to two possible mechanisms. The homoionic clinoptilolite form can be achieved by exchanging strongly bonding cations with  $\text{Na}^+$  in progressing steps by successively forcing concentrated  $\text{NaCl}$  solution.  $\text{Cd}^{2+}$  replacement, especially with having low mobility and strongly bonded cations, may make the conversion of  $\text{Na}^+$  with  $\text{Cd}^{2+}$  in regeneration steps easy when compared to other structural cations. The initially adjusted pH value of 4 changed during  $\text{Cd}^{2+}$  removal cycles and reached 5 in the effluent at breakthrough point. In the successive regeneration steps, the pH values decreased suddenly from 5 to minimum values of 3.9, 3.8, 3.5, 3.2, and 2.8, respectively, and equilibrated at approximately 4.3 for all cycles when the regeneration was stopped. The aluminum hydrolysis may lead to this considerable decrease in pH due to the possible increasing aluminum dissolution in progressing regeneration cycles.

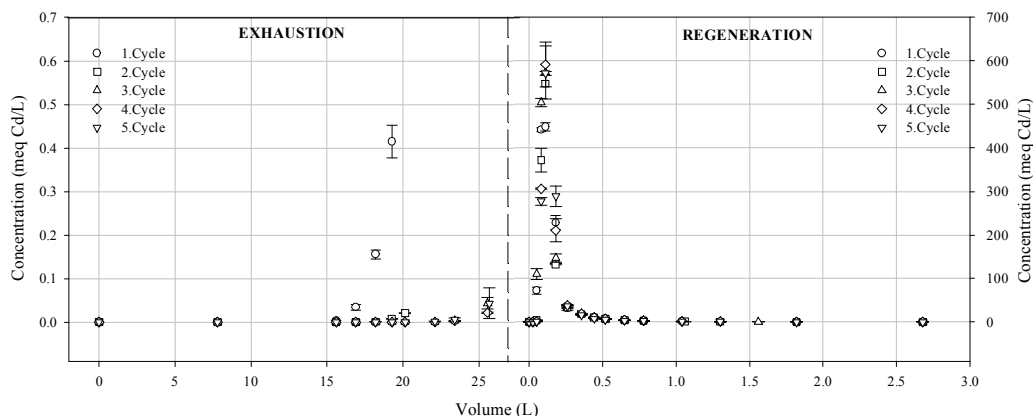


**Figure 1.** The exhaustion of clinoptilolite bed and elution of  $\text{Cd}^{2+}$  during regeneration

## **Lateral and vertical zeolite grade variations in the Tufo Lionato ignimbrite unit (Colli Albani, Roma, central Italy)**

**C. Giampaolo, S. Lo Mastro, D. De Rita, and G. Giordano**

*Università degli Studi Roma 3; Rome, Italy; Email: giampaol@uniroma3.it*

Zeolitized tuffs form during emplacement of pyroclastic products by alteration processes of the pyroclastic material in presence of sufficient magmatic water and at temperatures close to water vapor condensation (De Rita et al., 1986; Perez-Torrado et al., 1995; de' Gennaro et al., 1999; 2000). de' Gennaro et al. (2000) demonstrated that zeolitization of the Neapolitan yellow tuff took place soon after emplacement in a well-insulated thermal system in presence of hot aqueous solutions of hydromagmatic origin. They also observed a different grade of lithification of the tuff from the base to the top and with distance from the vent that they related to fluctuating emplacement conditions and thermal dispersion.

Behind the great importance of the zeolitization processes in relation to the eruptive and emplacement conditions, the nature and the type of zeolites and their distribution in the deposits are important factors controlling the geotechnical characteristics of the tuffs and their possible use on any practical scope. We have analyzed the distribution and the type of zeolites in the Tufo Lionato, which is the lower ignimbrite unit of the Villa Senni Eruption Unit, a large mafic ignimbrite eruption from the Colli Albani volcano, a few kilometres south of Roma (central Italy). The Tufo Lionato ignimbrite is radially distributed around the Colli Albani volcano over 1500 km<sup>2</sup> and occurs as far as 35 km from the vent. The unit ranges in thickness from less than 1 m to 15 m with the thickest deposits occurring within paleovalleys. The ignimbrite ash-matrix supported with up to 15% of scoria clasts, lava lithics, crystals (leucite, clinopyroxene, and phlogopite), and holocrystalline xenoliths. Over 99% of the facies' extent is affected by intense and pervasive zeolite and clay alteration and lithification giving the deposit an overall yellow-brown to reddish color. A relatively hot state of emplacement is inferred by the presence of scoria spatter clasts whose textures suggest deposition in a fluid or plastic state. Spatial and temporal changes in the dynamics of the pyroclastic density currents depositing the ignimbrite have been considered responsible of the different internal structures and facies relationships recognized in the ignimbrite in response to different topographic conditions and the distance from vents (Watkins et al., 2002).

We collected samples from three different stratigraphic sections representing proximal, median, and distal facies of the tuff. Two important different vertical lithofacies have been recognized in all sections: a lower massive lithoid facies and an overlying spatter-rich lithoid facies. Both lithofacies are massive and structureless with the exception of areas where the flow emplaced into paleotopographic slopes. The transition between the two facies is always gradational. In each section vertical sampling representative of the vertical facies variation has been performed. On random orientated samples semi-quantitative analysis of mineral content has been carried out by X-ray diffraction. Two main secondary mineral phases have been recognized: phillipsite and chabazite. The two mineral phases show a vertical symmetrical distribution respect to the deposit thickness. The presence of chabazite characterizes the base and the top of the unit in each section, whereas phillipsite is the prevailing phase in the central part of the unit. No lateral variation in this type of mineral distribution has been observed.

Dé Gennaro et al. (2000) observed a vertically variable zeolite content in the Neapolitan yellow tuff that they relate to a change in the physical conditions (water content and temperature) during emplacement of the unit. The reduction in lithification toward the base and top of the unit is ascribed by the authors to the heat loss towards the atmosphere and substrate. In our interpretation, a similar constant and unusual mineral distribution along the deposit thickness even in proximal, medial, and distal facies of the unit suggests that the chabazite/phillipsite ratio may reflect the vertical temperature gradient in the flow during its emplacement and its persistence during cooling conditions (geoaautoclave processes). Similar to the development of colonnade and entablature during the rapid cooling of lava flows, the vertical distribution of the chabazite/phillipsite ratio may be the result of slow cooling from the base upward and rapid cooling from the top downward.

This peculiarity behind helping to evaluate temperature, water content, and other physical conditions during ignimbrite emplacements can be used as a reading key to distinguish flow units constituting complex ignimbrite deposit and to evaluate the time interval between each unit emplacement.

## References

- dé Gennaro, M., Incoronato A., Mastrolorenzo G., Adabbo M. and Spina G. (1999) Depositional mechanism and alteration processes in different types of pyroclastic deposits from Campi Flegrei volcanic field (southern Italy). *Jour. Volc. Geoth. Res.* **91**, 303–320.
- dé Gennaro M., Cappelletti P., Langella A., Perrotta A. and Scarpati C. (2000) Genesis of zeolites in the Neapolitan yellow tuff: Geological, volcanological and mineralogical evidence. *Contr. Min. Petr.* **139**, 17–35.
- De Rita D., Parotto M. and Stocchi V. (1986) Le zeoliti, minerali possibili indicatori di fenomenologie idromagmatiche: Un'ipotesi di lavoro. *Mem. Soc. Geol. It.* **35**, 769–773.
- Watkins S.D., Giordano G., Cas R.A.F. and De Rita D. (2002) Emplacement processes of the mafic Villa Senni Eruption unit (VSEU) ignimbrite succession. Colli Albani Volcano, Italy. *Jour. Vol. Geoth. Res.* **118**, 173–203.



## **Zeolite characterization of Vico red tuff with black scoriae ignimbrite flow: The quarrying district of Civita Castellana (Viterbo, Italy)**

**C. Giampaolo<sup>1</sup>, L. Mengarelli<sup>1</sup>, E. Torracca<sup>1</sup>, and C. Spencer<sup>2</sup>**

<sup>1</sup>*Università degli Studi Roma TRE; Roma, Italy; Email: giampaol@uniroma3.it*

<sup>2</sup>*European Environmental Minerals Ltd.; UK*

This study reports the results of work undertaken on one of the major ignimbrite flows of northern Lazio in Italy, the so-called Vico red tuff with black scoriae. Since the Etruscan period this material has been used for the production of dimension stones.

A survey of bed thicknesses, carried out on the working faces of different quarries, reveals that previous literature data regarding overall volumes of material underestimated the size of the deposit. In the study area known as the quarrying district of Civita Castellana with its surface area of about 150 km<sup>2</sup>, a volume of not less than 5.5 km<sup>3</sup> has been estimated.

XRD analysis indicates moderate to high total zeolite content in the tuffs ranging from 29% to 67% with chabazite as the most abundant phase, mainly occurring in the matrix of the rock, and minor phillipsite mainly concentrated in the scoriae fraction.

The cationic exchange capacity (CEC) has been determined either directly after a cationic exchange process using Na<sup>+</sup> and K<sup>+</sup> and analysing the outcoming solution by ionic chromatography or approximately combining the results of the SEM chemical analysis with XRD results. The differences between the two applied methods are discussed. The CEC values range from 1.65 to 2.20 meq/g.

The chemical and mineralogical characteristics of this material combined with its high availability enable new horizons to be opened up for this georesource, with good prospects for diverse fields of application and a promising economic potential.

## Plant productivity and characterization of zeoponic substrates after three successive crops of radishes

J. E. Gruener<sup>1</sup>, D. W. Ming<sup>1</sup>, C. Galindo, Jr.<sup>2</sup>, and K. E. Henderson<sup>1</sup>

<sup>1</sup>NASA Johnson Space Center; Houston, Texas, USA; Email: douglas.w.ming@nasa.gov

<sup>2</sup>MEI Technologies; Houston, Texas, USA

The National Aeronautics and Space Administration (NASA) has developed advanced life support (ALS) systems for long-duration space missions that incorporate plants to regenerate the atmosphere (CO<sub>2</sub> to O<sub>2</sub>), recycle water (via evapotranspiration), and produce food. NASA has also developed a zeolite-based synthetic substrate consisting of clinoptilolite and synthetic apatite to support plant growth for ALS systems (Ming et al., 1995). The substrate is called zeoponics and has been designed to slowly release all plant-essential elements into soil solution. The substrate consists of K- and NH<sub>4</sub>-exchanged clinoptilolite and a synthetic hydroxyapatite that has Mg, S, and the plant-essential micronutrients incorporated into its structure in addition to Ca and P. Plant performance in zeoponic substrates has been improved by the addition of dolomite pH buffers, nitrifying bacteria, and other calcium-bearing minerals (Henderson et al., 2000; Gruener et al., 2003). Wheat was used as the test crop for all these studies.

The objectives of this study are to expand upon the previous studies to determine the growth and nutrient uptake of radishes in zeoponic substrates and to determine the nutrient availability of the zeoponic substrate after three successive radish crops.

### Experimental Methods

Zeoponic substrates (0.5–1.0 mm) consisted of clinoptilolite-rich tuff from the Ft. LeClede deposit in Wyoming exchanged with either NH<sub>4</sub><sup>+</sup> or K<sup>+</sup> (Allen et al., 1993), nutrient-substituted hydroxyapatite (Golden and Ming, 1999), and dolomite obtained from Baker Refractories (Gruener et al., 2003). Zeoponic substrates consisted of 36 wt.% NH<sub>4</sub>-exchanged clinoptilolite, 36 wt.% K-exchanged clinoptilolite, 18 wt.% synthetic apatite, and 10 wt.% dolomite.

Three radish crops were grown successively in the same zeoponic substrate (crops 1, 2, and 3). The experiment was then repeated in a new zeoponic substrate (crops 4, 5, and 6). Two control substrates consisted of peat:vermiculite:perlite potting mix and K-exchanged clinoptilolite. Eight pots per treatment (24 pots total) with 3 plants in each pot were arranged in a randomized block design. Control substrates were watered with half-strength Hoagland's solution. Radishes (cv. Cherry Belle) were grown in a controlled environmental plant growth chamber under the following conditions: T=23°C, RH=65%, 16 hour day/8 hour night, and 300 μmol/m<sup>2</sup>/sec photosynthetic photon flux. Each crop growth cycle was 21 days in length. Fresh and dry weights of shoots, edible storage roots, fibrous roots, and tissue analysis of vegetative parts were determined at the end of each cycle. Exchange cations on clinoptilolite were determined prior to and after growing three successive radish crops in the substrate (Ming and Dixon, 1987).

### Results and Discussion

Three crops of radishes were grown successively in the same zeoponic substrate, and then the procedure was replicated successively with a new zeoponic substrate (Table 1). There were no significant differences for the fresh weight produced in zeoponic substrates compared to the two control substrates irrigated with nutrient solutions. Zeoponic substrates have the ability to produce radish yields equivalent to substrates that use optimal nutrient solutions.

**Table 1.** Average fresh weight of the edible roots for radishes grown in zeoponic substrates.

Root fresh weight	Zeoponic substrate	Potting mix control substrate	K-clinoptilolite control substrate
	-----mass (g)-----		
Crop 1 (ave. of 8 pots)	9.23 (3.52) <sup>a</sup>	18.14 (3.94)	5.04 (3.50)
Crop 2 (ave.)	12.01 (3.43)	11.41 (4.99)	11.72 (3.53)
Crop 3 (ave.)	12.31 (3.61)	9.84 (3.41)	9.61 (2.68)
Average of first 3 crops	11.18 (3.52)	13.13 (4.11)	8.79 (3.23)
Crop 4 (ave.)	4.98 (1.76)	12.40 (5.18)	11.08 (3.30)
Crop 5 (ave.)	11.84 (4.83)	5.70 (3.05)	9.38 (3.01)
Crop 6 (ave.)	15.49 (4.56)	8.08 (2.84)	10.17 (2.84)
Average of second 3 crops	10.77 (3.72)	8.72 (3.69)	10.21 (3.05)
Average of 2 replicates	10.97 (3.62)	10.93 (3.90)	9.50 (3.14)

<sup>a</sup>Numbers in parentheses represent one standard deviation.

Plant tissue tests after each 21-day cycle indicated that nutrient uptake was adequate for optimum growth. Prior to plant growth experiments, the NH<sub>4</sub>-exchanged clinoptilolite had a NH<sub>4</sub>-cation exchange capacity (CEC) of 207 cmol<sub>(c)</sub>/kg, and the K-exchanged clinoptilolite had a K-CEC of 202 cmol<sub>(c)</sub>/kg. After three successive crops of radish growth, the average NH<sub>4</sub>-CEC was 107 cmol<sub>(c)</sub>/kg, and the average K-CEC was 158 cmol<sub>(c)</sub>/kg. Thus, after three successive crops of radish growth, the zeoponic substrates had 52% of the original NH<sub>4</sub>-N and 78% of the original K remaining on zeolite exchange sites. This suggests that zeoponic substrates are capable of long-term, slow-release fertilization for multiple crop cycles.

Radish yields in zeoponic substrates were equivalent to yields in control substrates irrigated with nutrient solutions. Zeoponic substrates also provided all of the plant-essential nutrients required for the growth of radishes. After three successive crops of growth, the zeoponic substrates had 52% of the original NH<sub>4</sub>-N and 78% of the original K remaining on zeolite exchange sites. Zeoponic substrates are capable of long-term, slow-release fertilization for multiple crop cycles.

## References

- Allen, E.R., Ming, D.W., Hossner, L.R., Henninger, D.L. and Galindo, C. (1995) Growth and nutrient uptake of wheat in a clinoptilolite-phosphate rock substrates. *Agronomy Journal*, **87**, 1052–1059.
- Golden, D.C. and Ming, D.W. (1999) Nutrient-substituted hydroxyapatites: synthesis and characterization. *Soil Science Society of America Journal*, **63**, 657–664.
- Gruener, J.E., Ming, D.W., Henderson, K.E. and Galindo, Jr., C. (2003) Common ion effects in zeoponic substrates: Wheat plant growth experiments. *Microporous and Mesoporous Materials*, **61**, 223–230.
- Henderson, K.E., Ming, D.W., Carrier, C., Gruener, J.E., Galindo, Jr., C. and Golden, D.C. (2000) Effects of adding nitrifying bacteria, dolomite, and ferrihydrite to zeoponic plant growth substrates. Pp. 441–447, in: *Natural Zeolites for the Third Millennium* (C. Colella & F.A. Mumpton, editors.), De Frede Editore, Naples, Italy.
- Ming, D.W., Barta, D.J., Golden, D.C., Galindo Jr., C. and Henninger, D.L. (1995) Zeoponic plant-growth substrates for space applications. Pp. 505–514, in: *Natural Zeolites '93: Occurrence, Properties, Use* (D.W. Ming & F.A. Mumpton, editors) Intern. Comm. Nat. Zeol., Brockport, NY.
- Ming, D.W. and Dixon, J.B. (1987) Quantitative determination of clinoptilolite in soils by a cation exchange capacity method. *Clays & Clay Minerals*, **35**, 463–468.

## **Crystal chemistry and genetic relationships of zeolites and associated minerals from Faeroe Islands**

**A. Guastoni<sup>1</sup> and G. Artioli<sup>2</sup>**

<sup>1</sup>*Università degli Studi di Padova; Padova, Italy; Email: [alessandro.guastoni@unipd.it](mailto:alessandro.guastoni@unipd.it)*

<sup>2</sup>*Università di Milano; Milano, Italy*

In the spring of 2000, the electric company of the Faeroe Islands (SEV) completed the drilling of a 12 km long tunnel in the tertiary basaltic rocks near Funningsfjörður, in the Island of Eysturoy, to drain water into a hydroelectric basin. The tunnel was drilled entirely in the Middle Basalt Series of the lava sequence, which are geologically part of the North Atlantic basalt province (Rasmussen and Noe-Nygaard, 1970). The lava flows of plagioclase-porphyratic and olivine basalts often show pipes, cavities and vesicles filled with secondary minerals, mostly zeolites. Indeed, the Faeroe Islands are a long-known locality for zeolite collectors and mineralogists (Currie, 1907; Görgey, 1910; Betz, 1981). An expedition jointly organized by the Department of the Earth Sciences of the University of Milano and by the Museum of Natural History extensively surveyed an 8 km long section of the tunnel and successfully collected zeolite samples for about two weeks in June 2000. Many museum-quality samples are now on display in the mineral collection of the organizing institutions. A brief account of the identification and the crystal chemistry of the zeolitic minerals is given.



**Figure 1.** Groups of mesolite fibers supporting several well formed stilbite-Ca crystals, overgrown on a layer of spherules composed of heulandite-Ca and thomsonite.

The zeolite mineral-samples were identified by X-ray powder diffraction, and the crystal chemistry was evaluated by SEM-EDS and EPMA point analyses.

The following zeolite minerals were identified: chabazite-Ca, heulandite-Ca, mesolite, stilbite-Ca, and thomsonite. They have different habits and genetic relationships. Associated minerals are calcite, hydroxyapophyllite, and okenite. The most frequent genetic sequences, in partial agreement with those reported by Betz (1981) are: heulandite-Ca→thomsonite, thomsonite→stilbite-Ca, thomsonite→chabazite-Ca, chabazite-Ca→stilbite-Ca, mesolite→stilbite-Ca, and heulandite-Ca →stilbite-Ca. The general crystallization sequence seems to indicate successive nucleation of zeolites with increasing Si/Al ratio, with the notable exception of

heulandite-Ca, which has a Si/Al ratio above 3 and often crystallizes before thomsonite at the contact with the rock. Hydroxyapophyllite crystallizes before or after stilbite.

A couple of interesting mineral associations have been found, which are both unusual and very attractive: a pink-red intergrowth of thomsonite and stilbite-Ca fine needles, and large transparent groups of aesthetical bow-tie stilbite-Ca crystals on a 5 cm thick bed of white fibrous okenite.

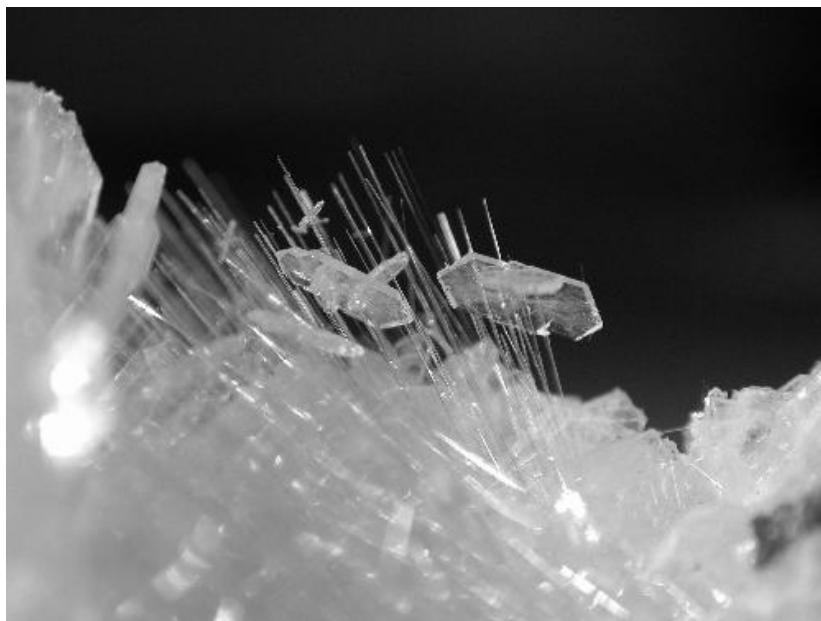


**Figure 2.** Perfectly crystallized stilbite-Ca crystals supported by thin mesolite fibers.

## References

- Betz, V. (1981) Zeolites from Iceland and the Faeroes. *Mineralogical Records*, **12**, 5-26.  
Currie, J. (1907) The minerals of the Faroes, arranged topographically. *Transactions of the Edinburgh Geological Society*, **9**, 1-68.  
Görgey, R. (1910) Ein Beitrag zur topographischen Mineralogie der Faröer. *Neues Jahrbuch für Mineralogie Beil.*, **29**, 269-315.  
Rasmussen, J. and Noe-Nygaard, A. (1970) Geology of the Faeroe Islands. *Geological Survey of Denmark I. Series No. 25*. Copenhagen, 142 pp.

## Effects of feeding clinoptilolite zeolite and acidogenic compounds to poultry

E. C. Hale III

*EcoCal Products, LLC; Brownstown, Indiana, USA; Email: [chale@goodegg.com](mailto:chale@goodegg.com)*

High levels of ambient ammonia in enclosed poultry housing facilities have adverse consequences in terms of bird health, productivity, and worker health. Significant respiratory tract damage (Anderson et al., 1964), increased susceptibility to Newcastle Disease (Anderson et al., 1964), and reduced egg production (Deaton et al., 1982) have been reported.

Poultry manure generally exhibits a basic pH (above 7 SU). Under these conditions, when uric acid present in the manure is enzymatically converted to ammonia, the volatile, neutrally charged ( $\text{NH}_3$ ) form of ammonia is predominant. At an acidic pH (below 7 SU) ammonia is protonated, forming ammonium ( $\text{NH}_4^+$ ), which is significantly less volatile than ammonia.

Acidogenic compounds are compounds that are fed, which directly or indirectly induce acidic conditions in manure at the point of excretion. Acidogenic diets have been tested in pigs (Kim et al., 2001) and laying hens (Hale, 2005; Hale, 2006; Van Ooijen, US Patent 5,562,916). In poultry, feeding sufficient amounts of acidogens to reduce manure pH to  $< 7$  SU has rendered results ranging from moderate increases in ammonia emissions to reductions of up to 20%, depending on the acidogen chosen and the amount fed. The reductions noted are generally believed to be due to interactions between acid anions and  $\text{NH}_4^+$ .

Zeolites are known to have gas adsorbent, molecular sieve, and cation-exchange properties. Clinoptilolite is a widely available natural zeolite that exhibits a significant preference for exchanging nitrogenous cations such as ammonium into its matrix. Zeolites are not digested and can pass through the gut with their cation-exchange properties intact. Feeding various naturally occurring and manmade zeolites to reduce manure ammonia emissions has rendered conflicting results (Nakaue et al., 1981; Amon et al., 1997; Cabuk et al., 2004; Hale, 2005). Topical amendment of poultry excreta with zeolites reduces odor (Xin, 2006) by acting as a gas adsorbent.

Initially, the effect of combining the two amendment strategies on manure ammonia emissions was explored in small flocks of 20 hens, with replicate analyses. The effects of combining either of two acidogens, gypsum ( $\text{CaSO}_4 \cdot 2\text{H}_2\text{O}$ ; obtained from US Gypsum) or sodium bisulfate ( $\text{NaHSO}_4$ ; obtained from the Jones-Hamilton Company), with a commercially available clinoptilolite (obtained from St. Cloud Mining) on manure ammonia emissions were determined using a Latin-square experimental design. Gypsum comprised 2.30%, 3.90%, or 5.25% of the experimental diets. Sodium bisulfate comprised either 0.50% or 0.75% of the experimental diets. Clinoptilolite comprised between 0.00% and 1.50% of the experimental diets. Industry standard diet formulations were fed as a control. All diets were nutritionally equivalent. The effect of combining the two acidogens was not explored. Ammonia emission reductions of up to 96.2% were observed in a laboratory setting.

The effect of one particular acidogen/zeolite combination comprising 5.25%  $\text{CaSO}_4$  and 1.25% clinoptilolite in the feed was further tested in a production environment. Populations of between 125,000 and 170,000 laying hens were fed the diet for periods of up to 11 months.

The combination reduced ammonia emissions by an average 66% during a 2-month feed trial. In an 11-month feed trial, the maximum reduction noted was 85%.

Effects of the diet on manure nitrogen, phosphorus, and potassium content during the 11-month feed trial were also determined. Manure was allowed to accumulate in an under-cage storage area for the entire 11-month period. At the end of the study, manure samples were collected from various locations and depths in the manure storage area. The results indicated that the amended diet increased manure nitrogen content by 37%, while phosphorus and potassium contents were reduced by 54% and 61%, respectively, compared to the control.

Where various  $\text{CaSO}_4$ /clinoptilolite diets were fed to small populations (20) hens for a period of 2 years, numerical production increases of up to 4% were noted compared to control diets. Production generally appears to peak slightly earlier for amended diets than for control diets; egg weights were not significantly different; and mortality, feed intake, and feed conversion ratios were not significantly different when hens were kept under the

same lighting, temperature, square inches of floor space per bird, and airflow conditions. No adverse effects were noted. Production scale effects of NaHSO<sub>4</sub>/clinoptilolite diets have not yet been explored.

## References

- Anderson, D.P., Beard, C.W. and Hanson, R.P. (1964) The adverse effects of ammonia on chickens including resistance to infection with Newcastle Disease virus. *Avian Diseases*, **8**, 369-379.
- Amon, M.M., Dobiec, R.W., Sneath, V.R., Phillips, V.R., Misselbrook, T.H. and Pain, B.F. (1997) A farm-scale study on the use of clinoptilolite zeolite and de-odorase for reducing odour and ammonia emissions from broiler houses, *Bioresource Technology*, **61**, 229-237.
- Cabuk, M., Alcicek, A., Bozkurt, M. and Akkan, S. (2004) Effect of yucca schidigera and natural zeolite on broiler performance. *International Journal of Poultry Science*, **10**, 651-654.
- Deaton, J.W., Reece, F.N. and Lott, B.D. (1982) Effect of atmospheric ammonia on laying hen performance. *Poultry Science*, **61**, 1815-1817.
- Hale, E.C. (2005) Reduction of ammonia emission, phosphorus excretion, and potassium excretion in laying hen manure through feed manipulation. *Proceedings, 2005 Animal Waste Management Symposium*, Research, Triangle Park, North Carolina.
- Hale, E.C. (2006) Effect of varying gypsum/zeolite feed rates and the use of sodium bisulfate as a dietary acidogen. Unpublished report to the United Egg Producers Environmental Science Panel.
- Kim, I.B. and Van Kempen, T. (2001) Determination of ammonia emission and urine pH as affected by different dietary sources of calcium and/or phosphorus in grow-finish pigs. *North Carolina State University Annual Swine Report*.
- Nakaue, H.S., Koelliker, J.K. and Pierson, M.R. (1981) Studies with clinoptilolite in poultry: II. Effect of feeding broilers and direct application of clinoptilolite (zeolite) on clean and reused broiler litter on broiler performance and house environment. *Poultry Science*, **60**, 1221-1228.
- Van Ooijen, J.A.C. Control of ammonia emission and odor, US Patent 5,562,916.
- Xin, H., Li, H., Liang, Y. and Richardson, J. (2006) Update on ammonia emission mitigation for egg facilities. *Iowa State University Animal Industry Report 2006*, A.S. Leaflet R2135.

## Iron-modified light expanded clay aggregates for the removal of arsenic from groundwater

M. N. Haque<sup>1,2</sup>, G. M. Morrison<sup>1</sup>, I. Cano-Aguilera<sup>3</sup>, and J. L. Gardea-Torresdey<sup>2,4</sup>

<sup>1</sup>*Chalmers University of Technology; Göteborg, Sweden*

<sup>2</sup>*University of Texas at El Paso; El Paso, Texas, USA; Email: mnhaque@utep.edu*

<sup>3</sup>*Universidad de Guanajuato; Guanajuato, Guanajuato, Mexico*

<sup>4</sup>*University of Texas at El Paso; El Paso, Texas, USA*

### Introduction

The development of efficient and economic new adsorbent materials for the removal of arsenic from groundwater is a priority in regions where human health is directly affected by elevated arsenic concentrations. Among many types of adsorbent or biomaterials, iron and/or iron-coated materials are the most commonly adopted adsorbents for arsenic removal from contaminated water. Several studies have been conducted to adsorb arsenic on various iron-coated materials, such as iron oxide-coated sand, iron-impregnated sand, and iron hydroxide-coated alumina.

In this study, iron-modified light expanded clay aggregates (Fe-LECA) were examined as a new adsorbent for the removal of arsenic from groundwater. Batch experiments were conducted to investigate how pH influences arsenic adsorption. Kinetic experiments were performed to determine the arsenic removal rates on Fe-LECA. Models were used to describe the experimental kinetics and equilibrium isotherms. Column experiments were performed to determine long-term arsenic removal rates by packed beds of Fe-LECA as a function of bed depth, different flow rate, coating duration, and initial concentration of iron salts for coating.

### Experimental Methods

LECA is a gardening material produced by Hassel Forsgarden (Göteborg, Sweden). The chemical composition of LECA is SiO<sub>2</sub> – 70%, Al<sub>2</sub>O<sub>3</sub> – 20%, FeO – 8.7%, and (CaO and MgO) – 1.3%. The LECA was ground and sieved to particle sizes of 0.25–0.50 mm. Sieved particles were washed with deionized water (25 g L<sup>-1</sup>) for 12 h, filtered off, and air-dried at 40 °C. To coat with iron, 50 g LECA was stirred with 500 ml of 0.1M FeCl<sub>3</sub>·6H<sub>2</sub>O salts in a beaker for 24 h. Then the LECA was separated from the solution after centrifugation for 5 min at 3,000 rpm, and washed with deionized water (pH 6.0) until no reddish color or precipitate formed upon addition of a few drops of 1:10-phenanthroline. One:ten-phenanthroline was used to indicate whether there was any iron in the washings. Washed particles were dried at 60 °C overnight in a hot air-flow oven. This material was used in all batch experiments as iron-coated light expanded clay aggregates (Fe-LECA).

For column experiments, the columns were filled with previously sieved, washed, and dried LECA. For the preparation of Fe-LECA, LECA was treated with the 0.1M FeCl<sub>3</sub>·6H<sub>2</sub>O solution at pH 6.0, where ferric oxides are practically insoluble. The preformed iron oxide suspension was passed through the column in upflow mode under recirculation to coat the surface of filtration media. The bed was subsequently washed with deionized water to remove iron oxide residuals that were not coated on the surface of the filter media. This washing action was finished when iron could not be detected in the outlet stream.

Standard batch experimental procedures together with column experiments were performed to get the results for kinetics, pH profile, isotherms, different flow rates with different bed depths, and coating durations. The determination of total arsenic in the collected samples was performed by hydride-generation atomic absorption spectrometry (HG-AAS, Perkin-Elmer MHS 15, and Perkin-Elmer Analyst 100).

### Results and Discussion

In this research, removal efficiency of arsenic from groundwater by Fe-LECA was carried out. Kinetics, pH profile, and isotherm studies were performed through batch experiments. The results showed that within 1 hour 80% of arsenic (3.12 mg of As/g of Fe-LECA) was adsorbed to Fe-LECA, followed by a slower rate of adsorption that prolonged the equilibrium, which occurred at 12 h. In the beginning, the solution pH dropped



from 7.0 (starting solution pH was 7.0) to 6.0, followed by a constant state until the next 24 h. The experimental data fitted the pseudo-first-order equation of Lagergren. A linear relationship of  $\ln(1/(Q_e - Q_t))$  with contact time was obtained with a correlation coefficient of 0.986; the rate constant  $k_1$  of the pseudo-first-order equation was found to be  $0.098 \text{ min}^{-1}$  at a  $1 \text{ mg L}^{-1}$  of arsenic concentration, which clearly represents a rapid adsorption to reach early equilibrium. Batch experiments having pH ranging from 2.0–10.0 were performed to determine the optimal pH value and found it at a pH range of 6.0–7.0. The sorption isotherm experiments were carried out for different arsenic concentrations ranging from 0.1 to  $100 \text{ mg L}^{-1}$  at pH 6.0, which was found to be optimal. Then the equilibrium isotherms were modeled using the Freundlich and Langmuir isotherm model. The Freundlich model ( $K_F = 1.121$ ,  $\beta = 0.862$ ,  $R^2 = 0.975$ ) fitted better than the Langmuir Model ( $K_L = 0.163$ ,  $q_{\max} = 3.32 \text{ mg of As/g of Fe-LECA}$ ,  $R^2 = 0.962$ ). From the batch experiments, electrostatic attraction and surface complexation were concluded to be the major arsenic removal mechanisms.

In addition, large-scale column experiments were conducted under different bed depths, flow rates, coating durations, and initial iron salts concentrations to determine optimal arsenic removal efficiency by the Fe-LECA column. The effect of flow rate on the arsenic sorption to Fe-LECA was carried out by changing the flow rates from 10 to  $40 \text{ ml min}^{-1}$  at a fixed bed depth of 50 cm. The breakthrough curve was at 425, 150 pore volumes at a flow rate of 10 and  $40 \text{ ml min}^{-1}$ , respectively. To determine the maximum hydraulic detention time, column experiments having different bed depths (15, 30, and 50 cm) were performed. The maximum breakthrough occurred at 450 pore volumes at a bed depth of 50 cm. So, the sorption capacity of the column can be increased by volumetric design, i.e., higher bed depth, but the ratio of column length to column diameter should be  $\sim 5$  to avoid plugging of the column and other undesirable effects. Coating of LECA using iron salts was examined for 3, 24, and 72 h to determine the optimum coating duration as well as the kinetics of iron coating to LECA for arsenic adsorption. The removal of arsenic was more efficient when the coating was performed for 24 h than for 3 h. However, no significant difference was noticed when the coating was performed for 72 h. This finding can be directly correlated with the amount of iron oxide coated onto the surface of the LECA, which was found to be almost equal for 24- and 72-h coatings (0.91 and 0.94 mg of Fe/g of Fe-LECA, respectively). The maximum arsenic accumulation was 3.31 mg of As/g of Fe-LECA when the column was operated at a flow rate of  $10 \text{ ml min}^{-1}$  and the LECA was coated with 0.1M  $\text{FeCl}_3$  suspension for 24 h. From the above mentioned column experiments, it is obvious that the removal of arsenic using Fe-LECA could occur on both the interior and exterior surface of the LECA through the proper modification of this material.

## Natural zeolite from southern Germany: Applications in concrete

F. Hauri

Hans G. Hauri Mineralstoffwerk; Bötzingen, Germany; Email: f.hauri@hauri.de

### Introduction

One of the deposits of natural zeolite in Germany is in the southwest on the edge of the famous Black Forest. Near the town of Freiburg is the little volcanic mountain called Kaiserstuhl. The volcanic material with the name phonolite contains 45% zeolite (= natrolite).

The rock is blasted, loaded with an elevator into trucks, and transported to the different crushers. Then we activate the material at 450°C to reduce the crystal water. After this treatment we grind the material very finely and store it in silos.

We market three standard products for application in concrete: Hydrolith F200, Hydrolith F500, and Kümix.

Hydrolith F200 is used in the production of the following concrete types: paving stones, concrete slabs, and ready-mixed concrete. The characteristic physical analysis of the product Hydrolith F200 is as follows: residue on 0.2 mm sieve is 2.9 %, size fraction < 0.040 mm is 81 %, and Blaine surface analysis is 5540 cm<sup>2</sup>/g

Hydrolith F500 is our finest product, 100% < 20 µm. This product is used, for example, in high-strength concrete pipes and high-load concrete supports.

Kümix is a mix of ground phonolite and clinker. With 48.5% clinker, 48.5% phonolite, and 3% gypsum, we produce a hydraulic binder. Kümix is used for constructing anchors. The main advantage is the enhanced ability to pump the product (more than 100 metres with a ratio of water/binder of 0.5).

### Experimental Methods

Hydrolith F200 is a material with pozzolanic activity. By using x-ray fluorescence analysis and an x-ray diffractometer we know the exact properties of our material. The following methods show us the performance of our product in concrete.

**Table 1.** Hydrolith F200 performance using Norm EN 197-1 method

Norm EN 197-1		75% CEM I 42,5 R + 25% Hydrolith	CEM I 42,5 R
Compression strength (MPa)	after 7 days	41.9	50.7
	after 28 days	57.3	58.3
Activity index (%)	after 7 days	83.0	
	after 28 days	98.0	

**Table 2.** Hydrolith F200 performance using Trass method

Trass Method (according to DIN EN 196 Part 1)		tensile strength in bending (N/mm <sup>2</sup> )	Compression strength (N/mm <sup>2</sup> )
Prisms 40 x 40 x 160 mm:	Hydrolith F200 720 g hydrated lime 180 g norm sand 1350 g water / binder ratio 0,45	5.5	13.6

For Hydrolith F500, the surface measured according to the Blaine method is 16,000 m<sup>2</sup>/g, or according to the BET method 9.4 m<sup>2</sup>/g. This product is used in high performance concrete. The French Research Centre (CERIB) has carried out intensive tests, of which the following results are interesting:

**Table 3.** Concrete mix proportions of high performance concretes

Ultrafine	Silica fume	Phonolith
Cement CEM I 52,5 PM ES	350	350
Ultrafine	30	30
Siliceous sand 0/5	700	712
Siliceous gravel 2/6	350	356
Siliceous gravel 5/12	700	712
Superplasticizer (phosphonate)	1.05	0.79
Water/Cement Ratio	0.43	0.44
Slump test (cm)	17	17

**Table 4.** Flexural strength

	Silica fume	Phonolith
28 days	5.4 MPa	5.2 MPa
90 days	5.5 MPa	5.5 MPa

**Table 5.** Comparison of Kümix to traditional cement

	CEM I 42.5 R	Kümix
Norm DIN EN 196		
Compression strength		
7days	50.7 MPa	35 MPa
28days	58.3 MPa	53 MPa
Surface Blaine method	4300 cm <sup>2</sup> /g	7900 cm <sup>2</sup> /g

## Results and Discussion

By substituting 25% standard cement strength class CEM I 42.5 R with 25% Hydrolith F200 we achieve results that can reduce CO<sub>2</sub> emissions. To produce one ton of cement 1.6 tons of limestone is required. During the firing process 600 kg CO<sub>2</sub> are emitted. An annual production of 50,000 tons of Hydrolith F200 results in a reduction of 30,000 tons CO<sub>2</sub>. This figure can be further improved by low energy production. By reducing the emission of CO<sub>2</sub> we can help towards achieving the aims of the Kyoto Protocol.

Phonolite with 45% zeolite is used in Germany, Switzerland, and France, not only in the concrete industry, but also as a feed additive and to improve the adsorption of mercury in waste incineration plants.

With a well-equipped laboratory and technical product expertise we shall be able to increase the use of natural zeolite in a wide variety of applications.

## Activated adsorption of chlorinated hydrocarbons on erionite

M. A. Hernández<sup>1</sup>, F. Rojas<sup>2</sup>, G. Rueda<sup>1</sup>, R. Portillo<sup>3</sup>, E. Campos Reales<sup>1</sup>, and V. Petranoskii<sup>4</sup>

<sup>1</sup>Instituto de Ciencias de la Universidad Autónoma de Puebla; Puebla, México; Email: mighern@siu.buap.mx

<sup>2</sup>Universidad Autónoma Metropolitana; Iztapalapa, Mexico

<sup>3</sup>Universidad Autónoma de Puebla; Puebla, Mexico

<sup>4</sup>Centro de Ciencias de la Materia Condensada, UNAM; Mexico

### Introduction

In zeolites the activated adsorption is a common effect. This kind of effect is due to the existence of steric barriers that hinder the diffusion of adsorptive molecules through very narrow channels, (Sing and Williams, 2004), thus requiring significant activation energies (i.e., sufficiently large temperatures) to permeate these capillaries into the cavities beyond. The existence of activated diffusion has been conceived theoretically for the case of hydrocarbon adsorptives (Laboy et al., 1999) entering microporous structures analogous to those studied in this work. The decrease of the amount adsorbed with temperature is a characteristic typical of physisorption; as the temperature increases, the trapping of adsorptive molecules becomes more difficult by reason of their mounting kinetic energy. Erionite (framework type ERI) is characterized by a three dimensional 8-MR channel system, along and perpendicular to the [001] direction, with access windows of 0.36 x 0.51 nm, (Meier and Olson, 2001). This work investigated the mechanism of trichloroethylene (TCE) adsorption in micropores. Adsorption in pores of molecular dimensions is shown to be an activated process that may contribute to slow contaminant uptake and release by aquifer sediments. In this work, erionite samples mined from diverse locations in Agua Prieta, Sonora, Mexico, are studied with respect to their adsorption behavior toward dichloroethylene, trichloroethylene, tetrachloroethylene, and carbon tetrachloride uptake. Both natural, dealuminated, exchanged with Ca erionites are employed for these sorption studies. The adsorption isotherms are measured at different temperatures by means of the gas chromatography (GC) peak maxima technique. The isosteric heats of adsorption at different adsorbate loadings are evaluated from the corresponding adsorption isotherm data through the Clausius-Clapeyron equation.

### Experimental Methods

High-purity chlorinated hydrocarbons were used as adsorptives. High-purity helium was used for GC determinations. The zeolites selected for this work are Mexican natural zeolites obtained from Agua Prieta in the state of Sonora, Mexico. The ERIN label accounts for the natural sample. Samples of dealuminated erionite zeolites were prepared at laboratory scale by means of an acid-leaching process; samples ERIH1, ERIH2 and the sample ERICa was prepared from ERIH2 and exchanged with CaCl<sub>2</sub>·2H<sub>2</sub>O. XRD patterns were determined by means of a Siemens D-500 diffractometer employing nickel-filtered Cu KR radiation. All N<sub>2</sub> adsorption isotherms were measured at the boiling point of liquid N<sub>2</sub> in an automatic volumetric adsorption system (Quantachrome AutoSorb-1LC). The adsorption isotherms of chlorinated hydrocarbons on ERIN, ERIH1, ERIH2 and ERICa adsorbents were measured at different temperatures by the GC technique using helium as the carrier gas. Data corresponding to the adsorption of chlorinated compounds on erionite samples were fitted to standard Freundlich, Langmuir, and Dubinin-Asthakov (DA) isotherm models through linear regression in order to determine the adsorption parameters pertinent to each of the above approaches.

### Results and Discussion

The XRD patterns of the ERIN, ERIH1, ERIH2 and ERICa samples were typical of erionite zeolites as described (Treacy et al., 2002).

N<sub>2</sub> adsorption isotherms at 76 K on ERI zeolites are IUPAC type I isotherms (Sing et al., 1985). The pore size distributions (PSDs) of the zeolites under study were obtained from DCCP method and exhibit a shallow bimodal distribution with pore size maxima occurring at 5.5 and 15.9 Å.

The rather similar uptakes of chlorinated molecules inside ERIN, ERIH1N, ERIH2, and ERICa substrates can be associated with an *activated diffusion* process. This kind of effect has been reported previously in

dealuminated clinoptilolite zeolites (Hernández et al., 2005). Chlorinated hydrocarbons adsorption isotherms at different temperatures on ERI zeolites are presented; the corresponding Freundlich and Langmuir linearized plots have shown to be consistent with the obtained results. The heats of adsorption of the chlorinated hydrocarbons increase with an increase in the adsorbate loading, then pointing to the existence of lateral interactions between adsorbed molecules.

## References

- Hernández, M.Á., Rojas, F., Lara, V.H. and Corona, L. (2005) A quantitative study of adsorption of aromatic hydrocarbons on dealuminated clinoptilolites. *Ind. Eng. Chem. Res.*, **44**, 2908–2916.
- Laboy, M.M., Santiago, I. and Lopez, G.E. (1999) Computing adsorption isotherms for benzene, toluene, and p-xylene in heulandite zeolite. *Ind. Eng. Chem. Res.*, **38**, 4938–4945.
- Meier, W. M. and Olson, D.H. (2001) Pp 58-59 in: *Atlas of Zeolite Structure Types* (Structure Commission, International Zeolite Association) Butterworths, London.
- Sing, K.S.W. and Williams, R.T. (2004) The use of molecular probes for the characterization of nanoporous adsorbents. *Part. Part. Syst. Charact.*, **21**, 71–79.
- Sing, K.S.W., Everett, D.H., Haul, R.A.W., Moscou, L., Pierrotti, R., Rouquerol, J. and Siemienieswka, T. (1985) Reporting physisorption data for gas/solid Systems. *Pure Appl. Chem.*, **57**, 603–619.
- Treacy, M.M.J., Higgins, J.B. and von Ballmoos, R. (1990) Collection of simulated XRD powder patterns for zeolites. *Zeolites*, **10**, 388S–389S.

## Thermodynamic properties of natrolite

G. L. Hovis<sup>1</sup> and P. S. Neuhoff<sup>2</sup>

<sup>1</sup>Lafayette College; Easton, Pennsylvania; USA; Email: [hovisguy@lafayette.edu](mailto:hovisguy@lafayette.edu)

<sup>2</sup>University of Florida; Gainesville, Florida; USA

### Introduction

Natrolite ( $\text{Na}_2\text{Al}_2\text{Si}_3\text{O}_{10}\cdot 2\text{H}_2\text{O}$ ) is a common rock-forming mineral in low-temperature, quartz-undersaturated environments such as zeolite-facies, olivine-phyric metabasalts, and pegmatitic portions of alkaline intrusions. In addition, it provides an important example of Si/Al order/disorder relations in zeolites. The degree of Si/Al ordering varies appreciably among stoichiometric natrolites, ranging from complete Si/Al ordering (Neuhoff et al., 2002) up to about 20% and 30% occupancy of Al in Si sites and Si in Al sites, respectively (Alberti et al., 1995). Complete Si/Al disorder is known only in the isostructural mineral gonnardite, which is generally Ca-bearing and exhibits Si/Al from 1.08 to 1.7. The present work employs HF solution calorimetry determinations of the enthalpy of formation ( $\Delta H_f$ ) of natrolite in varying states of Si/Al disorder to constrain calculations of the stability of natrolite geologic environments.

### Experimental Methods

Phase-pure separates of five natrolite samples (three previously studied by Neuhoff et al., 2002, plus two additional samples) were hand picked and ground in agate mortars. Purity and unit-cell dimensions were assessed by X-ray diffraction. The state of Si/Al disorder was independently assessed by  $^{29}\text{Si}$  magic angle spinning nuclear magnetic resonance (Neuhoff et al., 2002). Enthalpies of formation were calculated from heat-of-solution measurements conducted in a calorimeter system described by Hovis et al. (1998). Each sample was dissolved in 910.1 g (about one liter) of 20.1 wt% hydrofluoric acid (HF) at 323 K under isoperibolic conditions. Thermochemical cycles analogous to those employed by Neuhoff et al. (2004) were used to calculate  $\Delta H_f$  at 298.15 K from the heat-of-solution data (heat capacity data from Johnson et al., 1983 for natrolite were used to evaluate the change in heat content between 298.15 and 323.15 K).

### Results and Discussion

Site occupancies obtained from fits of  $^{29}\text{Si}$  MAS NMR data by Neuhoff et al. (2002, and this study) and heats of solution are listed in Table 1 along with calculated configurational entropies ( $S_{\text{CON}}$ ) and  $\Delta H_{f,298.15\text{K}}$  based on the formula unit listed above. It can be seen in Table 1 that  $\Delta H_{f,298.15\text{K}}$  for the studied samples varies on the order of  $\sim 5$  kJ/mol, although all samples are essentially within error of each other. There is a general trend for the more disordered samples to be less stable. One exception is the sample from Mont. St. Hilaire, which exhibits the most stable  $\Delta H_{f,298.15\text{K}}$  despite the fact that the fit of the  $^{29}\text{Si}$  MAS NMR spectrum (Table 1) indicated that this sample was the most Si/Al disordered. This reflects uncertainties in fitting of the NMR spectrum; the difference in the  $a$  and  $b$  unit-cell parameters for this sample (a proxy for the degree of Si/Al ordering in natrolite; Alberti and Vezzalini, 1981) is similar to that in the fully ordered sample from California, suggesting that the Mont St. Hilaire sample is nearly fully Si/Al ordered.

The results of the present study differ significantly from previous studies on natrolite. A prior determination of  $\Delta H_{f,298.15\text{K}}$  for natrolite by Johnson et al. (1983;  $-5718.6 \pm 5.0$ ) is substantially less energetic than those in Table 1, whereas the value determined by Kiseleva et al. (1996;  $-5750.5 \pm 8.0$ ) is significantly more stable than our data suggest. In the case of the Johnson et al. (1983) sample, this might in part reflect a slightly greater degree of Si/Al disorder, although the  $a - b$  difference in their sample is similar to that of the Greenland samples in this study. Kiseleva et al.'s (1997) datum cannot be explained by disorder, as the California sample in Table 1 is fully ordered yet  $\sim 18$  kJ/mol less stable than their sample. This disparity likely arose from the fact that a flowing atmosphere was not employed during Kiseleva et al. (1997) lead borate solution measurements. Our results are consistent with their observations of the enthalpy of disordering in natrolite; they found isocompositional tetranatrolite to be about 23.4 kJ/mol less stable than natrolite (of undetermined ordering state), whereas our results suggest a disordering enthalpy between fully ordered and fully disordered natrolite of  $\sim 30$  kJ/mol. The thermodynamic data generated in this study, unlike those determined previously by Johnson et

al. (1983) and Kiseleva et al. (1997), can be used to explain phase and compositional relations between natrolite and analcime as well as the discontinuous range of ordering states observed in natural natrolites.

**Table 1.** Site occupancies and calorimetric results

Sample	<sup>29</sup> Si MAS NMR data			$\Delta H_{\text{sol},323\text{K}}$ (kJ/mol)	$\Delta H_{\text{f},298\text{K}}$ (kJ/mol)
	$X_{\text{Al}(\text{Si}1)} = \frac{X_{\text{Al}(\text{Si}1)}}{X_{\text{Si}(\text{Al}1)}}$	$X_{\text{Al}(\text{Si}2)}$	$S_{\text{CON}}$ (J/molK)		
San Benito Co. CA (USA) <sup>1</sup>	0	0	0	-818.12 ± 2.61	-5732.7 ± 4.9
Marraat (Greenland) <sup>2</sup>	0.07	0.03	8.57	-823.31 ± 1.67	-5727.5 ± 4.5
Mont St. Hilaire, Quebec (Canada) <sup>3</sup>	0.09	0.05	10.5	-818.18 ± 1.95	-5732.7 ± 4.6
Marraat (Greenland)	0.06	0.03	5.49	-820.20 ± 1.74	-5730.7 ± 4.5
Ilímaussaq, (Greenland)	0.04	0.02	7.43	-821.47 ± 1.45	-5729.4 ± 4.4

<sup>1</sup>Sample NAT001 from Neuhoﬀ et al. (2002). <sup>2</sup>Sample NAT002 from Neuhoﬀ et al. (2002).

<sup>3</sup>Sample NAT003 from Neuhoﬀ et al. (2002).

## References

- Alberti, A., Cruciani, G. and Dauru, I. (1995) Order-disorder in natrolite-group minerals. *European Journal of Mineralogy*, **7**, 501–508.
- Alberti, A. and Vezzalini, G. (1981) A partially disordered natrolite; relationships between cell parameters and Si-Al distribution. *Acta Crystallographica, Section B: Structural Crystallography and Crystal Chemistry*, **37**, 781–788.
- Hovis, G.L., Roux, J. and Richet, P. (1998) A new era in hydrofluoric acid solution calorimetry: Reduction of required sample size below ten milligrams. *American Mineralogist*, **83**, 931–934.
- Johnson, G.K., Flotow, H.E., O'Hare, P.A.G. and Wise, W.S. (1983) Thermodynamic studies of zeolites: Natrolite, mesolite, and scolecite. *American Mineralogist*, **68**, 1134–1145.
- Kiseleva, I.A., Ogorodova, L.P., Melchakova, L.V., Belitsky, I.A. and Fursenko, B.A. (1997) Thermochemical investigation of natural fibrous zeolites. *European Journal of Mineralogy*, **9**, 327–332.
- Neuhoﬀ, P.S., Kroeker, S., Du, L.-S., Fridriksson, Th. and Stebbins, J.F. (2002) Order/disorder in natrolite group zeolites: A <sup>29</sup>Si and <sup>27</sup>Al MAS NMR study. *American Mineralogist*, **87**, 1307–1320.
- Neuhoﬀ, P.S., Hovis, G., Balassone, G. and Stebbins, J. (2004) Thermodynamic properties of analcime solid solutions. *American Journal of Science*, **304**, 21–65.

## **Zeolites and associated clay minerals from the altered Sheinovets caldera ignimbrites (eastern Rhodopes, southern Bulgaria)**

**R. Ivanova<sup>1</sup> and S. Gier<sup>2</sup>**

<sup>1</sup>*Bulgarian Academy of Sciences; Sofia, Bulgaria; Email: rossiv@geology.bas.bg*

<sup>2</sup>*University of Vienna; Vienna, Austria*

### **Introduction**

Intense collision-related volcanism took place in the eastern Rhodopes (southern Bulgaria) during the Paleogene. The erupted lava and pyroclastic rocks were assigned to four intermediate to basic phases alternating in time with five acidic ones (Yanev, 1998). Large volumes of acid pyroclastics, associated with caldera collapses, were produced during the first three acid phases (one Priabonian and two Rupelian).

The Sheinovets caldera is located in the easternmost parts of the eastern Rhodopes as only a part of it is currently exposed. The caldera is filled with a thick succession of pyroclastic flow and less fall deposits with interbedded epiclastics and biogenic limestones indicating submarine deposition. Rhyolite domes and dykes having perlite peripheries are also exposed (Ivanova, 2005). The volcanic glass is completely altered and the main alteration products are zeolites (mordenite, clinoptilolite, (rarely) analcime, stilbite, and erionite) accompanied by clay minerals, adularia, calcite, and opal-CT (Ivanova et al., 2001). Obtaining new data on zeolite chemistry and the distribution and characterization of associated phyllosilicates is the aim of the present study.

### **Experimental Methods**

The bulk mineralogy of the samples was determined by X-ray diffraction using D-500 SIEMENS diffractometer, CuK $\alpha$  radiation (40 kV, 30 mA), continuous scan. Diffraction data of the clay fractions were obtained with a Philips diffractometer (PW 3710, goniometer PW 1820), CuK $\alpha$  radiation (45 kV, 35 mA), step scan (step size 0.02° 2 $\theta$ , 1s per step). The < 0.2  $\mu$ m fractions were separated by centrifugation. The clay fractions were saturated with 1N KCl-solutions and 1N MgCl<sub>2</sub>-solutions. Oriented XRD mounts (made by dispersing approximately 7 mg of clay separate in 1 mL of water, pipetting the suspension onto a round glass slide, and drying at room temperature) were analyzed in air-dried, and after vapour solvation with ethylene glycol or glycerol at 60°C. Chemical analyses of zeolite and clay were performed on JEOL 733 Superprobe and Cameca SX 100 electron probe microanalyser (using 15 kV acceleration voltage, 20 nA beam current, 5Å beam diameter). SEM observations were carried out on some samples using a JEOL 733 Superprobe and a JEOL 6400.

### **Results and Discussion**

The new data obtained confirm the reported (Ivanova et al., 2001) changes in the vertical distribution of the alteration products. Adularia and opal-CT are the main components of the secondary associations in the lowermost exposed levels of the pyroclastic section. They are accompanied by clay minerals, calcite, and smaller amounts of zeolites (mordenite, clinoptilolite, and (locally) analcime). Authigenic albite has also been identified in some of the samples from the base of the section. Mordenite dominates in the middle parts while clinoptilolite is the most abundant secondary phase in the topmost parts of the pyroclastic sequence. Adularia and opal-CT are always present. Regarding their chemistry, Ca is the most abundant extra framework cation in clinoptilolite, Ca and Na are in almost equal quantities in mordenite but a significant increase of K content in both mordenite and clinoptilolite towards the upper part of the section has also been detected.



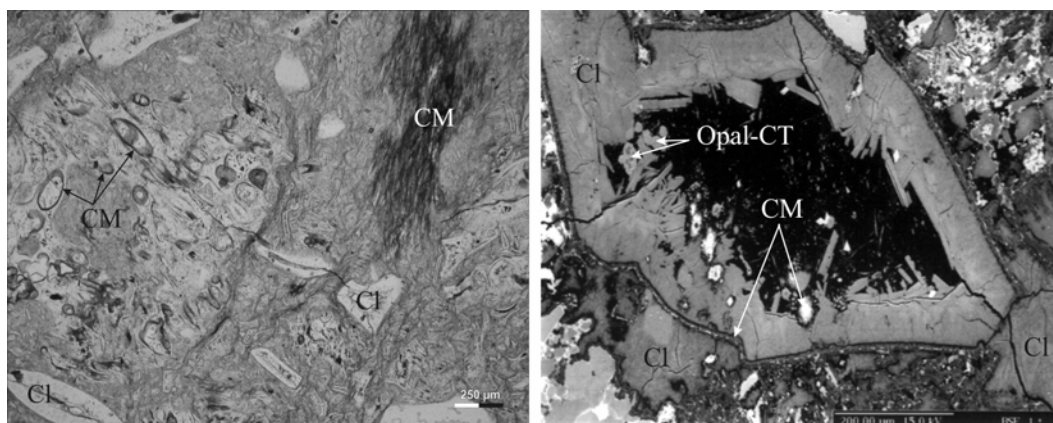


**Figure 1.** Microphotograph showing the alteration of different clasts in a pyroclastic flow unit (left). Back-scattered electron image of a zeolitized glass shard with two generations of clay minerals. (right) CM — clay minerals; Cl -clinoptilolite.

Different amounts of clay minerals are present in all samples but they seem to be more abundant in finer-grained varieties and in pumice-rich layers. Normally they precede the zeolite formation and coat the glass shards or fill in the pumice bubbles (Fig. 1). A second generation of phyllosilicate can often be found as irregular aggregates, located in the central parts of larger zeolitized glass shards. They are enriched in Fe (up to 20%), probably due to the ability of clays to incorporate cations, which cannot enter the zeolite structure and are in excess after the zeolitization has already occurred. The clay fractions ( $< 0.2 \mu\text{m}$ ) are dominated by illite-smectite mixed layer minerals.

The existence of a large, low-temperature, hydrothermal system (Hall, 1998), driven by the temperature gradient between the hot pyroclastic flow deposits and ambient marine water, is proposed by Ivanova et al. (2001) to explain the alteration of the pyroclastic sequence filling the Sheinovets caldera. The original volcanic features of pyroclastic rocks (type and size of the glass fragments, their initial temperature and rate of cooling, degree of vesiculation, etc.) seem to be of great importance to the distribution of alteration products on local scale.

## References

- Hall, A. (1998) Zeolitization of volcanoclastic sediments: The role of temperature and pH. *Journal of Sedimentary Research*, **68**, 739-745.
- Ivanova, R., Yanev, Y., Iliev, Tz., Koleva, E., Popova, T., and Popov, N. (2001) Mineralogy, chemistry and ion-exchange properties of the zeolitized tuffs from the Sheinovets caldera, Eastern Rhodopes (South Bulgaria). Pp. 95–103 in: *Studies in Surface Science and Catalysis* (A. Galarneau, F. Di Renzo, F. Fajula, and J. Vedrine, editors). 135, Elsevier, Amsterdam.
- Ivanova, R. (2005) Volcanology and petrology of the acid volcanic rocks from the Paleogene Sheinovets caldera, Eastern Rhodopes. *Geochemistry, Mineralogy and Petrology*, **42**, 23–45.
- Yanev, Y. (1998) Petrology of the eastern Rhodopes Paleogene acid volcanics, Bulgaria. *Acta Vulcanologica*, **10**, 265–277.

## Sorption of gases, cesium, and strontium by clinoptilolite-rich zeolites

J. M. Jablonski<sup>1</sup>, J. Krasen<sup>2</sup>, and A. Miecznikowski<sup>3</sup>

<sup>1</sup>Polish Academy of Sciences; Wrocław, Poland

<sup>2</sup>Geoexplorers International, Inc.; Denver, Colorado, USA

<sup>3</sup>Wrocław University of Technology; Wrocław, Poland; E-mail: miecznik@pwr.wroc.pl

Clinoptilolite-rich zeolites commonly occur in volcanic-sedimentary rocks. They are formed from volcanic ash if deposited in a saline, alkaline, lacustrine or marine environment. The crystallographic structure of clinoptilolite with an Si/Al ratio higher than 4 belongs to the monoclinic system and its space group is C2/m. However, a lower symmetry of Cm or C-1 is sometimes observed. The unit cell of the clinoptilolite structure has two dimensional channel systems. Along the Z-axis, channels of 10 and 8 tetrahedral (Al,Si)O<sub>4</sub> rings with 0.30–0.76 and 0.33–0.46 nm pore dimensions are formed. Along the X-axis, channels with 8-tetrahedral (Al,Si)O<sub>4</sub> rings with pore openings of 0.26–0.47 nm occur. (Fig. 1). Cavities are formed at the intersection of channels. Extra-framework exchangeable cations, such as Na, K, Ca, Mg, Sr, Cs, and others, that neutralize the negative electric charge of AlO<sub>4</sub> tetrahedra, are present in the channels and cages. Various molecules of CO, CO<sub>2</sub>, N<sub>2</sub>, NO<sub>x</sub>, H<sub>2</sub>O, CH<sub>4</sub>, and many others can be sorbed into the channels and cages.

### Experimental Methods

Samples of clinoptilolite-rich zeolites from the Tadeo Concession located in San Luis Potosi State, Central Mexico, were used for laboratory investigations. One series of samples was washed with warm water and dried and the second one was treated with two molar solution of hydrochloric acid (2M HCl). X-ray diffraction (XRD) patterns of both series of samples revealed that beside clinoptilolite, traces of amorphous silica and quartz also are present. The samples treated with 2M HCl diminished the degree of crystallinity of clinoptilolite-rich zeolite from 85% to 60%.

Cesium and strontium nitrate (Riedel de Haen, 99.9%) were used for preparation of the 0.05 and 0.25 molar solutions in doubly distilled water. Ion exchange was performed using 0.5g of clinoptilolite immersed in each of 5 cm<sup>3</sup> of prepared solutions with stirring for 24h at room temperature (293 K). After filtration, the amounts of cesium and strontium in solutions were measured by Inductively Coupled Plasma Atomic Emission Spectrometry (ICP AES, Applied Research Laboratories model 3410).

### Results and Discussion

Simulation of sorption of gases by clinoptilolite zeolite with the Cerius 2 Molecular Modeling Program version 4.7 resulted in the following amounts of molecules loaded (*n* per unit cell) at T=293 K and P=101kPa : *n*(CO)=3.69, *n*(CO<sub>2</sub>)=5.44, *n*(N<sub>2</sub>)=1.73, *n*(NO)=2.06, and *n*(NO<sub>2</sub>)=4.26.

The x-ray fluorescence spectroscopy (XRF) of clinoptilolite-rich zeolite revealed the following (in weight percent): SiO<sub>2</sub>=66.85, Al<sub>2</sub>O<sub>3</sub>=11.34, Fe<sub>2</sub>O<sub>3</sub>=1.78, MnO=0.026, MgO=0.75, CaO=2.03, Na<sub>2</sub>O=0.55, K<sub>2</sub>O=4.45, P<sub>2</sub>O<sub>5</sub>=0.03, LOI=12.37, for a Total=100.3. The amounts of trace elements measured in ppm are: Ba=573, Sr=1004, Y=45, Sc=5, Zr=221, Be=4, V=6. Si/Al ratio equals 5.01.

The results of ion sorption (exchange) as measured by ICP AES for cesium ( $\lambda$ =455nm) and strontium ( $\lambda$ =346nm) are presented in Table 1. The results show that clinoptilolite, washed only with water and dried, is able to sorb significantly greater quantities of cesium and strontium than that treated with hydrochloric acid. The lowering of sorption capacity could be due to the leaching of AlO<sub>4</sub> tetrahedra from the structure of zeolite during hydrochloric acid treatment.

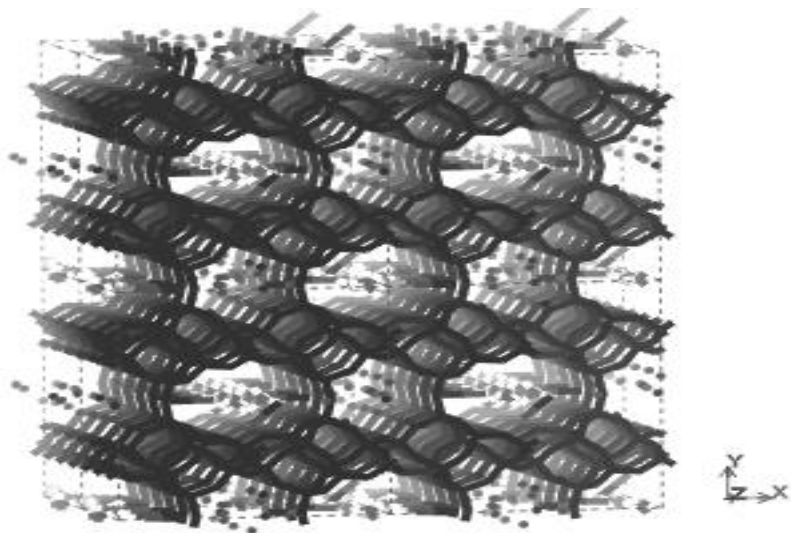
**Table 1.** Sorption of cesium and strontium by clinoptilolite-rich zeolite from Tadeo Concession, San Luis Potosi, Central Mexico, measured by Atomic Emission Spectrometry, grain 0.5–0.75mm

Cs $\lambda=455\text{nm}$						
Concentration before ion exchange M CsNO <sub>3</sub> M=moles	Cs before ion exchange mg/dm <sup>3</sup>	Cs after ion exchange mg/dm <sup>3</sup>	Cs(before)-Cs(after) mg/dm <sup>3</sup>	% of Cs ions sorbed from solution	Cs sorption by 1g of clinoptilolite mg/g	TREATED
0.2565	34091.4	17 756.2	16 335.2	47.9	163.4	Washed and dried
0.0513	6818.2	161.2	6656.8	97.6	66.6	Washed and dried
0.2565	34091.4	27850.7	6240.7	91.8	62.4	2M HCl
0.0513	6818.2	708.5	6109.8	89.6	61.1	2M HCl
0.0513	6818.2	769.9	6048.3	88.7	60.5	2M HCl

Sr $\lambda=346\text{nm}$						
Concentration before ion exchange M Sr(NO <sub>3</sub> ) <sub>2</sub>	Sr before ion exchange mg/dm <sup>3</sup>	Sr after ion exchange mg/dm <sup>3</sup>	Sr(before)-Sr(after) mg/dm <sup>3</sup>	% of Sr ions sorbed from solution	Sr sorbed by 1g of clinoptilolite mg/g	TREATED
0.2363	20704.6	17230.0	3474.6	16.8	34.7	Washed and dried
0.0473	4140.9	1724.5	2416.4	58.4	24.2	Washed and dried
0.2363	20704.6	21039.2	-334.6	0.0	-3.3	2M HCl
0.0473	4140.9	3298.1	842.8	20.3	8.4	2M HCl

Remarks: Sr in clinoptilolite-rich zeolite sample collected from in situ outcrop, determined by XRF 1004 ppm (or 1.004 mg). M=mole



**Figure 1.** View on (001) XY plane of the 8 unit cell of clinoptilolite zeolite. The channels of 10-(ellipsoidal) and 8-(circular) rings built of the (Al/Si)O<sub>4</sub> tetrahedrons, along [001] Z-axis are visible. Inside the channels are extra framework(exchangeable) cations and sorbed molecules are shown.

# Removal of paraquat pesticide residue from pre-treated wastewater using activated faujasite tuff from Jordan

**H. A. Jbara and K. M. Ibrahim**

*Hashemite University; Zarqa, Jordan; Email: Ibrahim@hu.edu.jo*

## Introduction

Water is a valuable but limited resource, especially in Jordan. Hence, Jordan has come to rely increasingly on wastewater treatment and reuse even though an increase in the production of chemical substances, including pesticides, are causing serious environmental problems. Therefore, it is necessary to act on removing them completely. The Jordanian faujasite tuff has suitable properties that enable it to be used for ion exchange processes (Ibrahim and Akasheh, 2004).

Faujasite tuff from Jabal Hannoun, NE Jordan, (Ibrahim and Hall, 1995) was selected to treat industrial effluent from a pesticide-producing factory. To determine optimum conditions with maximum efficiency, chemical and thermal activation were carried out and tested. The chemical activation included modification of the original sample by loading with Na, Ca, K, and Mg. Thermal activation was implemented at temperatures 200°C and 300°C. The original faujasite sample, along with the chemically and thermally activated forms, was characterized to verify their mineralogical, chemical, and technical specifications.

## Experimental Methods

Faujasite tuff samples with particle size between 1.00–0.425 mm were chemically activated by soaking at 80°C with 200 mL of 0.5 M solution of CaCl<sub>2</sub>, KCl, MgCl<sub>2</sub>, or NaCl to produce F-Ca, F-K, F-Mg, and F-Na forms, respectively. The original sample (F) and the chemically activated forms (F-Ca, F-K, F-Mg, and F-Na) were subjected to thermal activation by combustion under 200°C and 300 °C for 2 hours. Water adsorption capacity and percent of dehydrated water were measured at temperature range from 100–600°C.

Surface area was estimated using methylene blue. Cation exchange capacity (CEC) was determined following Mercer and Ames (1978).

Wastewater effluent from a pesticide factory containing paraquat (fungicide) was treated by the faujasite tuff using two routes. Route one represents direct contact of the wastewater effluent with the faujasite forms. The second route was pretreatment of the effluent by charcoal followed by treatment with faujasite. Comparison in the efficiency of the chemically and thermally activated faujasite using the two routes was carried out.

## Results and Discussion

Characterization of the faujasite forms shows noticeable variations in the CEC and surface area (Table 1). The former range from 152 meq/100g to 216 meq/100g, and the latter varies between 113 m<sup>2</sup>/g and 286 m<sup>2</sup>/g. These variations are most probably related by the selectivity of the faujasite minerals, which is controlled by ionic radius and charge of the exchangeable ions inside the faujasite structure. As shown in Table 1, variations in the hydration-dehydration are very narrow (< 2%).

**Table 1.** Specification of the original faujasite tuff sample and the chemically activated forms

Specification	Faujasite Forms				
	F	F-Ca	F-K	F-Mg	F-Na
Surface area (m <sup>2</sup> /g)	286	234	113	212	182
CEC (meq/100g)	178	152	216	168	178
Water adsorption capacity % at 200° C	6.9	6.5	7.2	7.3	6.5
Water adsorption capacity % at 300° C	7.9	8.4	8.4	8.0	8.0
Dehydration % at 200° C	9.2	7.9	8.2	9.2	7.6
Dehydration % at 300° C	10.8	9.1	8.9	9.7	9.9

Efficiency of faujasite forms in removing the paraquat is variable (≈ 27%). The average total organic carbon (TOC) value in the treated effluent was 41% compared to 100% in original influent. The best result was

obtained from F-Na (Fig. 1). Thermal activation of the faujasite forms at 200°C enhanced their efficiency to remove paraquat up to 142% and at 300°C to about 213%.

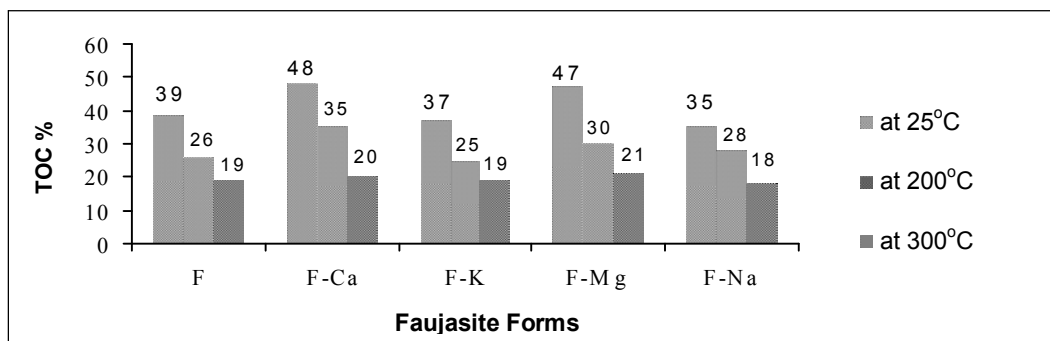


**Figure 1.** Efficiency of faujasite forms and their thermally activated forms in paraquat removal

Performance of the faujasite forms to remove paraquat from wastewater pretreated by charcoal was higher—up to 200% as illustrated in Figure 2.

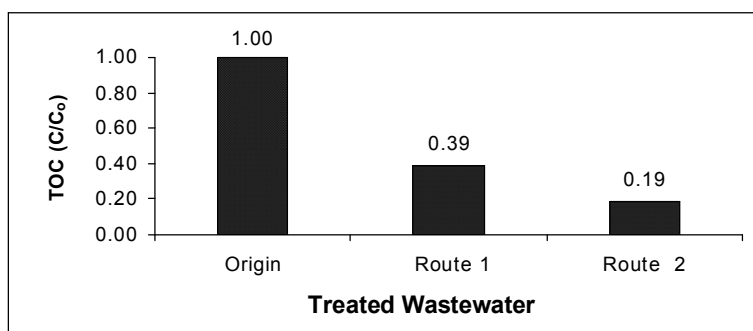


**Figure 2.** Faujasite performance during wastewater treatment using route one and route two

## References

- Ibrahim, K.M. and Akashah, T. (2004) Lead removal from wastewater using faujasite tuff. *Environmental Geology*, **64**, 865–870.
- Ibrahim, K.M. and Hall, A. (1996) The authigenic zeolites of the Aritayn Volcaniclastic Formation, northeast Jordan. *Mineral Deposita*, **31**, 514–522.
- Mercer, B.W. and Ames, L.L. (1978) Zeolite ion exchange in radioactive and municipal wastewater treatment. Pp. 451–462 in: *Natural zeolites; occurrence, properties and uses* (L. Sand and F.A. Mumpton, editors). Pergamon Press. Co., Oxford.

## Characterization of Mexican zeolitic rocks

M. J. Jiménez Cedillo<sup>1,2</sup>, M. T. Olguín Gutiérrez<sup>1</sup>, and M. J. Solache Ríos<sup>1</sup>

<sup>1</sup>*Instituto Nacional de Investigaciones Nucleares; Hidalgo. México; Email:mog@nuclear.inin.mx*

<sup>2</sup>*Universidad Autónoma del Estado de México; Toluca, México;*

### Introduction

Zeolitic tuffs have been found in different regions of Mexico; heulandite-clinoptilolite, mordenite, and erionite, among others, are the main components of these materials (Ostroumov et al., 2003; Ortiz, 2001; De Pablo-Galán and Chávez-García, 1996). Natural zeolites can be used as an economical sorbent of environmental pollutants because of their ion exchange capacity and adsorption properties. This paper attempts to contribute to the knowledge of the characteristics and ion exchange properties of two Mexican zeolites.

### Experimental Methods

One of zeolitic rocks was collected from the arroyo, municipio de la Haciendita, State of Chihuahua, Mexico, and the other was obtained as phillipsite from Compañía Comercializadora de Minerales no Metálicos.

The zeolitic rocks were ground and the grain size of 0.8 mm was chosen. The materials were treated with a sodium chloride solution, then washed until chloride ions were not found in the aqueous media, and dried at 100°C for five hours. The natural and sodium zeolitic materials were subjected to alkaline fusion or acid digestion, and the elemental composition was determined by atomic absorption spectroscopy.

Powder diffraction patterns of the zeolitic rock materials (not thermally treated and heated at 200, 400, 500, 600, 700, and 800°C) were obtained with a Siemens D500 diffractometer coupled to a copper anode X-ray tube. Conventional JCPDS patterns were used to identify the compounds. For scanning electron microscopy, the samples were mounted directly on the holders and covered with sputtered gold to avoid charging effects during observations with a Philips XL 30 electron microscope. The semi-quantitative analyses were done with a DX-4 system.

The surface area in each sample, heated previously at 60°C for 2 hours in a nitrogen atmosphere, was obtained by the Brunauer Emmet Telle (BET) method.

In order to determine the content of water in the materials, thermogravimetric analyses were performed using a TGA 51 TA Instrument in a nitrogen atmosphere with a heating rate of 10°C / minute up to 800°C. The cation exchange capacity was determined by the technique reported by Ming and Dixon (Ming and Dixon, 1987).

### Results and Discussion

In general, the elemental composition of the zeolitic rocks was similar; however, variations in the quantities of cations were observed. The main cations found in the samples were potassium, sodium, and magnesium. However, it has been reported that the main cations in other zeolitic rocks are Na<sup>+</sup>, K<sup>+</sup>, and Ca<sup>2+</sup> (Ming and Dixon, 1987).

The principal components found in the zeolitic rock from the state of Chihuahua were heulandite-clinoptilolite and quartz. The zeolitic rock identified as phillipsite had the same components; therefore, this zeolitic rock contains heulandite-clinoptilolite instead phillipsite. The X-ray diffractograms of the samples heated at different temperatures showed that the zeolitic rock from Chihuahua contains heulandite since changes were observed in the sample diffractogram at 400°C. It has been reported that heulandite is stable around 350–400°C and clinoptilolite is stable up to 700°C (Tsitsishvili et al., 1992). The commercial zeolitic rock labeled as phillipsite is composed of clinoptilolite since it is stable up to 700°C.

The chemical surface composition of the zeolitic rock samples obtained by EDS is Si, Al, Na, K, Ca, Mg, Fe, and O. The SEM image of the zeolitic rock samples revealed the presence of the characteristic crystals of clinoptilolite whose symmetry is monoclinic according to Mumpton and Clayton (1976).

It was found that the zeolitic rock from Chihuahua has a higher surface area than the zeolitic rock labeled as phillipsite, and the surface area is higher for the materials treated with sodium chloride than for the untreated ones. The thermogravimetric behavior of the zeolitic rocks depends on the origin and treatment of the samples.

The cation exchange capacities of the zeolitic rocks treated with sodium chloride was about twice as high as that found for the untreated ones.

We acknowledge the financial support from CONACyT, project 46219.

## References

- De Pablo-Galán, L.; Chávez-García, L.M. (1996) Diagenesis of oligocene vitric tuffs to zeolitas, Mexican volcano belt. *Clays and Clay Minerals*, **44**, 324–338.
- Ming, D.W. and Dixon, J.B. (1987) Quantitative determination of clinoptilolite in soils by a cation-exchange capacity method. *Clays and Clay Minerals*, **35**, 463–468.
- Mumpton, F. A. and Clayton, W. (1976) Morphology of zeolites in sedimentary rocks by scanning electron microscopy. *Clays and Clay Minerals*, **24**, 1–23.
- Ortiz, L. E. (2001). *Criterios y especificaciones concernientes a la exploración y valoración de minerales en la República Mexicana*. Dirección de Recursos Minerales. Gerencia de Recursos Mineros.
- Ostroumov, F.M., Ortiz, L.E., and Corona, C.P. (2003) *Zeolitas de México diversidad mineralógica y aplicaciones*. Sociedad Mexicana de Mineralogía.
- Tsitsishvili, G V., Andronikashvili, T.G., Kirov, G.N., and Filizova, L.D. (1992) *Natural Zeolites*. Ellis Horwood, England.

## Adsorption of pesticides on functionalized zeolites

**V. Jovanović, V. Dondur, L. Damjanović, G. Jordanov, and A. Daković**

*University of Belgrade; Belgrade, Serbia & Montenegro; Email: a.dakovic@itnms.ac.yu*

### Introduction

The extent of pesticide contamination of riparian environments has recently raised much concern because of the entry of these compounds into the food chain. Most agricultural pesticides are hydrophobic organic compounds; however, some of them are hydrophilic or ionic compounds. The wide range of pesticides used makes the design of an adsorbent that is efficient in removal of diverse pesticides extremely difficult. Functionalization of zeolites with cationic surfactants modifies the surface of these materials, changing the hydrophilic surface to hydrophobic (Daković et al., 2005). The aim of this work was to investigate the effectiveness of surfactant-modified clinoptilolite and FAU types of zeolites in the removal of the pesticides from aqueous solution.

### Experimental Methods

Clinoptilolite (CLI) from Zlatokop, Serbia, and a FAU zeolite (NaY, Si/Al = 2.5) purchased from Union Carbide were used. The Ca form of Y zeolite was prepared by standard ion exchange procedure using  $\text{Ca}(\text{NO}_3)_2$ . The long-chain quaternary ammonium compound disteardimethylammonium (DSDMA) chloride purchased from Clariant was used. The critical micellar concentration of surfactants in water solutions were determined by conductivity measurements. The adsorption of selected pesticides on surfactant-modified zeolites was investigated using a batch equilibrated method. The pesticides used in this study were technical grade. The adsorbed pesticides were washed off the zeolites with methanol, and gas chromatography was performed on those solutions.

An Agilent 6890N gas chromatograph, equipped with split/splitless-injector, Agilent 7683 autosampler, and DB-5MS column (30 m length, 250  $\mu\text{m}$  I.D., 0.25  $\mu\text{m}$  df bonded phase of 5% diphenyl-/95% dimethylpolysiloxane on fused silica), were used with an Agilent 5973 inert mass-selective detector. Ionization mode was positive electron impact (EI), 70 eV at 230°C. The injection port temperature was set to 250°C, the transfer line temperature to 280°C, and the quadrupole temperature to 150°C. Carrier gas flow was 1.5 mL/min helium (constant flow mode). The oven temperature program was ramped from 45°C (1.5 min holdup time) to 300°C (6°C/min) and the total run time was 44 min. The injection volume was 1  $\mu\text{L}$ .

### Results and Discussion

The adsorption of mixtures of four pesticides (dimethoate, malathion, fenitrothion, and deltamethrin) whose characteristics vary from hydrophilic to hydrophobic were performed on unmodified zeolites CLI and CaY, as well as on surfactant-modified CLI and CaY. The zeolites covered with a maximum amount of cationic surfactant were used. The maximum adsorption capacity of DSDMA on CLI and CaY was 158  $\mu\text{mol/g}$  and 77  $\mu\text{mol/g}$ , respectively. Zeolites that were not modified with cationic surfactants also showed adsorption of pesticides, but the amounts of adsorbed pesticides were lower than the values obtained for surfactant-modified zeolites. The highest adsorption indexes for pesticides were achieved on surfactant-modified CLI. The quantitative experimental results are summarized in Table 1.



**Table 1.** Adsorption index (I) of pesticides on unmodified and surfactant-modified CLI and CaY

Pesticides	I (%)			
	CLI	CaY	CLI/DSDMA	CaY/DSDMA
Dimethoate	56	48	84	78
Malathion	61	52	86	72
Fenitrothion	71	61	94	85
Deltamethrin	82	68	99	95

Water solubility of used pesticides and retention times are shown in Table 2.

**Table 2.** The water solubility and retention times for investigated pesticides

Pesticide	Water solubility (g/L)	Retention time (min)
Dimethoate	25	24.00
Malathion	0.14	28.17
Fenitrothion	0.02	27.78
Deltamethrin	$0.002 \cdot 10^{-3}$	42.48

Small molecules, such as fenitrothion and dimethoate, can enter the internal pores and channels of used zeolites and undergo dual-mode adsorption.

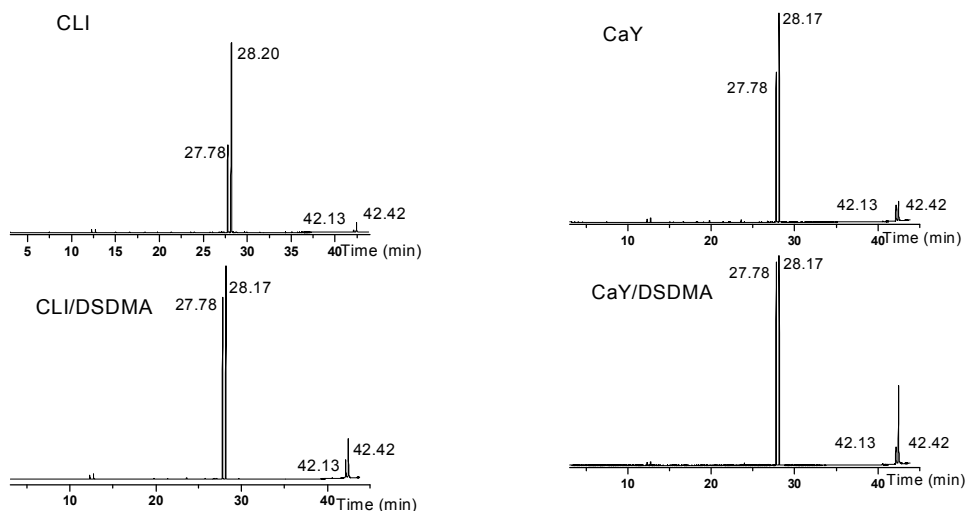


**Figure 1.** The gas chromatographs of adsorbed pesticides on unmodified and surfactant-modified CLI and CaY

Dimethoate, the smallest and the most hydrophilic molecule compared to the other used pesticides, is strongly bonded to zeolites and is not detected by gas chromatography.

The surface functionalization of zeolites can be a useful method for preparation of efficient adsorbents for pesticide elimination from aqueous solutions.

## References

- Daković A., Tomašević-Čanović M., Dondur V., Rottinghaus G.E., Medaković V. and Zarić S., (2005) Adsorption of mycotoxins by organozeolites, *Colloids Surface. B: Biointerfaces*, **46(1)**, 20.

## **The roles of zeolite in the nitrogen removal process and treatment of ammonium-rich wastewater using sequencing batch biofilm reactor (SBBR)**

**J. Y. Jung, D. H. Son, I. T. Yeom, and Y. C. Chung**

*Korea Institute of Science and Technology; Seoul, Korea; Email: jyjung@kist.re.kr*

The modified Z-SBBR is recommended for a new nitrogen removal process that has a special function of consistent ammonium exchange and bioregeneration of zeolite media. Three sets of sequencing batch biofilm reactors, packed with granular activated carbon and zeolite into the reactors, were tested to assess nitrogen removal efficiency. The control Z-SBBR reactor consisted of anoxic-fill, aeration-mixing, settling, and drain/idle phases, meaning that nitrogen removal efficiency was dependent on the decanting volume in a cycle. The operating order sequences in the Z-SBBR were changed in the modified Z-SBBR and AC-SBBR. Anoxic-fill phase was followed by aeration-mixing phase in the Z-SBBR, while aeration-mixing phase was followed by anoxic-fill phase in the modified Z-SBBR to carry  $\text{NH}_4^+$ -N over to the next operational cycle and to reduce total nitrogen concentration in the effluent. In the modified Z-SBBR, nitrification and biological regeneration occurred during the initial aeration-mixing phase, while denitrification and ammonium adsorption occurred in the following anoxic-fill phase. The changed operational sequence in the modified Z-SBBR to adapt the ammonium adsorption and biological regeneration of the zeolite-media could enhance nitrogen removal efficiency. As a result of the continuous operation, the nitrogen removal efficiencies of the control Z-SBBR and AC-SBBR were 75% and 79%, respectively, based on the 23% of decanting volume for a cycle. Meanwhile, the nitrogen removal efficiency of the modified Z-SBBR showed 94% through ammonium adsorption of the zeolite-media during anoxic phase before decanting.

### **Introduction**

Zeolite is well-known for its ability to preferentially remove ammonium ions from wastewater. Unlike synthetic ion exchange resins, zeolite is known to possess a higher selective ion-exchange capability for ammonium ion than  $\text{Ca}^{2+}$  and  $\text{Mg}^{2+}$ , even when the concentration of the latter is higher than the former (McLaren and Farquhar, 1973). Natural zeolite is mainly used to remove ammonium ions from secondary effluent by selective ion exchange (Mercer et al., 1970), but it is rarely tested for the wastewater of high ammonium nitrogen level, due to the chemical regeneration cost of the used zeolite (Koon and Kaufman, 1971).

Several researchers have developed hybrid biological-ion exchange systems, using the zeolite as ion exchange material (Semmens et al., 1981; Semmens and Porter, 1979). Green et al. (1979) and Lahav and Green (1998) recently presented a dual mode process consisting of ion exchange and bioregeneration mode in a single reactor using zeolites for ammonium removal, followed by bioregeneration. In addition to the ammonium removal step with bioregeneration, however, a denitrification step should be provided for complete nitrogen removal from the nitrogen stream generated from bioregeneration.

Jung et al. (1999) conducted studies on the bioregeneration and ammonium exchange capacity of the bio-flocculated zeolite, having powdered zeolite added to a sequencing batch reactor. However, they could not enhance overall nitrogen removal efficiency in a zeolite-added SBR. Therefore, modified zeo-SBR is recommended for nitrogen removal processes that have a special function of consistent ammonium exchange capacity and bioregeneration of the bio-flocculated zeolite as described in Jung et al. (2004).

The objectives of this study are to enhance nitrogen removal in a modified Z-SBBR process packed with granular zeolite by using the role of zeolite in a sequencing batch biofilm reactor.

### **Experimental Methods**

Three sets of sequencing batch biofilm reactors—AC-SBBR, Z-SBBR, and modified Z-SBBR— were tested to assess nitrogen removal efficiency. One liter of media was packed into the reactors. The size of granular zeolite was in the range of 2.37–4.74 mm. The real density and specific surface area of the zeolite was 1.73 g/ml and 44.9  $\text{m}^2/\text{g}$ , respectively. Meanwhile, the size of granular activated carbon was similar to zeolite but the real

density and surface area were 1.07 g/ml and 945.7 m<sup>2</sup>/g, respectively. The working volume of each reactor was 3 liters. The mixing conditions were maintained by recycling liquid in the bottom part of the reactor to the upper part of the reactor via a recycle pump. Aeration and mixing took place in the aerobic reacting phase. The temperature of the three reactors was maintained at 25°C using a water bath (LAUDA 12M). A programmable logic controller automatically controlled the whole operation including aerating, recycling, feeding, and draining. Seeding sludge obtained from a municipal wastewater treatment plant in Seoul, Korea, was screened with a No. 20 sieve (0.425 mm) in order to eliminate inert materials.

Three sequencing batch reactors were operated at a cycle of 24 hours. The 0.7 liter was drained during a cycle. Hydraulic retention time was 4.3 days. The operating condition of the control Z-SBBR reactor consisted of an anoxic-fill phase (0.25 h), an anoxic phase (7.75 h), an aeration-mixing phase (15 h), a settling phase (0.5 h), and a drain and idle phase (0.5 h). The operating condition of the modified Z-SBBR and AC-SBBR consisted of a first aeration-mixing phase (14.8 h), an anoxic-fill phase (0.25 h), an anoxic phase (7.75 h), a second aeration-mixing phase (0.2 h), a settling phase (0.5 h), and a drain and idle phase (0.5 h). In order to remove the remaining organics, 10 minutes of the second aeration-recycling period was provided in the modified Z-SBBR. Backwashing was conducted once a week to remove excess biomass in the reactor. The composition of the synthetic wastewater was glucose 469–937 mg/L, NH<sub>4</sub>Cl 764 mg/L (200 mg NH<sub>4</sub><sup>+</sup>-N/L), NaHCO<sub>3</sub> 1,500–3,500 mg/L, KH<sub>2</sub>PO<sub>4</sub> 44–88 mg/L, and other trace elements (Fe, Mn, Ca, Mg).

## References

- McLaren, J.R. and Farquhar, G.J. (1973) Factors affecting ammonia removal by clinoptilolite. *J. of Environmental Engineering Division*, **August**, 429–446.
- Mercer, B.W., Ames, L.L., Touhill, C.J., Van Slyke, W.J. and Dean, R.B. (1970) Ammonia removal from secondary effluents by selective ion exchange. *Journal of Water Pollution Control Federation*, **42**, R95–R107.
- Semmens, M.J., Kleive, J., Schnobrich, D. and Tauxe, G.W. (1981) Modeling ammonium exchange and regeneration on clinoptilolite. *Water Research*, **15**, 655–666.
- Green, M., Adriaan, M., Lahav, O. and Sheldon, T. (1996) Biological-ion exchange process for ammonium removal from secondary effluent. *Water Science Tech*, **34**(1-2), 449–458.
- Lahav, O and Green, M. (1998) Ammonium removal using ion exchange and biological regeneration. *Water Research*, **32**, 2019–2028.
- Jung J.Y., Chung, Y.C., Shin, H.S, Son, D.H. (2004) Enhanced ammonia nitrogen removal using consistent biological regeneration and ammonium exchange of zeolite in modified SBR process. *Water Research*, **38**, 347–354.

## Hydrothermal synthesis of microporous titanosilicates

V. Kostov-Kytin, S. Ferdov, B. Mihailova, and O. Petrov

*Bulgarian Academy of Sciences; Sofia, Bulgaria; Email: vkytin@clmc.bas.bg*

### Introduction

Microporous titanosilicates are closely related to natural zeolites and, of late, have drawn interest for various applications. Natural occurrences are mostly restricted to postmagmatic derivatives of peralkaline rocks (Pekov and Chukanov, 2005). More than 100 of these minerals are already reported (Chukanov and Pekov, 2005). These are zeolite-like compounds with frameworks built of tetrahedral (Si) fragments and transition elements (mainly Ti, but also Nb and Zr) having 6-fold, and, rarely, 5-fold coordination. Microporous titanosilicates often occur together with heterophyllo-silicate minerals that contain the same set of major cations (Ferraris and Gula, 2005). These materials are promising ion exchangers, sorbents, and catalyst carriers. In recent years, such phases, with or without mineral analogues, have been prepared by various synthesis techniques (Rocha and Anderson, 2000); however, their number is smaller than that provided by nature.

Aiming at optimization of the synthesis conditions for preparation of titanosilicates with desired pore systems and functionality, we explored the system  $\text{Na}_2\text{O}-\text{K}_2\text{O}-\text{TiO}_2-\text{SiO}_2-\text{H}_2\text{O}$ . Here we present results on the role of certain physicochemical parameters on the crystal type, size, morphology, and orientation of the run-products.

### Experimental Methods

The synthesis studies were held in the system:  $a\text{Na}_2\text{O}-b\text{K}_2\text{O}-c\text{TiO}_2-10\text{SiO}_2-675\text{H}_2\text{O}$  where  $0 \leq a \leq 9$ ,  $0 \leq b \leq 9$ ,  $a+b=9$ ,  $0.3 \leq c \leq 3.3$  at temperature  $200^\circ\text{C}$ , crystallization time 24 h and autogenous pressure. The reactants used were:  $\text{SiO}_2$ ,  $\text{TiCl}_4$ ,  $\text{NaOH}$ ,  $\text{KOH}$ , and distilled water. No organics were used as templates. The precursor gels were prepared by mixing the silicate alkaline aqueous solution with the hydrolyzed  $\text{TiCl}_4$  and subsequently transferred into 10 ml Teflon-lined autoclaves. In addition, kinetic investigations were carried out in the system:  $a\text{Na}_2\text{O}-b\text{TiO}_2-10\text{SiO}_2-675\text{H}_2\text{O}$ , where  $3 \leq a \leq 40$ ,  $1 \leq b \leq 6$  and synthesis duration varied from 16 to 240 h.

Phase identification and characterization were performed by powder X-ray diffraction analysis. SEM was used to examine morphology, size, and orientation of the run-products. Infrared, Raman and  $^{29}\text{Si}$  MAS NMR spectroscopic methods were applied to analyze the relationship between the chemical compositions of the initial synthesis gels and the favored crystalline titanosilicate phases formed upon hydrothermal treatment.

### Results and Discussion

Nine pure crystalline titanosilicate phases have been synthesized under the described conditions above. These are the microporous ETS-10, ETS-4 (zorite), STS (Ti analogue of the mineral umbite), GTS-1 and synthetic sitinacite, the layered AM-1 and AM-4 (Rocha and Anderson, 2000), and two dense titanosilicates which are analogous to the minerals natisite and paranatisite.

The role of the exchangeable cations as structure directing agents is evidenced by the formation of AM-1 instead of ETS-10 and ETS-4 instead of STS when Na replaces K in the potassium free system.

The crystal size and morphology of the run-products within the crystallization field of STS are strongly influenced by the  $\text{TiO}_2$  content in the initial gel (Fig. 1). Increasing its value promotes transition from large single crystals through intergrowths with decreasing size and degree of orientation of the building crystallites to spherical aggregates composed of microcrystallites.

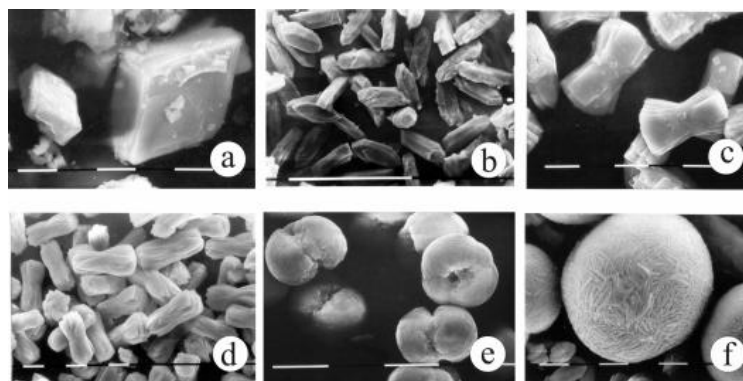


**Figure 1.** Micrographs of STS crystals and aggregates synthesized hydrothermally for 24 h in the system  $2\text{Na}_2\text{O}-7\text{K}_2\text{O}-x\text{TiO}_2-10\text{SiO}_2-675\text{H}_2\text{O}$ , where: a,  $x=0.3$ , bar length 10  $\mu\text{m}$ ; b,  $x=0.6$ , bar length 100  $\mu\text{m}$ ; c,  $x=0.9$ , bar length 10  $\mu\text{m}$ ; d,  $x=1.2$ , bar length 10  $\mu\text{m}$ ; e,  $x=1.5$ , bar length 10  $\mu\text{m}$ ; f,  $x=1.8$ , bar length 10  $\mu\text{m}$ .

In the potassium free system, the initial  $\text{Na}_2\text{O}/\text{TiO}_2$  ratio specifies the pH of the reaction medium in the range 12–13. It is found that lower  $\text{Na}_2\text{O}/\text{TiO}_2$  values favor the formation of layered and microporous materials, whereas at higher values titanosilicates with dense structures crystallize, preferentially. The kinetic investigations well confirm the validity of Ostwald's rule of successive phase transformations leading to the appearance of more thermodynamically stable products in the following sequence: AM-1—ETS-4—GTS-1—AM-4—sitinacite—paranatisite—natisite, i.e., from microporous and layered titanosilicates with low Ti content up to dense phases with high Ti content. The fact that the framework-topology type and phase morphology are quite sensitive to variations of the reaction medium allows precise tuning in the preparation of titanosilicates with tailored pore systems and functionality.

It is concluded that to increase the structural diversity of synthetic heterosilicates with useful properties it is necessary to vary the composition of framework and extraframework cations as well as to work in somewhat milder conditions concerning the pH and the temperature of the reaction medium.

## References

- Chukanov, N.V. and Pekov, I.V. (2005) Heterosilicates with tetrahedral-octahedral frameworks: Mineralogical and crystal-chemical aspects. *Reviews in Mineralogy & Geochemistry*, **57**, 105–143.
- Ferraris, G. and Gula, A. (2005) Polysomatic aspects of microporous minerals— Heterophyllosilicates, palysepiolites and rhodesite-related structures. *Reviews in Mineralogy & Geochemistry*, **57**, 69–104.
- Pekov, I.V. and Chukanov, N.V. (2005) Microporous framework silicate minerals with rare and transition elements: Minerogenetic aspects. *Reviews in Mineralogy & Geochemistry*, **57**, 145–171.
- Rocha, J. and Anderson, M.W. (2000) Microporous titanosilicates and other novel mixed octahedral-tetrahedral framework oxides. *European Journal of Inorganic Chemistry*, **5**, 801–818.

## The influence of zeolite-containing material on the respiratory activity of a leached chernozem contaminated by hydrocarbons

A. Krivosheeva<sup>1</sup>, N. Archipova<sup>2</sup>, V. Breus<sup>1</sup>, G. Khaidarova<sup>1</sup>, and I. Breus<sup>1</sup>

<sup>1</sup>Kazan State University; Kazan, Tatarstan, Russia; Email: ibreus@ksu.ru

<sup>2</sup>Kazan State Pedagogical University; Kazan, Tatarstan, Russia

### Introduction

Natural zeolites and zeolite-containing materials (ZCM) are intensively used as soil additives to improve soil fertility and also in remediation technologies (including phytoremediation) for soils and waste products contaminated by heavy metals, radioactive elements, and hydrocarbons (HC). These capabilities are due to the high sorption and cation-exchange capacities of zeolite and clay minerals and the presence of carbonates and other minerals, which improve physical and physical-chemical soil properties. But till now, the problem of the influence of ZCM on such an integral parameter of soil microbial activity as the intensity of CO<sub>2</sub> evolution (the characteristic of soil self-cleaning ability) has not been found out. The data on this problem for soils contaminated by heavy metals are poorly systematized and inconsistent (Mühlbachová et al., 2003; Usman et al., 2004). As to soils contaminated by HC, such data are practically absent. The last problem is one of the most important ecological problems in the Republic of Tatarstan. Here, oil recovery extends over 1,420 thousand hectares of the territory (more than 1/5 of the overall land area); the recovery of 1 ton of oil is accompanied by the destruction and contamination of 1–1.3 m<sup>3</sup> of soil.

### Experimental Methods

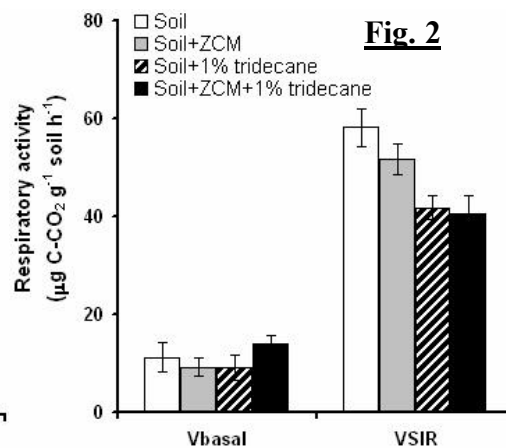
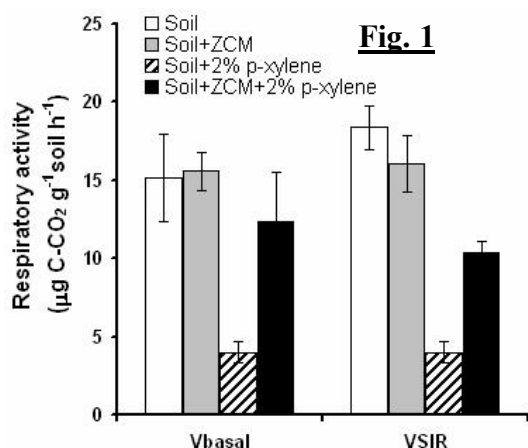
Two experiments on the influence of ZCM from the Tatarsko-Shatrashansky deposit (heulandite-clinoptilolite, 16%; clay minerals, 24%; calcite, 20%) on soil microbial respiratory activity were performed. The investigated soil was heavy loam leached chernozem (LCh), the most typical soil for oil-polluted areas. The soil was mixed with zeolite in order to give 25% zeolite amendment. The soil microbial respiratory activity was determined with the use of gas-chromatographic method by CO<sub>2</sub> evolution (Anderson et al., 1978). The basal respiration speeds (V<sub>basal</sub>) and substrate-induced respiration speeds (V<sub>sir</sub>) in LCh uncontaminated and contaminated by HC, with and without added ZCM, were measured. All of the experiments were made in triplicate. The ratio of V<sub>basal</sub> in the contaminated soil to the V<sub>basal</sub> in uncontaminated soil was used as a measure of the intensity of HC microbial degradation in LCh. The first experiment was carried out during 3 weeks under laboratory conditions at 22°C with soil contaminated by p-xylene (2 wt.%) at soil moisture of 20%. The variants of this experiment were formed as: LCh, LCh+ZCM, LCh+HC, LCh+HC+ZCM. The second greenhouse scale experiment was carried out during 4.5 weeks at 22–24°C and soil moisture of 20% in 1.5 kg vegetation pots with tridecane-contaminated soil (1 wt %). The variants of this experiment were the same as the four variants in the first one, but additionally four variants with plants (oats, *Avena sativa* L. and maize, *Zea mays* L.) were also tested.

### Results and Discussion

The introduction of ZCM into uncontaminated LCh did not reliably influence any determined parameters. Soil contamination with both p-xylene and tridecane results in decreasing V<sub>basal</sub> values of 70–75% and 15–20%, respectively (Figs. 1, 2). It testified of the stronger oppression of aromatic HC on microbial community of LCh when compared with aliphatic HC. Much more drastic decrease was observed on V<sub>sir</sub> values: in comparison with uncontaminated soil this effect was 80% for p-xylene and 40% for tridecane. Unlike the clean soil, the addition of ZCM into contaminated LCh changed soil microbial activity and, in particular, essentially improved it. As a result, in variants with added ZCM, the V<sub>basal</sub> values in soil polluted by p-xylene and tridecane increased 3 and 1.5 times, respectively. The increase of sustainability of soil microbial communities under ZCM influence was so essential that V<sub>basal</sub> values in contaminated LCh were close to (in the case of p-xylene) and even higher (in the case of tridecane) than V<sub>basal</sub> values without contamination. The effect of ZCM addition into contaminated LCh on V<sub>sir</sub> values was also positive but slightly less. However, the above-mentioned effect

of improvement of biological activity in LCh due to ZCM addition practically vanished when fodder plants (both oats and maize) were grown there. It should be also noted that ZCM use did not remove the negative influence of HC on plant growth. The depression of plant above-ground and root biomass in HC-polluted LCh was 65% and 55% for maize and 70% and 80% for oats, respectively.

Thus, our experimental results suggested that the addition of ZCM into contaminated heavy loam leached chernozem, a soil typical for European part of Russia, decreases stress of indigenous soil microbial community caused by aromatic p-xylene. Furthermore, in the case of tridecane contamination (1 wt %) soil microbial activity even slightly increases due to ZCM adding. The results of our additional laboratory experiments with sawdust (often used for the amelioration of clayey soils) suggest specific influence of ZCM on biological activity of leached chernozem. Unlike ZCM, this organic sorbent did not affect the sustainability of microbiocenose of HC contaminated soil.



The work was supported by Grants of International Scientific Technical Center, Project #2419 and Russian Foundation of Basic Research, Project 06-04-49098.

## References

- Mühlbachová, G., and Šimon, T. (2003) Effects of zeolite amendment on microbial biomass and respiratory activity in heavy metal contaminated soils. *Plant Soil Environ*, **49**(12), 536–541.
- Usman, A. R. A., Kuzyakov Y., and Stahr K. (2004) Effect of clay minerals on extrability of heavy metals and sewage sludge mineralisation in soil. *Chemistry and Ecology*, **20**(2), 1–13.
- Anderson, J. P. E., and Domsch, K. H. (1978) A physiologically active method for the quantitative measurement of microbial biomass in soils. *Soil Biology and Biochemistry*, **10**, 215–221.

## Metal nanodots formed and supported on chabazite surfaces

S. M. Kuznicki, D. J. A. Kelly, J. Chen, J. Bian, C. Lin, Y. Liu, D. Mitlin, and Z. Xu

University of Alberta; Edmonton, Alberta, Canada; Email: [steve.kuznicki@ualberta.ca](mailto:steve.kuznicki@ualberta.ca)

The formation of metal nanoclusters, nanodots, and nanowires is the subject of intense current scientific and engineering interest. With many of their properties manifested on a nano and sub- nano dimensional scale, molecular sieves would appear to be excellent candidates to be in the vanguard of such efforts (Tsapatsis, 2002).

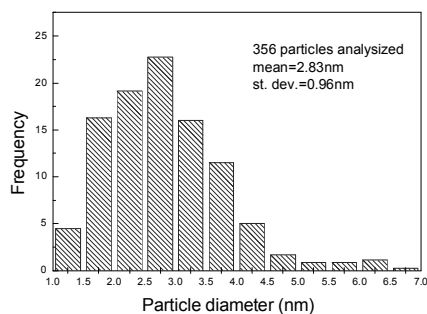
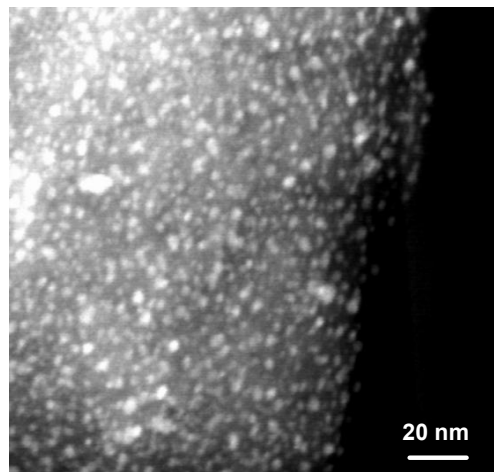


**Figure 1** TEM image of silver nanodots stabilized on the surface of upgraded chabazite. Showing particle size distribution on 1-5 nm, centered in 2.83 nm.

A wide range of techniques has been reported to synthesize metal nanoparticles. Silver nanoparticles and their formation have recently been summarized in a paper on silver nanoprisms (Metraux and Mirkin, 2005). While silver ensembles are well known to form within zeolite cavities under certain conditions, and much larger configurations often form freely on zeolite surfaces, we report high densities of uniform silver nanospheres on the order of 1-5 nanometers, centered in the regime of 3 nanometers, forming under a wide range of conditions on sedimentary chabazite surfaces. These nanospheres are stable to at least 500°C on the chabazite surfaces and remain as uniform nanoensembles under prolonged heating at that temperature. Twenty (20) weight percent or more of a zeolite metal nanosphere composite material may be composed of these silver particles.

Many useful properties might be expected from such nanostructured silver materials. Reversible mercury adsorption at temperatures as high as 300°C has been observed. Unusual antibacterial and antifungal properties have been observed, much stronger than silver ions alone. These properties differ greatly from those observed for bulk metallic silver. Nanosilver particles are well known antimicrobial agents (Burrell et al., 1995) finding increasing use in bandages and related applications.

Current techniques for nanosilver generation are expensive and cumbersome. Chabazite surface stabilization offers a new route to such materials. We know of no other technique that can generate such high concentrations of uniform silver nanospheres so easily, reproducibly, and economically. We believe that this effect emanates from the extremely polarizing surfaces of chabazite. While silver nanospheres form easily on chabazite surfaces, chemically upgraded chabazite induces the formation of even more uniform balls at even higher

concentration.

### References

- Burrell, R. E., Morris, L. R., Apte, P. S., Sant, S. B. and Gill, K. S. (1995) Anti-microbial materials. US Patent 5,837,275, filed Jun. 2, 1995, and issued Nov. 17, 1998.
- Metraux, G. S. and Mirkin, C. A. (2005) Rapid thermal synthesis of silver nanoprisms with chemically tailorable thickness. *Adv. Mater.*, 17(4), 412–415.
- Tsapatsis, M. (2002) Molecular sieves in nanotechnology era. *American Institute of Chemical Engineers*, 48(4), 654–660.



## Chemical upgrading of sedimentary Bowie, Arizona sodium chabazite

S. M. Kuznicki, C. Lin, D. J. A. Kelly, J. Bian, A. Koenig, J. Chen, Y. Liu, and Z. Xu

University of Alberta; Edmonton, Alberta, Canada; Email: [steve.kuznicki@ualberta.ca](mailto:steve.kuznicki@ualberta.ca)

Mineral chabazite is potentially the most polarizing of all molecular sieve adsorbents, including synthetics. As such, it is a prime candidate for many gas polishing applications and other uses where certain trace gases are to be collected and concentrated. Chabazite is such a strongly polarizing adsorbent (Maroulis et al., 1987a) that it can cleanly resolve oxygen from argon at ambient temperature by preferential interaction with the oxygen molecules (Maroulis et al., 1987b).

While samples of large crystals of essentially pure chabazite are well known (for example from Wasson Bluff, Nova Scotia, Canada), large, commercially exploitable deposits, like those at Bowie Arizona, invariably have the chabazite co-formed with significant amounts of other natural zeolites such as clinoptilolite and erionite. Because of its unusually strong interactions with appropriate adsorbates, pure chabazite, available on an industrial scale, could open new opportunities for the utilization of natural zeolites.

It has been reported that raw sodium Bowie chabazite ore can be recrystallized by caustic digestion into an aluminum-rich version of the chabazite structure with Si/Al that can approach 1.0 (Kuznicki et al., 1988). The more siliceous phases of the chabazite ore, clinoptilolite and erionite, selectively dissolve in alkaline medium, reforming with the chabazite as an apparent template. While such semi-synthetic high aluminum chabazite analogs manifest the expected increase in cation exchange capacity (to as high as 7.0 meq/g) and demonstrate high selectivity towards heavy metals from solution, especially lead (Kuznicki et al., 1991), these aluminum-rich materials are unstable toward rigorous dehydration and therefore cannot be sufficiently activated to be employed as selective gas adsorbents.

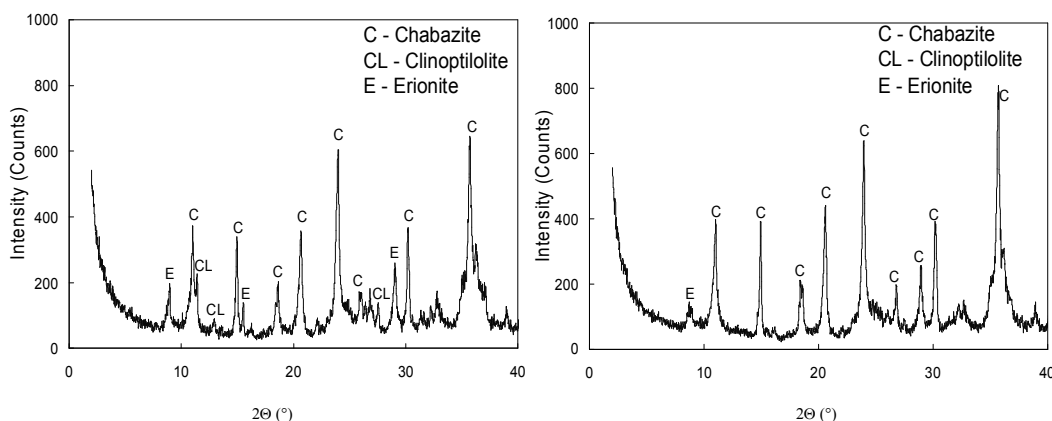


**Figure 1.** XRD powder pattern of raw chabazite ore (left) and upgraded chabazite (right) for  $2\theta \approx 0\text{--}40^\circ$ .

We report that sodium Bowie chabazite ore may be reformed and upgraded in an alkaline medium to a semi-synthetic purified and upgraded chabazite with elemental compositions resembling the original chabazite component of the ore (Si/Al  $\sim 3.0\text{--}3.5$ ), if substantial excess soluble silica is present in the reaction/digestion medium. In this process, essentially all of the clinoptilolite and much of the erionite is dissolved and reformed into chabazite, but not at the high aluminum content found in solely caustic digestion. This new, semi-synthetic, purified and upgraded chabazite is stable towards the rigorous dehydration needed to activate it as an adsorbent. Also, if the process is conducted on granules of the chabazite ore (which are of generally poor mechanical

strength) the granules gain greatly in mechanical strength as the clinoptilolite and erionite, which are recrystallized into chabazite, appear to bind the edges of the existing chabazite platelets.

Preliminary testing on these more uniform, upgraded semi-synthetic chabazites indicate that they have enhanced adsorbent properties for molecules such as water, form stronger acid sites (in the H form), and show an enhanced propensity to form uniform dispersions of metal nanospheres (such as silver) on their surfaces compared to the raw chabazite ore from which they are derived.

## **References**

- Kuznicki, S. M. and Whyte, Jr., J. R. (1988). Ion-exchange agent and use thereof in extracting heavy metals from aqueous solutions. US Patent 5,071,804, filed Sep. 8, 1988, and issued Dec. 10, 1991.
- Kuznicki, S. M. and Whyte, Jr., J. R. (1991). Ion-exchange agent and use thereof in extracting heavy metals from aqueous solutions. US Patent 5,223,022, filed Jul. 1, 1991, and issued Jun. 29, 1993.
- Maroulis, P. J., Coe, C. G., Kuznicki, S. M., Clark, P. J. and Roberts, D. A. (1987a). Selective adsorption process using an oxidized ion-exchanged dehydrated chabazite adsorbent. US Patent 4,744,805, filed Jul. 1, 1987, and issued May 17, 1988.
- Maroulis, P. J., Coe, C. G., Kuznicki, S. M. and Roberts, D. A. (1987b). Selective chromatographic process using an ion-exchanged, dehydrated chabazite adsorbent. US Patent 4,747,854, filed Jun. 25, 1987, and issued May 31, 1988.

## Natural zeolite bitumen cracking and upgrading

**S. M. Kuznicki, W. C. McCaffrey, J. Bian, E. Wangen, and A. Koenig**

*University of Alberta; Edmonton, Alberta, Canada; Email: [steve.kuznicki@ualberta.ca](mailto:steve.kuznicki@ualberta.ca)*

With advancing technology in recovery and processing, the oilsands of North America may well represent the world's largest available petroleum reserve (Alberta Chamber of Resources, 2004). The oil or bitumen these sands yield offers several unique problems. The oil recovered is much more viscous than normal petroleum and must be diluted with expensive solvents before it can be transported by pipeline for chemical upgrading. The bitumen also contains much higher levels of contaminants than typical crude. Levels can be literally an order of magnitude higher for sulfur, nitrogen, and metals than encountered in traditional petroleum.

Single pass, disposable cracking agents could improve the performance of Visbreaking processes and enhance the economics of field upgrading of in situ-derived bitumen. Such agents would need to be much less expensive than current commercial cracking catalysts while manifesting substantial activity. If such materials could also begin upgrading by removing sulfur, nitrogen, and/or metals, an additional benefit could be derived. Zeolite's well-known properties as catalysts and adsorbents would seem to offer promise for such a multifunctional field-upgrading approach.

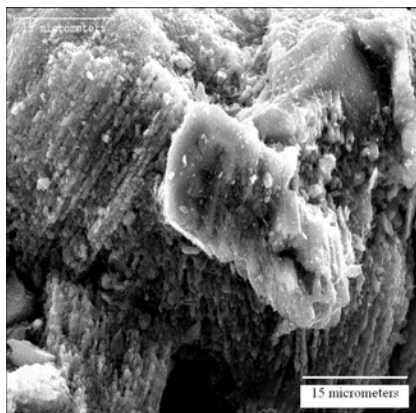


**Figure 1** SEM image of upgraded chabazite showing platy morphology with high exterior surface area.

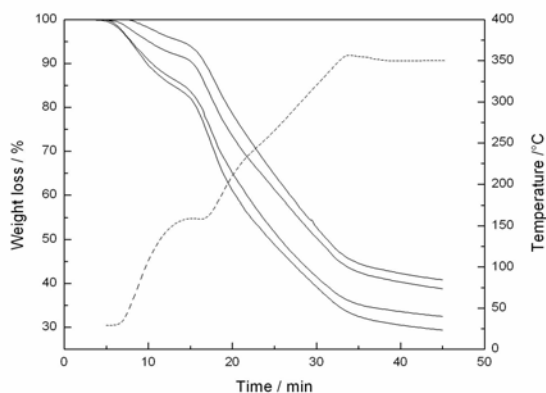


**Figure 2.** TG simulated distillation curves of extractable products (under vacuum, ASTM D1160-03, 2005). From top to bottom: no catalyst present, H-Y added, modified mineral chabazite added, upgraded chabazite added.

Owing to unique chemical and morphological properties (Fig. 1), the mineral zeolite chabazite was chosen for modification and testing. Under mild cracking conditions (1 hour at 400°C in a sealed microreactor), catalyst-bearing oil sand produced extractable products of significantly lower viscosity that contained substantially more middle distillates and less residue (Fig. 2) than raw oil sand processed under identical conditions, where only thermal cracking reactions would be expected.

Model cracking studies using hexadecane indicate that these modified mineral zeolites may, in fact, be more active cracking agents than undiluted premium commercial FCC catalyst. Ammonia desorption studies (Auroux, 2006) indicate that individual acid sites available from chabazite may be qualitatively stronger than those of H-Y zeolite. Additionally, substantial sulfur and nitrogen were removed from the bitumen and left in the residual sand waste product. Such materials may offer promise for partial upgrading schemes to reduce in-field solvent requirements and enhance initial product quality.

## References

- Alberta Chamber of Resources (2004) *Oil sands technology: Unlocking the potential*. Edmonton, Canada, 92 pp.
- ASTM Active Standard (2005) D1160-03 Standard test method for distillation of petroleum products at reduced pressure. *ASTM book of standards*, **05.01**.
- Auroux, A. (2006) Acidity and basicity: Determination by adsorption microcalorimetry. Pp. 1-108 in: *Molecular Sieves - Science and Technology* (H. G. Karge and J Weitkamp, editors). 5, Springerlink, Berlin. Also available online at <http://www.springerlink.com> (accessed January 13, 2006).

## **A molecular modeling investigation of cation and water adsorption in crystalline titanosilicate materials.**

**J. P. Larentzos<sup>1</sup> and E. J. Maginn<sup>2</sup>**

<sup>1</sup>*Sandia National Laboratories; Albuquerque, New Mexico, USA; Email: jlarent@sandia.gov*

<sup>2</sup>*University of Notre Dame; Notre Dame, Indiana, USA*

Remediation of high-level nuclear waste requires efficient separation of trace amounts of radioactive elements from alkaline waste solutions in order to minimize disposal volume required for vitrification. Development of highly selective ion exchangers with increased capacity and kinetics is desired for a more cost-effective separation process. Crystalline titanosilicates with sitinakite topology have demonstrated the ability to selectively remove cesium, strontium, and the actinides, and are thus under investigation to gain a fundamental understanding of the origins of selectivity and to enhance ion exchange performance.

Molecular simulations have the potential to be valuable design tools in guiding future synthesis efforts. The accuracy of molecular simulations is critically dependent upon the quality of the intermolecular force field used to describe the interactions. In this work, an intermolecular force field is developed to describe the nature of the interactions among the counterbalancing cations, water molecules, and the titanosilicate framework. The electronic structure is computed through plane-wave pseudo-potential density functional theory (DFT) simulations and extended to classical, force-field based simulations.

Grand canonical Monte Carlo simulations are conducted to compute adsorption isotherms, adsorption energies, and isosteric heats of adsorption for water in the acid-exchanged titanosilicate. The water loading at saturation is in excellent agreement with results obtained from neutron diffraction experiments. The adsorption energies at low water loading agree well with DFT calculations. The force field is shown to be superior to a previously derived, empirically fitted force field, where better agreement of water positions, orientations, and occupancies with neutron diffraction experiments is observed.

Finally, we apply the new force field to the Na<sup>+</sup>, Cs<sup>+</sup>, and Sr<sup>2+</sup> exchanged titanosilicates and niobium substituted counterparts. Replica exchange Monte Carlo and grand canonical Monte Carlo simulations are conducted to investigate hydration effects on the titanosilicate counterbalancing cations. Through replica exchange Monte Carlo simulations, there is evidence of cation redistribution as water loading increases. The preferred cation and water locations and occupancies at saturation are predicted to be in excellent agreement with experimental powder diffraction results.

## Sustaining plant growth in conditions of extreme metal pollution

P. J. Leggo<sup>1</sup> and B. Ledésert<sup>2</sup>

<sup>1</sup>University of Cambridge; Cambridge, UK; Email: Leggo@esc.cam.ac.uk

<sup>2</sup>Université de Cergy-Pontoise, Neuville-sur-Oise, France

A new strategy of soil amendment is presented that will greatly enhance the scope of phytoremediation. In cases of extreme metal pollution, waste sites remain barren of vegetation; consequently, a critical factor is how to supply sufficient plant nutrients to sustain growth.

The utilization of an organo-zeolitic soil amendment is put forward as an answer to this problem because, unlike the use of synthetic chemicals, it provides a natural source of plant nutrients by greatly increasing the nitrifying bacterial population of the soil (Leggo, 2000). The organo-zeolitic material is a mixture of poultry manure and crushed zeolitic tuff, rich in clinoptilolite. Ammonium ions, produced from the biological decomposition of protein, are taken into the zeolite pore structure. When the mixture is added to a soil, the ammonium ions are back-exchanged, typically, by potassium into the soil pore water. Once in the soil pore water, the ammonium ions are then oxidized by nitrifying bacteria. This results in a large increase of available nitrate-nitrogen. Commonly, increases of three orders of magnitude with respect to a clean, unamended soil control occur in soil leachates. As a by-product of the ensuing enzyme reactions, free hydrogen ions are produced that have the effect of dissociating metal cations from soil particles causing extensive mineralization in the soil environment. Again, as in the case of the increase in the nitrate concentration, metal cation concentrations in leachates are increased by two orders of magnitude relative to clean, unamended soil controls. It appears from this work that the adequate nutrient range for spring wheat (*Triticum aestivum*, L) for elements such as N, P, K, Ca, Mg, and Na is not exceeded in the highly mobilized soil because plant growth fully utilizes the amount of the elements mobilized (Leggo and Ledésert, 2001).

Furthermore, in moist conditions, we have shown that zeolite crystal surfaces become covered in biofilm (Leggo and Ledésert, 2006). Recent work demonstrates that bacteria enclosed in biofilm can survive and remain functional in highly metal polluted environments (Kemner et al., 2005). In our work, the aqueous leachate chemistry of plant substrates shows that nitrifying bacteria remain fully functional in metal-polluted substrates that normally are highly phytotoxic. We have now sustained the growth of metal-tolerant plants (*Arabidopsis halleri*, *Brassica napus* and *Salix viminalis*) in sediments that have extreme metal concentrations measured in weight percentages.

### References

- Kemner, K.M., O'Loughlin, E.J., Kelly, S.D. and Boyanov, M.I. (2005) Synchrotron x-ray investigations of mineral-microbe-metal interactions. *Elements*, **1.4**, 217-221.
- Leggo, P.J. (2000) An investigation of plant growth in an organo-zeolitic substrate and its ecological significance. *Plant and Soil*, **219**, 135-146.
- Leggo, P.J., and Ledésert, B. (2001) Use of organo-zeolitic fertilizer to sustain plant growth and stabilize metallurgical and mine-waste sites. *Mineralogical Magazine*, **65.5**, 563-570.
- Leggo, P.J., Ledésert, B., and Christie, G. (2006) The role of clinoptilolite in organo-zeolitic-soil systems used for phytoremediation. *The Science of the Total Environment*, **363**, 1–10.

## Competitive adsorption of polycyclic aromatic hydrocarbons on organo-zeolites

J. Lemić, M. Tomašević–Čanović, S. Milošević, M. Adamović, and S. Milićević

*Institute for Technology of Nuclear and Other Mineral Raw Materials; Belgrade, Serbia and Montenegro; E-mail: j.lemic@itnms.ac.yu*

### Introduction

Complex mixtures of hazardous chemicals such as polycyclic aromatic hydrocarbons (PAHs) in contaminated soil and groundwater can have severe and long-lasting effects on health. Extensive research has been conducted using various adsorbents to bind PAHs in contaminated water. Cetylpyridium-exchanged, low-pH montmorillonite clay was shown to be an effective sorbent for a variety of PAHs in water (Groisman et al., 2004). Ake et al. (2003) demonstrated the effectiveness of a matrix (sand)-immobilized organoclay for the cleaning up of PAHs and pentachlorophenol from groundwater.

The main objective of this research was to investigate the adsorption of polycyclic aromatic hydrocarbons on organo-zeolites. The hydrophobic character of the surface of the organo-zeolites was investigated in water vapor adsorption experiments. The effects of adsorbent size, SDBAC loading, and initial concentration of PAHs on the adsorption efficiency were determined. The adsorption was studied under batch and column conditions.

### Experimental Methods

A clinoptilolite-rich zeolite tuff was obtained from the Beocin Mine in Serbia and Montenegro. According to XRPD analysis, the clinoptilolite content is ~80% and the main impurities in the zeolite are quartz, feldspar, and carbonate. The sample was sieved to the following particle sizes: 0–0.4 mm (Z I), 0.4–0.8 mm (Z II), and 0.8–3.0 mm (Z III). The zeolite was modified using steryl dimethylbenzylammonium chloride (SDBAC) solutions of four initial concentrations: 50, 75, 100, and 150 mmol/dm<sup>3</sup> in order to achieve SDBAC/ECEC ratios of 0.67, 1.0, 1.33, and 2.0. To measure the ability of the obtained organo-zeolites to adsorb water vapor, the dried samples were kept in a 100% relative humidity of atmosphere (saturated solution of NaCl) for 24 h.

A concentrated solution of a mixture of phenanthrene, fluorene, fluoranthene, pyrene, and benz[a]anthracene in acetone was prepared for the experiments. The same quantity (5 g) of the organo-zeolite samples (of different size and SDBAC loading) was added to 500 cm<sup>3</sup> of PAHs solution having a concentration of 10 µg/dm<sup>3</sup> of the individual PAHs (total concentration of PAHs in the solution was 50 µg/dm<sup>3</sup>). In order to investigate the influence of the initial concentration of the solution, 0.5 g samples of OZ II 75 (Roman and Arabic numerals denote particle size and SDBAC loading) were shaken with 500 cm<sup>3</sup> of different solutions of PAHs, in which the individual concentrations of PAHs ranged from 6.0–80.0 µg/dm<sup>3</sup> (total concentrations ranging from 30–400 µg/dm<sup>3</sup>). The column experiment was conducted using a vertical glass column of 150 mm height and 7 mm diameter. The column was filled with 2 g (68 mm height) of sample OZ II 75. The feed was introduced using a peristaltic pump at a flow rate of about 6 cm<sup>3</sup>/min. The initial concentration of the PAHs solution was 50 µg/dm<sup>3</sup>.

### Results and Discussion

The adsorption of water vapor decreased linearly with increasing surfactant loading up to 75 mmol/kg, when a minimum on the adsorption curves can be observed. With loadings above 75 mmol/kg, the water adsorption increased, which can be ascribed to an intensification of the hydrophilic properties of the organo-zeolite samples.

For the unmodified zeolite (0.4–0.8 mm), the adsorption indexes of the PAHs were less than 50%, except for benzantracene at 79%. The maximal adsorption (100%) for all PAHs, at a given concentration of solution, was achieved on the sample OZ II 75, the surface of which was covered with a monolayer of surfactant. With further increasing of the SDBAC on the zeolite surface (bilayer coverage, Sullivan et al., 1998), the adsorption efficiency decreased only for fluorine (OZ II 100–82% and OZ II 150–91%). The results showed that only fluorine and phenanthrene were not completely adsorbed on the organo-zeolite samples.

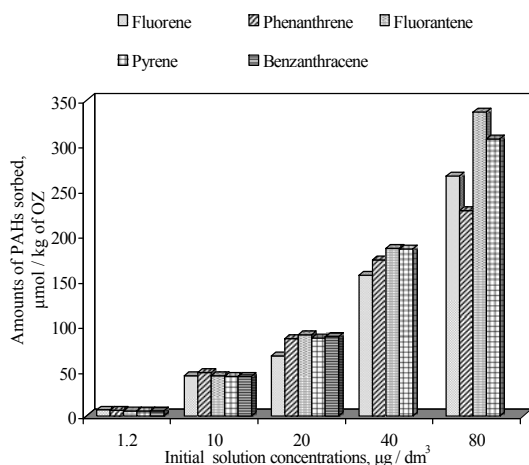


**Figure 1.** Amounts of PAHs adsorbed versus the initial concentration of the solution

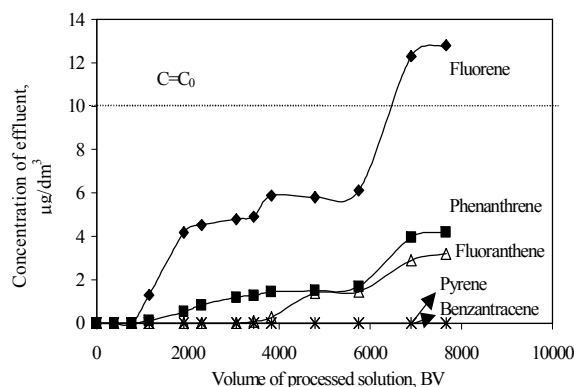


**Figure 2.** Breakthrough curves of the PAHs

At individual PAHs concentrations of  $80 \mu\text{g/dm}^3$  (total PAHs concentration in solution was  $320 \mu\text{g/dm}^3$  (Fig. 1), sample OZ II 75 had the highest affinity for the adsorption of fluoranthene ( $68 \mu\text{g/dm}^3$ ). The amounts of the other PAHs adsorbed decreased in the order: pyrene ( $62 \mu\text{g/dm}^3$ ), fluorine ( $44 \mu\text{g/dm}^3$ ), and phenanthrene ( $40 \mu\text{g/dm}^3$ ). The first PAH to appear in the effluent solution was fluorine after 770 ( $2.0 \text{ dm}^3$ ) bed volumes (BV) had passed through the column. Phenanthrene and fluoranthene appeared after 1300 BV and 3800 BV. The concentration of fluorene in the effluent after 6120 ( $16 \text{ dm}^3$ ) of solution (Fig. 2) had passed through the column was greater than the initial concentration. Thus, further adsorption was followed by desorption of the least hydrophobic PAH.

## References

- Ake, C.L., Wiles, M.C., Huebner, H.J., McDonald, T.J., Cosgriff, D., Richardson, M.B., Donnelly, K.C. and Phillips, T.D. (2003) Porous organoclay composite for the sorption of polycyclic aromatic hydrocarbons and pentachlorophenol from groundwater. *Chemosphere*, **51**, 835–844.
- Groisman, L., Rav-Acha, C., Gerstl, Z. and Mingelgrin, U. (2004) Sorption of organic compounds of varying hydrophobicities from water and industrial wastewater by long- and short-chain organoclays. *Applied Clay Science*, **24**, 159–166.
- Sullivan, E.J., Carey, J.W. and Bowman, R.S. (1998) Thermodynamics of cationic surfactant sorption onto natural clinoptilolite. *Journal of Colloid and Interface Science*, **206**, 369–380.



## Computational and experimental studies of the structure and dynamics of water in natural zeolites

**D. W. Lewis<sup>1</sup>, D. Salih<sup>2</sup>, A. R. Ruiz-Salvador<sup>3</sup>, H. Emerich<sup>4</sup>, W. van Beek<sup>4</sup>, C. L. I. M. White<sup>1</sup>, and M. A. Green<sup>1,2</sup>**

<sup>1</sup>*University College London; London, United Kingdom; Email: d.w.lewis@ucl.ac.uk*

<sup>2</sup>*Royal Institution of GB; London, United Kingdom*

<sup>3</sup>*University of Havana; Havana, Cuba*

<sup>4</sup>*Swiss-Norwegian Beam Lines, European Synchrotron Radiation Facility; Grenoble Cédex, France*

We will describe a number of computational and experimental studies of the structure and behavior of water in natural zeolites. We combine theoretical and experimental measurements of the static and dynamic structure of water as a function of different hydration levels, brought about through changes in both pressure and temperature. For the Leonhardite-Laumontite system we demonstrate how pressure can lead to increased hydration. For Goosecreekite we show how increasing the temperature leads to a lowering of the dynamic behavior of the intrazeolitic water.

### Introduction

The interactions between zeolite frameworks and the cations and water present within the micropores are critical not only to their formation but also to their application in fields such as ion-exchange. Subtle changes in structure and hydration levels are particularly important in the use of naturally occurring deposits of minerals as part of long-term radioactive waste storage depositaries (Bish et al., 2003), more so if conditions lead to so-called superhydration (e.g., Lee et al., 2004). Thus, a detailed characterization of the structural and dynamic properties of intrazeolite water is paramount in our understanding of zeolite behavior.

In a series of combined computational and experimental studies we are investigating the changes in the structure and dynamics of intrazeolitic water in a number of model natural zeolites. Through careful characterization we are able to identify and isolate a variety of different behaviors and thus quantify their contribution to the structure and stability of the zeolite structure as a whole.

### Results and Discussion

We will outline the development of computer modeling methods for the determination of dehydration pathways in zeolites using the specific case of Laumontite (White et al., 2004): we show how our method reproduces both long-range and short-range structure and also the energetics of dehydration. We shall also show how we were able to predict—independently experimentally shown (Lee et al., 2004)—how increased pressure leads to increased water content in this material (converting “Leonhardite” to Laumontite). We shall provide a further analysis of our results in light of the experimental work.

We shall extend our discussion of water-cation and water-framework interaction through our experimental and computational studies of Goosecreekite. Although all the water molecules directly coordinate to the extra-framework calcium in this structure, the material exhibits a number of well-defined stages during dehydration. Furthermore, we have isolated metastable partially dehydrated phases. Thus, we have performed a variety of experimental studies of this dehydration process including, using a unique setup on the SNBL at the ESRF, whereby we are able to perform a combined synchrotron powder X-ray diffraction and Raman spectroscopy measurement of the dehydration process. Preliminary results are shown below. We have been able to correlate the structural and vibrational changes through four different regimes. We have also performed quasi-elastic neutron scattering experiments that quantify the degree and nature of the H<sub>2</sub>O motion within the zeolite pores. Simultaneously, molecular dynamics simulations of the same systems were performed, and we find not only strong correlation between the various techniques but are also now able to provide a detailed molecular-level mechanism for the observed transitions in the long- and short-range structural order and the dynamics of the zeolitic water. Indeed, we show how partial dehydration leads to a *loss* of water mobility; indeed, we see a partial freezing of water at 120°C.

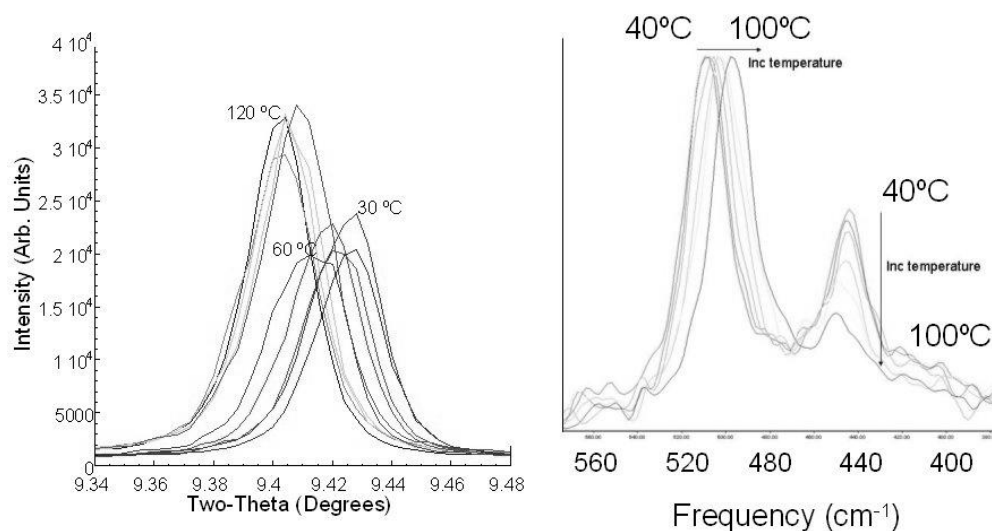


**Figure 1.** In situ dehydration of the first water molecules from Goosecreekite—combined (left) X-ray diffraction and (right) Raman spectroscopy.

From these two studies we are now able to identify and distinguish (and quantify) the various contributions that framework-cation, cation-water, water-water, and water-framework contributions make to the evolution of zeolite stability and will discuss these in the context of zeolite formation and application.

## References

- Bish, D.L., Vaniman, D.T., Chipera, S.J. and Carey, J.W. (2003) The distribution of zeolites and their effects on the performance of a nuclear waste repository at Yucca Mountain, Nevada, USA. *American Mineralogist*, **88**, 1889–1902.
- Lee, Y., Hriljac, J.A. and Vogt, T. (2004) Pressure-induced migration of zeolitic water in laumontite. *Physics and Chemistry of Minerals*, **31**, 421–428.
- White, C.L.I.M., Ruiz-Salvador, A.R. and Lewis, D.W. (2004) Pressure-induced hydration effects in the zeolite laumontite. *Angewandte Chemie International Edition*, **43**, 469–472.

## **Grain size effect on chromate sorption and transport through surfactant-modified zeolite columns**

**Z. Li**

*University of Wisconsin – Parkside; Kenosha, Wisconsin, USA; Email: li@uwp.edu*

In this study, zeolite aggregates with particle sizes of 3.4–4.8 mm, 1.4–2.4 mm, and < 0.4 mm were modified by hexadecyltrimethylammonium (HDTMA) bromide, a cationic surfactant, to surfactant bilayer coverage. Batch chromate sorption and column chromate transport experiments were performed to evaluate the effect of particle size on chromate sorption and retention. The 3.4–4.8 mm surfactant-modified zeolite (SMZ) had an HDTMA loading level of 80 mmol/kg and a concurrent counterion bromide loading level of 34 mmol/kg. The chromate retardation factor ( $R$ ) was 60. The 1.4–2.4 mm SMZ had an HDTMA loading level of 130 mmol/kg and an  $R$  of 80. The < 0.4 mm SMZ had an HDTMA loading level of 250 mmol/kg, a bromide loading level of 110 mmol/kg, and an  $R$  of 500. The results show that particle sizes of the SMZ play an important role in designing and using SMZ as permeable barriers for groundwater remediation.

### **Introduction**

Remediation of groundwater containing anionic contaminants presents a great challenge. Because of its low cost, SMZ has been studied for potential uses as a permeable barrier material to remove anionic contaminants from water for more than 10 years. Sorption of anionic contaminants such as chromate and nitrate was attributed to surface anion exchange resulted from bilayer formation of sorbed surfactant on zeolite surfaces when excess surfactants were present (i.e., beyond 100% of the zeolite's external cation exchange capacity) (Li and Bowman, 1997; Li et al., 1998). Uptake of chromate by SMZ could be as high as 160 mmol/kg, or 19 g/kg (Vujaković et al., 2000). However, most of these studies were limited to batch tests, although a preliminary pilot scale test was performed using SMZ to remove chromate from water (Bowman et al., 2001). The chromate retardation factor ( $R$ ) increased by two orders of magnitude in column test using surfactant-modified illite (Li et al., 2002). However, due to its low hydraulic conductivity, surfactant-modified illite can only be used as an impermeable barrier.

The primary goal of this study was to investigate the effect of particle size of SMZ on chromate sorption and retardation from batch and column flow through tests for results to shed lights on further optimal use of SMZ for groundwater remediation.

### **Experimental Methods**

The zeolite used (from St. Cloud Mine in Winston, NM) was in an aggregate form with particle sizes of 3.6–4.8 mm, 1.4–2.5 mm, and < 0.4 mm. The size of individual crystals in the aggregates is in the micrometer range. The zeolite was modified by hexadecyltrimethylammonium bromide to 80, 130, and 250 mmol/kg for 3.6–4.8 mm, 1.4–2.5 mm, and < 0.4 mm zeolites, respectively.

Chromate batch sorption tests were performed by combining 2.5 g of SMZ and 10.0 mL chromate solution at varying concentrations in 50 mL centrifuge tubes. The mixtures were shaken and centrifuged, and the supernatants were analyzed for equilibrium chromate concentration. Chromate sorption was determined from the difference between initial and final solution concentrations.

Chromate transport experiments were performed using plastic columns (2.16 cm internal diameter and 10.7 cm in length). Raw zeolite and SMZ each were packed in duplicates and were fed with DI water at 20 mL/h to saturate the columns. The input chromate concentrations ranged from 11 to 15 mg/L. About 10–20 pore volumes (PVs) of chromate solution were fed through unmodified columns, and then DI water fed until the effluent concentration reached zero. The modified columns were fed with the chromate solution until 10–20 PVs after full breakthrough, then with DI water until the effluent chromate concentration was below 0.20 mg/L. Samples were analyzed for chromate, HDTMA, and bromide concentrations. The breakthrough curves were fitted by HYDRUS-1D.

## Results and Discussion

Chromate sorption on SMZ followed a Langmuir isotherm (Li and Bowman, 1997; Li et al., 1998):

$$S = \frac{K_L S_m C}{1 + K_L C} \quad (1)$$

Chromate sorption capacity and intensity increased as the SMZ particle size decreased (Figure 1). Unmodified zeolite has an  $R$  of 1, indicating no retardation of chromate (Figure 2 insert), while SMZ increased the  $R$  value significantly (Figure 2). The  $R$  values are 60, 80, and 500 for 3.6–4.8 mm, 1.4–2.5 mm, and < 0.4 mm SMZ, respectively, contrasted to 150 for surfactant-modified illite (Li et al., 2002). The inverse relationship between particle size and  $R$  shows that care must be taken to maintain a higher hydraulic conductivity while achieving a larger  $R$  when using SMZ as a permeable barrier for groundwater remediation. Furthermore, slow, but persistent, desorption of HDTMA from the upper layer of the surfactant bilayer coupled with desorption of counterion bromide may eventually render the sorbed surfactant into a monolayer configuration.

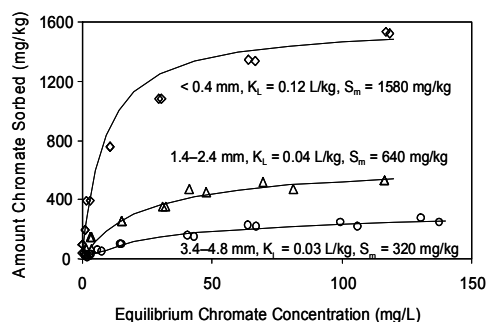


Figure 1. Chromate sorption isotherm on SMZ.

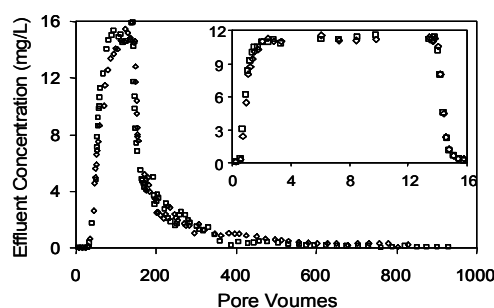


Figure 2. Chromate transport through 1.4–2.4 mm SMZ and raw zeolite (insert).

## References

- Bowman, R.S., Li, Z., Roy, S.J., Burt, T., Johnson, T.L. and Johnson, R.L. (2001) Pilot test of a surfactant-modified zeolite permeable barrier for groundwater remediation. Pp. 161-185 in: *Physical and Chemical Remediation of Contaminated Aquifers* (S. Burns and J. A. Smith, editors.) Kluwer Academic Publishers.
- Li, Z. and Bowman, R.S. (1997) Counterion effects on the sorption of cationic surfactant and chromate on natural clinoptilolite. *Environ. Sci. Technol.*, **31**, 2407-2412.
- Li, Z., Anghel, I., and Bowman, R.S. (1998) Sorption of oxyanions by surfactant-modified zeolite. *J. Dispers. Sci. Technol.*, **19**, 843-857.
- Li, Z., Alessi, D., Zhang P. and Bowman R.S. (2002) Organo-illite as a low permeability sorbent to retard migration of anionic contaminants, *J. Environ. Engineer.*, **128**, 583-587.
- Vujaković, A.D., Tomašević-Čanović, M.R., Daković, A.S., and Dondur, V.T. (2000) The adsorption of sulphate, hydrogenchromate and dihydrogenphosphate anions on surfactant-modified clinoptilolite." *Applied Clay Sci.*, **17**, 265-277.

## Natural zeolite occurrences in New Mexico

V. W. Lueth

*New Mexico Tech; Socorro, New Mexico, USA; Email: vwlueth@nmt.edu*

New Mexico contains a wide variety of zeolite occurrences ranging in size from microcrystals in vugs to altered ash deposits (approximately 1.6 x 4.9 km of 10 m thick) that constitute the largest domestic zeolite producer in the United States. Large volcanic fields, extensive areas of hydrothermal alteration, variable climate, and active tectonism all contribute to the wide variety and distribution of these minerals. The largest and most widespread zeolite occurrences are associated with rocks emplaced during two major pulses of regional magmatism.

The largest of the volcanic events was the development of the Mogollon-Datil and Boot Heel volcanic fields that erupted from 35 to 25 Ma (Chapin et al., 2004). These rocks are associated with the large-scale and commercially mined zeolite deposits at Chloride and Buckhorn. In addition to those occurrences, museum-quality specimens of zeolite minerals can be found almost anywhere in the volcanic fields with notable mineralization along the Gila River, at Alum Mountain, and associated with the Taylor Creek tin deposits. The mineralogy of occurrences predominantly consists of chabazite, stilbite, heulandite, mesolite, analcime, and lesser amounts of levyne and tompsonite hosted by altered andesite.

The last volcanic episode of regional volcanism is associated with emplacement of mostly basaltic rocks along the Rio Grande rift over the last 5 Ma (Chapin et al., 2004). In these occurrences, the zeolites generally occur as vesicle fillings in only a select number of lava flows. The young ages of the flows and lack of significant burial probably inhibits the number of occurrences in these rocks. Notable localities do exist, however, mainly at Arroyo del Oso.

Zeolites are also associated with sulfide ore mineralization in a number of deposits. The Continental Mine, near Fierro, has produced a number of fine specimens of heulandite, stilbite, and scolecite hosted by skarn. The zeolites represent a significant period of retrograde alteration in this deposit and others, including some pegmatites.

Rock and mineral collectors have discovered most of the zeolite occurrences in New Mexico attesting to the value of these amateurs to science. Northrup (1996) lists 14 zeolite mineral species of which only 5 were reported in scientific journals. Collectors first reported all of the others in mineral symposia proceedings. A survey of zeolite minerals in the New Mexico Bureau of Geology and Mineral Resources Mineral Museum shows 7 additional confirmed species not reported in the literature and supplied by collectors. New discoveries are made annually with some of the most recent being a new chabazite locality in the Bear Mountains of Socorro County and apophyllite from the Servietta basalt flows northwest of Española. The wide distribution of volcanic rocks coupled with relative remoteness of the state bodes well for the discovery of additional occurrences and zeolite minerals.

### References

- Chapin C.E., McIntosh, W.C. and Chamberlin, R.M. (2004) The late Eocene-Oligocene peak of Cenozoic volcanism in southwestern New Mexico. Pp. 271–294 in: *The Geology of New Mexico—A geologic history* (G.H. Mack and K.A. Giles, editors). New Mexico Geological Society Special Publication 11.
- Northrup, S.A. (1996) *Minerals of New Mexico*. Third Edition revised by Florence LaBruzza, University of New Mexico Press, Albuquerque, 346 pp.

## Quantitative mineralogy and genetic history of the natural zeolite deposits of coastal Ecuador

L. Machiels<sup>1</sup>, F. Morante<sup>2</sup>, R. Snellings<sup>1</sup>, J. Elsen<sup>1</sup>, and C. Paredes<sup>2</sup>

<sup>1</sup>*Katholieke Universiteit Leuven; Heverlee, Belgium; Email: lieven.machiels@geo.kuleuven.be*

<sup>2</sup>*Escuela Superior Politécnica del Litoral; Guayaquil, Ecuador*

### Introduction

Recent discoveries indicate the presence of a large zeolite deposit in Coastal Ecuador, west of Guayaquil (Lopez et al., 2002; Morante, 2004; Machiels, 2005). The zeolite-bearing rocks are found in the Cayo formation, a rock unit of Cretaceous age consisting of marine volcanoclastic and interstratified sedimentary rocks. The rocks are found in an area of more than 1000 km<sup>2</sup> large, cropping out in a horst-type mountain range west of Guayaquil, bordered by recent sedimentary basins in the north, south, and east and by a fault zone in the west.

The zeolite minerals possess a wide range of local applications in agriculture (fertilizer), the cement industry (pozzolana), and in the treatment of mining and city waste waters (extraction of heavy metals, protons, and ammonia). There are large vertical and lateral variations in lithology and mineralogy through the rock unit; therefore, exploitation is restricted to thin green tuff layers that make up only 10–20% of the rock unit. To achieve an optimal exploitation of the deposit, a detailed study of its depositional setting, mineralogy, and diagenetic to low-grade metamorphic history is required. This abstract presents the results of a master thesis and the first results of a Ph.D. research that started in October 2005.

### Experimental Methods

Three cross-sections were sampled through the Cayo formation and its neighbouring rock units, among which is the section along the Perimetral highway, proposed as the new type locality of the Cayo formation by Benítez (1995). At some locations, detailed 50 m sections were sampled through volcanoclastic sequences to investigate small-scale lithological and mineralogical variations. To obtain a precise XRD quantification of all authigenic minerals, samples were hand ground to < 500 µm, spiked with 10% of ZnO internal standard, and ground in methanol to < 10 µm using a McCrone micronizing mill. Grain size was checked by infrared spectroscopy. Random mounts were prepared using the side-loading technique and were placed in an equilibration chamber of RH 52.0% for at least 16 hours prior to XRD measurement. For the quantitative interpretation of the data, two independent methods, a profile summation method (RockJock<sup>®</sup>) and the Rietveld method (Topas Academic<sup>®</sup>), were used. Some zeolite samples were exchanged to a K-rich form to achieve an optimal fit with crystallographic data; others were heat-treated prior to XRD measurement to distinguish between clinoptilolite and heulandite. Thin sections were investigated with optical microscopy and SEM-EDX analysis. Major elements were measured by AAS.

### Results and Discussion

The Cayo formation consists of decametric sequences of coarse- to fine-grained volcanoclastic sediments, interpreted as submarine ignimbrites (pyroclastic block and ash flow deposits, 70–80% of rock unit), interstratified with air fall tuffs, minor turbidites, and pelagic sediments. Volcanoclastic material originated from an andesitic (ignimbritic sequences) to rhyolitic (fine grained green tuffs) source, which was probably a volcanic arc related to an intra-oceanic subduction zone of Late Cretaceous age.

Zeolite minerals dominate the entire outcrop area of the Cayo formation, except the base of the rock unit at the Perimetral freeway section and some small hydrothermally altered zones near recent faults related to the uplift of the area. In the eastern region (Guayaquil), a member of the clinoptilolite-heulandite solid solution series, a Ca-rich heulandite, is present in most samples. Laumontite and mordenite are less common and analcime is rare. In the central region, south of Isidro Ayora, ignimbritic sequences at the top of the rock unit have a mineralogy similar to the Guayaquil section, but the basal part of the rock unit, more than half of the section, is dominated by green mordenite tuffs. In the western region, at the Rio Ayampe cross-section,

heulandite is common in ignimbritic sequences, while mordenite (associated with minor heulandite) is common in rhyolitic tuffs and some sedimentary rocks. Wairakite was found in a small fault bounded by uplifted blocks.

A burial metamorphic model is proposed to explain the actual distributions of authigenic minerals in the area. Two major zones can be distinguished along the Perimetral highway section, comparable to zonations described in similar deposits (e.g. Coombs, 1954). A zeolite-rich zone is found at the top of the section (zone 1, thickness ~ 1.5 km) and an albite-quartz-calcite (laumontite) zone is found in the basal part (zone 2, thickness ~ 1.5 km). In zone 1, heulandite is the dominant zeolite. Interstratifications of heulandite-, mordenite-, laumontite- and analcime-rich layers can be explained by differences in elemental composition, grain size, and permeability. The basal part of ignimbritic sequences consists of lapilli tuffs and is dominated by heulandite associated with feldspars (volcanic plagioclase and K-feldspar, probably partially albitized), pyroxenes (volcaniclastic augite and clinoenstatite), calcite in vein and matrix, quartz (< 10%, partially volcaniclastic), Fe-Ti oxides, celadonite, smectite, and chlorite. Fine-grained crystal tuffs are rich in detrital feldspar and quartz; sedimentary rocks have a high authigenic quartz content and a low zeolite content. The heulandite percentage is typically around 30–40 %, but varies through a single sequence. Laumontite occurs as vein fillings and replaces heulandite in the matrix of some lapilli tuffs in the basal part of zone 1. Prograde reactions (formation of laumontite, calcite, and albite) are clearly favored in permeable coarse-grained lapilli tuffs. Along the Perimetral highway three mordenite-rich green rhyolitic tuff layers were found (one currently exploited). Mordenite is associated with minor heulandite, quartz, and smectite; zeolite content is up to 85%. Zone 2 consists of similar lithologies as zone 1 but is dominated by albite, quartz, and calcite and in some samples small amounts of laumontite. The model developed can be useful for indicating future zeolite exploitation areas.

## References

- Benítez, S. (1995) Evolution géodynamique de la province côtière sud-équatorienne au crétacé supérieur-Tertiaire. *Géology Alpine*, **71**, 3-163.
- Coombs, D.S. (1954) The nature and alteration of some Triassic sediments from Southland, New Zealand. *Transactions of the Royal Society of New Zealand*, **82**, 65-109.
- López, K., Morante, F., Botto, L. and Adhemazar, J. (2002) Geología y mineralogía de zeolitas al Oeste de Guayaquil, provincia del Guayas-Ecuador. Pp. 250-253 in: *Memorias del XV congreso geológico boliviano, Santa Cruz*.
- Machiels, L. (2005) Geologische en mineralogische studie van de zeolietafzettingen van de Cayo formatie aan de kust van Ecuador. Master's thesis, Katholieke universiteit Leuven, Leuven, België, 91 pp.
- Morante, F. (2004) Las zeolitas de la Costa de Ecuador (Guayaquil): Geología, caracterización y aplicaciones. Ph.D. thesis, Universidad Politécnica de Madrid. Escuela Técnica Superior de Ingenieros de Minas de Madrid, Madrid, España, 382 pp.

## Structural investigation of $\text{Zn}^{2+}$ sorption on clinoptilolite tuff

**K. Margeta<sup>1</sup>, N. Zabukovec Logar<sup>2</sup>, N. Novak Tutar<sup>2</sup>, K. Maver<sup>3</sup>, I. Arcon<sup>3</sup>, V. Kaucic<sup>2</sup>, and S. Cerjan-Stefanovic<sup>1</sup>**

<sup>1</sup>University of Zagreb; Zagreb, Croatia; Email: kmargeta@fkit.hr

<sup>2</sup>National Institute of Chemistry; Ljubljana, Slovenia

<sup>3</sup>Nova Gorica Polytechnic; Nova Gorica, Slovenia;

### Introduction

Studies investigating the possibility of using natural zeolites for zinc removal from wastewaters based on equilibrium and dynamic ion exchange on natural and synthetic zeolites were already published (Shahwan et al., 2005; Cerjan–Stefanović et al., 1996). Here we report on the microscopic, diffraction, and X-ray absorption spectroscopic analyses of a  $\text{Zn}^{2+}$ -modified zeolite tuff with emphasis on the determination of the local environment of zinc in order to improve the understanding of the sorption mechanism of  $\text{Zn}^{2+}$ .

### Experimental Methods

Natural zeolite, obtained from a large sedimentary deposit in Vranjska Banja, Serbia and Montenegro, was used in this work. The sample was crushed in an agate mortar and washed with distilled water in order to remove the surface dust. Grain size fractions below 0.063 mm were chosen for the experiment because they were proven to enable the highest uptake of metal cations. 5.000 g of the sample was pretreated with 100 mL of 2 mol/L solutions of NaCl or  $\text{CaCl}_2$ , respectively. Of the Na-treated and Ca-treated zeolites, 1.000 g were placed in 100 mL of 500 mol/L solutions of  $\text{ZnCl}_2$ . Desorption of  $\text{Zn}^{2+}$  was performed by treating 1.000 g of the  $\text{Zn}^{2+}$ -modified samples with 100 mL of 2 mol/L solution of NaCl. The bulk chemical compositions of the natural zeolite (PZ1-Zn), Na-pretreated  $\text{Zn}^{2+}$ -modified (NaZ-Zn), and Ca-pretreated  $\text{Zn}^{2+}$ -modified (CaZ-Zn) samples were determined by the classical chemical analysis (Trgo et al., 2005). The size and the morphology of the crystals in the samples were studied by using a scanning electron microscope (JEOL JSM 5800). Elemental analyses of the three samples were also carried out using Energy Dispersive X-ray Spectroscopy (EDXS) analysis within the LINK ISIS 300 system, attached to the same microscope. The X-ray powder diffraction (XRPD) patterns were collected at room temperature on a Siemens D-5000 diffractometer using  $\text{CuK}\alpha$  radiation (1.5406 Å). X-ray absorption spectra of Zn samples and reference compound (ZnO) were measured in the energy region of the Zn K-edge in transmission mode at E4 beamline of the HASYLAB synchrotron facility at DESY in Hamburg, Germany. Zn samples were prepared as self-supporting pellets with absorption thickness ( $\mu\text{d}$ ) of about 2.5 above the Zn K-edge.

### Results and Discussion

The chemical analyses showed that the natural zeolite partly converted to the sodium and calcium forms by the NaCl and  $\text{CaCl}_2$  treatments, i.e., the content of the  $\text{Na}^+$  and  $\text{Ca}^{2+}$  ions increased while at the same time the content of the other exchangeable ions decreased. After zinc loading, the content of sodium and calcium decreased and the content of the rest of the cations remained practically unchanged. X-ray diffraction analysis revealed the presence of clinoptilolite, feldspar, and quartz phases and confirmed that the framework structures remained undistorted during the sodium, calcium, and zinc treatments. The metallographic preparation of the sample by polishing the crystals embedded in the epoxy film enabled a cross-sectional view of the crystallite grains and a detailed elemental analysis of all major phases (Fig. 1). In the  $\text{Zn}^{2+}$ -modified samples, zinc was found only in one phase, i.e., in small dark grey crystallites where the Si/Al ratio and the presence of other elements corresponded to the clinoptilolite phase. Besides clinoptilolite, large crystallites of feldspars and quartz were detected (bright grey).



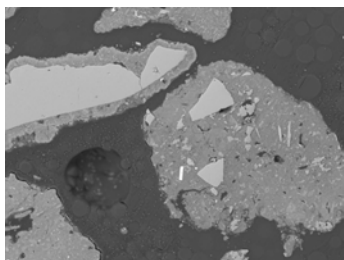


**Figure 1.** SEM picture of polished crystallites of Zn<sup>2+</sup>-modified zeolite sample.

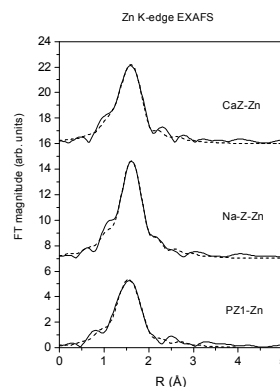


**Figure 2.** Fourier transforms of k<sup>3</sup>-weighted Zn EXAFS

Zn K-edge EXAFS spectra of the PZ1-Zn, NaZ-Zn and CaZ-Zn samples were quantitatively analysed for the coordination number, distance, and Debye-Waller factor of the nearest coordination shells of zinc. EXAFS fit for PZ1-Zn in the R range from 1 Å to 2.3 Å shows that zinc atoms are coordinated to four oxygens, two at 1.94 Å and two at 2.09 Å, which indicates that Zn atoms in the sample are located at sites with distorted tetrahedral symmetry. On the other hand, EXAFS fit for NaZ-Zn shows that zinc atoms are coordinated to six oxygens, four at 2.04 Å and two at 2.20 Å, indicating that Zn atoms in the sample are located at sites with distorted octahedral symmetry. Additionally, EXAFS fit for CaZ-Zn shows that zinc atoms are coordinated to six oxygens at 2.04 Å, indicating octahedral symmetry of zinc (Fig. 2). Pretreatment of zeolite tuff therefore affects the sorption mechanism and local structure of Zn<sup>2+</sup>. Preliminary X-ray photoelectron spectroscopy depth analysis showed that most of the zinc is distributed on the surface of the crystallites.

We thank the support by the Slovenian Research Agency through the research programmes P1-0021 and P1-0112, the EC-Research Infrastructure Action under the FP6 "Structuring the European Research Area" Programme (through the Integrated Infrastructure Initiative "Integrating Activity on Synchrotron and Free Electron Laser Science"). Access to synchrotron radiation facility of HASYLAB (beamline E4, project II-04-065) is acknowledged. We would like to thank Konstantin Klementiev of HASYLAB for expert advice on beamline operation.

## References

- Cerjan-Stefanović, Š., Ćurković, L. and Filipan, T. (1996) Metal ion exchange by natural zeolites. *Croatica Chemica Acta*, **69**, 281–290.
- Shahwan, T., Zünbül, B., Tunusoğlu, Ö. and Eroğlu, A.E. (2005) AAS, XRPD, SEM/EDS, and FTIR characterization of Zn<sup>2+</sup> retention by calcite, calcite-kaolinite, and calcite-clinoptilolite minerals. *Journal of Colloid and Interface Science*, **286**, 471–478.
- Trgo, M., Peric, J. and Vukojevic Medvidovic, N. (2005) Investigations of different kinetic models for zinc ions uptake by a natural zeolitic tuff *Journal of Environmental Management, In Press, Corrected Proof, Available online 26 October 2005*.

## Peculiarities of sorption extraction of oil products from aquatic environment

**T. Martynova**

*Technical College of Jerusalem; Jerusalem, Israel; Email:bravo50@mail.ru*

### Introduction

There are rather contradictory opinions on treating media for organic impurities of different composition using carbon- and silicon-containing sorbents. The objective of this paper is to investigate the nature of sorption-based extraction of organic substances using the economically justified materials of carbon, slag, and natural and synthetic zeolites.

### Experimental Methods

Filtrating materials (Table 1) were selected based on the results of known assessments of their efficiency of oil product extraction. Clinoptilolite and synthetic zeolite were tested using NMR method.

**Table 1.** Mechanical and physical properties of filtering materials

Material	Strength, %	Size, mm	Density, g/cm <sup>3</sup>	
			Bulk	Actual
Fuel slag	Not more than 30.00	1.30	0.76	0.86
Natural zeolite	No less than 75.00	0.63–1.30	0.82	2.38
Synthetic zeolite	Not more than 45.00	3.15 (granules)	1.00	0.98
Activated carbon	No less than 90.00	1.30	0.96	1.20

Studied were modeled mixtures consisting of aromatic compounds. Toluene and naphthalene were selected as models since aromatic compounds (including condensed naphthalene types) are a part of many oil products such as benzene, kerosene, crude oil, diesel fuel, etc. Moreover, toluene and naphthalene molecules have notably different sizes, which allow comparative assessment of their penetration ability into the zeolite cavities.

### Results and Discussion

Zeolite selectivity towards toluene is explained by the small size and mobility of aromatic carbon molecules, and by activity of methyl radicals towards reagents and solvents. Mixtures with lower concentration of toluene are almost completely absorbed by natural zeolite. Natural zeolite is efficient enough for the treatment of industrial waste water containing different types of oil products of different phases. The large cavities of zeolites are more efficiently plugged with homogeneous organic phases than with suspended mixtures. Sorbents whose surface has charged centers sorb molecules with manifold relations and  $\pi$ -electrons more efficiently than linear molecules. Thus, zeolite's selectivity towards toluene is explained by small dimensions of aromatic carbon and high mobility of molecules, as well as by activity of methyl radicals towards reagents and solvents. Olefins (condensed compounds of naphthalene type) with higher positive charge than that of the core of the mineral with non-homogeneous surface and differently oriented centers of charges are more efficiently absorbed by natural zeolite—up to 7.4% and 3.7%, respectively, than by synthetic zeolite—up to 4.0 and 1.5%, respectively. Sorption of aromatic compounds by zeolites is known to be due to sorbent interaction with metal cations available in the zeolite structure (in the amount of 0.6–8.5 mass % and higher). Selectivity of metal cations towards extracted impurities reduces in the series:  $\text{Ni}^{2+} > \text{Fe}^{3+} > \text{Cu}^{2+} > \text{Co}^{2+} > \text{Cr}^{3+} > \text{Mn}^{2+}$ . This selectivity series of metals agrees with reduction in the value of their electron potential. That is, the higher the electron potential, the more active the electron acceptor of this metal. It should be noted that sorption on zeolites depends on the size of their inlet window. If the window size does not exceed 0.4–0.6 nm, then sorption occurs with surface metal cations only. The voltage of electrostatic field inside and on the surface of cavities is not high and grows insignificantly due to cations of  $\text{Ca}^{2+}$  and  $\text{Mg}^{2+}$ . Reduction in the effect of dispersion forces on the sorption takes place in the series:  $\text{Al}^{2+} > \text{Fe}^{2+} > \text{Fe}^{3+} > \text{Ca}^{2+} > \text{Mg}^{2+} > \text{Na}^+ > \text{K}^+$ .

Chemical modification of zeolite, resulting in the change of cation composition, affects the number of electron-generating centers of the mineral. Thus, acid treatment of minerals results in the reduction in the activity of electron-generating centers of the mineral. Availability of free pairs of electrons in those centers allows partial regeneration of organic substances and splitting of complex compounds into elementary ones with lesser size of molecules, which facilitates their absorption by zeolite. It has been noted that sorption capacity of flint zeolite with active cations is higher with respect to toluene. A study of the process of phenol alkylation with methanol (using zeolite catalyst) demonstrated that with the growth of silicon oxide concentration in zeolite and with temperature rise of the medium, the rate of alcohol conversion and its gasification grow as well. Toluene sorption by clinoptilolite (up to 66%) and montmorillonite (up to 20%) containing zeolite (preliminarily calcinated at 100°C for 1 hour) fails. Toluene molecules in clay materials are probably located parallel to the rings of the mineral structure and are maintained in the zeolite cavities due to interaction of structural hydroxyl groups of metal cations and oxygen nuclei with a system of  $\pi$ -electrons in the aromatic ring of toluene. Toluene compounds with a more ordered system of charges are more efficiently sorbed by synthetic zeolite—up to 50.8% as their surface is evenly oriented by available charges.

Reduction in sorption capacity of carbon sorbents against changes in the sorption value of natural zeolite and synthetic zeolite can be explained both by the nature of sorbent porosity and hemoactivation nature of external (zeolites and carbon) and internal (zeolite) space. Use of synthetic zeolites raises the efficiency of treatment by 10–15%, whereas natural zeolite is characterized by a more sustainable filtration cycle. For this reason natural zeolites are more suitable for oil product extraction from industrial waste water. Carbon-containing materials are rather efficient for water treatment from organic compounds. The treatment process represents itself molecular sorption on porous materials. Compounds with ordered electron structure (of toluene type) are more efficiently sorbed by synthetic zeolites. Complex compounds (of naphthalene type) with acceptor properties (or subjected to chemical initiation) are more efficiently sorbed by natural zeolites. Modification of natural zeolites results in their hemoactivation, which considerably raises the efficiency of water cleaning from oil products.

## Removal of *Giardia lamblia* and model organism *Saccharomyces cerevisiae* from contaminated waters through the use of surfactant-modified zeolite (SMZ)

D. Meier and R. S. Bowman

New Mexico Institute of Mining and Technology; Socorro, New Mexico, USA; Email: dmeier@nmt.edu

Over the past two decades, *Giardia lamblia* has become the most common cause of waterborne disease in humans in the United States and infects millions of people across the globe in both sporadic and epidemic events. *Giardia* is ubiquitous in surface waters and has also been detected in groundwater sources. Due to the serious global concerns presented by the persistence of *G. lamblia* in the environment, there is a worldwide demand for water treatment techniques that are inexpensive, efficient, and effective for the removal of *G. lamblia* from drinking water supplies.

Surfactant-modified zeolite (SMZ) provides a possible solution to the removal of *G. lamblia* from drinking water supplies. Schulze-Makuch et al. (2003) found that the sorptive properties of SMZ can be utilized to remove 100% of some biological pathogens, including bacteriophages and *Escherichia coli*, from contaminated waters. The success of the application of SMZ to the removal of these pathogens led to the hypothesis that *G. lamblia* will adsorb to SMZ and lead to the successful removal of the organism from drinking water. Batch experiments and flow-through experiments were designed and executed to determine the removal efficiencies of *G. lamblia* by SMZ from water. The organism *Saccharomyces cerevisiae* was used to test and refine the experimental design of the flow-through column experiments. *S. cerevisiae* is an ideal analog for *G. lamblia* due to the fact that it is very well characterized, in addition to having size and surface properties similar to *G. lamblia*.

The zeolite used in this study is a natural clinoptilolite-rich tuff from the St. Cloud mine, Winston, NM. XRD analysis found a mineral composition of 74% clinoptilolite, 5% smectite, 10% quartz/cristobalite, 10% feldspar, and 1% illite (Sullivan et al., 1997). The raw zeolite has an external surface area of 14 m<sup>2</sup>/g (Schulze-Makuch et al., 2003). The aggregate size of the material used in these studies is 1.4 to 2.4 mm (8-14 mesh size), with a bulk density of 0.9 g/cm<sup>3</sup> (Bowman et al., 2001). Bowman et al. (2000) reported the maximum surfactant loading (MSL) of the raw zeolite to be 140 mmol hexadecyltrimethylammonium (HDTMA)/kg zeolite.

Three different materials were used to determine microbial removal efficiencies: hydrophobic SMZ, cationic SMZ, and raw zeolite. To prepare the cationic and hydrophobic preparations, untreated zeolite was washed with HDMTA-Cl to the desired surfactant loading. A cationic SMZ preparation requires treatment of the raw material to the maximum MSL. The hydrophobic SMZ was prepared by treating the raw zeolite to only 2/3 MSL.

A series of batch experiments was performed using the three treatments. The data from the batch experiments were plotted to determine the linear sorption coefficients for each material. Following the batch experiments, six column experiments were run. The scaling of the column experiments was adjusted to minimize the influence of physical filtering and hydrodynamic forces. The columns used in this study were sterile syringes packed with the appropriate SMZ formulation. *G. lamblia* or *S. cerevisiae* suspensions were fed through the columns at a constant rate. Initial and final concentrations were measured for the column experiments. This column design allowed for the use of small sample volumes and the column outlet could be connected directly to a filter membrane for organism collection and counting. Breakthrough curves were developed for both *S. cerevisiae* and *G. lamblia*.

The *S. cerevisiae* was cultured in the laboratory using a pure strain of the organism from Ward's Natural Science (Rochester, NY) and a dextrose broth (EMD Chemicals, Darmstadt, Germany). The yeast colonies were grown in glass flasks on a shaker for 24 hours at a temperature of 30°C to optimize growth. At the end of the growth period, the yeast was rinsed and deactivated in a solution of potassium sorbate at 50°C for thirty minutes. The deactivated cells were resuspended in a phosphate buffer solution (PBS) at a pH of 6.5. The colonies suspended in PBS were then used in the batch and column experiments. The results of the *S. cerevisiae* experiments were used to optimize the experiments to measure removal of *G. lamblia*.

The *G. lamblia* cysts were obtained from Waterborne, Inc. (New Orleans, LA) in a formalin and Tween 20 solution, at a concentration of approximately 625,000 cysts/L. The cysts were filtered, rinsed and re-suspended in PBS, at a pH of 6.5. The PBS cyst suspensions were then used in the batch and column experiments.

Concentrations of *S. cerevisiae* and *G. lamblia* in influent and effluent samples were determined by direct counting methods using black, 0.45- $\mu\text{m}$  filter membranes.

## References

- Bowman, R.S., Hinkle, S.R., Kroeger, T.W., Stocking, K. and Gerba, C.P. (2001) Bacteriophage adsorption during transport through porous media: Chemical perturbations and reversibility. *Environmental Science and Technology*, **25**, 2088-2095.
- Bowman, R.S., Sullivan, E.J. and Li, Z. (2000) Uptake of cations, anions and nonpolar organic molecules by surfactant-modified Clinoptilolite-rich tuff. Pp. 287-297 in: *Natural Zeolites for the Third Millennium* (C. Colelle and F.A. Mumpton, editors). Naples, Italy.
- Salazar, C. (2004) Evaluation of surfactant-modified zeolite for control of Cryptosporidium and Giardia species in drinking water. Masters thesis, New Mexico Institute of Mining and Technology, Socorro, New Mexico, 84 pp.
- Schulze-Makuch, D., Bowman, R.S., Pillai, S.D. and Guan, H. (2003) Field evaluation of the effectiveness of surfactant modified zeolite and iron-oxide-coated sand for removing viruses and bacteria from ground water. *Ground Water Monitoring and Remediation*, **23**, 68-75.
- Sullivan, E.J., Hunter, D.B., and van Genuchten, M.T. (1997) Topological and thermal properties of surfactant-modified clinoptilolite studied by tapping-mode atomic force microscopy and high-resolution thermogravimetric analysis. *Clays and Clay Minerals*, **45**, 42-53.

## Hydraulic-loading and NaCl concentration effect on regeneration of exhausted homoionic natural zeolite

Z. Milán, K. Ilangoan, C. de las Pozas, and O. Monroy

Universidad Autónoma Metropolitana; Iztapalapa, México; Email: z\_milan\_2000@yahoo.com

### Introduction

Many wastewater treatment systems do not allow the removal and recovery of nutrients, and final effluents are disposed with nitrogen and phosphorous compounds. Primarily, three different methods have been developed for ammonia and nitrogen removal from wastewater: Air stripping, ion exchange, and biological nitrification/denitrification (Milán et al., 1997).

Natural zeolites have been widely used in ion exchange, but usually the regeneration costs can amount up to 50% of the total ammonia removal costs. However, there are no engineering criteria for regenerating exhausted zeolites based on brine concentration and hydraulic-loading rates (USEPA, 1971). In this study, regeneration efficiencies curves were developed to find suitable hydraulic loading at two NaCl concentrations.

### Experimental Methods

The natural zeolite (60% clinoptilolite and 5% mordenite) used in the experiments was obtained from the Etlá deposit in Oaxaca, Mexico. This zeolite was transformed to sodic homoionic zeolite as described elsewhere (Milán et al., 1997). The homoionic zeolite had a particle size between 1.0–2.0 mm. Glass ion exchange columns (20 cm height, 3.5 cm internal diameter) were packed with stock treated zeolite with 58% porosity and 0.81 g/mL apparent density ( $55 \pm 2$  g zeolite mass/column).

The average value of ammonia influent concentration was 120 mg/L (from  $\text{NH}_4\text{NO}_3$ ), which was downflow fed at 2 BV/h (bed volume per hour) to packed homoionic zeolite columns (sorption capacity  $22.5 \pm 0.9$  mg  $\text{NH}_4^+$ /g of zeolite). After system saturation, the regeneration of the exhausted homoionic zeolites was tried at three different upflow hydraulic loadings of 4-, 6- and 8 BV/h, with two NaCl concentration solutions of 2- and 4M.

In a second experiment, the influence of exhaustion-regeneration cycles on ammonium sorption capacity was determined. In each cycle, columns were regenerated at 6 BV/h (with both NaCl solutions) and were again exhausted at 2 BV/h. A total of four exhaustion-regeneration cycles were carried out. Between cycles, samples from packed zeolites were taken. In all experiments, triplicate samples of effluents were done at one-hour intervals. Ammonium and sodium concentrations were determined by selective electrode and spectrometric adsorption atomic, respectively (APHA, 1989).

### Results and Discussion

The results obtained in the regeneration studies were represented by ammonium removal from exhausted zeolite as  $(C_0 - C_i)/C_0$ , for both regeneration solutions applied at the different hydraulic loadings. Average value of the initial ammonium content ( $C_0$ ) of exhausted zeolite mass was  $1238 \pm 6$  mg.  $C_i$  as the ammonium content time variations in exhausted zeolite mass. For both NaCl concentrations, the curves of  $(C_0 - C_i)/C_0$  showed an equilibrium between 4 and 6 hours of operation. But, two hours was the optimal regeneration time, when the rate of efficiencies change is less or equal to half of the previous value.

In all systems, the first two hours of operation appear to have a great influence on the process kinetics. In the same way, at 8 BV/h regeneration load, the ammonium removal during the first 15 minutes was not the expected amount as compared to 4 and 6 BV/h. For instance, at two hours, accumulative leached ammonium, applying 4 M NaCl concentration was 0.9 and 0.7 g for 6 and 8 BV/h, respectively. This fact denoted a great influence of a high linear velocity applied to the systems.

In general, there was a major effect of hydraulic loading on the ammonium output from the exhausted zeolites, this being an important aspect influencing the efficiency of regeneration, principally in the first operation hours where the relationship between sodium and ammonium concentrations in liquid-solid interface

are the highest. Diffusion, the controlling step in this process, explains why the deeper ionic exchange sites could not be reached (Break, 1974).

Based on the last, it was determined the macro- and self-diffusivity in all systems. Related to macro-diffusivity, there was not a great difference between the behaviour of systems fed with both regenerant solutions. However, the values of self-diffusivity showed an influence of liquid retention time, being the controlling diffusion and also the criterion for absence of macropore diffusion control, similar to other studies (Iglezakis et al., 2002; Karger, 2003).

In reference to results of ion content of zeolite after its regeneration, the sodium content per zeolite gram diminished as the applied hydraulic load increased. There were differences among results of regenerated zeolites at 2 M NaCl solution when the load was increased in 2 BV/h, approximately 5% sodium content. Regenerated zeolites at 6 BV/h had the greatest sodium content for both NaCl concentrations. Analyzing the load effect at the same NaCl concentration, operating the systems at 6 BV/h halved the time needed to reach 60% removal comparing to 4 BV/h, while at 8 BV/h tripled the required operation time, with major NaCl consumption. The suitable operation conditions are around 6 BV/h, according to  $(C_o - C_i)/C_o$  curves and self-diffusivity values, which dictate that system behavior is favored as: 6 BV/h > 4 BV/h > 8 BV/h.

Despite of the cyclic behavior of ammonium and sodium content in packed zeolite between each exhaustion-regeneration cycle, the ion concentration in zeolite denotes a little diminution of both ions, among cycles. From the second regeneration cycle forward, the loading breakthrough point diminished two hours for each cycle. The last could be due to zeolite mass lost provoked by stress forces of flow and by high conductivity values of regenerant solutions (U.S. EPA, 1971).

## References

- APHA-AWWA-WPFC (1989) *Standard methods for examination of water and wastewater*. 17<sup>th</sup> edition. (American Public Health Association), Washington.
- Breck, W. D. (1974) *Zeolite molecular sieves: Structure, chemistry and use*. Interscience publication. New York.
- Iglezakis, V. J. Loizidou, M. D. and Grigoropoulou, H. P. (2002) Equilibrium and kinetic ion exchange studies of  $Pb^{2+}$ ,  $Cr^{3+}$ ,  $Fe^{3+}$  and  $Cu^{2+}$  on natural clinoptilolite. *Water Research* **36**, 2784–2792.
- Karger, J. (2003) Measurement of diffusion in zeolites-A never ending challenge. *Adsorption* **9**, 29–35.
- Milán, Z. Sánchez, E. Weiland, P. De las Pozas, C. Borja, R. Mayari, R. and Roviroso, N. (1997) Ammonia removal from anaerobically treated piggery manure by ion exchange in columns packed with homoionic zeolite. *Chemical Engineering Journal* **66**, 65–71.
- U.S.EPA (1971) Optimization of ammonia removal by ion exchange using clinoptilolite. Project No. 17080 DAR. *Water Pollution Control Research Series*, Berkeley, California, USA.

## Analysis of zeolite exchange capacity cations

W. J. Miles

*Miles Industrial Mineral Research; Denver, Colorado, USA; Email: w\_miles@hotmail.com*

Cation exchange capacity (CEC) of zeolites is created by negative charges in their three dimensional framework structures. To neutralize these negative charges, cations migrate to zeolites and collect in the channels created within the zeolite structure. These cations do not become part of the zeolite crystal structure.

Cations are preferentially attracted to zeolite by their positive charge, and by the volume of cations and their water of hydration. The size and shape of the aperture of the main zeolite channels vary among zeolite minerals. These differences of size and shape of main channels within three dimensional zeolite structures result in preferences of some cations over other cations. If the zeolite channel opening is small compared to the cross section of a cation with its water of hydration, more energy is required for this cation to migrate into the channel than another cation that has a smaller cross-section.

For example, chabazite has a decided preference for larger cations:  $\text{Ti} > \text{K} > \text{Rb} > \text{NH}_4 > \text{Pb} > \text{Na} > \text{Ca} > \text{Mg} > \text{Li}$ . Clinopillolite cation selectivity is:  $\text{Cs} > \text{Rb} > \text{NH}_4 > \text{Sr} > \text{Na} > \text{Ca} > \text{Fe} > \text{Al} > \text{Mg} > \text{Li}$ . Conversely, the displacement trend is the opposite of selectivity. Type A synthetic zeolite is more selective for Ca than for Na, explaining its use as a water softener in phosphate-free detergents.

In some zeolite structures, dominant cations alter x-ray diffraction patterns significantly. For example, when calcium is the dominant cation, the  $[(\text{Al}_2\text{O}_{10})_{16}(\text{SiO}_2)_{24}]\cdot n\text{H}_2\text{O}$  zeolite structure is classified as chabazite; however, when sodium is the dominant cation, this structure is classified as herschelite. Two other isostructural zeolites with different dominant cations are analcime, when sodium is dominant, and wairakite, when calcium is dominant. With two other isostructural zeolites, natrolite is present with sodium as the dominant cation, and scolecite is present when calcium is the dominant cation.

In addition to the measurement of the exchange capacity of a zeolite mineral by displacement with  $\text{NH}_4^+$ , determination of the cations displaced by  $\text{NH}_4^+$  gives significant information for potential applications or uses of a zeolite resource. This presentation will give a method for displacement of the cations associated with a zeolite and subsequent analysis for each. Each zeolite is slurried with an excess of 1N ammonium acetate to displace the exchangeable cations. After filtration and collection of the supernatant, the zeolite is slurried several times until all cations are displaced. The displaced cation solution is evaluated for a range of cations. In addition to analysis of the ammonia remaining at zeolite exchange sites, the sum of the individual cations gives the total exchange capacity. Knowledge of the individual cations associated with a zeolite mineral resource can be used for determining cation absorbent applications.



## **X-Ray diffraction identification of smectite clays associated with zeolite minerals**

**W. J. Miles**

*Miles Industrial Mineral Research; Denver, Colorado, USA; Email: w\_miles@hotmail.com*

Zeolites are formed by the reaction of solid materials with water. Common source materials include biogenic amorphous silica, volcanic glass, smectite clays such as montmorillonite, and decomposition products of granites such as feldspars and quartz. Both clay minerals and zeolites can form from these parent materials. Major environmental factors control the formation of clays or zeolites from these sources such as pH, dissolved alkali and alkaline earth cations, and silicic acid. Other important factors that determine the type of zeolite formed include the temperature and pressure of the altering material and ionic strength of pore water. Most zeolite occurrences in sedimentary rocks are categorized by several types of geologic environments such as saline alkaline lakes, saline alkaline soils and land surfaces, deep-sea sediments, open hydrologic systems, hydrothermal alteration systems, and burial diagenetic and metamorphic environments.

Smectites are layer silicate clay minerals with charge defect structures that create negative charges at the clay platelet surfaces that require exchangeable cations for neutrality. The exchangeable cations associated with smectites are typically an order of magnitude less than the cation exchange capacity of zeolite minerals. However, the smectite clays contribute to the total cation exchange capacity of zeolite minerals when measured by displacement with ammonium cations.

X-ray diffraction (XRD) analysis for smectites associated with zeolites is difficult if typical XRD powder patterns are carried out without additional examination. Smectites, including montmorillonite, are capable of hydrating the interlayer space between clay sheets. Typically, divalent cations such as magnesium and calcium are hydrated so that the layer spacing is approximately 14 Å, while monovalent cations such as sodium give variable spacing with humidity near 12 Å. When a zeolite sample is slurried with deionized or distilled water, and the slurry is coated on an amorphous glass slide, the dispersed clay platelets typically settle horizontally as the slurry dries, resulting in a dried oriented film.

Examination of the oriented film by XRD analysis shows enhanced layer spacing of the clay minerals, improving identification. When the oriented film is exposed to ethylene glycol vapor, the layer spacing of smectite clays expand to approximately 17 Å, clearly demonstrating their presence at low concentrations that typically cannot be detected by powder patterns. Other clay minerals such as kaolinite or illite do not expand with ethylene glycol vapor. Some smectite clays can be identified below 5% concentrations by this method.

This presentation will give an analytical XRD method that demonstrates the benefits of thin films and their expansion by ethylene glycol vapor for x-ray diffraction identification and quantification of smectite clays associated with zeolite minerals.

## The investigation of zeolite-containing material as a potential sorbent for petroleum hydrocarbons

A. Mishchenko, A. Krivosheeva, V. Breus, S. Neckludov, and I. Breus

Kazan State University; Kazan, Russia; Email: [ibreus@ksu.ru](mailto:ibreus@ksu.ru)

### Introduction

One of the modern approaches to remediation of soil and ground-water contaminated by petroleum hydrocarbons (HC) is considered to be combined sorption/biodegradation cleaning assisted by natural sorbents. Recently a number of modern methods were proposed for modifying of mineral sorbent surfaces by cationic surfactants to make sorbents more hydrophobic (Li *et al.*, 2000; Sharmasarkar *et al.*, 2001). Here the application of cheap native zeolite-containing materials (ZCMs) could be promising for ecological purposes. Such sorbents simultaneously are characterized by high cation-exchange capacities (due to the presence of zeolites) and high specific surface areas (due to clay minerals).

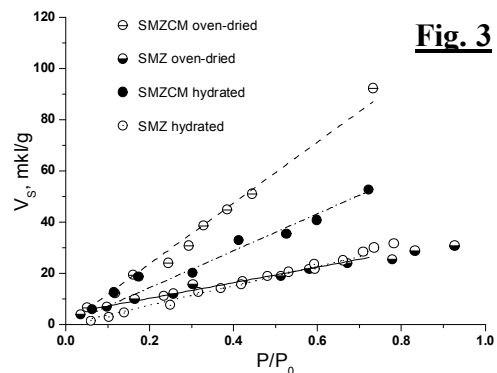
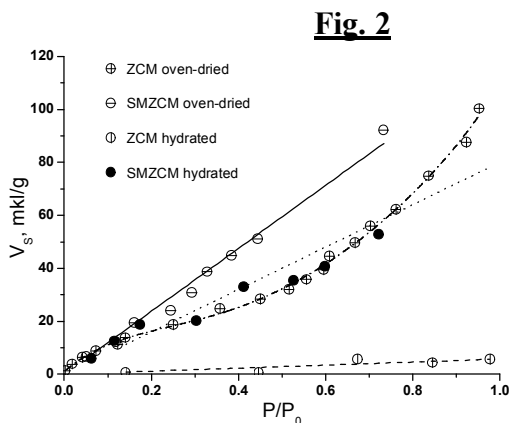
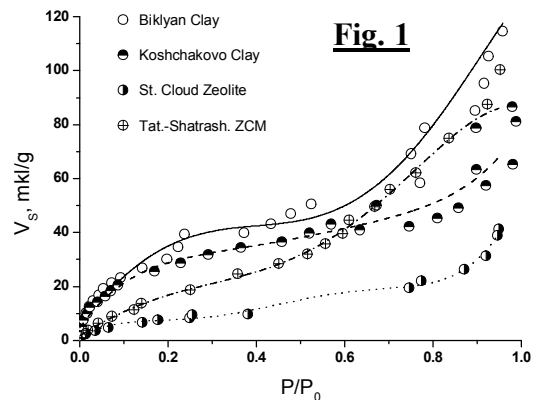
### Experimental

In the present work, the sorption capacity of natural (ZCM) and organo-modified by HDTMA (SMZCM) zeolite-containing material from Tatarsko-Shatrashansky deposit (Tatarstan, Russia: heulandite-clinoptilolite, 16%; clay minerals, 24%) with regard to benzene, toluene and p-xylene was studied. The vapor-phase sorption investigations (static headspace gas-chromatographic analysis was used) allowed us to determine ZCM sorption capacities under different moisture conditions (from oven-dried up to completely water-hydrated, RH=100%). For comparison, in the same experimental conditions the sorption of these three HC was studied on natural and surfactant-modified (SMZ, modified by HDTMA) zeolites from St.Cloud deposit (New Mexico, USA: clinoptilolite, 74%; smectite, 5%; quartz, 10%; feldspar, 10%; illite, 1%) provided by Prof. Robert Bowman. Besides, the sorption isotherms of benzene on two bentonite clay samples from Biklyansky and Koshchakovsky deposits (Tatarstan, Russia) were determined. The obtained sorption isotherms were represented as HC sorption values vs. HC thermodynamic activities at the constant temperature. To compare our results with literary data on HC water-phase sorption on surfactant-modified zeolites we have translated solute concentration scale into thermodynamic activity scale. The activity of the component was calculated from  $a = N\gamma$ , where  $N$  is the molar fraction of a compound in solution and  $\gamma$  is the activity coefficient (reference data).

### Results and Discussion

The obtained functionalities for benzene, toluene and p-xylene were similar on the whole; here the data only for benzene are presented. Vapor-phase sorption values of dried natural ZCM were sufficiently higher (more than two times) as compared with St.Cloud zeolites, Fig.1. Such difference was due to the presence of significant amount of clay minerals (up to 15-20%) in ZCM. So, benzene sorption values for different mineral sorbents shown that the ZCM activity was intermediate between the activities of more active clays and less active St.Cloud zeolites. The sorbent moistening up to completely hydrated state brought on decreasing of benzene sorption practically up to zero both for ZCM and St.Cloud zeolites. The organo-modification resulted in increasing ZCM sorption capacity, both for oven-dried (2.5 times as much) and water-saturated SMZCM (more than tenfold), Fig.2. The similar but little less sorption effect (1.5 times as much and tenfold, respectively) was observed also after organo-modifying of St.Cloud zeolites. Fig.3 shows that SMZCM, both dried and hydrated, had higher sorption capacity (fivefold and twofold, respectively) in comparison with SMZ. Even in comparison with dried SMZ the sorption values of hydrated SMZCM were 2-3 times as higher. To compare SMZ sorption coefficients determined from water solution (Li *et al.*, 2000) and vapor phase we have done translation-recalculation mentioned above. Here we have found the identical ranges of sorption selectivity for three HC on SMZ: benzene > toluene > p-xylene. It pointed out that in the case of water-phase sorption the translation from "solution" coordinates to "thermodynamic" ones allows to "subtract" sorbate-solvent interactions and thus to estimate the mechanism of sorbate-sorbent interactions - as in case of vapor-phase sorption.

Further, sorption coefficients ( $K_d$ ,  $K_{oc}$ ) for SMZCM, SMZ and surfactant-modified smectites were compared and probable HC sorption mechanisms were discussed. The negative correlation between  $K_d$  and HC molar refraction values brought out the steric obstacles in HC sorption and respectively - sorbate molecule diffusion into organo-modifier phase as a predominant sorption mechanism. The obtained results show that organo-modifying of cheap native clay-rich ZCM leads to significant increasing its sorption capacity with regard to petroleum HC. This could open new areas of ZCM application to environmental remediation, namely to the purification of HC gas mixtures at any moisture contents and to HC soil remediation. The use of cheaper organic modifiers as well as SMZCM inoculation by active strains of HC-oxidating microbes should promote much greater increasing sorbent efficiency and its much lower cost.



The work was supported by ISTC #2419, RFBR 06-04-49097, Postdoctoral fellowship CRDF REC-007 and Grant of President of Russia MK-2439.2005.5

## References

- Li, Z., Burt, T., and Bowman, R.S. (2000) Sorption of ionizable organic solutes by surfactant-modified zeolite. *Environmental Science and Technology*, **34**, 3756-3760.
- Sharmasarkar, Sh., Jaynes W.F. and Vance G.F. (2000) BTEX sorption by montmorillonite organo-clays: TMPA, Adam, HDTMA. *Water, Air, and Soil Pollution*, **119**, 257–273.

## Sorption of lead by a Mexican heulandite-clinoptilolite- rich tuff

M. M. Llanes Monter<sup>1,2</sup>, M. T. Olguín Gutiérrez<sup>1</sup>, and M. J. Solache Ríos<sup>1</sup>

<sup>1</sup>*Instituto Nacional de Investigaciones Nucleares, México, D.F.; Email: mog@nuclear.inin.mx.*

<sup>2</sup>*Universidad Autónoma del Estado de México, México.*

### Introduction

The levels of lead in the environment depend on several factors such as industrial development and urbanization. Natural zeolites have been used in sorption processes because they are inorganic cation exchangers that exhibit high ion exchange capacity, selectivity, low cost, and compatibility with the natural environment (Arellano et al., 1995; Kesraoul-Ouki et al., 1993; García-Sosa and Solache-Ríos, 1997; Curcovic et al., 1997; Zamzow et al., 1990; Ouki and Kavannagh, 1999).

Several natural zeolites have been investigated for the separation of heavy metals from aqueous solutions and it was found that the process depends on the size of the crystals, the type of zeolite exchangeable cations, the treatment time, and the temperature, among others (Godelitsas and Armbruster, 2003).

Different models can be applied to the sorption of ions by different materials. Although good correlations may be obtained, not all of the models are applicable to every process. Therefore, the goal of this paper was to determine the ion exchange behavior of lead by a Mexican heulandite-clinoptilolite rich tuff at pH values where the  $\text{Pb}^{2+}$  was the principal species present in the solution and in the absence of any precipitate of hydrolyzed lead species in the sorption process. Freundlich and Langmuir isotherm models were also considered in order to compare the lead sorption behavior.

### Experimental Methods

A heulandite-clinoptilolite rich tuff from Etla, Oaxaca in Southeast Mexico (17°14'N, 97°13'W) was ground and sieved. The grains used in this work were between 0.4 and 0.8 mm. The hydration temperature was determined in order to estimate the quantity of zeolite in the tuff (Ortiz, 2002). A weighted quantity of the material was heated for 5 hrs at 623 K, then it was left for some hours in a desiccator at room temperature. Later some milliliters of water were added and the temperature was measured.

The zeolitic material was treated with a 5-M NaCl solution for 8 days, washed with deionized water until no  $\text{Cl}^-$  was detected in the washing solution using an  $\text{AgNO}_3$  test. The Na-treated heulandite-clinoptilolite rich tuff was then dried.

Observations of the heulandite-clinoptilolite rich tuff, before and after lead sorption, were carried out. The samples were mounted directly on the sample holders and coated with gold. Finally the images were observed at 10 and 20 keV using a Phillips XL30 electron microscope. The chemical compositions, including Al/Si ratio, of the zeolitic samples were determined by an EDS system coupled to the electron microscope.

Powder diffractograms of the samples were obtained with a Siemens D500 diffractometer coupled to a copper anode X-ray tube. The conventional diffractograms were used to identify the compounds and to verify crystalline structure.

Aliquots (10 mL) of different lead nitrate solution concentrations were put in contact with 100 mg of the heulandite-clinoptilolite rich tuff under occasional stirring. The aqueous phases were separated from the solids by centrifugation after some period of time has elapsed. The zeolitic samples were washed, dried, and finally left in a humid medium to equilibrate with water. Lead and sodium were determined using a GBC 932 plus atomic absorption spectrometer at wavelength 283.3 nm and 589.6 nm, respectively.

### Results and Discussion

Clinoptilolite is the most important mineral component of the tuff [JCPDS card 39-1383,  $\text{KNa}_2\text{Ca}_2(\text{Si}_{29}\text{Al}_{17})\text{O}_{72}$ ] and minor quartz is also present (JCPDS card 33-1161,  $\text{SiO}_2$ ). The SEM images of the natural zeolite and the material treated with sodium show a morphology typical of sedimentary clinoptilolite-rich tuffs (Mumpton and Clayton, 1976)—coffin- and cubic-like crystals.

The elemental analysis determined by EDS of both the zeolitic material and the material treated with the NaCl solution indicated that  $\text{Na}^+$  ions in solution were exchanged by  $\text{K}^+$ ,  $\text{Ca}^{2+}$ , and  $\text{Mg}^{2+}$  from the zeolitic material.

The hydration temperature was  $8.83 \pm 0.76$  K, which reveals, according to Ortiz (2002), that the zeolitic material contains from 60–80% of clinoptilolite, consistent with the value given above.

According with the equivalent fractions of As and Az, an ion exchange isotherm type “b” at pH 3 was obtained. It was observed that the entering cation shows a selectivity reversal with increasing equivalent fraction in the zeolite (Breck, 1973); this behavior was similar at pH 2.

The isotherms obtained at pH values 4 and 5 were type “a” and these results show the selectivity for lead ions by the zeolitic material over sodium ions (separation factor  $\alpha_{\text{Na}}^{\text{Pb}} > 1$ ). The isotherm obtained at pH 5 showed that ion exchange was incomplete, which may be due to the equilibrium pH, which was 6 for 0.002, 0.005, 0.01, 0.015, and 0.02 M lead nitrate solutions. Under these conditions, lead precipitates as  $\text{Pb}(\text{OH})_2$ .

Ion exchange treatment could be applied satisfactorily to sorption of lead by a Mexican heulandite-clinoptilolite-rich tuff. For comparison purposes, the results were treated with the Langmuir and Freundlich models. The Langmuir model often has been used to describe the adsorption of heavy metals, for example, cadmium adsorption on peat (Söukand et al., 2002). The experimental values fit the Freundlich model better than the Langmuir model because of the heterogeneity of the natural materials.

It is important to consider the nature of the sorption process before choosing a model to describe the interaction between the metal ions and the sorbent.

## References

- Arellano, F.; García-Sosa, I.; Solache-Ríos, M. (1995) Sorption of Co and Cd by zeolite Y. *J. Radioanal. Nucl. Chem. Letters*, **199**, 107-113.
- Kesraoul-Ouki, S.; Cheeseman, C.; Perry, R. (1993) Effects of conditioning and treatment of chabazite and clinoptilolite on the lead and cadmium removal. *Environmental Science and Technology*, **27**, 1108-1116.
- García-Sosa, I.; Solache-Ríos, M. (1997) Sorption of cobalt and cadmium by Mexican erionite. *J. Radioanal. Nucl. Chem.*, **218**, 77-80.
- Curcovic, L.; Cerjan, S. S.; Filipan, T. (1997) Metal ion exchange by natural and modified zeolites. *Water Res.*, **31**, 1379-1382.
- Zamzow, M. J.; Eichbaum, B. R.; Sandgren, K. R.; Shanks, D. E. (1990) Removal of heavy metals and other cations from wastewater using zeolites. *Separation Science and Technology*, **25**, 1555 – 1569.
- Ouki, S. K.; Kavannagh, M. (1999) Treatment of Metals-Contaminated Wastewaters by Use of Natural Zeolites. *Water Science and Technology*, **39**, 115-122.
- Godelitsas, A.; Armbruster, T. (2003) HEU-type zeolites modified by transition elements and lead. *Microporous and Mesoporous Materials*, **61**, 3-24.

## Time dependent $\text{Zn}^{2+}$ and $\text{Pb}^{2+}$ removal with clinoptilolite and release of exchangeable ions

N. Morali, V. Çağın, and İ. İmamoğlu

Middle East Technical University; Ankara, Turkey; Email: [nihan.morali@tubitak.gov.tr](mailto:nihan.morali@tubitak.gov.tr)

### Introduction

Discharge of heavy-metal-containing wastewaters into receiving water causes detrimental effects on human health and the environment. Therefore, there is a need to treat heavy-metal-containing wastewaters before discharging them into the environment. Recently, natural zeolites have gained attention in wastewater treatment as appropriate materials for removing heavy-metal ions due to their unique physical and chemical properties, their abundance in many deposits, and especially their local availability, combined with a recovery potential for both metals and the mineral. Natural zeolites, especially clinoptilolite, are abundant in the world. Turkey has very high reserves for clinoptilolite. Therefore, investigation of the potential of this natural material in wastewater treatment may lead to its establishment as a viable alternative to conventional heavy-metal treatment technologies.

### Experimental Methods

The clinoptilolite sample used throughout this study originated from the Bigadiç deposit located near Balıkesir in Western Anatolia, Turkey. The clinoptilolite content of the sample is about 80%, with 13% quartz and 5–6% biotite as the other phases detected in the sample. The chemical composition of the sample is given as weight %:  $\text{SiO}_2$ -71.83;  $\text{Al}_2\text{O}_3$ -11.68;  $\text{Fe}_2\text{O}_3$ -1.15;  $\text{CaO}$ -3.39;  $\text{MgO}$ -1.25;  $\text{Na}_2\text{O}$ -0.43;  $\text{K}_2\text{O}$ -3.70;  $\text{MnO}$ -0.03  $\text{TiO}_2$ -0.07; and  $\text{H}_2\text{O}$ -2.60. Throughout the studies, two types of clinoptilolite were used: (1) as-received clinoptilolite and (2) conditioned clinoptilolite. No pretreatment was applied to as-received clinoptilolite samples; they were ground and sieved to 0.18–0.80 mm size fraction, dried at 105°C for 24 h, and stored in a desiccator. Conditioning process was accomplished by shaking 10 g as-received clinoptilolite in 250 mL of 2 M NaCl solution at 150 rpm and 30°C for 24 h. The sample was then washed with deionized water until no  $\text{Cl}^-$  was detected, dried at 105°C for 24 h, and stored in a desiccator.

Kinetic studies were carried out with 10 g clinoptilolite/1000 mL solution and the sampling times were 2, 5, 10, 20, 30, and 60 minutes and 3, 6, 10, 24, and 48 h. At each sampling, 10 mL of the sample was drawn from the system and analyzed for  $\text{Zn}^{2+}$  or  $\text{Pb}^{2+}$  and  $\text{Na}^+$ ,  $\text{K}^+$ ,  $\text{Ca}^{2+}$ , and  $\text{Mg}^{2+}$  in the liquid phase. For selected samples  $\text{Si}^{4+}$  measurements were also made. The initial pH of solutions was adjusted to 4. The studied concentrations were selected depending on the previous equilibrium experiments and the lowest concentration (150 mg/L for  $\text{Zn}^{2+}$ /as-received clinoptilolite system, 400 mg/L for  $\text{Zn}^{2+}$ /conditioned clinoptilolite system, and 1000 mg/L for  $\text{Pb}^{2+}$ /as-received clinoptilolite system) where the maximum metal removal capacity that had been observed was used. Kinetic studies were carried out under two conditions: pH-uncontrolled and pH-controlled. In pH-uncontrolled conditions, after an initial pH adjustment (to pH=4) the system pH was left uncontrolled. However, in pH-controlled kinetic studies, pH-control was accomplished throughout the reaction time (48 h) via keeping the pH of suspension at around 4 by the use of a Cole Parmer pH/ORP Controller and 0.1 N  $\text{HNO}_3$  solution.

### Results and Discussion

In  $\text{Zn}^{2+}$ /as-received clinoptilolite systems, the effective capacity of clinoptilolite is reached within 10 h under pH-uncontrolled conditions. However, under pH-controlled conditions, a distinct fluctuation in  $\text{Zn}^{2+}$  uptake is observed with the final capacity being lower than the pH-uncontrolled case. For  $\text{Zn}^{2+}$ /conditioned clinoptilolite systems, the removal within the first 6 h is slightly enhanced for pH-controlled cases when compared to pH-uncontrolled conditions. Further addition of  $\text{H}^+$  ions release the retained  $\text{Zn}^{2+}$  in the clinoptilolite structure, and at the end of 48 h, a slightly lower capacity is attained. The lower capacities attained for pH-controlled systems could be attributed mainly to weak bonding of  $\text{Zn}^{2+}$  ions to the clinoptilolite structure. The added  $\text{H}^+$  ions upset  $\text{Zn}^{2+}$  ions bound to the clinoptilolite structure and as more  $\text{H}^+$  ions are introduced to the system,  $\text{Zn}^{2+}$  ions are replaced by  $\text{H}^+$  ions in the structure. Also, with  $\text{H}^+$  addition, more surface sites are protonated, the availability of

negatively charged surface sites are lowered affecting the electrostatic attraction between negatively charged surfaces and  $\text{Zn}^{2+}$  ions, inhibiting  $\text{Zn}^{2+}$  ions being included in the clinoptilolite structure. On the other hand, in  $\text{Pb}^{2+}$ /as-received clinoptilolite system, external  $\text{H}^+$  addition has no influence on effective capacity. In both pH-controlled and pH-uncontrolled systems,  $\text{Pb}^{2+}$  ions seem to be strongly bound to the clinoptilolite structure.

Investigation of exchangeable ions ( $\text{Na}^+$ ,  $\text{K}^+$ ,  $\text{Ca}^{2+}$ ,  $\text{Mg}^{2+}$ ) released from a clinoptilolite structure and heavy-metal ions ( $\text{Zn}^{2+}$ ,  $\text{Pb}^{2+}$ ) taken into a clinoptilolite structure, together with  $\text{Si}^{4+}$  dissolution rate of clinoptilolite gives information about possible mechanisms and the extent of ion exchange. Time dependent release of exchangeable ions in  $\text{Zn}^{2+}$ /clinoptilolite systems demonstrates a discrepancy between  $\text{Zn}^{2+}$  ions removed from solution and exchangeable ions released from the structure. At the initial times of uptake, the amount of  $\text{Zn}^{2+}$  ions removed from the solution are generally greater than the exchangeable ions released. The results indicate that positively charged  $\text{Zn}^{2+}$  ions or  $\text{Zn}^{2+}$  species are initially attracted to clinoptilolite's negatively charged surfaces and then start to move within the pores and channels of clinoptilolite exchanging with its extraframework cations, which is indicated by a slow increase of exchangeable ions as a function of time.

In  $\text{Pb}^{2+}$ /as-received clinoptilolite systems, the uptake of  $\text{Pb}^{2+}$  increases with time and so does the amount of exchangeable ions released into the solution. However, this release could not solely be due to the ion exchange process, since considerable concentrations of  $\text{Si}^{4+}$  are detected, indicating dissolution of clinoptilolite. The degree of dissolution is higher in  $\text{Pb}^{2+}$ /as-received clinoptilolite systems when compared to  $\text{Zn}^{2+}$ /clinoptilolite systems. Also, dissolution of clinoptilolite is more pronounced in pH-controlled systems, owing to introduction of  $\text{H}^+$  ions to the system, inducing clinoptilolite dissolution.

Due to the complexity of clinoptilolite-metal solution interaction, it is very difficult to differentiate between exchangeable cations released as a result of ion exchange with heavy-metal ions and those released due to dissolution of clinoptilolite. In order to observe the rate of change of clinoptilolite dissolution and the resulting concentration of exchangeable ions in metal-free solutions, behavior of as-received clinoptilolite in a metal-free solution was also investigated. When the results of deionized water/clinoptilolite systems are compared with that of heavy-metal/clinoptilolite systems, it is found that higher pH values are attained in a heavy metal-free medium. This is mainly due to higher chance of  $\text{H}^+$  ions interacting with clinoptilolite and the absence of heavy-metal ions which tend to decrease pH via hydrolysis.

Up to the 24<sup>th</sup> h, discrepancies between the total amount of exchangeable ions and the amount of metal uptake is insignificant, and also the amount of ions released stayed almost constant until the 3<sup>rd</sup> h, at which point it starts to increase. Together with the results of  $\text{Si}^{4+}$  release with time, it is clear that the increase in exchangeable ions is due to the dissolution of clinoptilolite. As the amount of  $\text{Si}^{4+}$  released to solution increases from the 24<sup>th</sup>–48<sup>th</sup> h, there is a remarkable increase in the exchangeable ion amount even though no further increase in pH is observed. The general trend shows that with an increase in pH, extent of dissolution is also increased.

## Investigation of heavy metal ( $\text{Cu}^{2+}$ , $\text{Ni}^{2+}$ , $\text{Zn}^{2+}$ , $\text{Pb}^{2+}$ ) uptake by clinoptilolite and release of exchangeable ions

N. Morali, V. Çağın, and İ. İmamoğlu

Middle East Technical University; Ankara, Turkey; Email: [nihan.morali@tubitak.gov.tr](mailto:nihan.morali@tubitak.gov.tr)

### Introduction

Heavy metals pose a serious threat to the environment if discharged untreated. Treatment technologies developed for their removal tend to be very expensive and therefore not widely applicable. Natural zeolites, particularly clinoptilolite, recently have gained attention in wastewater treatment as low-cost ion exchangers. Turkey has very high reserves for zeolites (approximately 50 billion tons), and therefore their use in removal technologies presents a viable alternative to conventional treatment technologies. In this study, clinoptilolite is investigated for its use in removal of  $\text{Cu}^{2+}$ ,  $\text{Ni}^{2+}$ ,  $\text{Zn}^{2+}$ , and  $\text{Pb}^{2+}$  ions from aqueous solutions from the aspect of ionic species exchanged and for the possible pathways of heavy metal removal.

### Methods

The clinoptilolite used in this study was obtained from a sedimentary deposit in Bigadiç basin located in Western Anatolia, Turkey. The zeolite sample was firstly characterized by XRD analysis. The chemical composition of the sample, which had 80% clinoptilolite content, was (% wt):  $\text{SiO}_2$ —71.83;  $\text{Al}_2\text{O}_3$ —11.68;  $\text{Fe}_2\text{O}_3$ —1.15;  $\text{MgO}$ —1.25;  $\text{CaO}$ —3.39;  $\text{Na}_2\text{O}$ —0.43;  $\text{K}_2\text{O}$ —3.70;  $\text{MnO}$ —0.03;  $\text{TiO}_2$ —0.07;  $\text{H}_2\text{O}$ —2.50. Equilibrium experiments for heavy metal removal were carried out for both as-received and conditioned clinoptilolite. Clinoptilolite was conditioned in batch reactors with 2M NaCl at 30°C for 24 hours at 150 rpm with a solid/liquid ratio of 10 g/250 mL. Prior to determination of exchange capacity of the clinoptilolite for removal of  $\text{Cu}^{2+}$ ,  $\text{Ni}^{2+}$ ,  $\text{Zn}^{2+}$  and  $\text{Pb}^{2+}$ , different initial pHs were analyzed for their effects on the removal and the optimum initial pHs were determined. All experiments were carried out with 100 mL solution and 1 g clinoptilolite (particle size of 0.15-0.80 mm) in batch reactors at a constant temperature of  $25^\circ\text{C} \pm 2^\circ\text{C}$  at 125 rpm for 48 hours. The metal concentration ranges were; 5-1500 mg/L, 5-10000 mg/L, 5-400 mg/L, 100-5000 mg/L for  $\text{Cu}^{2+}$ ,  $\text{Ni}^{2+}$ ,  $\text{Zn}^{2+}$  and  $\text{Pb}^{2+}$ , respectively, for as-received clinoptilolite and 10-1500 mg/L, 10-10000 mg/L, 10-2000 mg/L and 100-10000 mg/L for  $\text{Cu}^{2+}$ ,  $\text{Ni}^{2+}$ ,  $\text{Zn}^{2+}$  and  $\text{Pb}^{2+}$ , respectively, for conditioned clinoptilolite. Heavy metal ion concentrations as well as the exchangeable ions ( $\text{Na}^+$ ,  $\text{K}^+$ ,  $\text{Ca}^{2+}$ ,  $\text{Mg}^{2+}$ ) released from the clinoptilolite structure were measured before and after reaching equilibrium for each concentrations tested.

### Results and discussion

As a result of equilibrium studies carried out with as-received clinoptilolite, the Langmuir isotherm model was found to best fit the experimental data points with maximum sorption capacities of 0.31 meq/g for  $\text{Cu}^{2+}$ ; 0.32 meq/g for  $\text{Ni}^{2+}$ ; 0.13 meq/g for  $\text{Zn}^{2+}$  and 0.50 meq/g for  $\text{Pb}^{2+}$ . Investigation of the ions released from clinoptilolite structure as a result of equilibrium studies exhibited different uptake capacities for different heavy metal ions and this may be attributed to different hydrated radii of heavy metal ions and accessibility of these ions to the sites occupied by exchangeable ions. For example, in this study, clinoptilolite had the highest capacity for  $\text{Pb}^{2+}$ , which led to the highest amount of  $\text{K}^+$  release from clinoptilolite structure.

If ion exchange was the only mechanism involved in heavy metal uptake by clinoptilolite, a balance would be expected between the ions released from and taken into clinoptilolite structure. In  $\text{Cu}^{2+}$ ,  $\text{Ni}^{2+}$ , and  $\text{Zn}^{2+}$  removal studies, the total amount of exchangeable cations release was higher than the total amount of metal uptake at equilibrium in the reactors having the lowest and the highest studied metal concentrations. For  $\text{Pb}^{2+}$  studies, on the other hand, the above situation is valid for the whole studied concentration range. Dissolution of clinoptilolite was considered as the main reason for this phenomenon in all cases. The type of dissolution depends on the pH (either low or high) and the ionic strength of the solutions. Therefore, considerable pH increase to the basic pH ranges due to protonation (interaction with  $\text{H}^+$  ions) of clinoptilolite, complex formation within the clinoptilolite structure and further detachment of these complexes with increasing ionic strength of the solution can be given as the factors that were considered to be the reasons for the dissolution



phenomenon in the reactors at equilibrium that have the lowest and highest initial studied metal concentrations, respectively.

Surface precipitation is also reported as another possible prevailing mechanism in the systems of concern in the literature. At high metal concentrations, formation of metal-hydroxyl complexes, especially metals with low solubility products (e.g.  $\text{Cu}^{2+}$  in this case), might inhibit the uptake of free metal ions into the clinoptilolite structure and ion exchange process. At higher  $\text{Cu}^{2+}$  concentrations, for example, the formation of  $\text{Cu}(\text{OH})_x$  complexes most probably results in surface precipitation, inhibits the possible ion exchange process and results in a lower uptake capacity when compared to the ones obtained in the reactors containing relatively lower initial studied  $\text{Cu}^{2+}$  concentrations.

In reactors having the median initial  $\text{Cu}^{2+}$  and  $\text{Ni}^{2+}$  concentrations (60-600 mg/L for  $\text{Cu}^{2+}$  and 100-3000 mg/L for  $\text{Ni}^{2+}$ ), however, total amount of metal uptake was considerably higher than that of exchangeable cations release and this was interpreted in terms of adsorption processes.

The results of the equilibrium studies carried out with conditioned clinoptilolite revealed that conditioning process enhances the uptake capacity of clinoptilolite considerably. The maximum removal capacities with the conditioned clinoptilolite were as follows: 0.55 meq/g for  $\text{Cu}^{2+}$ ; 0.43 meq/g for  $\text{Ni}^{2+}$ ; 0.39 meq/g for  $\text{Zn}^{2+}$  and 1.1 meq/g for  $\text{Pb}^{2+}$ . Examination of the exchangeable cations for these experiments revealed that despite generation of a  $\text{Na}^+$ -form clinoptilolite was aimed in conditioning process,  $\text{Ca}^{2+}$  and  $\text{Mg}^{2+}$  ions are still encountered in the suspensions whereas almost no  $\text{K}^+$  ions are detected except during  $\text{Pb}^{2+}$  removal.

When the balance between the amounts of ions released from and taken into the conditioned clinoptilolite structure was examined, a similar trend was observed particularly in  $\text{Cu}^{2+}$  and  $\text{Ni}^{2+}$  removal studies as before. This was considered to be an indication of the lack of dependence of conditioning process on the degree of prevailing mechanisms for these two metals. However, results of the  $\text{Zn}^{2+}$  removal study revealed that although conditioning did not result in any change in the trend, it seems to lead to a better stoichiometry between the total amount of exchangeable cations release and amount of  $\text{Zn}^{2+}$  uptake. In contrast to all other equilibrium studies carried out with conditioned clinoptilolite, in the  $\text{Pb}^{2+}$  removal study, there seems to be a change both in the trend (balance shifts in favor of total amount of  $\text{Pb}^{2+}$  uptake with increasing initial concentration) and in the degree of the difference between the total amount of exchangeable cations release and amount of  $\text{Pb}^{2+}$  uptake.

The capacities obtained in this study give promising outcomes for the Turkish clinoptilolite, indicating the potential for this natural material for heavy metal removal. However, clinoptilolite exhibits different removal capacities for different heavy metals in the order  $\text{Pb}^{2+} > \text{Ni}^{2+} \approx \text{Cu}^{2+} > \text{Zn}^{2+}$  for as-received clinoptilolite and  $\text{Pb}^{2+} > \text{Cu}^{2+} > \text{Ni}^{2+} > \text{Zn}^{2+}$  for conditioned clinoptilolite.

Investigation of exchangeable ions demonstrates that ion exchange is the predominant mechanism involved in the heavy metal uptake. Besides, indications of adsorption of heavy metal complexes onto clinoptilolite structure, dissolution of clinoptilolite during the uptake process and surface precipitation, particularly for  $\text{Cu}^{2+}$ , may also take part in the metal-clinoptilolite interactions.

## **Study of the effects of natural zeolite from the Tsagaantsav deposit on dynamics of pH, volatile fatty acids, and ammonia of rumen contents of one-year-old sheep**

**D. Narmandakh<sup>1</sup>, M. Zolzaya<sup>2</sup>, and Sh. Demberel<sup>3</sup>**

<sup>1</sup>*University of Colorado at Denver, USA; Email: nar2063@yahoo.com*

<sup>2</sup>*Institute of Veterinary Medicine; Ulaanbaatar, Mongolia*

<sup>3</sup>*Mongolian State University of Agriculture; Ulaanbaatar, Mongolia*

### **Introduction**

In Mongolia, where pasture-based animal husbandry exists under severe climatic conditions, the prevention and curing of animal diseases and the growing of young animals (lambs, kids, calves ) with minimal morbidity and mortality are actual problems. Livestock populations die in numbers due to emaciation, disorders of metabolism, and digestive malfunctions caused by poor feed because of the nutritive value loss of pasture plants during winter and spring seasons. Our research suggests that minimization of these factors is necessary; therefore, we are now studying the possibility of using natural zeolite from Tsagaantsav in Mongolia as a preventive and curative agent and feed supplement.

### **Experimental Methods**

In total, eight native Mongolian one-year-old sheep in pasture conditions, with analogues of their body weight, were selected for the experiment and divided into two groups in April. The four sheep of the experimental group were given natural zeolite from Tsagaantsav in a daily dose of 10 g to each sheep before grazing while the sheep of the control group were naturally grazing on the pasture.

These sheep underwent surgical operations to create fistulae on their rumen; then samples were taken using special pipettes through these fistula after the surgical wounds healed. Samples were taken at 1.5-, 3-, 5-, and 7 hours before and after grazing; pH, ammonia, volatile fatty acids (VFAs) and their fractions were measured and compared. The sheep of the experimental group received zeolite through the fistula in doses of 10 g daily for a week; then relevant measurements were made.

### **Results and Discussion**

For grazing sheep, rumen cud pH, which is equal to 7.0 on an empty stomach, changed to 6.53–6.46 ( $p < 0.005$ ) 3 to 5 hours after giving zeolite and grazing, and then to  $6.33 \pm 0.15$  after 7 hours.

Concentration of ammonia in rumen liquid during the empty stomach period was 17.50 mmol/L, whereas the ammonia concentration in the control group was 6–10 mmol/L less at 1.5 to 3.0 hours after receiving zeolite and grazing. The ammonia concentration was similar for the groups with and without receiving zeolite after 7 hours (Table 1). The natural zeolite from Tsagaantsav deposit in Mongolia tends to decrease the ammonia concentration and pH level in the rumen.

The total amount of VFAs in rumen fluid increased in the sheep of both the experimental and control groups for the first 3 hours after grazing, and then gradually reduced. The increase was greater in the group using zeolite for initial 1.5 hours, but it was not significant (Table 1).

**Table 1.** Effects of zeolite from the Tsagaantsav deposit on some characteristics of the rumen in sheep

Groups	Characteristics	Hours of sampling				
		0 M ± m	1.5 M ± m	3 M ± m	5 M ± m	7 M ± m
Experimental	PH	7.0 ± 0.11	6.53 ± 0.15	6.56 ± 0.15	6.46 ± 0.15	6.33 ± 0.15
	Ammonia					
	/mmol/L	17.50 ± 0.61	24.93 ± 1.18	23.59 ± 0.33	23.06 ± 0.56	21.72 ± 0.34
	VFAs,/mmol/L	64.77 ± 6.33	124.58 ± 11.6	120.6 ± 15.3	114.1 ± 18.9	105.4 ± 11.6
Control	PH	7.27 ± 0.1	6.80 ± 0.01	6.46 ± 0.15	6.63 ± 0.31	6.66 ± 0.15
	Ammonia					
	/mmol/L	17.51 ± 0.33	31.41 ± 0.89	33.16 ± 0.36	26.84 ± 0.74	24.62 ± 0.28
	VFAs,/mmol/L	55.82 ± 5.07	105.4 ± 8.94	124.6 ± 9.82	117.6 ± 17.6	104.5 ± 75.8

For sheep in the experimental group, the amount of acetic acid in the VFAs found in the rumen cud decreased after 3 hours while propionic acid increased significantly and the butyric acid and its isomer – isobutyric acid increased slightly for the initial five hours. For the sheep in the control group, the decrease of acetic acid was significant, and the amount of butyric acid increased 13–22% after grazing. Percentages of valeric and isovaleric acids were stable ranging around 1.0 and 1.8%.

From the study results, we found that the use of zeolite in daily doses of 10 g resulted in the reduction of ammonia concentration and environmental pH of rumen of native Mongolian sheep in pasture conditions and had no significant effect on the total concentrations of VFAs; however, the zeolite intensifies the fermentation of propionic acid after grazing. Higher porosity and absorbency of natural zeolite reduces degradation of feed proteins in the rumen of sheep; also, the greater content of minerals in zeolite exerts a positive effect on the activities of microorganisms in rumen cud.

We can see that during the spring season, when the nutritive values of pasture plants are minimal, the amount of ammonia produced in the rumen increased (Kutas, 2005); fermentation was caused by dominant actions of acetic, butyric, and isobutyric acids, and the sheep lost body weight because of internal toxication (Demberel, 2005).

## References

- Kutas, F.A. (2005) Gardasóqi hason allatok korai elvalasztasanakm ementes ellettani alapjai. Allateqeszseguqi es takormonyorasi kozlemenyek. *Phylaxia*, **2**, 78–84.
- Narmandakh, D. (2005) Electrophysiological characteristics of stomach and effect of zeolite on digestion of young ruminant animals. Thesis, Ulan-Ude University, 171–174.

## Direct measurement of partial molar heats of hydration in zeolites by differential scanning calorimetry

P. S. Neuhoﬀ and J. Wang

University of Florida; Gainesville, Florida, USA; Email: neuhoﬀ@ufl.edu

### Introduction

Characterization and thermodynamic modeling of reversible dehydration reactions in zeolites is critical for evaluating their stability relations in geologic environments and their application in heat pump technologies. Thermodynamic properties for zeolite dehydration reactions determined by calorimetric and phase equilibrium techniques are often inconsistent; these discrepancies are often attributed to differences between samples and differential reference and standard states employed in these techniques (e.g., Bish and Carey, 2001). The present study presents a new calorimetric technique in which the heat of immersion in water vapor is measured in a simultaneous differential scanning calorimeter (DSC)-thermogravimetric analyzer (TGA) under isothermal conditions. Although similar techniques have previously been employed (e.g., Pires et al., 2000) to determine integral enthalpies of hydration ( $\Delta H_{\text{hyd}}$ ), we show below that simultaneous evaluation of the DSC and TGA signals provides a means of directly evaluating partial molar enthalpies of hydration ( $\Delta h_{\text{hyd}}$ ) as a function of degree of hydration. Direct detection of degree of reaction progress by TGA eliminates many of the complications attending ambiguous reference states in other calorimetric techniques. This technique also shows promise for investigating slow hydration reactions accompanied by small heat signals.

### Experimental Methods

Experiments were conducted on phase-pure separates of natural analcime and chabazite that were hand ground in an agate mortar and sieved to the 20–40  $\mu\text{m}$  size fraction. Calorimetric experiments were conducted on a Netzsch STA 449C Jupiter simultaneous DSC-TGA apparatus. Gas flow was maintained at  $\sim 30$  ml/min using mass flow controllers. The samples were dehydrated by dynamic heating in dry  $\text{N}_2$  from ambient temperature to 1023 K at 15 K/min and then allowed to cool under dry  $\text{N}_2$  to the experimental temperature. After equilibration (10–30 minutes) under dry gas, at the experimental temperature until both the DSC and TGA baselines stabilized, the gas stream was changed to humid  $\text{N}_2$  (10–13 mbar water vapor pressure) and the sample allowed to react until the DSC and TGA baselines stabilized again.

### Results and Discussion

Figure 1a shows the DSC and TGA response of analcime during immersion in water vapor at 489 K. Solution between hydrated and dehydrated analcime is ideal (Ogorodova et al., 1996), in which case  $\Delta H_{\text{hyd}}$  and  $\Delta h_{\text{hyd}}$  should be identical for all compositions along the solution. The rehydration in Figure 1a is initially relatively rapid (as shown by the peak in the first derivative of the TGA signal, dTGA) and then decays exponentially. The DSC signal in this experiment reflects the enthalpy of the hydration reaction, with the area under the DSC peak being the integral heat of hydration. In the case of analcime, however, rehydration is so slow that the sample did not fully rehydrate even over the 17.5 hour total course of this experiment. Because the DSC signal is relatively small, errors associated with baseline uncertainty induce large uncertainties in  $\Delta H_{\text{hyd}}$ . It can be seen in Figure 1a that the shape of the DSC signal and that of dTGA are virtually identical. Given the ideal behavior noted in analcime, this suggests that the dependence of the DSC signal on the rate of uptake of  $\text{H}_2\text{O}$  (the dTGA signal) provides a measure of  $\Delta h_{\text{hyd}}$ . The DSC and dTGA signals at one minute intervals in Figure 1a are plotted against each other in Figure 1b, and it can be seen that these data define a linear trend ( $R^2 > 0.998$ ) with a slope corresponding to  $\Delta h_{\text{hyd}} = -85.5$  kJ/mol  $\text{H}_2\text{O}$  which compares well with previous measurements of  $\Delta H_{\text{hyd}}$  (e.g., Ogorodova et al., 1996; Johnson et al., 1982).

Chabazite appears to contain at least three energetically distinct populations of water molecules (e.g., Fialips et al., 2005). At the vapor pressures employed in this study, we were able to achieve rehydration of the two most energetic of these at 373 K. Comparison of the DSC and dTGA signals analogous to that in Figure 1a clearly distinguishes these populations and leads values of  $\Delta h_{\text{hyd}}$  consistent with previous studies. In addition,

the results show clear evidence of exchange of water between sites during rehydration that may be associated with solvus behavior that is not apparent in previous calorimetric and phase equilibrium studies.

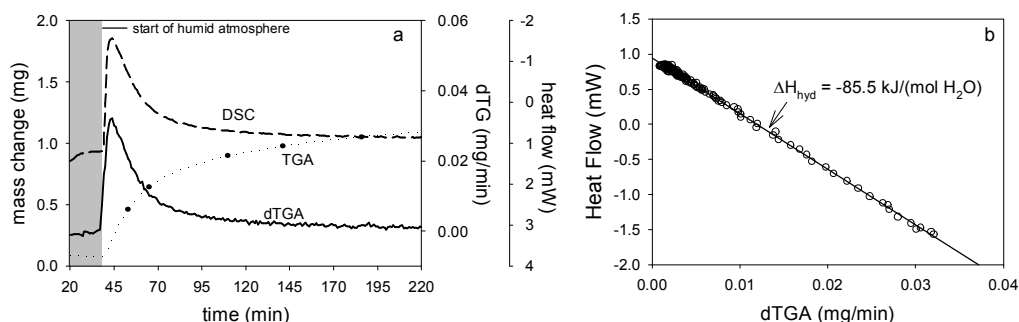


**Figure 1.** Isothermal immersion experiments on analcime at 489 K. a) Variation of the DSC, TGA, and dTGA signals with time after immersion. Gray region is initial equilibration step (dry atmosphere), white region is the immersion step under humid atmosphere. b) Comparison between the DSC and dTGA signals shown in part a (open circles). The linear regression of these data shown by the line is consistent with  $\Delta H_{\text{hyd}} = \Delta h_{\text{hyd}} = -85.5 \text{ kJ}/\text{mol}(\text{H}_2\text{O})$ .

## References

- Bish, D.L., and Carey, J.W. (2001) Thermal properties of natural zeolites. Pp. 403–452 in: *Natural Zeolites: Occurrence, Properties, Applications* (D.L. Bish and D.W. Ming, editors). Reviews in Mineralogy and Geochemistry **45**, Mineralogical Society of America and Geochemical Society.
- Fialips, C.I., Carey, J.W., and Bish, D.L. (2005) Hydration-dehydration behavior and thermodynamics of chabazite. *American Mineralogist*, **69**, 2293–2308.
- Johnson, G.K., Flotow, H.E., O'Hare, P.A.G., and Wise, W.S. (1982) Thermodynamic studies of zeolites: Analcime and dehydrated analcime. *American Mineralogist*, **67**, 736–748.
- Ogorodova, L.P., Kiseleva, I.A., Mel'chakova, L.V., Belitskii, I.A., and Fursenko, B.A. (1996) Enthalpies of formation and dehydration of natural analcime. *Geochemistry International*, **34**, 980–984.
- Pires, J., Brotas de Carvalho, M., Carvalho, A.P., Guil, J.M., and Perdigón-Melón, J.A. (2000) heats of adsorption of n-hexane by thermal gravimetry with differential scanning calorimetry (TG-DSC): A tools for textural characterization of pillared clays. *Clays and Clay Minerals*, **48**, 385–391.

## **Isotope-geochemical evidence for uranium retardation in zeolitized tuffs at Yucca Mountain, Nevada, USA**

**L. A. Neymark<sup>1</sup>, J. B. Paces<sup>1</sup>, S. J. Chipera<sup>2</sup>, and D. T. Vaniman<sup>2</sup>**

<sup>1</sup>*U.S. Geological Survey; Denver, Colorado, USA; Email: lneymark@usgs.gov*

<sup>2</sup>*Los Alamos National Laboratory; Los Alamos, New Mexico, USA*

### **Introduction**

Retardation of radionuclides by sorption on minerals in the rocks along downgradient ground-water flow paths is a positive attribute of the natural barrier at Yucca Mountain, Nevada, the site of a proposed high-level nuclear waste repository. Alteration of volcanic glass in nonwelded tuffs beneath the proposed repository horizon produced thick, widespread zones of zeolite- and clay-rich rocks with high sorptive capacities. The high sorptive capacity of these rocks is enhanced by the large surface area of tabular to fibrous mineral forms, which is about 10 times larger in zeolitic tuffs than in devitrified tuffs and about 30 times larger than in vitric tuffs. The alteration of glass to zeolites, however, was accompanied by expansion that reduced the matrix porosity and permeability. Because water would then flow mainly through fractures, the overall effectiveness of radionuclide retardation in the zeolitized matrix actually may be decreased relative to unaltered vitric tuff.

Isotope ratios in the decay chain of <sup>238</sup>U are sensitive indicators of long-term water-rock interaction. In systems older than about 1 m.y. that remain closed to mass transfer, decay products of <sup>238</sup>U are in secular radioactive equilibrium where <sup>234</sup>U/<sup>238</sup>U activity ratios (AR) are unity. However, water-rock interaction along flow paths may result in radioactive disequilibrium in both the water and the rock, the degree of which depends on water flux, rock dissolution rates,  $\alpha$ -recoil processes, adsorption and desorption, and the precipitation of secondary minerals.

The effects of long-term water-rock interaction that may cause radionuclide retardation were measured in samples of Miocene-age subrepository zeolitized tuffs of the Calico Hills Formation (Tac) and the Prow Pass Tuff (Tcp) from borehole USW SD-9 (Engstrom and Rautman, 1996) near the northern part of the proposed repository area. Mineral abundances and whole-rock chemical and U-series isotopic compositions were measured in unfractured core samples (depth interval 451.1 to 633.7 m) representing rock matrix, in rock-fragment rubble (about 1 cm) representing zones of higher permeability (assuming that the rubble core indicates a broken zone in the rock mass rather than an artifact of drilling), and in samples from surfaces of natural fractures representing potential fracture pathways. Uranium concentrations and isotopic compositions also were measured in samples of pore water obtained by ultracentrifugation or by leaching rock samples with deionized H<sub>2</sub>O. The concentrations and isotopic compositions of loosely bound U adsorbed on reactive mineral surfaces were obtained by analyzing 1 M sodium acetate (NaOAc) leachates of whole-rock samples.

### **Experimental Methods**

Mineral abundances were measured at Los Alamos National Laboratory by X-ray powder diffraction methods using the full-pattern quantitative analysis program FULLPAT. Major and trace-element chemical compositions were determined at the US Geological Survey (USGS) laboratory in Denver by several techniques including standard X-ray fluorescence spectroscopy (XRF) and inductively coupled plasma-mass spectrometry (ICP-MS). Uranium concentrations and isotopic compositions were measured at the USGS using a thermal ionization mass spectrometer (TIMS). Reproducibility of TIMS analyses was about 1% (2 $\sigma$ ) for elemental concentrations and 0.2% for U isotope ratios. Atomic isotope ratios were converted to activity ratios using known decay constants.

### **Results and Discussion**

The most common secondary minerals in 35 samples of the zeolitized tuff are clinoptilolite (0.5 to 76.3 %), opal-CT (6.5 to 21.8 %), mordenite (1.2 to 22.4 %), and smectite (0.1 to 44 %). Fracture surfaces have more smectite (median value of 6.1%) than unfractured and rubble core (median value of 3.2%).

Trends of concentrations with depth for whole-rock samples from the upper 50 m of the Tac document accumulation of Ca accommodated by loss of Na as a result of downward water movement and cation exchange

within the zeolitized rock sequence, consistent with published results (Vaniman et al., 2001). However, systematic variations with depth and zeolite abundance are not observed for U concentrations over this same depth interval.

Uranium contents in NaOAc leachates (0.012 to 0.071  $\mu\text{g/g}$  rock) represent a mobile U component adsorbed on mineral surfaces or in readily acid-soluble secondary minerals. Compared with whole-rock analyses, these data indicate that the adsorbed U comprises 0.3 to 1.7 percent of total rock  $^{238}\text{U}$ . These data allow estimates of the time-integrated *in situ* U partition coefficient ( $K_d = C_s/C_w$ , where  $C_s$  and  $C_w$  are concentrations in the solid and water, respectively) under natural flow conditions. Use of median U concentrations in pore water (5 ng/mL) and NaOAc leachates (0.035  $\mu\text{g/g}$  rock) yields an estimate of the  $^{238}\text{U}$   $K_d$  value of about 7 mL/g. This value is larger than the value of 0.5 mL/g obtained for crushed tuffs from laboratory batch experiments that currently is used for zeolitized units at Yucca Mountain (BSC, 2004, Table 5-1).

Whole-rock samples of unfractured core, rubble core, and fracture surfaces have similar  $^{234}\text{U}/^{238}\text{U}$  AR ranging from 0.92 to 1.16, indicating both enrichments ( $^{234}\text{U}/^{238}\text{U}$  AR > 1) and depletions ( $^{234}\text{U}/^{238}\text{U}$  AR < 1) in the daughter  $^{234}\text{U}$  relative to the parent  $^{238}\text{U}$ . In contrast to the rock samples, all pore water and rock leachate samples have elevated  $^{234}\text{U}/^{238}\text{U}$  AR ranging from 1.1 to 5.2. Whole-rock  $^{234}\text{U}/^{238}\text{U}$  AR greater than 1 for these zeolitized rocks contrast with data from samples of the welded part of the Topopah Spring Tuff (Tpt), the proposed repository horizon, that invariably have  $^{234}\text{U}/^{238}\text{U}$  AR < 1. The depletion in  $^{234}\text{U}$  in Tpt rocks is caused by preferential removal of  $^{234}\text{U}$  by the percolating water as a result of  $\alpha$ -recoil processes. Therefore, the large  $^{234}\text{U}/^{238}\text{U}$  AR in pore water and in U sorbed on mineral surfaces indicate that  $^{234}\text{U}$  removed from overlying units is transported in percolating water and retained in underlying zeolitized units. U-series isotope data for whole-rock samples from subrepository units having  $^{234}\text{U}/^{238}\text{U}$  AR > 1 also strongly support the potential for retention of U from percolating water by zeolitized rocks and indicate that amounts of retardation of radionuclides may be greater than currently credited to zeolitized rocks at Yucca Mountain.

## References

- BSC (2004) Technical Basis Document No. 10: Unsaturated zone transport, Revision 1, 266 p., Bechtel SAIC Company, LLC, Las Vegas, Nevada. Accessed March 6, 2006, at <http://www.lsnnet.gov> (LSN# NRC000024904).
- Vaniman, D.T., Chipera, S.J., Bish, D.L., Carey, J.W. and Levy, S.S. (2001) Quantification of unsaturated-zone alteration and cation exchange in zeolitized tuffs at Yucca Mountain, Nevada, USA. *Geochimica et Cosmochimica Acta* **65**, 3409-3433.
- Engstrom, D.A. and Rautman, C.A. (1996) Geology of the USW SD-9 Drill Hole, Yucca Mountain, Nevada, SAND96-2030, 128 p., Sandia National Laboratories, Albuquerque, New Mexico. Accessed March 6, 2006, at <http://www.lsnnet.gov> (LSN# DEN000707221).

## About features of ion exchange, mathematical modeling, and calculation of dynamic ion-exchange processes on natural clinoptilolites

**V. A. Nikashina**

*Russian Academy of Sciences; Moscow, Russia; Email: nikashina@geokhi.ru*

Among other methods, the ion-exchange method plays an important role in water decontamination. The well-grounded choice of optimized conditions and modes under which to carry out the ion-exchange process has essential practical importance and value. The shortest scientific way to determine optimal conditions or forecast ion-exchange process results lies in the mathematical modeling of every stage (sorption, regeneration). Modeling allows the calculation of modes of dynamic ion-exchange processes based on the minimal number of experimental data—depending on the quite different parameters (depth of a sorbent bed, flow rate, a sorbent grain size, degrees of its regeneration, etc.). For this reason, modeling becomes the important investigation phase for deciding on practical tasks using natural clinoptilolites.

The theory of ion-exchange dynamics, with the purpose of modeling and calculating various ion-exchange processes, has been developing for many years in the Sorption Methods Laboratory of Vernadsky Institute of Geochemistry and Analytical Chemistry of the Russian Academy of Sciences (Venitsianov and Rubinstein, 1983; Senyavin et al., 1972). As a result, the Sorption Methods Laboratory has a bank of solutions for the ion-exchange (sorption) dynamics problems for the unicomponent systems described by film-, particle-, and mixed-diffusion kinetics, and by various types of isotherms, as well as for multicomponent systems that are ready for use as programs or as schedules (sets of the dimensionless breakthrough curves, together with several simple formulas for which practical use cannot cause difficulties). This bank allows researchers to calculate the broad specifications of practically all important problems because a lot of cases of complex multicomponent systems can be reduced to simple unicomponent ones. The choice of model for the dynamic ion-exchange process is based on the following estimations:

- theoretical and real system components taken from the isotherm character of sorbed ions (linear values, Langmuir constants, rectangular, etc.)
- definition of the equilibrium constants necessary for the calculation characteristics (constants of ion exchange ( $K_{ij}$ ) or the distribution coefficient ( $G_{ij}$ )).
- definition of kinetic characteristics of investigated ion-exchange process—film-diffusion kinetic coefficient ( $\beta$ ) and particle diffusion coefficient ( $D$ ). These characteristics can be obtained from independent sources: the equilibrium characteristics from ion-exchange isotherms; the kinetic characteristics from a thin layer method (Boyd et al., 1947) or from data from dynamic breakthrough curves, both kinetic coefficients and equilibrium coefficients (Nikashina et al., 1995). The value  $\beta$  can also be determined from values of equivalent electroconductivity of exchanging ions, taking into account the hydrodynamics principles (Senyavin et al., 1972).
- relative contributions of film- and particle-diffusion in dynamic processes depending on flow rate, particle size of sorbent, and so on (Senyavin et al., 1972).

As we know, in contrast with the ion-exchange proceeding on many organic resins, the ion-exchange on zeolites is characterized by a number of specific features. One of the major features is the existence of two kinetic stages in zeolites (Thompson and Tassopoulos, 1986; Brown et al., 1971).

We have solved the problem of sorption dynamics for bidisperse particles in our laboratory (Khamizov, 1998); but its use in practice is difficult. Therefore, we have made a tentative estimation of the opportunities for using available solutions of sorption dynamics for modeling and calculating the ion-exchange processes on natural zeolites. This estimation shows that using existing mathematical models of sorption dynamics for calculating the processes on zeolites is possible if the sorption of a target component is described by a linear or nearly linear isotherm.

The analysis of the many problems associated with decontaminating, i.e., removing radioactive impurities or heavy metal ions, natural water and wastewaters indicates that despite the multicomponent composition and



complexity of a solution, in most cases it is possible to reduce multicomponent problems to single component problems because, as a rule, the sorption isotherms of the pollutants are linear on natural clinoptilolites. This substantially facilitates the problem of mathematical modeling of the decontamination ion-exchange processes and allows for the use of the above mentioned solutions and approaches. Concrete examples are presented for using known theoretical solutions of the sorption dynamics for modeling and calculating ion-exchange processes to decontaminate surface potable waters of radionuclides, underground potable waters of superfluous strontium and ammonium, and atomic power station wastewaters of  $^{137}\text{Cs}$  and  $^{90}\text{Sr}$ . On the basis of the received initial data, calculations are carried out of breakthrough times of the technological filters loaded with clinoptilolite, depending on column operating conditions in each considered case.

## References

- Boyd, G.E., Adamson, A.W. and Meyers, L.S. (1947) The exchange adsorption of ions from aqueous solutions by zeolites. *Journal of American Chemical Society*, **69**, 2836–2848
- Brown, L.M., Sherry, H.S. and Krambek, F.J. (1971) Mechanism and kinetics of isotopic exchange in zeolites. *Journal of Physical Chemistry*, **75**, 3846–3855.
- Khamizov, R.Kh. (1998) Physico-chemical basis of integrated development of ocean mineral resources. Ph.D. thesis, Vernadsky Institute of RAS, Moscow, Russia, 332 pp.
- Nikashina, V.A., Galkina, N.K., Komarova, I.V., Anfilov, B.G. and Argin, M.A. (1995) Evaluation of clinoptilolite-rich tuffs as ion-exchangers. Pp. 289–297 in: *Natural Zeolites '93: Occurrence, Properties, Use* (D.W. Ming and F.A. Mumpton, editors). Int. Comm. Natural Zeolites, Brockport, New York.
- Senyavin, M.M., Rubinstein, R.N., Venitsianov, E.V., Komarova I.V., Galkina, N.K. and Nikashina, V.A. (1972) *Fundamentals of Calculation and Optimization of Ion-Exchange Processes*. Nauka, Moscow, 172 pp. (in Russian).
- Thompson, P.W., and Tassopoulos, M.A. (1986) Phenomenological interpretation of two-step uptake behaviour by zeolites. *Zeolites*, **6**, 9–12.
- Venitsianov, E.V. and Rubinstein, R.N. (1983) *Dynamics of Sorption from Liquids* (M.M. Senyavin, editor). Nauka, Moscow, 240 pp. (in Russian).

## Study of natural zeolites in Vernadsky Institute

**V.A. Nikashina**

*Russian Academy of Sciences; Moscow; Russia; Email: nikashina@geokhi.ru*

Research on clinoptilolite-containing tuffs in the sorption methods laboratory of the Vernadsky Institute of Geochemistry and Analytical Chemistry (RAS) has been carried out since 1971 in the following basic directions:

1. Comparative studies on ion-exchange properties of natural clinoptilolites of various deposits (determination of exchange capacities, equilibrium and kinetic characteristics of ion-exchange processes, an estimation of clinoptilolite's selectivity to various ions depending on composition and concentration of a solution, and also mineralogical composition and structure clinoptilolites), and also the definition of mechanical durability, chemical stability and other properties.

2. Mathematical modeling and calculation of ion-exchange processes on clinoptilolites of various deposits based on the initial equilibrium and kinetic data obtained in item 1 and their use for the solution of optimization problems.

3. The solution of concrete practical problems with use of natural zeolites based on developed methodology. The choice of modes of the developed technological processes carried out based on their equilibrium and kinetic characteristics, modeling and calculation (see items 1, 2).

Main applications from the solved problems :

- a) The decontamination of drinking water with ionic impurities (radionuclides—Cs 137, Sr 89,90, some heavy metals). Results of this research has been approved for one water-treatment plant in Moscow.

Clinoptilolite is applied in the technological scheme of water purification, as a filtering agent instead of quartz sand or any other filtering agent, and as a barrier to toxic ionic impurities (heavy metals, radionuclides, etc. in case of short-term pollution of water as a result of emergency emissions etc.).

The estimation of time of the protective action of a clinoptilolite filter on ionic impurities depends on the conditions of the filtration (length of a layer of loading, solution flow rate, etc.) based on the mathematical modeling and calculation.

- b) The decontamination of underground potable water containing excess stable strontium and iron. Institute Atomenergoproekt designed a treatment station for removing strontium and iron from the underground drinking water supply for the Desnogorsk settlement, Smolensk region, following initial data and recommendations by us. There is a patent.

- c) The decontamination of atomic power station special laundry waters containing radioactive Sr and Cs was developed together with the Institute of Nuclear Research and Nuclear Power of the Bulgarian Academy of Sciences. Mathematical modeling and calculation of the ion-exchange process of special laundry waters decontamination have been carried out.

4. A databank of equilibrium and kinetic characteristics of Russian zeolites was created and the quantitative estimation of efficiency of zeolites of various deposits for the solution of the various practical problems was carried out.

5. Modifying natural clinoptilolite. Research on zeolite modification by organic and inorganic compounds was undertaken with the purpose of expanding the use of clinoptilolite.

- a) Modification by polyhexamethyleneguanidine (PGMG) with use of the cross-linker agent, epichlorohydrine, has allowed the design of a sorbent for simultaneous cation-exchange, anion-exchange, and bactericidal properties. There is a patent. Very high selectivity of this sorbent to carbonate uranium complex has been shown. The sorbent can be effectively used for treating surface drinking water from radionuclides, heavy metals, and uranium.

- b) Modification with magnetite has led to creation of a sorbent with magnetic properties with preservation of selectivity for radionuclides. The sorbent can be used for removal of radionuclides from highly turbid solutions and soils. There are patents.

- c) The opportunity to design geochemical barriers based on modified clinoptilolites is considered.

## The role of interfacial water in the clinoptilolite-heulandite zeolite system

N. W. Ockwig<sup>1</sup>, T. M. Nenoff<sup>1</sup>, L. L. Daemen<sup>2</sup>, M. T. Hartl<sup>2</sup>, and R. T. Cygan<sup>1</sup>

<sup>1</sup>Sandia National Laboratories; Albuquerque, New Mexico, USA; Email: [nockwig@sandia.gov](mailto:nockwig@sandia.gov).

<sup>2</sup>Los Alamos National Laboratory; Los Alamos, New Mexico, USA

This study focuses on understanding the role of interfacial water in zeolites as a function of ion exchange ability and selectivity, plus intercalated cation solvation. In particular, our current efforts are focused on the HEU-CLI zeolite systems, where classical molecular dynamics (MD) and experimental spectroscopic observations are being studied and correlated as a function of Si/Al and cation identity. Large-scale MD simulations are used to derive equilibrium structures, enthalpies, and the dynamical behavior of various hydration states of these phases. Among the most abundant naturally-occurring zeolitic aluminosilicate phases heulandite (HEU) and clinoptilolite (CLI), are formulated as  $[\text{Ca,Na,K,Li}]_{4-6}[\text{Al}_6(\text{Al,Si})_4\text{Si}_{26}\text{O}_{72}] \cdot 24\text{H}_2\text{O}$ . These isostructural minerals can be synthesized over a range of Si/Al values (from 2.5 to 6) with a wide variety of charge-compensating cations, and have an underlying HEU topology. The topology is composed of an array of three distinct types of channels. Two of these channels, defined by 10-member ( $4.4 \times 7.2$  Å) and 8-member ( $4.1 \times 4.7$  Å) aluminosilicate rings, are aligned parallel to the crystallographic *c*-axis and are perpendicularly intersected by the third and final type of channel, defined by 8-member ( $4.0 \times 5.5$  Å) aluminosilicate rings, which are parallel to the crystallographic *a*-axis. The distinction between these two materials is based on both their Si/Al values and thermal stabilities. Clinoptilolite has a silica-rich (Si/Al > 4) composition and a thermal stability exceeding 500°C while heulandite (Si/Al < 4) exhibits structural degradation at temperatures above 350°C. Because there are abundant deposits of clinoptilolite, extensive work on the development of its commercial applications in gas separations, ion exchange, agriculture, and waste water remediation have been widely reported. However, despite these extensive efforts relatively little is understood about the role interfacial water plays in the viability of these materials for a given application. This presentation will primarily highlight our computational efforts towards understanding the behavior of water in these materials.

### References

- Arcoya, A.; González, J.A.; Llabre, G.; Seoane, X.; Travieso, N. (1996) Role of the counteractions on the molecular sieve properties of clinoptilolite. *Microporous Materials*, **7**, 1-13.
- Yang, S.; Navrotsky, A.; Wilkin, R. (2001) Thermodynamics of ion-exchanged and natural clinoptilolite. *American Mineralogist*, **86**, 438-447.
- Jobic, H. (1992) Molecular motions in zeolites. *Spectrochimica Acta*, **48A**, 293-312.
- Joshi, M.S.; Joshi, V.V.; Choudhari, A.L.; Kasture, M.W. (1997) *Materials Chemistry and Physics*, **48**, 160-163.
- Ward, R.L.; McKage, L. (1994) *Journal of Physical Chemistry*, **98**, 1232-1237.

## Comparison of water quality improvement by natural mordenite and bamboo coal inside the biotope, Japan

M. Okamoto, T. Kobayashi, and E. Sakamoto

*Kyushu International University; Kitakyushu, Japan; Email: okamoto@econ.kiu.ac.jp*

### Introduction

We have investigated the capability of natural mordenite for removing nitrogen from river water. In this study, we determined the removal capability under laboratory conditions and at full scale in an artificial biotope using natural mordenite and bamboo coal. We measured such properties as pH, COD,  $\text{NH}_4^+$ ,  $\text{NO}_2^-$ ,  $\text{NO}_3^-$  and total N of actual river water under the same experimental conditions.

We have also compared the purification ability of natural mordenite, bamboo coal (which has no ion exchange capability), and glass (which has no adsorption ability at all).

### Experimental Methods

The Shakutake River biotope is set up parallel to the Shakutake River (Fig.1), where drainage of Nogata City, Fukuoka Prefecture and the Onga River tributary are present. The biotope was completed in August, 2001. The dimensions of the biotope are length 26 m, width 6 m, and depth 0.8 m. Natural zeolite (about 17 tonnes) was placed in one half and bamboo coal (about 3 tonnes) in the other half. The zeolite is from a Ca-rich source in Fukushima Prefecture. Water was pumped at about 5 L/sec from the Shakutake River and passed through the zeolite and bamboo coal, then returned to the river. The residence time was about 10 hours. Water was sampled from the zeolite tank, the bamboo char tank, and sites S1 to S4 (Fig. 1) before the Shakutake River confluence. The pH, EC, DO, ORP, cations, anions, COD, and coliforms were measured. The biological measurements were carried out in order to observe the difference between the zeolite tank and microorganisms in the water from bamboo char tank.

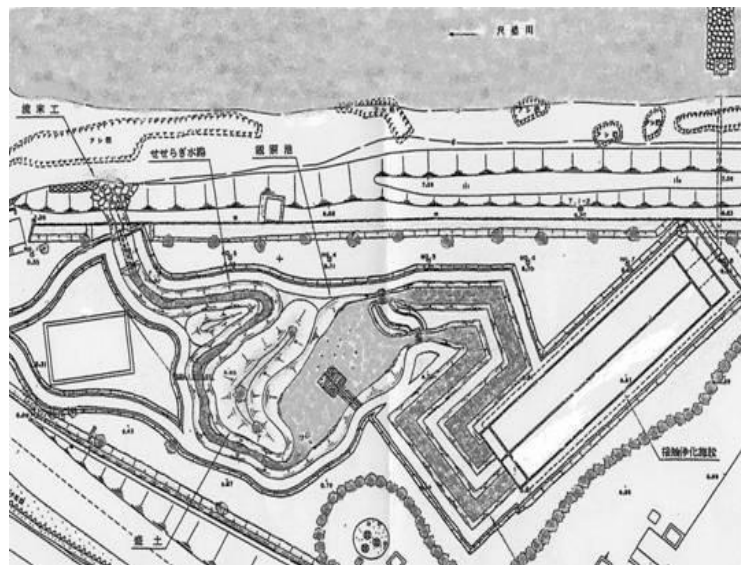


**Figure 1.** Schematic diagram of the Shakutake River biotope. The sampling points S1 to S4 are shown.

## Results and Discussion

There was no difference in pH among sites S1, S2, S3 and S4.  $S1 > S3 > S2$  for DO and COD. The values of  $N-NH_3$  and  $N-NO_3$  are shown in Fig. 2.  $N-NO_3$  increased, while  $N-NH_3$  decreased after passage through each tank in November, 2001 four months after the beginning of the experiment. Nitrification was encouraged especially in the zeolite tank. There was hardly any change at S1, S2, and S3 in May and September, 2003, after 2 years.

In the zeolite tank, the ORP was +10 mV and the color of the waterway brown in May, 2003. In the bamboo char tank the ORP was -14 mV and the color of the waterway was black. A food chain was established in the zeolite tank including black snail and algae.

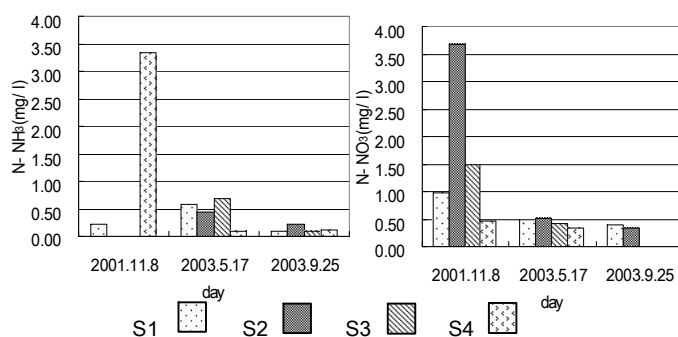


**Figure 2.** The change in nitrogen concentrations  $NH_3-N$  (left) and  $NO_3-N$  (right) depending on the date of analysis. Data for sampling locations S1 to S4 are shown.

## Magnetic modified natural clinoptilolite from Bigadic region, Turkey.

Ö. Orhun and, Z. Dikmen

Anadolu University; Eskişehir, Turkey; E-mail: oorhun@anadolu.edu.tr

The papers on magnetic modification processes were originally published about synthetic zeolites and studies still continue (Petridis et al, 2003, Čapek et al, 2005). The literature review, which we have done up to now, shows that there is no study about magnetic modification process for natural zeolites or that we haven't found one even if there were one.

In this study, magnetic modified forms of natural clinoptilolite obtained from Bigadic region, Turkey, have been prepared and then characterized using methods such as XRD, XRF, DTA, and DSC. The ion exchange, adsorption, and magnetic properties of these samples have been investigated. The magnetic modified forms of natural clinoptilolite samples have been prepared in the following way: The natural clinoptilolite samples that have dimensions smaller than 63  $\mu\text{m}$  have been separated by sieving. The natural clinoptilolite samples were mixed and intensively ground with powder forms of  $\text{NiCl}_2 \cdot 6\text{H}_2\text{O}$  and  $\text{CoCl}_2 \cdot 6\text{H}_2\text{O}$  salt in a mortar. The resulting powder mixture was slowly heated up to 550 °C at 0.5 °C/min and maintained at this temperature for 6 hours. The solid sample was cooled and washed with de-ionized water until no  $\text{Cl}^-$  ions were detected in the eluted water. The mixture solid sample was then dried at 80 °C during 16 hours (Čapek et al, 2005).

Ion exchange isotherms, ion selectivity-sequence and ion exchange capacities of the prepared samples have been determined. Also, the adsorption isotherms of various gases on modified clinoptilolites have been obtained. The magnetic properties of the samples have been determined by means of Vibrating Sample Magnetometer.

### References

- Čapek, L., Kreibich, V., Dědeček, J., Grygar, T., Wichterlová, B., Sobalík, Z., Martens, J.A., Brosius, R. and Tokarová, V. (2005) Analysis of Fe species in zeolites by UV–VIS–NIR, IR spectra and voltammetry. Effect of preparation, Fe loading and zeolite type. *Microporous and Mesoporous Materials*, **80**, (1-3), 279-289.
- Petridis, D., Bourlinos, B.A. and Zboril, R. (2003) A simple route towards magnetically modified zeolites. *Microporous and Mesoporous Materials*, **58**, 2, 155-162.

## First reported occurrence of clinoptilolite-rich tuff deposits in the Mexican Volcanic Belt (state of Michoacan, southwestern Mexico)

M. Ostrooumov and I. Ostrooumova

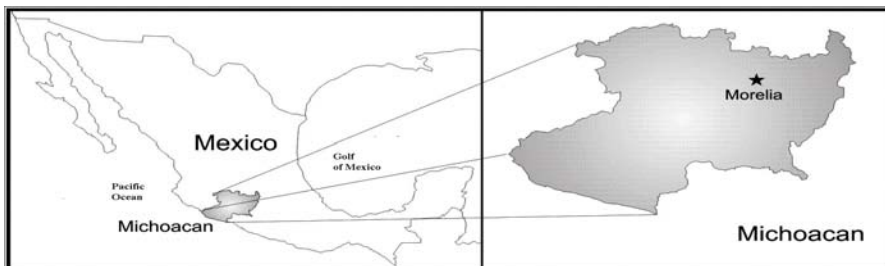
*University of Michoacan; Morelia, Michoacan, Mexico; Email: ostroum@zeus.umich.mx*

The most studied and well-known deposits of natural zeolites in Mexico are those of Oaxaca (southern Mexico) and Sonora (northern Mexico). They seem to be also the most important of the country in terms of estimated amounts (Ostrooumov, 2002): Oaxaca, Laollaga Municipality, 15,120,000 tons (clinoptilolite, mordenite); Sonora, El Cajon deposit (Rayon Municipality), 10,000,000 tons (clinoptilolite); Sonora, Agua Prieta deposit (Agua Prieta Municipality), 3,000,000 tons (erionite). These deposits formed during the Oligocene and Miocene, when intensive volcanic activity produced large pyroclastic deposits, mainly in the geological provinces of the Sierra Madre del Sur and the Sierra Madre Occidental (Pablo Galan et al., 1996). on the contrary, no data have been so far reported on the occurrence of relevant zeolite deposits in the central part of the country, namely in the Mexican Volcanic Belt (MVB) geological province.

As a result of geological and mineralogical investigations, large accumulations of sedimentary clinoptilolite have been found in the zeolitic tuffs from the MVB geologic province in the state of Michoacan (southwestern Mexico). Zeolites have been observed in volcanic sequences of recent geological age (Fig. 1) that have been located around the Laguna de Cuitzeo and near Morelia (capital of Michoacan). The dominant lithologies are andesites and basalts (Upper Miocene), pyroclastic flow deposits (Pliocene-Miocene), and Quaternary basalts. The pyroclastic flows can be differentiated into two main units. The lower unit is characterized by a pink-gray, glassy ash-flow tuff with phenocrysts of quartz, sanidine, albite, and traces of biotite, rare lithics, and pumice fragments up to 1 cm. Rhyolitic bubble-wall glass shards are partly altered to authigenic smectite, and opal-C. Sanidine crystals from a glassy ash-flow tuff south of Laguna de Cuitzeo yielded a radiometric age of 2.8 Ma (Pasquarè et al., 1991). The upper unit is a pale-green tuff that substantially devitrified to zeolite. The principal authigenic mineral is clinoptilolite (up to 90-95 wt%), coexisting with altered volcanic glass, mordenite, and opal-C.

Analytical techniques (XRD, SEM-EDS, XRF, IR, and Raman spectrometry) allowed the identification of the primary composition of the glassy pyroclastic rocks and their diagenetic evolution. The results confirm the first discovery of clinoptilolite-rich tuff deposits and allowed the crystal-chemical characterization of the clinoptilolite.

Geological and mineralogical features of the investigated deposits lead us to hypothesize a potential economic interest for this area. However, further exploration is required to evaluate fields of application of these important resources and to define correct strategies mainly aimed to the environmental preservation of the Morelia area and other industrial parts of this region of Mexico.



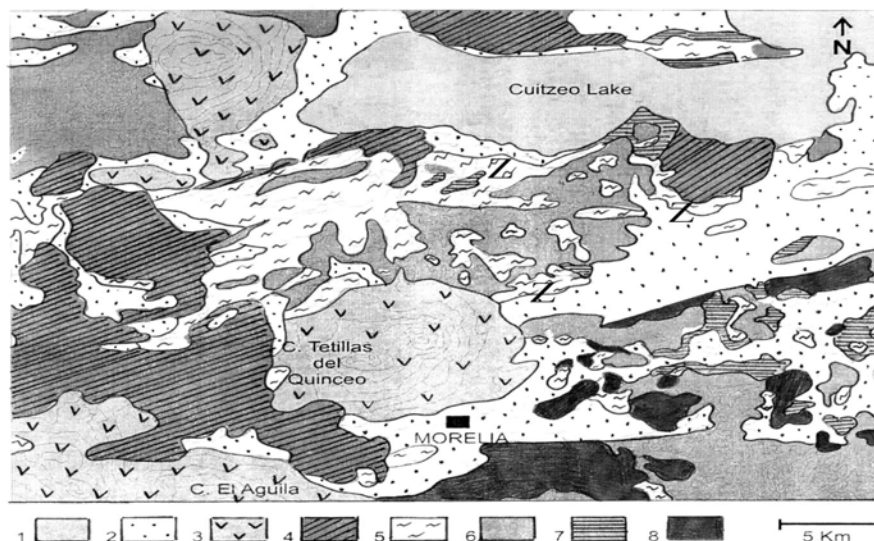


**Figure 1.** Simplified geological map of Morelia area: 1, Cuitzeo Lake; 2, Alluvial deposits; 3, Scoria cones and related pyroclastic flows; 4, andesites and basalts (Quaternary); 5, pyroclastic flow deposits (2.8 million yr BP); 6, andesites and basalts (Upper Miocene); 7, lacustrine and fluviolacustrine deposits (Upper Miocene–Lower Pliocene); 8, ignimbrites (Middle and Upper Miocene); Z, clinoptilolite-rich tuff deposits.

## References

- Ostrooumov, M. (2002) Zeolitas de México: diversidad mineralógica y aplicaciones. Sociedad Mexicana de Mineralogía, <<http://www.geocities.com/smexmineralogia/zeolitas.htm>>
- Pablo Galan, L., Chavez Garcia, M., and Cruz Sanchez, M. (1996) Sedimentary zeolites in the Sierra Madre del Sur and Sierra Madre Occidental, Mexico. *Revista Mexicana de Ciencias Geológicas*, **13** (2), 188-200.
- Pasquarè, G., Ferrari, L., Garduño, V.H., Tibaldi, A., and Vezzoli L. (1991) Geologic map of the central sector of the Mexican Volcanic Belt, states of Guanajuato and Michoacan, Mexico. Geological Society of America, Map and Chart Series, MCH072.



## **Analysis of physical and chemical properties of natural zeolite in the southeast region of Mongolia**

**J. Oyuntseteg and R. Lkhagvajav**

*Mongolian Academy of Science; Ulaanbaatar, Mongolia; Email: oyuntsetsegi@yahoo.com*

Mongolia is rich in natural zeolites. Since 1960, Mongolia and Russian geologists had discovered more than 30 deposits and occurrences of zeolite. Estimated resources are 2.5 billion tons by P1 classification. Spatially concentrated in the East Mongolian volcanic belt, they belong to distinctive type of zeolites of igneous limonitic and hydrothermal genesis dating back to the Upper Jurassic and Early Cretaceous periods. The main content of the valuable component in zeolite is 40–90 %. The main zeolite is clinoptilolite. Minor amounts of chabazite, geylandite, analcime, and ferrierite are sometimes recorded.

Zeolites of the southeast region of Mongolia are mainly characterized by clinoptilolite-montmorillonite assemblages, containing up to 80% of crystalline phases, and their total volume of pores is 0.6 cm<sup>3</sup>/g. These zeolites have high porosity (up to 51%), satisfactory hardness (no less than 35%), and abrasion (not more than 60%), acid-resistance (pH for the start of the crystal destruction is less than 1), and thermal stability (crystal structure breakdown temperature is 600–800°C), and they are not carcinogenic (content of such toxic elements as arsenic, lead, and mercury in the minerals does not exceed 0.001 mg/g of zeolite and are able to absorb radioactive isotopes of cesium and strontium). The average technological parameters of natural zeolites in the southeast region deposits are as follows: Silicate module, SiO<sub>2</sub>/Al<sub>2</sub>O<sub>3</sub> 4.01–4.71, with volumetric capacity 0.65–1.22 mg-equiv/g

The authors revealed the correlative dependence of the process parameters on the crystal-mineralogical and physicochemical properties in the studied natural zeolites. Analyzing the available database (crystal-mineralogical, physicochemical, and technological characteristics of certain zeolite-bearing materials (and/or zeolite)), one can determine the possible main direction in the implementation of the given mineral and the method of modifying zeolite for particular purposes.

## **Experimental and thermodynamic modeling study of multicomponent ion-exchange of alkali and alkaline-earth metals in clinoptilolite**

**R.T. Pabalan and F.P. Bertetti**

*Southwest Research Institute®; San Antonio, Texas, U.S.A.; Email: rpabalan@swri.edu*

Ion-exchange processes in natural systems generally involve more than two cations, but little published data are available for multicomponent ion-exchange reactions. Experimental data on ternary and more complex mixtures are needed to develop and evaluate thermodynamic models that can be used to predict ion-exchange equilibria in natural systems. In this study, ternary and quaternary ion-exchange experiments were conducted involving the alkali and alkaline-earth cations  $\text{Na}^+$ ,  $\text{K}^+$ ,  $\text{Cs}^+$ ,  $\text{Sr}^{2+}$ , and  $\text{Ca}^{2+}$  and clinoptilolite, a zeolite mineral that is locally abundant in the saturated and unsaturated zones of Yucca Mountain, Nevada, which is the potential site for a high-level waste repository. The clinoptilolite used in the experiments was prepared by pulverizing a sample of clinoptilolite-rich tuff from Death Valley Junction, California, and purifying the 200–325 mesh fraction. Homoionic forms of  $\text{Na}^+$ -,  $\text{K}^+$ -, and  $\text{Ca}^{2+}$ -clinoptilolite were prepared by reacting at 75 °C the purified zeolite with 3-M chloride solutions of  $\text{Na}^+$ ,  $\text{K}^+$ , or  $\text{Ca}^{2+}$ . The ternary ion-exchange experiments consisted of reacting weighed amounts of homoionic clinoptilolite powder with known volumes of solution mixtures of  $\text{Na}^+ + \text{K}^+ + \text{Cs}^+$ ,  $\text{Na}^+ + \text{K}^+ + \text{Sr}^{2+}$ , and  $\text{Na}^+ + \text{K}^+ + \text{Ca}^{2+}$  at constant solution normality. The quaternary ion-exchange experiment studied a  $\text{Na}^+ + \text{K}^+ + \text{Ca}^{2+} + \text{Sr}^{2+}$  system.

A thermodynamic model based on the Wilson equation was used to model the ion-exchange data. The parameters for the Wilson equation and the equilibrium constants for the binary ion-exchange reactions were derived from published binary ion-exchange data. A correlation method that has been applied to predictions of formation constants of aqueous hydroxo-metal complexes was used to help constrain the equilibrium constants derived from the binary isotherm data. The Wilson model, with parameters derived only from binary ion-exchange data, was used to predict ternary and quaternary ion-exchange equilibria. A comparison of experimental data for ternary and quaternary systems and thermodynamic model predictions indicates that the Wilson model adequately reproduces multicomponent ion-exchange equilibria. The results suggest that it is possible to use the Wilson model to evaluate multicomponent ion-exchange involving alkali and alkaline-earth metals in natural systems.

This abstract was prepared to document work performed by the Center for Nuclear Waste Regulatory Analyses (CNWRA) for the U.S. Nuclear Regulatory Commission (NRC) under Contract No. NRC-02-02-012. The activities reported here were performed on behalf of the NRC Office of Nuclear Material Safety and Safeguards, Division of High-Level Waste Repository Safety. This abstract is an independent product of CNWRA and does not necessarily reflect the view or regulatory position of NRC.

# Application of natural zeolites in the production of controlled-release fertilizers

**A. Pawelczyk and A. Popowicz**

*Wroclaw University of Technology; Wroclaw, Poland; Email: adam.pawelczyk@pwr.wroc.pl*

## Introduction

Commonly used mineral fertilizers contain nutrients in water-soluble forms that are therefore easily available for plants. On the one hand, these fertilizers create opportunities to intensify agricultural production, but on the other hand, they endanger the natural environment due to leaching and migration of soluble compounds into surface waters and groundwaters.

Techniques that allow efficient utilization of nutrients contained in fertilizers employ compounds of lower water-solubility, fertilizer granulation, coating the granulated product with substances that moderate the release of components, as well as using fillers or carriers of absorptive and ion-exchange features (Mumpton, 1999; Pawelczyk, 2005).

This work presents the results of research on the production of granulated fertilizers based on natural zeolite and diammonium phosphate (DAP), as well as of the research on the kinetics of  $\text{NH}_4^+$  and  $\text{PO}_4^{3-}$  ions released in modeled conditions simulating a natural soil state.

## Experimental Methods

Batches of mineral fertilizers were produced based on blending DAP with natural zeolite to achieve a varying content of phosphorus and nitrogen. Both non-modified and modified zeolites were utilized. The modification consisted of heating the zeolite up to 250°C for 5h. Fertilizers were granulated using biodegradable binding agents in the form of modified starch (Creamix1230CS, Adanet CS), as well as polysaccharides-carboxymethylcellulose (CMC) sodium salts (JELOCEL-S AS-10/2). Lysimetric tests were performed to determine the rate of the leaching of nutrients from the fertilizers.

During the research, natural clinoptilolite zeolite from Slovakian deposits with a chemical formula of  $(\text{Ca}, \text{K}_2, \text{Na}_2, \text{Mg})_4\text{Al}_8\text{Si}_{40}\text{O}_{96}24\text{H}_2\text{O}$  was used. Properties of the zeolite are given in Table 1.

**Table 1.** Properties of natural zeolite used in the research

Effective diameter of pores	0.4 nm	Fe <sub>2</sub> O <sub>3</sub>	0.7–1.9%
Volume weight	1600–1800 kg/m <sup>3</sup>	K <sub>2</sub> O	2.2–3.4%
Porosity	24–32%	Si/Al	4.8–5.4%
Water absorption	34–36%	Clinoptilolite	84%
SiO <sub>2</sub>	65.0–71.3%	Cristobalite+quartz	8–9%
Al <sub>2</sub> O <sub>3</sub>	11.5–13.1%	Clay mica	4%
CaO	2.7–5.2%	Plagioclase	3–4%

A laboratory drum granulator with a rotation speed control was used to granulate the powdered fertilizers. The model bed used to characterize nutrient-leaching consisted of pre-rinsed < 2-mm grain-size pit sand.

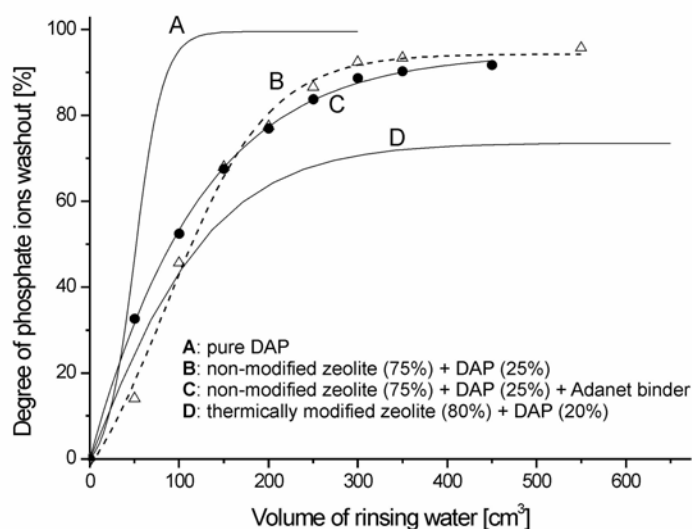
Phosphorus in samples of fertilizers and eluates was analyzed using a Varian Cary 50 spectrophotometer. Nitrogen was analyzed using a distillation method, and hardness tests of the granules were performed with an Erweka TBH 20 tablet tester.

## Results and Discussion

Table 2 and Figure 1 show that the use of binding agents did not consistently increase either the hardness or leaching-resistance of granules in the process of granulation of the fertilizer batches. Zeolite-DAP blends are a very good mixture for obtaining resistant grains. In most cases the mechanical strength of the granules obtained without binding additives was even higher than those with binder.

**Table 2.** Selected results of hardness measurements of granules of selected fertilizer samples, fraction 3.15–5 mm. Average values for 10 granules are given.

Kind of the zeolite	Zeolite mass fraction in the fertilizer [%]	Binder (Adanet)	Hardness [Newton]	Grain size [mm]
non-modified, drum granulator	75	yes	26.10	3.69
non-modified, drum granulator	75	no	34.22	4.28
non-modified, drum granulator	50	yes	28.7	4.13
non-modified, drum granulator	50	no	30.3	4.03
non-modified, drum granulator	25	yes	30.3	4.26
non-modified, drum granulator	25	no	26.5	3.86
thermally modified, drum granulator	80	no	25.8	4.59
thermally modified, hand granulated	80	no	14.2	3.89

**Figure 1.** Results of lysimetric tests of the granular fertilizers

Lysimetric tests showed that after rinsing the model soil beds, the release of  $\text{PO}_4^{3-}$  and  $\text{NH}_4^+$  ions into solutions was several times lower in the zeolite fertilizers than in pure DAP. The last were completely leached from the model bed after rinsing it with only 100  $\text{cm}^3$  of water. Zeolite-based fertilizers retained  $\text{PO}_4^{3-}$  and  $\text{NH}_4^+$  ions more tightly, even when greater volumes of washing water were used. Particularly, the fertilizer based on thermally modified zeolite retains about 67% of  $\text{PO}_4^{3-}$  after rinsing the bed with 100  $\text{cm}^3$  of water.

In conclusion, zeolite-based fertilizers can be a very interesting alternative for products obtained using other techniques, such as coatings, binders, fillers, and varying solubilities and granulation.

## References

- Mumpton, F. (1999) Uses of natural zeolites in agriculture and industry. *Proceedings of the National Academy of Sciences of the United States of America*, **96**, 3463–3470.
- Pawelczyk, A. (2005) Application of zeolites in processes of pollutants removal from liquid wastes. *Polish Journal of Chemical Technology*, **7**, 40–45.

## **On the geology of the zeolite deposit Beli Plast in NE Rhodopes, Bulgaria**

**P. I. Petrov**

*University of Mining and Geology St. Ivan Rilski; Sofia, Bulgaria; Email: ppetrov@mail.mgu.bg*

There are six deposits of zeolites in the Eastern Rhodopes of Bulgaria. The deposits are associated with the first Oligocene acidic volcanism (Beli Plast, Gorna Krepost, Most, Golobradovo and Ljaskovetz) and to the second Oligocene acidic volcanism (Bilia Bair). The zeolites from the deposits Beli Plast, Gorna Krepost, Most, Golobradovo and Bilia Bair are clinoptilolitic types while those from the Ljaskovetz deposit are mordenitic. The estimated reserves of clinoptilolite rocks total 722,000 th.t. and those of mordenite total 114 th.t. The Beli Plast deposit is composed of thick- to moderately thick-layered rocks with a white, red or pink color. Its total thickness is 70 m and reserves of clinoptilolite rocks are 37 000 th.t. The zeolites are composed of modified volcanic glass and pumice fragments of various dimensions from less than 1 mm to more than 5 cm. The volcanic glass and pumice fragments are replaced mainly by clinoptilolite (72-96%) and small amounts of either celadonite or montmorillonite, stilbite, quartz, opal-cristobalite, adularia, and illite. The clinoptilolite crystals fill cavities in the rocks. On the basis of the cation composition the zeolites are of two chemical types: calcium clinoptilolite ( $\text{Ca} > \text{K} + \text{Na}$ ) and potassium clinoptilolite ( $\text{K} + \text{Na} > \text{Ca}$ ;  $\text{K} > \text{Na}$ ). The minerals have a cation exchange capacity of 1.37 meq/g. The Beli Plast deposit has been developed. Three grain size fractions (5.0-2.5 mm, 2.5-0.8 mm, and  $< 0.8$  mm) are produced from this deposit. The first fraction is used for drying of gases, for improvement of soil structure, and to increase the efficiency of fertilizer. The second fraction is employed for filtration of potable water, for addition to the fodder of chickens, for deodorization of farms, and as a medium for planting of strawberries, trees, etc. The third fraction is used as a filler in soap manufacture and for addition to the fodder of pigs, cows, calves and chickens.

The clinoptilolite rocks from the Beli Plast deposit could be used for: 1) Zeolite substrates (mineral soils). The substrate is obtained by a comparatively simple chemical treatment of crushed clinoptilolite rock. It ensures normal yield for several years with only water irrigation. The sterility of the substrate along with its chemical and physical properties makes it an ideal medium for growing high quality seedlings. The method was patented in Bulgaria, USA, Italy and France. The clinoptilolite substrate Balkanine was used for plant cultivation in the SVET Space Greenhouse on board the MIR orbital station, 2) Molecular sieves, materials that, because of their internal structure, can selectively adsorb molecules according to the molecules' size and/or shape. Adsorption may also be used for purification, bulk separation, drying, refrigerants and cryosorption. 3) Addition to the diets of farm animals to aid nutrition by increasing the feed-conversion value. 4) Carriers of herbicides, fungicides, pesticides and recultivation of soils contaminated with herbicides. 5) Purification of waste water from nuclear power plants. The waters from our atomic station for many years have been purified with green clinoptilolite rocks. 6) Deodorant for farms, as a fertilizer, and in soil amendments. 7) Removal of organisms from human and animal wastes as well as heavy metals and radioisotopes; 8) Fillers in polymers. 9) Fillers in papers and cardboard. 10) Potable and industrial water filters.

## Magnetic and structural characterization of modified Romanian clinoptilolite

R. Pode<sup>1</sup>, E. Popovici<sup>2</sup>, V. Pode<sup>1</sup>, and V. Georgescu<sup>3</sup>

<sup>1</sup>University of Timisoara; Timisoara, Romania; Email: rodica.pode@rectorat.utt.ro

<sup>2,3</sup>University of Iasi; Iasi, Romania

### Introduction

Soil pollution by heavy metals can result from the extraction and processing of non-ferrous ores, aluminum, chemical fertilizers and cement, and also from coal-fired power stations. An alternative method that can be used to reduce pollution of soil by heavy metal ions involves the use of natural zeolites. The increase of soil pollution led to new materials and technologies for pollution abatement. The ion exchange properties of zeolites makes these materials potentially useful for mitigating pollution of soil by heavy metals. However, the use of zeolites for sticky textures face problems related to zeolite-polluted environment phase separation after pollution abatement treatment. These problems led to the initiation of research with the aim of synthesizing new materials based on magnetite-supported zeolites that have, besides adsorption capacity, magnetic properties that would facilitate phase separation (Pode et. al, 2002).

Studies carried out on very highly granulated zeolite samples have shown that magnetization occurred only at the surface of the particles (Pode et. al, 2001). Without knowing the magnetization depth, it was required to synthesise homogeneous samples of modified zeolite, starting with very fine ground natural zeolite, to determine the optimal conditions.

The present paper is aimed at establishing a relationship between synthesis conditions, magnetic characteristics, and structural characteristics of the adsorbent based on magnetite-supported clinoptilolite.

### Experimental Methods

The starting material for this study was natural zeolite from Mirsid-Romania, with particle size of about 63  $\mu\text{m}$ . The clinoptilolite content of the natural zeolite determined by x-ray diffraction was about 65 wt%.

To get clinoptilolite-based adsorbent with magnetic properties, various concentrations of ferrous-ferric solutions at the required stoichiometric ratio for magnetite precipitation, were heated up to 75°C. Then the solution was added to the activated zeolite at a pre-set  $\text{Fe}_3\text{O}_4$ /zeolite mass ratio corresponding to full precipitation of magnetite. This step was carried out by slowly adding a 25%  $\text{NH}_3$  solution under intense stirring. The temperature during the precipitation process was kept between 85–90°C. Finally, the samples of adsorbent were filtered, washed, and dried.

To assess magnetic characteristics, clinoptilolite particles were shaped as pellets (20 mm diameter) in a non-magnetic frame. Each sample contained the same quantity of modified adsorbent. The magnetic characteristics of the samples prepared in various conditions were measured by an induction method (50 Hz magnetic field) at room temperature using a Howling-type device with the aim of determining the optimum magnetic behaviour. The device was provided with a computerized acquisition data system. The XRD investigations on the zeolite samples were carried out by using  $\text{Co K}_\alpha$  radiation with a DRON-3 installation.

### Results and Discussion

The working conditions for adsorbent synthesis are shown in Table 1, for representative samples.

**Table 1.** Parameters of synthesizing modified clinoptilolite samples

Sample #	Fe <sub>3</sub> O <sub>4</sub> : zeolite mass ratio	Concentration of ferrous-ferric solutions (% wt.)	NH <sub>3</sub> Excess (% wt.)	Duration of NH <sub>3</sub> addition (hours)
1	1:5	3	100	2
2	1:5	5	100	2
3	1:7	5	100	2
4	1:5	5	50	2
5	1:5	5	100	1

The magnetization processes of the samples were investigated by recording both magnetization ( $M$ ) and differential susceptibility ( $\chi = dM/dH$ ) plots.

The experiments carried out on our samples showed that magnetization and differential susceptibility plots (or magnetic hysteresis curves) had the same basic shape for all samples.

The variation of synthesis parameters determined a variation of the quantity of magnetite included in the samples, expressed by an induced signal that would be labelled  $\Delta U$ . This signal ( $\Delta U$ ) is proportional to both magnetization and quantity of magnetic material included in each sample. The samples studied in this work were measured in the same installation, with the same geometry and identical mass of samples. Therefore, one can conclude that  $\Delta U$  correspond to the quantity of magnetic material included in zeolite channels, because the magnetization (i.e., the magnetic moment of the unit volume of magnetic material) was the same for all samples. For the studied samples, both the  $\Delta U$  and differential susceptibility ( $\chi$ ) values were determined. Thus, these values were used to set up the relationship between synthesis conditions and magnetic characteristics. The results showed the major influence of ammonia excess and ammonia addition time on the magnetic properties of the samples.

The conditions that favoured the formation of modified clinoptilolite with good magnetic characteristics were as follows: Fe<sub>3</sub>O<sub>4</sub>/zeolite mass ratio—1/5; concentration of ferrous-ferric solution—3%; ammonia excess—100%; duration of ammonia addition—2 hours.

Powder diffraction patterns for the samples were measured and compared to a reference sample (labelled sample 0) made of untreated clinoptilolite. Data obtained by XRD and magnetic measurements were in good agreement.

The authors wish to thank the MATNANTECH Scientific Authority (Project No.1/S1-2005) for supporting this research.

## References

- Pode, V., Todinca, T., Pode, R., Dalea, V., Popovici, E. (2002) Pb(II) ion exchange on zeolite-supported magnetite. Characterization of process by effective diffusivity coefficient. *Studies in Surface Science and Catalysis*, **142b**, 1825–1831.
- Pode, V., Georgescu, V., Dalea, V., Pode, R., and Popovici, E. (2001) A new adsorbent with magnetic properties based on natural clinoptilolite. *Studies in Surface Science and Catalysis*, **135**, CD.

# Clinoptilolitized pyroclastic rocks from Oaxaca (south Mexico): A mineralogical and technological study

N. Popov<sup>1</sup>, Y. Yanev<sup>2</sup>, Tz. Iliev<sup>2</sup>, and T. Popova<sup>1</sup>

<sup>1</sup>*Institute of Cryobiology and Food Technologies; Sofia, Bulgaria; Email: iliana\_nacheva@abv.bg*

<sup>2</sup>*Geological Institute, Bulgarian Academy of Sciences; Sofia*

## Introduction

The largely zeolitized complex of Mid-Tertiary ignimbrites of Sierra Madre Occidental has been the subject of many studies. Our study is focused on the zeolitization in the southernmost parts of this series, in the state of Oaxaca (in Sierra Madre del Sur). Two quarries for construction materials have been sampled, located 7–8 km NE of Oaxaca City. The aim is to provide new data on the petrographic and chemical composition of the zeolitized pyroclastics, their absorption characteristics and their possible utilization as zeolite material in agriculture.

## Experimental Methods

The samples have been studied under petrographic microscope Amplival-pol, the morphology and chemical composition of zeolites by Jeol 733 Superprobe (WDS, using 15 kV acceleration voltage, 1 nA beam current and 5 µm beam diameter) and by XRD semiquantitative analysis, all at the Geological Institute, Sofia. Chemical composition of the zeolitized pyroclastics and CEC (Cation Exchange Capacity) measurements were performed by the method of Ming et al. (1993) with Cs<sup>+</sup> ions at the Institute of Cryobiology and Food Technologies, Sofia.

## Results and Discussion

**Petrographic and chemical composition of the pyroclastics.** The studied rocks are probably products of pyroclastic flows and consist of: shards in average 0.1 mm in size, in single cases up to 0.5–0.6 mm; pumice fragments most commonly 0.5–0.7 mm, rarely up to 1 mm (with spherical or spindle-shaped bubbles); few plagioclase (An<sub>20.8-22.1</sub>Or<sub>5.3-5.7</sub>) phenocrysts up to 1 mm in size; quartz, biotite, magnetite, single zircon grains and lithics (probably andesite and single clasts from the crystalline basement). The chemical composition of the studied rocks is presented in Table 1.

**Table 1.** Chemical composition of the zeolitized pyroclastic rocks (in wt%)

Quarry	SiO <sub>2</sub>	TiO <sub>2</sub>	Al <sub>2</sub> O <sub>3</sub>	Fe <sub>2</sub> O <sub>3</sub>	MgO	CaO	Na <sub>2</sub> O	K <sub>2</sub> O	L.O.I.	Total
1	67.89	0.10	11.72	1.54	0.24	0.97	3.99	1.96	10.79	99.20
2	69.72	0.09	11.75	1.74	0.28	1.80	1.16	3.91	9.26	99.71

**Zeolitization.** All shards and pumice fragments are replaced by zeolites (almost always clinoptilolite) and light-green clay minerals. Zeolites form bands of microcrystalline mass, alternating with bands of clay minerals. Only on the walls of the central leached cavity of larger shards and in pumice bubbles, short-platy crystals are formed (size below 0.01 mm), rarely larger elongated-platy (up to 0.1 mm), all with heulandite habit and positioned parallel to the cavity walls. From a chemical point of view, they are alkaline clinoptilolites: sodic (Na<sub>4.53-5.27</sub>K<sub>0.2-1.66</sub>Ca<sub>0.27-0.42</sub>Al<sub>5.7-6.89</sub>Si<sub>29.06-30.16</sub>O<sub>72</sub>·24H<sub>2</sub>O) in the first quarry and potassic to K-Ca-Na (K<sub>1.57-2.92</sub>Na<sub>0.81-1.5</sub>Ca<sub>0.95-1.42</sub>Al<sub>5.47-6.85</sub>Si<sub>29.07-30.43</sub>O<sub>72</sub>·24H<sub>2</sub>O) in the second one, which explains the difference in the chemical composition of the zeolitized pyroclastics (Table 1).

Mordenite needles up to 20–30 µm long, commonly strongly twisted, overgrow the platy clinoptilolite crystals. Sometimes they form spherulites.

The clay minerals are deposited on the walls of the shards and the bubbles in pumice fragments, rarely filling them. In the first quarry, celadonite is sharply predominating and imparts the green color of the zeolitized pyroclastics. It forms small (below 0.1 mm) spheres irregularly scattered within the rock.

**The ion-exchange properties** of the studied zeolitized pyroclastics are similar to those in other parts of the world, for instance, the Eastern Rhodopes zeolitized rocks in Bulgaria (Raynov et al., 1997). These properties



are directly related to the chemical composition of the clinoptilolite (Table 2) and indicate a possible utilization in technological fields, such as agriculture.

**Table 2.** Cation exchange capacity (CEC) in meq/100g

Quarry	K <sup>+</sup>	Na <sup>+</sup>	Ca <sup>2+</sup>	Mg <sup>2+</sup>	Total	C.E.C.
1	12.78	119.62	16.12	0	148.52	135
2	24.29	28.27	43.32	0	95.88	94

**Use.** Mineral substrata have been prepared to cultivate plants based on patent No 4.337.078. The substratum from sample 2, irrespective of its lower CEC, showed better agricultural indices due to its more favorable cation composition.

These features suggest the production of zeolite sorbents and substrata for direct growth of plants and improvement of soil structure in view of a possible decrease of the imported chemical fertilizers.

## References

- Ming, D., Allen, E., Galindo, C. and Henninger, D. Methods for determining cation- exchange capacities and compositions of natural exchangeable cations of clinoptilolite. NASA Johnson Space Center, SN 14, Houston, Texas 77058
- Ming, D.W., Allen, E.R., Galindo, C. Jr., and Henninger, D.L. (1993) Methods for determining cation exchange capacities and compositions of native cations for clinoptilolite. Pp 31–35 in: *Memoirs of the 3rd International Conference on the Occurrence, Properties, and Utilization of Natural Zeolite, Vol. 2* (G.R. Fuentes and J.A. Gonzales, eds.).
- Petrov, G., Petkov, I., Etropolski, Ch., Dimitrov, D., Popov, N. and Uzonov, N. (1982) *Substrate for the Cultivation of Agricultural Crops and Rooting of Green Cutting in Greenhouses and in Open Air*. US Patent 4.337.078.
- Raynov, N., Popov, N., Yanev, Y., Petrova, P., Popova, T., et al. (1997) Geological, mineralogical and technological characteristics of zeolitized (clinoptilolitized) tuffs deposits in the Eastern Rhodopes, Bulgaria. Pp. 263–275 in: *Natural Zeolites, Sofia '95* (G. Kirov, L. Filizova, and O. Petrov, editors). Pensoft, Sofia - Moscow.

## Pedogenic origin of clinoptilolite and heulandite in magnesium-rich sedimentary deposits (Madrid Basin, Spain)

M. Pozo<sup>1</sup>, J. Casas<sup>2</sup>, J. A. Medina<sup>1</sup>, M. I. Carretero<sup>3</sup>, and J. A. Martín Rubí<sup>4</sup>

<sup>1</sup>Universidad Autónoma de Madrid; Madrid, Spain; Email: manuel.pozo@uam.es

<sup>2</sup>C.S.I.C.; Madrid, Spain

<sup>3</sup>Universidad de Sevilla; Seville, Spain

<sup>4</sup>Instituto Geológico y Minero de España; Madrid, Spain

### Introduction

The Intermediate Unit of Miocene age in the Madrid Basin (central Spain) is well known for its large deposits of different Mg-clay mixed layers including sepiolite, saponite, stevensite and kerolite-stevensite, all of them associated to the named Magnesian Unit (Pozo and Casas, 1999). The occurrence of zeolites, however, has been rarely reported. The scarce development of these minerals seems to be related with both the lack of fine pyroclastic deposits (e.g. tuffs) and the mostly Mg-rich hydrochemistry. In this work, zeolite-bearing sedimentary materials belonging to the Intermediate Unit of Miocene age from Madrid Basin were studied.

Sampling was done in two different points of the Madrid Basin: Esquivias area (ESQ) and Pinto area (PIN). Seventy samples from three lithological sections were collected and examined. Zeolites are mainly related to four lithofacies: 1-Green mudstones (GM). 2-Pinkish brown mudstones (PM). 3-Carbonated mudstones (dolocretes) (D). 4-Massive to laminated grey sands (GS). It is noteworthy that lithofacies 1 and 2 are common in both sampled zones but lithofacies 3 and 4 are only frequent in PIN and ESQ areas, respectively. Mudstone and carbonate lithofacies show abundant pedogenic features including pedality, root bioturbation, dessication, nodulization, and slickensides. The sedimentary sequence in ESQ is interpreted as a marginal lake facies (mud flat) but considered palustrine facies in PIN area.

### Experimental Methods

The mineralogy of the zeolite and clay samples were examined by means of X-ray diffraction (XRD) and SEM-EDX. Clay mineralogy was identified from the < 2 µm fraction. Air dried, glycolated, and heated (550°C) oriented slides were prepared from each sample. The small size and low content of zeolites in mudstones required different typologies of separation including sieving and hand picking. Chemical composition of single zeolite crystals was determined by electron microprobe analysis. The textural relationship between clays and zeolites has been recognized by a petrographical study in thin sections.

### Results and Discussion

The mineralogical study allowed the identification of different assemblages within the differentiated lithofacies: GM (saponite > illite-kaolinite-quartz-feldspar-dolomite-opal CT-barite-zeolites), PM (stevensite-kerolite-stevensite mixed layers > illite-calcite-quartz-zeolites), GS (feldspars (plagioclase>K feldspars)-phyllosilicates-quartz-zeolites) and D (dolomite-phyllosilicates-barite-zeolites). The highest content (up to 15 wt.%) in zeolites was observed in green mudstones whereas carbonates displayed the lowest one (< 5 wt.%). The pedogenic features observed in these lithofacies and its mineralogy (smectites, zeolites, dolomite, barite) is characteristic of alkaline paleosoils (Retallack, 1990).

The mineralogical analysis of zeolites by means of XRD point to a composition belonging to the clinoptilolite-heulandite group. In order to classify them, the thermal test proposed by Boles (1972) was followed. Both heulandite and clinoptilolite were identified. The SEM-EDX examination confirmed the XRD results showing laths, plates, and typical coffin-shaped crystals. Zeolites occurred as small (120–500 µm) euhedral crystals, often coating and/or infilling root molds, cracks, and, less commonly, intergranular porosities. Opal CT was also identified mostly in the samples of ESQ. Presence of opal CT lepispheres, coating zeolite crystal faces, indicates a high supply of silica in pore water.

Petrographical observations display evidence that zeolites are genetically later than Mg-clays and dolomite, but earlier than opal CT precipitation. Therefore, the growth of these zeolites cementing secondary porosities

suggests a change in the pH and chemistry of pore waters. Indeed, a pH higher than 8, low activity of  $Mg^{+2}$  (fixed in Mg-clays and dolomite), and an increase in Si and Al would be decisive in the formation of zeolites instead clay minerals (Hay, 1978).

The chemical analyses of single zeolite grains (electron microprobe) indicate the predominance of heulandite in PIN mudstones. On the other hand, clinoptilolite is the main zeolite in ESQ mudstones. These chemical analyses allow us to calculate the following average formulae for studied zeolites: Pinto zeolites:  $(Si_{28.57} Al_{7.54}) O_{72} (Mg_{1.28} Ca_{1.95} Na_{0.18} K_{0.42})$  and Esquivias zeolites:  $(Si_{29.26} Al_{6.88}) O_{72} (Mg_{1.13} Ca_{1.51} Na_{0.11} K_{0.91})$ .

On the basis of Si and Al ratio (Ming and Mumpton, 1989), the pH conditions for heulandite formation were more alkaline than those of clinoptilolite. This fact is well correlated with the predominance of carbonates and opal CT in lithofacies containing heulandite or clinoptilolite, respectively.

In the Madrid Basin, clinoptilolite-heulandite formed in marginal lake sediments (mud flat, palustrine fringe) by reaction of detrital silicates with  $Ca^{2+}$ - $Na^{+}$ - $K^{+}$ -rich pore waters, concentrated close to the land surface by evaporative pumping and evapotranspiration. Poorly ordered clay minerals and other non-clay silicates (e.g., feldspars) were probably the main reactants. In PIN mudstones, the common occurrence of carbonates (dolocretes) seems to favor the formation of heulandite. However, in ESQ mudstones the presence of non-cemented sandy inserts could be the way for silica-laden ground waters, which propitiate the clinoptilolite and opal CT authigenesis. Therefore the compositional variability of the studied zeolites is well correlated with pH but also with the mineralogy of hosted sedimentary deposits. As a conclusion, an authigenic origin of clinoptilolite-heulandite in alkaline paleosoils with pH ranging between 8–10 is inferred.

## References

- Boles, J.R. (1972) Composition, optical properties, cell dimensions and thermal stability of some heulandite group zeolites. *American Mineralogist*, **57**, 1463–1493.
- Hay, R.L. (1978) Geological occurrence of zeolites. Pp 135–143 in: *Natural Zeolites: Occurrence, Properties, Use*. (Sand and Mumpton, editors). Pergamon Press, Inc. Elmsford, N.Y.
- Ming, D.W. and Mumpton, F.A. (1989) Zeolites in soils. Pp. 873–911 in: *Minerals and Soil Environments*. (J.B. Dixon and S.B. Weed, editors). Soil Science Society of America.
- Pozo, M. and Casas, J. (1999) Origin of kerolite and associated Mg clays in palustrine-lacustrine environments. The Esquivias deposit (Neogene Madrid Basin, Spain). *Clay Minerals*, **34**, 395–418.
- Retallack, G.J. (1990) *Soils of the Past*. Unwin Hyman, Boston, 520 pp.

## Characterization of zeolite modified with cation active polyelectrolyte and its effect on biological wastewater treatment

P. Princz<sup>1</sup>, B. Koczka<sup>2</sup>, K. Marthi<sup>2</sup>, G. Pokol<sup>2</sup>, and S. E. Smith<sup>3</sup>

<sup>1</sup>Living Planet Environmental Research, Ltd.; Budaors, Hungary; Email: pprincz@living-planet.hu

<sup>2</sup>Technical University of Budapest; Budapest, Hungary

<sup>3</sup>University of Florida; Gainesville, Florida, USA

The bound organic carbon (BOC) content, chemical stability, and homogeneity of clinoptilolite-rich zeolitic tuff ( $C_z$ ) modified with cation active polyelectrolyte (CAP), as well as the effect of CAP-modified  $C_z$  (CAPMZ) on carbonaceous biochemical oxygen demand (CBOD), nitrogenous biochemical oxygen demand (NBOD), reaction rate, and order in laboratory batch experiments were determined. Full-scale biological degradability experiments using CAPMZ at a wastewater treatment plant (WWTP) were carried out. We found that the BOC content of CAPMZ was 2.3 mg<sub>BOC</sub>/g<sub>C<sub>z</sub></sub>. CAPMZ was stable to pH 9 and its homogeneity was 3.5%. CAPMZ increased the reaction rate and decreased the reaction order of the biochemical oxidation of organic constituents in wastewaters.

### Introduction

The most common wastewater (WW) treatment method is aerobic biological, in which the organic and inorganic pollutants are decomposed and converted to gases and cell tissue by bacteria in the presence of oxygen. The culture of bacteria forms a living, activated sludge. The capacity and the loadability of WWTPs depend on the activity and settling characteristics of the activated sludge. These sludge parameters, however, can be improved with the addition of  $C_z$  into the raw WW.

Since both the  $C_z$  and bacteria have negative surface charges, the adsorption of bacteria on the  $C_z$  surface is hindered. The  $C_z$ -bacterium bond is formed and attributed to the extracellular polymers (ECP) produced by the bacteria, since the ECP molecules can bridge the bacteria and the  $C_z$  surface.

If positively charged CAP molecules are bonded to the  $C_z$  particles, the CAP molecules are able to bind the bacterium flocs to themselves, i.e., to the  $C_z$  in a prompt reaction by their free, positively charged groups. The CAP molecules attached to the  $C_z$  particles change the sorption characteristics of zeolite crystals, because its external cation exchange capacity is converted to an anion exchange, i.e., CAPMZ can adsorb not only cations, but anions, as well.

This paper demonstrates the properties of a CAPMZ and its effects on biological degradability of WWs.

### Experimental Methods

Materials:  $C_z$  samples, with a particle size range of 50–110  $\mu\text{m}$ , were obtained from the Bodrogkeresztúr Zeolite Mine in Hungary. CAP of polyacrylamine type [poly-2-hydroxypropyl-N, N-dimethyl ammonium chloride,  $(\text{C}_5\text{H}_{12}\text{NOCl})_n$ ,  $n = 360$ , molecule weight: 50,000] was used for surface modification of  $C_z$ .

The dry modification method was applied for manufacturing CAPMZ. The bound CAP content of CAPMZ was determined in the form of BOC by total organic carbon (TOC) measurements. CAPMZ were washed through with TOC-free water to remove the mechanically adhered CAP molecules. Thereafter, the TOC of the unwashable, bound CAP content of CAPMZ was determined.

Examination of the stability of  $C_z$ -CAP bond was as follows: CAPMZ was suspended in TOC-free water. The suspension was intensively stirred and the TOC concentration in the aqueous phase was measured as a function of pH and time.

The thermogravimetric (TG) method combined with a mass selective (MS) detector was used to determine the homogeneity of CAPMZ. The MS detector measured the quantity of the methyl ( $\text{CH}_3^+$ ) ions liberated from a 3 mg CAPMZ sample at a high temperature.

The effect of CAPMZ on CBOD and NBOD was tested by the determination of the oxygen requirement of a communal WW sample with and without CAPMZ. During the CBOD measurements, nitrification was suppressed with a nitrification inhibitor. Measurements were accomplished according to Standard Methods.

Dissolved oxygen (DO) concentrations in the samples were measured with an oxygen membrane electrode. Fujimoto's method was used for calculating the ultimate CBOD (UCBOD) values.

Biological degradability tests were carried out to determine the effect of CAPMZ on the reaction rate and reaction order of biochemical oxidation. The mixture of a WW sample and activated sludge was aerated in a 50 L batch reactor. In parallel experiments CAPMZ was added to the WW-activated sludge mixture. The chemical oxygen demand (COD), biochemical oxygen demand (BOD<sub>5</sub>) and NH<sub>4</sub>-N concentration in the control and CAPMZ samples were determined as a function of time.

The WW treatment technology (WWTT) employing CAPMZ was installed at the WWTP located at Veresegyháza in Hungary. One of the cleaning lines of the WWTP was fed with CAPMZ, while the other one served as a control.

## **Results and Discussion**

The data of TOC measurements and stability tests showed the BOC content of CAPMZ was 2.3 mg/g and 92% of the CAP-C<sub>z</sub> bonds remained stable in an aqueous suspension of pH 9. Since the pH of communal WW is always less than 9, the CAP-C<sub>z</sub> connection can be considered stable in the process of biological WW treatment.

Homogeneity, characterized by the standard deviation (SD) of the TG-MS measurements of seven CAPMZ samples, was 3.5%.

The batch scale tests showed that CAPMZ accelerated the aerobic decomposition of organic matters, but did not increase the amount of the biodegradable constituents of WW.

CAPMZ suspended in WW decreased the reaction order and increased the reaction rate of the biological oxidation of organic matters by 20–30%.

The pilot scale experiments, in conjunction with the laboratory ones, showed that applying CAPMZ, resulted in significantly better effluent water quality and verified that CAPMZ additive was capable to increase the loadability of WWTP expressed in COD (5–40%), BOD (5–40%), NH<sub>4</sub>-N removal (20–80%), phosphorous removal (15–20%) and suspended solids removal (30–40%).

The NATO Science for Peace Program with the National Office for Research and Technology in Hungary supported this research.

## Combustion treatment of $\text{Co}^{2+}$ and $\text{Cs}^+$ exchanged Mexican clinoptilolite

R. Rodríguez-Trejo<sup>1,2</sup>, P. Bosch<sup>2</sup>, and S. Bulbulian<sup>1</sup>

<sup>1</sup>*Instituto Nacional de Investigaciones Nucleares; Col. Escandón, México D. F.; Email: rosas@correo.unam.mx*

<sup>2</sup> *Universidad Nacional Autónoma de México; Ciudad Universitaria, México D. F.*

Although clinoptilolite has often been proposed to retain  $\text{Co}^{2+}$  and  $\text{Cs}^+$ , the resulting exchanged zeolite is not a safe material as it may be leached. Several methods to trap those radionuclides have been proposed. The most frequently used is the thermal treatment of the resulting aluminosilicate. However, this method is expensive as it requires a very long treatment time. In this work, we studied the effectiveness of a new method that consists of the combustion of the sample with urea. The advantage of this method is that urea combustion is highly exothermic and produces instantaneous collapse of the zeolite network.

The  $\text{Co}^{2+}$  and  $\text{Cs}^+$  exchanged zeolites were thermally and combustion treated until vitrification. Desorption of  $\text{Co}^{2+}$  and  $\text{Cs}^+$  from those treated solids was tested by leaching with 1 N NaCl solution. The  $\text{Co}^{2+}$  and  $\text{Cs}^+$  content were determined by neutron activation and the solids were characterized by X-ray diffraction, IR-spectroscopy, and scanning electron microscopy (SEM). As the calcining temperature increased, the crystallinity of  $\text{Co}^{2+}$  and  $\text{Cs}^+$  exchanged zeolites decreased. The retention of  $\text{Co}^{2+}$  and  $\text{Cs}^+$  in thermally treated, exchanged zeolites is slightly higher than in combustion-treated zeolites ignited at 1,000 °C. The difference is attributed to the different compounds (amorphous and crystalline) formed during the treatments.

### Introduction

Nuclear wastewaters from nuclear plants or industries may contain radioactive atoms in solution. As the disposal of such polluted liquids is hazardous, the radioactive ions have to be retained in non-leaching solids to be deposited in nuclear burial sites.

Zeolites have a high-exchange capacity and are more resistant to radioactivity and temperature than other exchanged materials; but, if in contact with water, exchanged zeolites may leach. To address this problem, the most commonly proposed solution is thermal treatment. The exchanged minerals have to be treated thermally up to vitrification or to formation of other crystalline compounds. In this way, the radioactive materials are encapsulated. However, with time and radioactivity, defects and cracks may appear in the initially safe compounds. Thus, new treatments have to be attempted in order to avoid leaching and reduce costs.

In this study, we chose two radioactive cations,  $\text{Co}^{2+}$  and  $\text{Cs}^+$ , as they are both representative of nuclear wastes. The chosen cationic exchanger is clinoptilolite with Si/Al ratio 5.0, and with an exchangeable-cation “window” size between 0.28 nm and 0.75 nm. The collapse temperature of clinoptilolite in air is 750 °C. Hence, the effect of window size and Si/Al ratio on properties of combustion or thermally treated materials must be considered.

The purpose of our work is thus to compare the immobilization of  $\text{Co}^{2+}$  and  $\text{Cs}^+$  in exchanged clinoptilolite by treating the samples thermally or by a combustion process with urea ( $\text{CH}_4\text{N}_2\text{O}$ ) ignited at different temperatures. The last method is known to provide ceramics or vitreous compounds because urea combustion is highly exothermic. This technique is inexpensive and has not been tested in nuclear waste disposal.

### Experimental Methods

The zeolite was left for 8 days in a 5 N NaCl solution. The resulting material was labeled NaC. The sample NaC was shaken for 1 day with  $\text{Co}(\text{NO}_3)_2$  or  $\text{CsNO}_3$  0.06 N solutions in order to obtain the respective  $\text{Co}^{2+}$  and  $\text{Cs}^+$  exchanged zeolites. The solids were then separated from the residual content of  $\text{Co}^{2+}$  and  $\text{Cs}^+$  in the remaining solution. In each experiment, the content of cobalt or cesium was determined by neutron activation analysis.

The samples exchanged with the  $\text{Co}(\text{NO}_3)_2$  solution are labeled as  $\text{Co}_2\text{NaC}$ , and those exchanged with  $\text{CsNO}_3$  are labeled as  $\text{CsNaC}$ . Some of the  $\text{Co}^{2+}$  and  $\text{Cs}^+$  exchanged zeolites were calcined in air from 600 to 1,000 °C (thermal treatment = TT) for 3 hours. In the other experiment, exchanged zeolite was mixed with urea

and distilled water. Then, the mixture was transferred into an oven preheated up to 500, 750, or 1,000 °C, for 5 minutes (combustion treatment = TC).

All zeolite powders were studied by X-ray diffraction to identify the crystalline compounds.

Non-treated and combustion-treated samples at 1,000°C were analyzed by infrared spectroscopy.

A scanning electron microscope (SEM) was used to determine the sample morphologies from 750 to 1,000 °C.

## **Results and Discussion**

In clinoptilolite-based preparations (NaC, Co,NaC, and Cs,NaC) albite was present and, if Co or Cs were exchanged, a small fraction of the sample turned out to be amorphous. The cell parameters for clinoptilolite samples NaC, Co,NaC, and Cs,NaC were estimated.

Cobalt and cesium act as modifiers in the zeolite structure and, therefore, the compounds obtained by heating an exchanged zeolite with  $\text{Co}^{2+}$  or  $\text{Cs}^+$  are different than those obtained with the monocationic sodium zeolite. The compounds and leaching results of NaC were compared to the corresponding exchanged materials that were thermally or combustion treated..

In the Co,NaC samples TT at 800 and 1,000 °C, the amount of  $\text{Co}^{2+}$  leached out is  $4.9 \pm 2.5$  % and  $3.7 \pm 1.3$  %, respectively. When the same Co,NaC samples were treated as TC at 750 and 1,000 °C, the amount of cobalt leached from the sample was  $11.7 \pm 3.1$  % and  $3.1 \pm 1.5$  %, respectively. The percentages of  $\text{Co}^{2+}$  lost in both treatments were similar for similar temperatures within the experimental error range.

The amount of  $\text{Cs}^+$  leached from the Cs,NaC sample TT at 800 and 1,000 °C was  $54.8 \pm 2.4$  % and  $1.5 \pm 0.3$  %, respectively. When the same Cs,NaC sample was treated as TC at 750 and 1,000°C, the amount of cesium leached from the sample was  $20.1 \pm 1.2$  % and  $10.3 \pm 0.8$  %, respectively. In the Cs,NaC sample TT at 800 °C, which was composed of 56 % Cs,NaC and 44 % albite, a large number of coffin-like crystals were observed; they are characteristic of clinoptilolite. They are located on top of larger particles, probably albite. Although the combustion-treated clinoptilolite at 750 °C contains 80 % clinoptilolite and 20 % albite, no clinoptilolite crystals were visible. Only a thick-layered material was found; then again, the zeolite crystallites must be occluded into such material. If the temperature was increased to 1,000°C, both materials turned out to be a heterogeneous mixture where no zeolite crystals were observed. The combustion-treated sample was more dispersed than the thermally treated sample.

To be sure that no remnants of urea were present in the 1,000 °C combustion-treated samples, the infrared spectra of the non-treated and 1,000°C combustion-treated materials were compared. No urea was found in the heated samples. Such was the case in all combustion-treated samples ignited at 1,000°C. This result is in agreement with the X-ray diffraction results previously presented.

## Removal of the human pathogen *Giardia intestinales* from groundwater

C. Rust<sup>1</sup>, D. Schulze-Makuch<sup>1</sup>, and R. Bowman<sup>2</sup>

<sup>1</sup>Washington State University; Pullman, Washington, USA; Email: colleen\_rust@wsu.edu

<sup>2</sup>New Mexico Tech; Socorro, New Mexico, USA

### Introduction

Microbial contamination of groundwater is a serious concern worldwide. For many countries, groundwater provides approximately 40% of the potable water used for human consumption. Cyst-forming protozoans such as *Giardia intestinales* can survive for extended periods of time in groundwater systems with temperatures of less than 10°C, can migrate significant distances, and are relatively resistant to standard municipal water system chlorination practices. Though dormant outside the host, as few as ten cysts can result in a human infection (Casemore et al., 1997).

Pathogenic bacteria, viruses, and protozoans tend to be negatively charged in the pH range of most groundwaters. Thus, naturally occurring and modified materials such as surfactant-modified zeolites (SMZ), which have net positive surface charges and hydrophobic properties, are suitable as barriers to impede pathogen migration in aquifer systems (Fig. 1). In our experiments SMZ has been used to remove *E. coli* and the bacteriophage MS-2 from sewage water with a high success rate (*E. coli* 100%, MS-2 > 90%) (Schulze-Makuch et al., 2003). Testing was conducted both in the laboratory and the field to test the removal efficiency of SMZ for *Giardia intestinales* and its analogs.

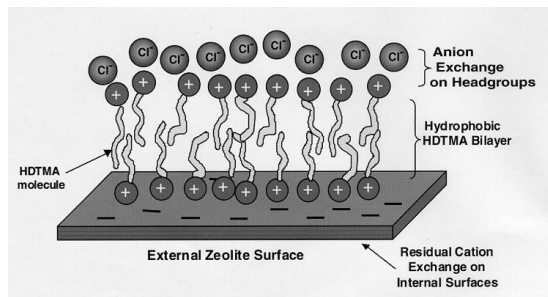


**Figure 1.** Schematic of the surface of the SMZ from Schulze-Makuch et al. (2002)

### Experimental Methods

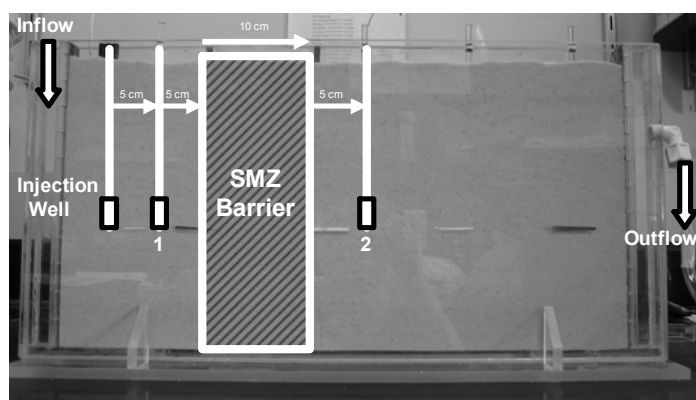
Three different SMZ formulations were prepared using zeolite from the St. Cloud mine in Winston, New Mexico (Bowman et al., 2001) (Table 1). Five different experimental runs were conducted under varied conditions (including use of raw zeolite and sand only) with a 10-cm-wide barrier of SMZ to test the removal efficiency of SMZ for *Giardia intestinales* using the *Giardia* cysts and microsphere analogs. The model aquifer was filled with coarse silica sand to mimic realistic natural field conditions (Fig. 2). CaCl<sub>2</sub> water, typical of western United States water chemistries, was used as a baseline, and then

bromide, microspheres (analog for *Giardia*), and *Giardia intestinales* cysts were used. The arrival of the tracer down gradient of the SMZ barrier was compared to the arrival in the absence of the barrier to evaluate the effectiveness of each SMZ formulation.

The coarse-grained Cationic SMZ (1.4–2.4 mm) formulation was further tested at our field site using water amended with microspheres to simulate *Giardia* cyst behavior. The field site is an existing multiple well site at the University of Idaho in Moscow. The wells are completed in the Lolo Basalt Formation—a highly heterogeneous and anisotropic fractured basalt aquifer system typical of the subsurface of most of eastern Washington and northeastern Oregon.

The SMZ pathogen field filter was installed directly in the well bore, and the concentrations of microsphere-amended ground-water were measured before and after filtration. Pumping over an extended period was continued in order to test the lifetime of our prototype filter system. Our tests and results were targeted at developing a prototype filter system for removing a multitude of human pathogens in drinking water.



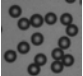



**Figure 2.** Model aquifer set-up with a 0.07 gradient

## Results and Discussion

All formulations of SMZ were effective at removing *Giardia intestinales* cysts from the groundwater, but removal rates were not as high as for bacteria and viruses in the earlier experiments (Schulze-Makuch et al., 2003). The removal efficiency varied with the particular formulation of the SMZ used (Table 1). The SMZ filtration material with the highest removal rate, shown by our model aquifer runs, is the Hydrophobic SMZ. The field test of coarse Cationic SMZ was not as effective as shown in earlier laboratory tests.

**Table 1.** Removal rates of SMZ formulations during the laboratory experiments

 	Hydro-phobic	Fine Cationic	Coarse Cationic	Raw Zeolite	Sand Only (no barrier)	Lehner, 2004 Hydrophobic
<b>8 <math>\mu</math>m microspheres</b> (fluorescent polystyrene)	<b>99.8 %</b>	98.2 %	86.9 %	96.9 %	N/A	5 $\mu$ m microspheres 99.2 %
<b>8 <math>\mu</math>m <i>Giardia</i> cysts</b> (non-viable)	<b>100.0 %</b>	67.1 %	76.2 %	37.5 %	66.7 %	10 $\mu$ m microspheres 67.2 %

## References

- Bowman, R.S., Li, Z., Roy, S.J., Burt, T., Johnson, T.L. and Johnson, R.L. (2001) Pilot test of a surfactant-modified zeolite permeable barrier for groundwater remediation. Pp. 161-185 in: *Physical and chemical remediation of contaminated aquifers* (J.A. Smith and S. Burns, editors). Kluwer Academic/Plenum Publishers, New York.
- Casemore, D.P., Wright, S.E. and Coop, R.L. (1997) Pp. 65–92 in: *Cryptosporidium and Cryptosporidiosis* (R. Fayer, editor). CRC Press, Boca Raton, Florida.
- Lehner, T., Schulze-Makuch, D., Langford, R. and Bowman, R.S. (2004) Removal of Pathogenic Parasites using Surfactant-Modified Zeolite Barriers in a Model Aquifer. Master's thesis, University of Texas at El Paso, 1-81 pp.
- Schulze-Makuch, D., Bowman, R.S., Pillai, S.D. and Guan, H. (2003) Field Evaluation of the Effectiveness of Surfactant Modified Zeolite and Iron-Oxide-Coated Sand for Removing Viruses and Bacteria from Ground Water *Ground Water Monitoring and Remediation*, **23**, 68.

## Dehydration behavior in natural zeolite of the heulandite group: An in situ NIR study

K. Sadhana<sup>2</sup>, K. Shiva Prasad<sup>1</sup>, P. S. R. Prasad<sup>1</sup>, and S. Ramana Murthy<sup>2</sup>

<sup>1</sup>National Geophysical Research Institute; Hyderabad, India; Email: psrprasad@ngri.res.in

<sup>2</sup>Osmania University; Hyderabad, India Email: psrprasad@ngri.res.in

### Introduction

Thermal-induced variations in the molecular arrangements in zeolites are important in understanding their stability and also in distinguishing the isostructural members of a family. The reversible dehydration behavior of zeolites is particularly important in ion exchange processes. The repetitive dehydration may cause defects in the zeolites, particularly during irreversible dehydration, and may modify the physico-chemical properties of zeolites (Bish and Carey, 2001; Gottardi and Galli, 1985; Moroz et al., 2003). The dehydration in zeolites often triggers the proton exchange between network cations leading to formation of structural hydroxyls (Prasad et al., 2005).

Vibrations of water and hydroxyls are very prominent in infrared spectroscopy, making this technique a promising tool to investigate the dehydration-induced variations in the molecular linkages. Mid-IR spectra cover all the modes belonging to T-O-T framework modes as well as bending ( $\approx 1600\text{ cm}^{-1}$ ) and stretching modes ( $\approx 3400\text{ cm}^{-1}$ ) of zeolitic water. On the other hand, combinations of stretching and bending vibrations ( $\delta\text{HOH}$  and  $\delta\text{T-OH}$ ) are well separated in the near IR region allowing us to draw valuable information on the molecular linkages of hydroxyls during the dehydration (Prasad et al., 2005).

Heulandite  $[(\text{Na}, \text{K})\text{Ca}_4(\text{Al}_9\text{Si}_{27}\text{O}_{72})\cdot 24\text{H}_2\text{O}]$  and clinoptilolite  $[(\text{Na}, \text{K})_6(\text{Al}_6\text{Si}_{30}\text{O}_{72})\cdot 20\text{H}_2\text{O}]$  are the two zeolites belonging to the framework topology HEU. These zeolites belong to the same crystal class, monoclinic with  $C_2/m$  symmetry. The zeolites belonging to HEU group are classified in three categories based on their thermal behavior: (1) The dehydration of a zeolite heated to a temperature around 473 K is completely reversible and known as phase A. If heated to 540 K, phase A transforms to phase B, which does not rehydrate immediately to phase A but inverts to an intermediate phase I; prolonged heating at 725 K destroys the lattice, (2) Reversible dehydration when heated to a temperature higher than 473 K upon cooling from 673 K, the zeolite (at ambient temperature) shows a mixture of phases of A, B, and I. The lattice resists destruction up to 825 K and over, and (3) The sample undergoes continuous reversible dehydration and the lattice is not destroyed up to 1025 K (Gottardi and Galli, 1985).

The aim of the present work is to investigate the thermal behavior of a zeolite belonging to the HEU group. The formation of hydroxyl during dehydration and rehydration by the breakage of T-O-T linkages are studied using in situ NIR spectroscopy in the temperature range 300–825 K.

### Results and Discussion

The samples are characterized using differential scanning calorimetry, x-ray diffraction, and mid-IR spectroscopy. The x-ray diffraction and differential scanning calorimetry data match well with reported data of Gottardi and Galli (1985). The pattern observed in DSC is similar to that of clinoptilolite. The mid-IR spectrum matches well with the reported data of Mozgawa (2001). However, no distinction is possible between heulandite and clinoptilolite on mid-IR spectra alone. Three peaks in the water stretching regions 3622, 3403, and 3238  $\text{cm}^{-1}$  and a single peak at 1642  $\text{cm}^{-1}$  are observed. The prominent peaks at 1173, 1079, 1042, 798, 779, 695, 516, and 467  $\text{cm}^{-1}$  are observed in the framework structural mode region (400–1250  $\text{cm}^{-1}$ ). The NIR spectra in the wavenumber region 4000–8000  $\text{cm}^{-1}$  have overtones at 7046 and 6794  $\text{cm}^{-1}$  and a combination band at 5223  $\text{cm}^{-1}$ . However, a mode at 4527  $\text{cm}^{-1}$  is observed and may be assigned to SiOH. The total peak area of water modes is proportional to the total water content in the mineral (Prasad et al., 2005). The thermal variations in the total peak area of second order water modes (overtones- $\Delta$ ; combinations -o) monitored in the temperature range 300–825 K are shown in Figure 1. Filled symbols are during the heating cycle, while the open symbols are in the cooling cycle. As shown in Figure 1, the water content in the zeolite decreases continuously with increase in temperature and vanishes at 675 K, indicating complete dehydration. All the water molecules are regained (about 95%) while cooling in a shorter time period (12 hrs). The variations of the

combination mode involving Si-OH are worth noticing. The total peak area increased to a temperature of 675 K and monotonically decreased to 800 K. Upon cooling, this mode shows an increase in total peak area (almost the same as at 675 K) indicating an increase in hydroxyl content. These results are in agreement with Moroz et al. (2003) who reported accumulation of acid defective centers on re- and dehydration cycles. We shall address the effect of these defect centers on conductivity in our future work.

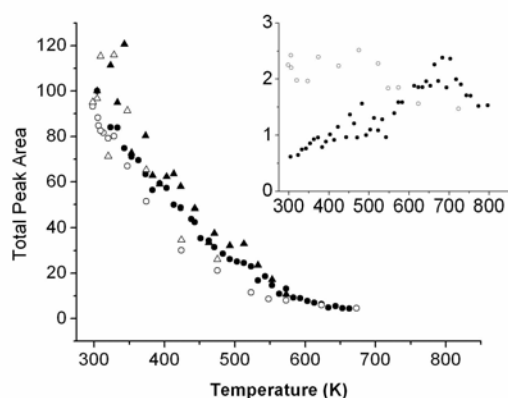


Figure 1

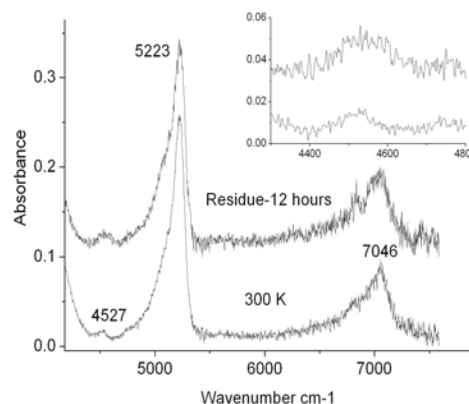


Figure 2

**Figure 1.** Thermal variations of second order modes (overtones  $\Delta$  & combinations-O) during heating (solid symbols) and cooling (open symbols). Inset shows the variations of  $4527\text{ cm}^{-1}$  mode.

**Figure 2.** Observed spectral profile of zeolite sample in its virgin and residual (cooled from 825 K and collected after 12 hrs) forms in the wavenumber region  $4000\text{--}8000\text{ cm}^{-1}$ .

## References

- Bish, D.L. and Carey, J.W. (2001) Thermal behavior of natural zeolites (D.L.Bish and D.W.Ming editors). *Reviews in Mineralogy & Geochemistry*, **45**.
- Gottardi, G. and Galli, E. (1985) *Natural Zeolites*. Springer-Verlag, Berlin.
- Mozgawa, W. (2001), The relation between structure and vibrational spectra of natural zeolites, *J. Molecular, Molecular Structure*, **596**, 129–137.
- Prasad P.S.R, Prasad, K.S. and Murthy S.R. (2005) Dehydration behavior of natural stilbite: An *in-situ* FTIR study. *American Mineralogist*, **90**, 1636.
- Moroz, N.K, Afanassyev, I.S, Paukshtis, E.A. (2003) Accumulation of acid sites on natural clinoptilolite under recurring dehydration. *Phys. Chem. Minerals*, **30**, 243–247.

## Zeolite facies metamorphism in the Hvalfjörður area, Iceland

R. S. Selbekk and T. Weisenberger

Albert-Ludwigs University, Freiburg, Germany; Email: [rune.selbekk@minpet.uni-freiburg.de](mailto:rune.selbekk@minpet.uni-freiburg.de)

The Hvalfjörður area, 30 km north of Iceland's capital Reykjavik, belongs to the sequence of late Tertiary to early Quaternary flood basalts with a minor interlayer of hyaloclastites and rhyolites (Rutten, 1958). The basalts are affected by a low temperature metamorphism caused by the burial of the lava succession and higher heat flow influenced by the Laxárvogur and the Hvalfjörður volcanic centers. Low-grade zeolite facies metamorphism of basaltic lavas in the Hvalfjörður field area results in two distinct mineral parageneses that can be correlated to events in the burial and hydrothermal history of the lava pile. Stage 1a marks a near-surface alteration in which celadonite and silica were precipitated along primary pores. During burial, hydrolysis of olivine and glass led to the formation of mixed layers of chlorite/smectite clays. The chlorite content of stage 1b precipitation increases with increasing burial depth, corresponding to increasing temperature. Stage 2 occurred after burial and is marked by zeolite mineralization, caused by higher heat flow, from the Laxárvogur volcanic center (Weisenberger, 2005).

Altogether twelve different zeolites were found in the Hvalfjörður area: analcime, chabazite, epistilbite, garronite, heulandite, laumontite, levyne, mesolite, stilbite, stellerite, thomsonite, and yugawaralite. Based on the work done by Walker (1960), zeolites were grouped into zeolite zones. In total, three separate depth and temperature-controlled zeolite zones are described in the Hvalfjörður area: the upper chabazite/thomsonite zone, the middle mesolite zone, and the lowest laumontite zone. The mineralization temperature for zeolites increases from the upper chabazite/thomsonite zone to the lower laumontite zone. From empirical correlations between the depth distribution of zeolite zones and the temperatures of formation of zeolites in the geothermal system, a geothermal gradient of 133°C/km can be estimated, which is usual for central volcanoes. This indicates the occurrence of a Laxárvogur volcanic center, which can be supported by the geochemistry of volcanic rocks and tectonic features in the Hvalfjörður area.

### References

- Rutten, M.G. (1958) Geological reconnaissance of the Esja-Hvalfell-Armannsfell area, southwestern Iceland. *Verhandelingen van het Koninklijk Nederlands Geologisch-Mijnbouwkundig Genootschap, Geologische Seris XVII*, 219–298.
- Walker G.P.L. (1960) Zeolite zones and dike distribution in relation to the structure of the basalts of eastern Iceland. *Journal of Geology*, **68**, 515–528.
- Weisenberger, T. (2005) Zeolite facies mineralisation in the Hvalfjörður area, Iceland. Diploma thesis, University Freiburg, Germany, 142 pp.

## Natural zeolites and bentonite characteristics affecting $K^+$ and $NH_4^+$ sorption and desorption behaviour

A. S. Sheta<sup>1</sup>; A. M. Falatah<sup>2</sup>, and M. Al-Sewailem<sup>2</sup>

<sup>1</sup>Ain Shams Univ.; Cairo, Egypt; Email: Sheta11us@yahoo.com

<sup>2</sup>King Saud Univ.; Riyadh, Saudi Arabia

### Abstract

The zeolite group is one of the tectosilicates that are characterized by three dimensional framework structures with cation exchange capacity (CEC) greater than phyllosilicates such as bentonite mineral. The behaviour of  $K^+$  and  $NH_4^+$  with these minerals is important for increasing fertilizer efficiency of  $K^+$  and  $N^+$ . The main objective of this research was to study the sorption characteristics of  $K^+$  and  $NH_4^+$  by bentonite and five zeolite minerals (i.e. analcime, chabazite, phillipsite, clinoptilolite 1 and 2). Results indicated that  $K^+$  sorption follow the Langmuir equation at two stages. The 1<sup>st</sup> stage is at a low concentration of up to 600 ppm  $K^+$  while the 2<sup>nd</sup> stage is in 800–1600 ppm range. Binding energies ( $k_d$ ) at the 1<sup>st</sup> stage range from (2.7–14.66)10–2 Lmg<sup>-1</sup> and maximum adsorption (b) in the range of 2.23–30.3 mg g<sup>-1</sup>. At the 2<sup>nd</sup> stage, the  $k_d$  values range from (1.3–7.41)10–3 and the b values range from 18.52–59.17 mg g<sup>-1</sup>. The highest b value was obtained with phillipsite followed by chabazite, bentonite, and clinoptilolite 1 and 2. Data of sorbed  $K^+$  indicated that the amount of  $K^+$  extracted decreased with the increase of extractions. Phillipsite shows the highest amount of extracted  $K^+$  while the lowest amount was found with clinoptilolite. Ammonium sorption data fit with the Freundlich equation whereas bentonite, chabazite, and phillipsite minerals show a greater ability to adsorb  $NH_4^+$ . Desorption data indicated that most of the sorbed ammonium was extracted in the 1<sup>st</sup> extraction by KCl. Analcime mineral was capable of retaining  $NH_4^+$  in the nonexchangeable form followed by phillipsite and clinoptilolite 1 and 2. We concluded that the ability of zeolites to retain  $K^+$  and  $NH_4^+$  was high and there was differences between the studied minerals in sorption and desorption characteristics. On the other hand, bentonite, the most common clay mineral in arid and semiarid regions, shows an intermediate ability between the studied zeolite minerals for  $K^+$  and  $NH_4^+$  sorption.

## Dehydration and rehydration mechanism in natural natrolite: An FTIR study

K. Shiva Prasad and P. S. R. Prasad

*National Geophysical Research Institute; Hyderabad, India; Email: psrprasad@ngri.res.in*

### Introduction

The water in zeolites dehydrates continuously and reversibly, depending on the structural modifications caused during dehydration (Bish and Carey, 2001). The dehydration of the zeolites triggers the migration of extra framework cations in order to compensate for charge during the loss of water molecules. In general, the extra framework cations coordinate to framework oxygens by altering the T-O-T angles. The variations in the framework are at times so severe that they break the T-O-T linkages (Bish and Carey, 2001; Gottardi and Galli, 1985).

Water molecules are very prominent in infrared spectroscopy, making this technique a promising tool to investigate the dehydration and molecular linkages (Prasad et al., 2005).

Natrolite [ $\text{Na}_{16}(\text{Al}_{16}\text{Si}_{24}\text{O}_{80})\cdot 16\text{H}_2\text{O}$ ] is a fibrous zeolite belonging to the NAT topology. The loss of water molecules in natrolite occurs at around 625 K. Reeuwijk (1972) studied the transformations in natrolite using x-ray diffraction and thermal analysis and reported a single sharp water loss at 625 K and the transformations of natrolite  $\alpha$ - and  $\beta$ -meta natrolite at around 550 K and 775 K, respectively. Natrolite rehydrates until the structure becomes amorphous at 785°C (Reeuwijk, 1972; Bish and Carey, 2001). The aim of the present study is to understand the dehydration and rehydration behavior in natrolite demarcating the modifications in network molecular linkages. However, to the best of our knowledge no studies have been reported on dehydration and rehydration behavior using IR spectroscopy.

### Results and Discussion

The sample is characterized by using x-ray diffraction, thermal analysis, and IR spectroscopy. The x-ray diffraction patterns and the mid-IR spectrum match well with the reported data (Gottardi and Galli, 1985; Mozgawa, 2001). The differential scanning calorimetry (DSC) has shown two endothermic peaks at around 675 K and 820 K. The peak at 675 K corresponds to the water loss and the peak at around 820 K corresponds to the transformation of  $\alpha$ -meta natrolite to  $\beta$ -meta natrolite. The differential thermogravimetry (DTG) has shown a single water loss at around 600 K. The absence of the water loss at around 820 K in DTG confirms the transformation of  $\alpha$ -meta natrolite to  $\beta$ -meta natrolite could be a structural change. The IR spectrum of natrolite has three major peaks around 3540, 3326, and 3186  $\text{cm}^{-1}$  in the water stretching region and a single peak at around 1634  $\text{cm}^{-1}$  in the water bending region. These modes were monitored to understand the dehydration and rehydration behavior. The thermal variations in the total peak of these modes (measure of total water content in the mineral) are monitored. The parameter, total peak area, has decreased continuously with temperature and disappeared at around 650 K. Upon cooling of  $\alpha$ -meta natrolite, it regained 85% of the water molecules in four days with marginal variations in the network modes. Spectral variations are similar for  $\beta$ -meta natrolite, but the recovered water molecules are around 78%. The rate of recovery of water molecules is comparatively slower in  $\beta$ -meta natrolite. Further, the modes in the wavenumber region 400–1250  $\text{cm}^{-1}$  were monitored to understand the dehydration, rehydration behavior, and structural changes induced during dehydration. The IR spectrum of natrolite in the wavenumber region 400–1250  $\text{cm}^{-1}$  has major peaks at 1093, 1063, 1041, 981, 966, 720, 679, 625, 578, 543, 512, 486, and 442  $\text{cm}^{-1}$  at 300 K, as seen in Figure 1. The bands in the wavenumber region 950–1250  $\text{cm}^{-1}$  correspond to the internal vibrations of  $\text{TO}_4$  tetrahedra. And the bands in the wavenumber region 400–800  $\text{cm}^{-1}$  correspond to the pseudo-lattice modes (Mozgawa 2001). The mode at around 720  $\text{cm}^{-1}$  corresponds to the four membered rings. The thermal evolution of these peaks in the sample, heated to temperatures of 650 K and 773 K are shown in Figures 1A and 1B, respectively.

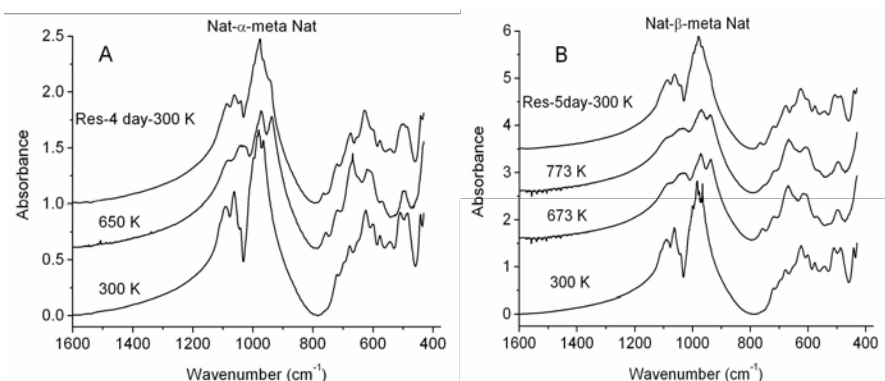


**Figure 1:** Thermal evolution of the mid-IR spectra of natrolite heated to 773 K (Fig. 1A) and 650 K (Fig. 1B) in the wavenumber region 400–1600  $\text{cm}^{-1}$ .

During the dehydration of natrolite the bands at 966 and 720  $\text{cm}^{-1}$  decreased continuously. Bish and Carey, (2001) observed an abrupt decrease in the unit cell parameters of natrolite when it transforms to  $\alpha$ -meta natrolite at 625 K by the rotations of the tetrahedral accompanied by the movement of Na atoms. The transformation of natrolite to  $\alpha$ -meta natrolite is observed by the growth of bands around 937, 758, and 721  $\text{cm}^{-1}$  at 550 K, as seen in Figure 1A. The transformation to  $\beta$ -meta natrolite is observed by the broadening of the bands at 937, 758, and 721  $\text{cm}^{-1}$  at 773 K, as seen in Figure 1B. The rehydration of the sample heated to 650 K ( $\alpha$ -meta natrolite) and 773 K ( $\beta$ -meta natrolite) recovered all the modes within a period of four and five days, respectively. The residue spectra of the samples heated to 650 K and 773 K retained the band at around 758  $\text{cm}^{-1}$  indicating partial recovery of the structural changes induced during dehydration. The natrolite transformed to  $\alpha$ -meta natrolite rehydrates faster than that transformed to  $\beta$ -meta natrolite.

## References

- Bish, D.L. and Carey, J.W. (2001) Thermal behavior of natural zeolites (D.L. Bish and D.W. Ming, editors). *Reviews in Mineralogy & Geochemistry*, **45**, 403pp.
- Gottardi, G. and Galli, E. (1985) *Minerals and Rocks, Natural zeolites*. Springer-Verlog, Berlin Heidelberg.
- Mozgawa, W. (2001) The relation between structure and vibrational spectra of natural zeolites. *J. Molecular Structure*, **596**, 129-137.
- Prasad, P.S.R., Prasad, K.S. and Murthy, S.R. (2005) Dehydration of natural stilbite: An in situ FTIR study. *American Mineralogy*, **90**, 1636-1640.
- Reeuwijk, L.P. (1972) High temperature phases of zeolites of the natrolite group. *American Mineralogy*, **57**, 499-510.

## Computational studies of the nucleation and growth of zeolites

B. Slater<sup>1</sup>, D. Salih<sup>1</sup>, M. Mora-Fonz<sup>2</sup>, C. R. A. Catlow<sup>1,2</sup>, and D. W. Lewis<sup>2</sup>

<sup>1</sup>Royal Institution of Great Britain; London, United Kingdom; Email: ben@ri.ac.uk

<sup>2</sup>University College London; London, United Kingdom

We will describe our efforts in modeling the fundamental processes that lead to the formation of zeolites. We will consider the chemistry of silica solutions, including the effect of pH and temperature, and describe in detail the reactions that lead to the formation of small silicate and aluminosilicate oligomers in solution. We will also consider the growth of zeolite surfaces through the addition of solution species and the structure-directing role of inorganic cations on this growth process.

### Introduction

In order to understand the fundamental molecular processes that lead first to the formation of nucleation centers then to the formation of zeolite crystals, we must be able to observe the structure and reactivity of an array of silicate and aluminosilicate species, together with typically metal cations, in highly basic aqueous media under conditions of elevated temperature, and often, pressure. Although many experimental methods are available to probe such chemistry, each brings difficulties of both performing the experiments and of analyzing the resulting data.

Computational methods, in principle, allow us to study at a variety of length-scales the interactions of the species involved. We will describe here the development of methods that allow the accurate and self-consistent description of the reactions of silicate and aluminate species. Then we shall probe, through the selection of a model system, how the presence of different metal cations directs the growth of crystal surfaces.

### Results and Discussion

We show how a combination of relatively low-cost density functional theory methods and a dielectric continuum description of the aqueous medium (Mora Fonz, 2005) can describe the deprotonation of small silicate species, correlating very well with available experimental data. However, we will emphasize that care must be taken to explicitly account for specific solvation.

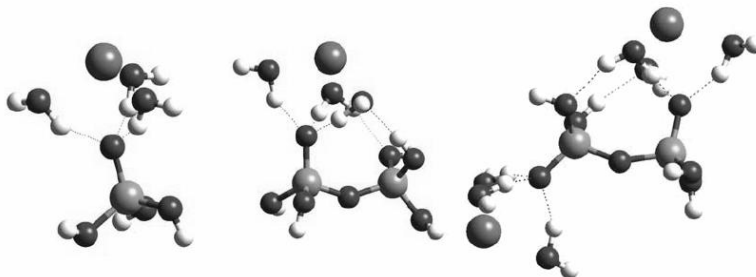


**Figure 1.** Examples of silicate fragments considered. From the left,  $\text{Si(OH)}_3\text{O}^-$ ,  $(\text{OH})_3\text{Si-O-Si(OH)}_2\text{O}^-$  and  $^-\text{O(OH)}_2\text{Si-O-Si(OH)}_2\text{O}^-$  together with  $\text{Na}^+$  counterions and appropriate solvent molecules.

Reaction	Free energy (kJ mol <sup>-1</sup> )		Reference
	Calc	Expt	
$\text{H}_3\text{O}^+(\text{H}_2\text{O})_3 + \text{OH}^-(\text{H}_2\text{O})_4 \rightarrow (\text{H}_2\text{O})_4 + (\text{H}_2\text{O})_5$	-97	-101	Paterson (1986)
$\text{Si(OH)}_4 + \text{NaOH}(\text{H}_2\text{O})_3 \rightarrow \text{SiO(OH)}_3\text{Na}(\text{H}_2\text{O})_3 + \text{H}_2\text{O}$	-29	-33	Iler (1979)
$\text{SiO(OH)}_3\text{Na}(\text{H}_2\text{O})_3 + \text{NaOH}(\text{H}_2\text{O})_3 \rightarrow \text{SiO}_2(\text{OH})_2\text{Na}_2(\text{H}_2\text{O})_6 + \text{H}_2\text{O}$	-17	-18	Sefcik and
$\text{Si}_2\text{O(OH)}_6 + \text{NaOH}(\text{H}_2\text{O})_3 \rightarrow \text{Si}_2\text{O}_2(\text{OH})_5\text{Na}(\text{H}_2\text{O})_3 + \text{H}_2\text{O}$	-35	-38	McCormick (1997)

**Table 1.** Prototypical deprotonation and condensation reactions—calculated and experimental free energies.



Considering now the growth of zeolite surfaces, we have sought to understand the role of extra-framework cations within zeolite formation by examining the synthetic ABW and JBW structures. These two materials are topologically distinct yet are formed using very similar synthetic conditions, where the Si:Al composition is identical (1:1) but the alkali source is NaOH for JBW synthesis and LiOH for ABW synthesis. Using the approach described earlier, DFT calculations have been performed to understand how the extra-framework cation influences the process of oligomerisation in solution. Separately, we have investigated the surface structure of the slowest and fastest growing surfaces of ABW and JBW using a combination of interatomic potential and first-principles calculations. We find that basic conditions strongly favor the formation of 4 rings in the case of Li compared to Na whilst lower pH conditions appear to favor Na in preference to Li. The significance of this result is that ABW can be constructed entirely by 4 rings at the surface, whilst JBW consists of dimers, 4 and 6 rings. The preliminary results seem to indicate that under similar thermodynamic and basic conditions, 4 rings are formed more plentifully in the case of the Li mediated synthesis, suggesting that cation directed formation of different topologies may be driven by solution phase processes. Similarly, the Na mediated synthesis results in a higher proportion of dimers to 4 rings, which may explain why the JBW topology is formed.

We hope to demonstrate that our results can explain many of the experimental observations on the pre-nucleation stage of zeolite formation and to not only rationalize both the relative growth rates of different zeolite surfaces but to also explain the influence of templating cations on these growth processes.

## References

- Iler, R. K. (1979) *The chemistry of silica: solubility, polymerization, colloid and surface properties, and biochemistry*. Wiley, New York..
- Mora Fonz, M. J., Catlow, C. R. A., and Lewis, D.W. (2005) Oligomerization and cyclization processes in the nucleation of microporous silicas. *Angewandte Chemie-International Edition*, **44**, 3082-3086.
- Pearson, R.G. (1986) Ionization-potentials and electron-affinities in aqueous solution. *Journal Of The American Chemical Society*, **108**, 6109-6114.
- Sefcik, J., and McCormick, A. V. (1997) Thermochemistry of aqueous silicate solution precursors to ceramics. *AIChE Journal*, **43**, 2773-2784.

## Studying the composition and properties of zeolite-containing rocks of Tatar-Shatrashane occurrence

V. I. Sukharenko, S. I. Usenko, L. I. Borisova, T. V. Serova, and T. A. Morozova

*All-Russian Scientific Research Institute of Experimental Physics; Sarov, Russia; Email: suh-v@yandex.ru*

### Introduction

Zeolites that are aluminosilicates of alkaline and alkaline-earth elements have found wide application in various fields of science and industry. It is economically efficient to use native zeolites without separating them from the parent rock. In order to investigate the potential environmental protection application of the zeolite-containing rock (ZCR) of one Tatarstan Republic deposit, the composition and properties of ZCR were studied.

### Experimental Methods

Atomic emission spectroscopy (AES), and atomic absorption spectrometry (AAS) methods, electron diffraction analysis (ED), X-ray diffraction analysis (XRD), and optical microscopy methods were used to determine the chemical and phase composition of ZCR and to identify zeolites. Differential thermal analysis (DTA) and thermogravimetric analysis (TGA) methods were used to study the behavior of ZCR heated in the mode of dynamically varying temperatures. The morphological composition of ZCR and the effect of water, benzene, and p-xylene absorption on ZCR were investigated using the optical microscopy method. The bulk density and the specific surface were determined using the bottle method and gas chromatography method.

### Results and Discussion

The above described experimental methods allowed to identify heulandite ( $\text{Ca}(\text{Si}_7\text{Al}_2)\text{O}_{18} \cdot 6\text{H}_2\text{O}$ ) with a phase content of 19%, as the unique zeolite present in this ZCR. Silicon is found to be the basic element of the parent rock; iron and calcium are also available in significant quantities; the percentage of aluminum, titanium, and magnesium is lower; with potassium, copper, and cerium also present. Aluminosilicates, such as kaolinite and muscovite, as well as quartz, magnetite, and calcite with the quantitative phase content of 0.17%, 10.2%, 49.7%, 1.8%, and 20%, respectively, exist as discrete particle systems.

The specific surface value was measured using the gas chromatography method based on the direct dependence between the specific surface of adsorbent and the amount of argon adsorbed by a monomolecular layer onto the sample's surface at the temperature of liquid nitrogen. The results of measurements of the specific surface of the test sample in its original state and after its dehydration were  $40.0 \text{ m}^2/\text{g}$  and  $45.4 \text{ m}^2/\text{g}$ , respectively. The general porosity of the test samples of ZCR calculated using the relative and bulk density values was found to be 70%.

Morphological composition of ZCR was examined. It consists of porous and dense formations. When porous formations come in contact with water, the result is air release and their complete fragmentation into small particles. Contacts of dense particles with water cause separation of the surface porous layer alone, while the internal dense layer remains unchanged. Contacts of ZCR with benzene and p-xylene cause fragmentation of neither porous nor dense formations and lead to the appearance of an organic-film. The effect is not observed if previously moistened particles of ZCR contact with benzene and p-xylene.

The behaviour of ZCR by thermogravimetric analysis shows that, up to  $1000^\circ\text{C}$ , ZCR displays 7 endoeffects of various intensities and results in partial conversion into gaseous products (16.8 wt.%). One can assume that heating of the samples causes ZCR dehydration, decarbonization, and  $\alpha\text{-SiO}_2$ - $\alpha$ -tridymite polymorphous conversion at  $850^\circ\text{C}$ . Dehydration can be attributed to the presence of heulandite, muscovite, and kaolinite. Dehydration takes place within the range of temperatures  $30$ – $600^\circ\text{C}$  and the total water loss is 7.7 wt.%. Investigation of ZCR dehydration processes (the observation period was 40 minutes) at temperatures of  $85^\circ\text{C}$  and  $250^\circ\text{C}$ , typical for dehydration of heulandite, demonstrated losses of mass of the ZCR test sample equal to 2.5 wt.% and 3.8 wt.%, respectively. At a temperature of  $30^\circ\text{C}$ , the mass loss was 1.9 wt.%. The initial water content in ZCR, determined by the test sample dehydration up to its permanent weight at temperature  $105^\circ\text{C}$ , was 3.0 wt.%.

The zeolite-containing rock, with its physical and chemical parameters obtained, is assumed to be used for studying processes of hydrocarbon contaminants accumulation and migration in the upper horizons of soils.

This work is carried out within the framework of International Project #2419, with financial support by the United States of America under contract with the International Science and Technology Center (ISTC), Moscow.

# Selectivity of clinoptilolite for $\text{Na}^+$ , $\text{Cu}^{2+}$ , $\text{Zn}^{2+}$ , and $\text{Pb}^{2+}$ evaluated by a Margules empirical model coupled with a linear free energy correlation approach

J. C. Torres and J. C. Gubulin

International Institute of Ecology; São Carlos, São Paulo, Brazil; Email: [juan.iie@iie.com.br](mailto:juan.iie@iie.com.br)

Among other factors, the selectivity of a solid phase for ions at any isotherm point is basically affected by the innate properties of the exchanging ions in solution and in the particular solid phase and also by the departure from ideality of ions in both solid and solution phases.

The ion-lattice interactions of  $\text{Na}^+$ ,  $\text{Cu}^{2+}$ ,  $\text{Zn}^{2+}$ , and  $\text{Pb}^{2+}$  with clinoptilolite were quantified and interpreted using the classical Margules model (MM) for solid solutions. The binary empirical parameters ( $A_{ij}$  and  $A_{ji}$ ) of the model were derived from the binary isotherm data. Ion exchange experiments were conducted equilibrating a homoionic ( $M_1$ )-clinoptilolite ( $\text{CEC}=1.86 \times 10^{-3} \text{ eq g}^{-1}$ ; Na-form:  $\text{Na}_{4.911}\text{K}_{.421}\text{Ca}_{.395}\text{Mg}_{.113}[\text{Al}_{5.829}\text{Fe}_{.446}\text{Si}_{29.613}\text{O}_{72}] \cdot 18.2\text{H}_2\text{O}$ ) and aqueous solutions of two competing cations at 30°C and total normality of 0.005 N. The activity coefficients for the aqueous cations and nitrate, as the background anion, were estimated from the electrolyte ion-interaction model developed by Pitzer (1991). The standard free energy of exchange ( $\Delta G^\circ$ ) was derived from the values of its equilibrium constants ( $K$ ) evaluated from the empirical model.

The free energies calculated by the Margules model,  $\Delta G^\circ_{\text{MM}}$ , were equated with a linear free energy correlation model (Wang and Xu, 2000),  $\Delta G^\circ_{\text{LCA}}$ , that correlates thermodynamic parameters with cation properties. The  $\Delta G^\circ_{\text{MM}}-\Delta G^\circ_{\text{LCA}}$  couplings for (2-2)-monovalent and (1-2)-heterovalent exchange systems permitted the evaluation of the parameters in the linear free energy correlation approach (LCA), which are constants for a given isostructural mineral family.

If nonideality corrections for both solution and zeolite phases are considered,  $\Delta G^\circ_{\text{MM}}=\Delta G^\circ_{\text{LCA}}$ , then the linear equation for the Gibbs free energy of exchange reaction may be written as:

$$\Delta G^\circ_{\text{MM}} = a_{M_1X}^* (\Delta G^\circ_{nM_2^{z_2+}} - \Delta G^\circ_{nM_1^{z_1+}}) + \beta_{M_1X}^* (r_{M_2^{z_2+}} - r_{M_1^{z_1+}}) - (\Delta G^\circ_{fM_2^{z_2+}} - \Delta G^\circ_{fM_1^{z_1+}}) + b_{M_1X}^* \quad (1)$$

where  $a_{M_1X}^*$ ,  $\beta_{M_1X}^*$  ( $\text{KJ mol}^{-1} \text{\AA}^{-1}$ ) and  $b_{M_1X}^*$  ( $\text{KJ mol}^{-1}$ ) are constants,  $\Delta G^\circ_{nM_2^{z_2+}}$  and  $\Delta G^\circ_{fM_1^{z_1+}}$  are the standard free energies of non-hydration and formation of host (“1”) and counter (“2”) ions and  $r_{M_1^{z_1+}}$ , the ionic radius of cation  $M_1^{z_1+}$ . The values for the constants in the linear expression of the Gibbs free energy using clinoptilolite as solid phase (“X”) were calculated by least squares analysis and are given in Table 1. The constant  $b_{M_1X}^*$ , which depends on the standard Gibbs free energies of formation of the host mineral and the host cation, was considered only for the (1-2)-exchange systems. The small differences between the values of  $a_{M_1X}^*$  and  $\beta_{M_1X}^*$  found for the two system types may be due to different exchange site groups existing in the clinoptilolite structure. In this case, monovalent cations such as  $\text{Na}^+$  may occupy sites not populated by divalent cations.

The parameters calculated by applying the Margules model to the binary exchange data showed good linear correlation with the Gibbs free energies evaluated from the metal cation properties (Figure 1). Since the quantity  $RTz_2A_{12}$  is associated with zeolite framework stabilization when cation  $M_2^{z_2+}$  (infinitely diluted) replaces cation  $M_1^{z_1+}$  from a homoionic  $M_1$ -zeolite, the selectivity of an exchanger phase for cations in multicomponent systems can be evaluated from independent binary empirical parameters. In addition, for a pair of exchanging cations, the estimation of  $\Delta G^\circ_{\text{LCA}}$  using the linear parameters allows the evaluation of  $K$ ,  $A_{12}$  and  $A_{21}$  with which other (2-2)- and (1-2)-clinoptilolite systems can be predicted (isotherm) at any total solution normality and 303 K.

For the two types of exchange systems studied, both empirical parameters ( $A_{12}$  and  $A_{21}$ ) and the standard Gibbs free energies of reaction became more negative as the difference in the physical properties of the

exchanging cations increased. Likewise, Gibbs free energies of exchange approaches zero as the properties of the pair of exchanging cations become more similar. In the case of  $\text{Na}^+/\text{Pb}^{2+}$  exchange system, properties such as charge density, polarizability and ionic radius may favor the interaction of  $\text{Pb}^{2+}$  with crystallographic sites generally restricted to relatively large monovalent cations such as  $\text{Na}^+$ . From the results obtained, the selectivity of clinoptilolite for the aqueous cations studied at 0.005 N and 303 K followed the sequence:  $\text{Pb}^{2+} \gg \text{Na}^+ > \text{Cu}^{2+} \approx \text{Zn}^{2+}$ .

Table 1. Gibbs free energies from the empirical model and parameters from MM-LCA couplings

Exchange System $M_1^{z_1+} \square M_2^{z_2+}$	$\Delta G^\circ_{\text{MM}}$ (KJ/mol)	$\Delta G^\circ_{\text{MM}} - \Delta G^\circ_{\text{LCA}}$ couplings		
		$a_{M_1X}^*$	$\beta_{M_1X}^*$	$b_{M_1X}^*$
$2\text{Na}^+ \square \text{Zn}^{2+}$	6.71			
$2\text{Na}^+ \square \text{Cu}^{2+}$	5.49	0.988	329.34	-69.28
$2\text{Na}^+ \square \text{Pb}^{2+}$	1.54			
$\text{Zn}^{2+} \square \text{Cu}^{2+}$	1.37			
$\text{Zn}^{2+} \square \text{Pb}^{2+}$	-3.03	1.001	335.01	-
$\text{Cu}^{2+} \square \text{Pb}^{2+}$	-4.33			

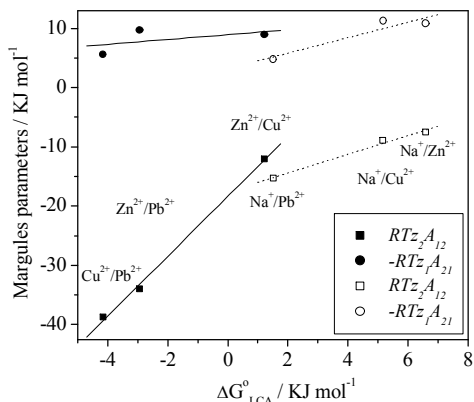


Figure 1. Margules empirical parameters and standard Gibbs free energies (LCA) of binary (1-2)- and (2-2)-exchange systems. (2-2)-systems:  $\{ RTz_2A_{12} = -18.37 + 5.04\Delta G^\circ_{\text{LM}}; -RTz_1A_{21} = 8.92 + 0.41\Delta G^\circ_{\text{LM}} \}$ , (1-2)-systems:  $\{ RTz_2A_{12} = -17.56 + 1.57\Delta G^\circ_{\text{LM}}; -RTz_1A_{21} = 3.18 + 1.31\Delta G^\circ_{\text{LM}} \}$ .

## References

- Pitzer, K.S. (1991) Activity Coefficients in Electrolyte Solutions. Boca Raton. Chapter 3.  
Wang, Y. and Xu, H. (2000) Prediction of trace metal partitioning between minerals and aqueous solutions: A linear free energy correlation approach. *Geochimica et Cosmochimica Acta* **65**, 1529-1543.

## Mexican surfactant-modified natural zeolite as an adsorbent of azo dyes from aqueous solution

J. Torres Pérez<sup>1,2</sup>, M. Solache Ríos<sup>1</sup> and M. Olguín Gutiérrez<sup>1</sup>

<sup>1</sup>*Instituto Nacional de Investigaciones Nucleares; México; Email: mog@nuclear.inin.mx*

<sup>2</sup>*Universidad Autónoma del Estado de México; Mexico*

### Introduction

The removal of color from textile effluents is one of the challenging problems in the field of environmental chemistry (Hammer and Hammer (Jr.), 1996). Azo dyes are presently the most important compounds, contributing to about 20–40% of the total dyes used for coloring. Recently the sorption for dye removal from aqueous solutions using aluminosilicates has been reported (Ho et al., 2001; <sup>a</sup>Armagan et al., 2004; Al-Bastaki and Banat, 2004; Bouberka et al., 2005). The removal of azo dyes everzol Black, everzol Red 239, and everzol Yellow (<sup>b</sup>Armagan et al., 2004) by natural and surfactant-modified clinoptilolite show that natural zeolite have limited adsorption capacities of the reactive dyes but are substantially improved upon modifying its surface with hexadecyltrimethylammonium bromide. Therefore the aim of this paper was to evaluate the adsorption of two azo dyes from aqueous solutions (mono- or bi-component) onto a surfactant-modified Mexican natural zeolite.

### Experimental Methods

The clinoptilolite-rich tuff from Villa de Reyes, San Luis Potosí, México was milled and sieved. The grain size used in this work was from 0.8–1.0 mm.

Zeolitic material was treated with a NaCl solution under reflux and the phases were separated. The zeolitic sample was washed with deionized water until there was no presence of chloride ions. The sodium treated clinoptilolite-rich tuff was then dried.

Zeolitic materials treated with NaCl were mixed with a HDTMA-Br solution, the mixture was shaken at 303 K. Then, the zeolitic material was separated from the solution and it was washed, until the concentration of HDTMA-Br in the washing solutions was less than 10% of the initial concentration. The surfactant was determined by using an ultraviolet-visible spectrophotometer analyzer at  $\lambda = 195$  nm. Finally the solid samples were left to dry for two days at room temperature.

Powder diffractograms of the zeolitic samples were obtained with a Siemens D500 diffractometer coupled to a copper anode X-ray tube. The conventional diffractograms were used to identify the compounds and to verify crystalline structure.

For scanning electron microscopy (SEM) observations, the natural zeolite samples before and after dye sorptions were mounted directly on the holders, covered by sputtering with gold, and then observed at 10 and 20 kV in an XL 30 Philips electron microscope. The microanalysis was done with an EDS system.

Samples of natural organo-zeolite were put in contact with 20 mL of different concentrations of mono- and bi-component dye solutions (from 2.5–20.0 mg/L). The aqueous and solid phases were shaken for 5 hours at room temperature. The samples were centrifuged and decanted; dyes were analyzed in the liquid phases as described above.

### Results and Discussion

Both clinoptilolite and quartz were the principal components found in the zeolitic samples and there were no clay minerals observed. It was observed that HDTMA conditioned zeolite samples showed no significant changes in the position of the most intense diffraction peaks. The powder diffraction pattern of the surfactant-modified Mexican natural zeolite after the azo dye sorptions did not show any important changes.

SEM images and EDS analysis show similar morphologies and slight differences in the chemical composition of the untreated and treated natural zeolite.

The presence of sulfur (~ 0.3% wt.) in the modified natural zeolite after the dye sorption process confirms the interaction between the dye and the surfactant bonded to the zeolite surface.

The isotherm data obtained in this work was fitted to the Langmuir and Freundlich models (Slejko, 1985) in order to describe the azo dye sorption behavior in a surfactant-modified clinoptilolite-rich tuff from Villa de Reyes, San Luis Potosí (México).

In general the correlation coefficients were higher using the Langmuir model rather than the Freundlich model.

The experimental data was treated with the extension of Langmuir competitive equations (Pagnanelli et al., 2002; Pagnanelli, et al., 2003). In general the larger the multi-component Langmuir adsorption constant of one dye, the larger the competition effect of this dye on the adsorption of the other.

We acknowledge financial support from CONACyT, project 46219 and we thank L. Carapia and the technicians of the Chemistry Department (ININ) for technical support.

## References

- Al-Bastaki, N., Banat, F. (2004) Combining ultrafiltration and adsorption on bentonite in a one-step process for the treatment of colored waters. *Resources, Conservation and Recycling* **41**, 103-113.
- Armagan, B.; Turan, M.; Çelik, M. (2004a) Equilibrium studies on the adsorption of reactive azo dyes into zeolite. *Desalination* **170**, 33-39.
- Armagan, B.; Turan, M.; Ozdemir, O.; Çelik, M. (2004b) Color removal of reactive dyes from water by clinoptilolite. *Journal of Environmental Science Health A. Tox. Hazard Subst. Environ. Eng.* **39**, 1251-1261.
- Bouberka, Z.; Kacha, S.; Kameche, M.; Elmaleh, S.; Derriche, Z. (2005) Sorption study of an acid dye from an aqueous solutions using modified clays. *Journal of Hazardous Materials* **119**, 117-124.
- Hammer, M. J.; Hammer, M. J. (Jr.). (1996) *Water and Waste Water Technology*, Third Edition, Prentice Hall Inc., USA.
- Ho, Y.; Chiang, C.; Hsu, Y. (2001) Sorption kinetics for dye removal from aqueous solution using activated clay. *Separation Science and Technology* **36**, 2473-2488.
- Pagnanelli, F.; Esposito, A.; Veglio, F. (2002) Multi-metallic modeling for biosorption of binary systems. *Water Research* **36**, 4095-4105.
- Pagnanelli, F.; Mainelli, S.; Centofanti, M.; Veglio, F.; Toro, L. (2003) *Biosorption of binary metal systems onto an olive pomace: equilibrium modeling*. The sixth Italian Conference on Chemical and Process Engineering, Pisa, Italy.
- Slejko, F. (1985) *Adsorption Technology: a step-step approach to process evaluation and application*. USA, Marcel-Decker Inc.

## **Intraparticle diffusion of Pb, Cu, and Zn ions during exchange processes on the natural zeolite clinoptilolite**

**M. Trgo, N. Vukojević Medvidović, J. Perić**

*University of Split; Split, Croatia; Email: mtrgo@ktf-split.hr*

### **Introduction**

It is well known that natural zeolites behave as good ion exchangers for removal of heavy metal ions from aqueous solutions. But the selectivity of natural zeolite for a particular ion depends on the type of zeolite and on the type, hydrated radius, and concentration, of exchangeable ion in the solution (Colella, 1999). Examination of ion exchange kinetics, determination of diffusion rate, diffusion coefficients, and the mechanism that controls the overall process are important for application of these processes in practice. The diffusion kinetics of heavy metal ions is often examined on natural zeolite clinoptilolite which shows high selectivity for these ions, e.g., for lead ions. This paper examines the kinetics of lead, copper, and zinc ion exchange on clinoptilolite. The kinetic parameters of the ion exchange process have been calculated using the empirical homogeneous diffusion model.

### **Experimental Methods**

Experiments have been carried out with samples of natural zeolite from the Vranjska Banja deposit that contains ~80% clinoptilolite. A natural sample has been milled and dry sieved producing the 0.04–0.10 mm fraction, and preconditioned to the Na form. The aqueous solutions of lead, copper, and zinc have been prepared by dissolving the salts in doubly distilled water. Exact concentrations of these ions were determined complexometrically using highly selective indicators. Experiments of ion exchange were performed by means of the batch method, in mixtures of 1 g of zeolitic sample and 100 ml of heavy metal ion solution (Pb or Cu or Zn) of similar initial molar concentration at the temperature of  $23 \pm 1^\circ\text{C}$  in glass vessels isolated from atmosphere. At different contact times, the experiment was interrupted, the suspension filtered, and the concentration of heavy metal ions remaining in the filtrate was determined. In the clinoptilolite-lead ion system, the equilibrium was attained faster than in systems with copper and zinc ions, so that experimental performance had to be changed and repeated. Examinations with lead ions were repeated in one vessel with the volume of 3000 ml, by stirring a suspension of 20 g of zeolite with 2000 ml of lead solution. At different time intervals (from 1.5 min to 60 min), 10-mL portions were sampled and centrifuged, and the remaining concentration of lead determined. The zeolite samples after saturation with heavy metal ions were analysed by SEM and EDX.

### **Results and Discussion**

Figure 1 shows the plots of experimental results for lead, copper, and zinc bound per gram of zeolite relative to time. The rate of removal is initially fast for all examined ions, where the exchange of lead is the fastest and equilibrium is attained in ~22 minute (Fig. 1b). Maximum exchange levels for lead and copper ions are very close but significantly higher than that for zinc ions. This order is in accordance with the selectivity order found in the literature (Colella, 1999). The time needed for equilibration is prolonged for copper and zinc, and it is achieved in ~500 minutes.



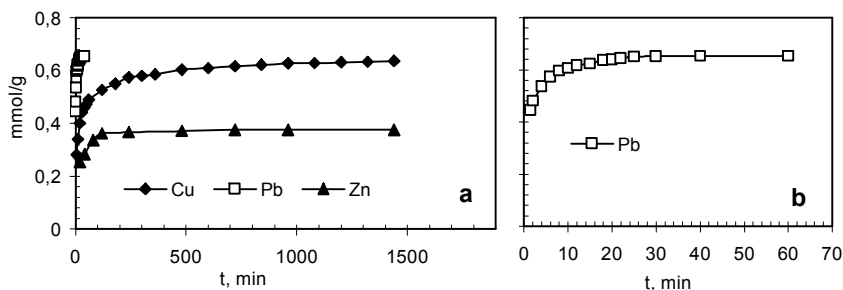


**Figure 1.** The quantity of Pb, Cu, and Zn bound vs. time: a) comparison of all three ions, b) Pb ions excluded.

In our previous studies, we concluded that the diffusion through the zeolitic particle is the rate-determining step, and that the diffusion rate does not depend on initial concentrations of the Pb, Cu, or Zn ions (Trgo et al., in press 2006). The kinetics of intraparticle diffusion is described by the empirical homogeneous diffusion model for the condition  $t \rightarrow t_{\infty}$  that assumes the constancy of diffusion rate from the surface of the zeolite particle to the exchangeable site (Sparks, 1998). The application of this kinetic model to the experimental results yields linear dependence for lead and non-linear curves for copper and zinc ions. These non-linear curves have inflection points that separate each curve into two areas. These areas have been linearised and the diffusion coefficients have been calculated according to the model equation. The values of diffusion coefficients show that the diffusion of lead ion is fastest and does not change with time, and that the diffusion of copper and zinc is slower and decreases with time. This phenomenon can be explained by the order of hydrated ionic radius of particular exchangeable ions ( $Pb < Zn < Cu$ ), as well as by their tendency for forming monovalent hydroxy species. These effects could be responsible for the higher mobility of ions through the framework structure of the zeolitic particle that contributes to its higher selectivity and exchange capacity.

## References

- Colella, C. (1999) Environmental applications of natural zeolitic materials based on their ion exchange properties. Pp. 207-224 in: *Natural Microporous Materials in Environmental Technology* (P. Misaelides, F. Macasek, T.J. Pinnavaia and C. Colella editors). Kluwer Academic Publishers, Dordrecht.
- Panayotova, M., and Velikov, B. (2002) Kinetics of heavy metal ions removal by use of natural zeolite. *Journal of Environmental Science and Health*, **A37**, 139-147.
- Sparks, D.L. (1998) Kinetics of sorption/release reactions on natural particles. Pp. 413-448 in: *Structure and Surface Reactions of Soil Particles* (P.M. Huang, N. Senesi, J. Buffle editors). John Wiley and Sons, London.
- Trgo, M., Perić, J., and Vukojević Medvidović, N. (2006) A comparative study of ion exchange kinetics in zinc/lead - modified zeolite clinoptilolite systems. *Journal of Environmental Management* (in press).

## Pollutant removal of stormwater from traffic areas using zeolite-containing substrates

M. Upmeyer

*Zeobon GmbH; Bad Honnef, Germany; Email: martin.upmeyer@zeobon.com*

Traffic areas, in many cases, show high loads of pollutants. According to German regulations, the direct infiltration of contaminated water in underground facilities without pretreatment is not permitted. The presented system for cleaning contaminated stormwater consists of a hydrodynamic separator, a plastic storage chamber, and a zeolite containing substrate.

Small scale box experiments were conducted to prove the effectiveness of the zeolite-containing substrate. Because of the good results of the laboratory experiments, local water authorities decided to equip a newly populated area with the infiltration system.

### Introduction

In densely populated areas there is often not enough space for topsoil water infiltration facilities. In addition this stormwater, in many cases, is contaminated with heavy metals, mineral oils or polycyclic aromatic hydrocarbons that can endanger the soil and groundwater. In Germany the use of infiltration devices such as swales or swale-trench systems is recommended by water authorities. Therefore, the use of a treatment plant in combination with a highly adsorptive substrate can be an appropriate solution.

The designed system consists of three units: a hydrodynamic separator, a plastic storage chamber, and a quantity of zeolitized tuff with a high content of natural zeolite. The retention of water before infiltration is ensured by the plastic storage chamber. The volume of the chamber was calculated according to German ATV-DVWG-worksheet A 138. The substrate consists of a mixture of lava, zeolitized tuff, and limestone. The tuff used is from Bystre/Slovakia with a clinoptilolite content of 80%.

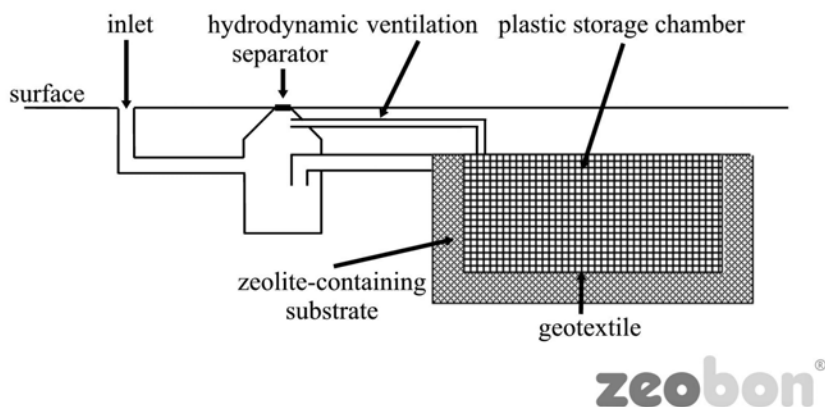


**Figure 1** Stormwater infiltration system

### Experimental Methods

Laboratory experiments were carried out at the University of Essen. Adsorption capacity of the substrate for artificial waste water was determined using lysimeters with a 52x52 cm<sup>2</sup> surface area. The contaminant concentration was similar to motorway runoff water in Germany; the freight applied in two weeks corresponds quantitatively to the complete freight of a year.

## Results and Discussion

The results of the laboratory test are shown in table 1 (*measurement below detection limit in italics*). Mineral oils and polycyclic aromatic hydrocarbons (PAH) are removed very well by the substrate. The amount of heavy metals removed in the laboratory experiments vary from 68.8% to 97.7%.

As pollution retention of the system works by means of sedimentation (hydrodynamic separator), filtration (in the storage chamber) and adsorption + chemical precipitation (in the zeolite-containing substrate), even an higher retention is expected in the field experiments due to biological degradation.

The system has been build for the first time in a new district in Leverkusen (near Cologne) in spring 2006. We estimate first results regarding the cleaning efficiency by the end of 2006.

**Table 1** Adsorption properties of the zeolite-substrate (Geiger & Fach 2003)

parameter	unit	series A			series B		
		artificial runoff	percolated water	reduction	artificial runoff	percolated water	reduction
mineral oil	mg/l	0.120	<0.100	>16.7%	0.420	<0.020	>95.2%
PAH	µg/l	16.550	0.110	99.3%	26.300	<0.050	>99.8%
Cd	mg/l	0.010	<0.001	>90.0%	0.004	<0.001	>75.0%
Zn	mg/l	0.388	0.121	68.8%	0.413	0.050	87.9%
Cu	mg/l	0.098	0.208	---	0.089	0.026	70.8%
Pb	mg/l	0.241	0.008	96.7%	0.173	<0.008	>95.4%
Ni	mg/l	0.047	0.014	70.2%	0.060	<0.004	>93.3%

## References

- Geiger, W.F., Fach, S. (2003) Adsorption of stormwater pollution in infiltration plants using synthetic soils (German – original title: Rückhalt von Inhaltsstoffen aus Niederschlagsabflüssen durch den Einbau definierter Böden in Versickerungsanlagen), 10 p, appraisal, University Duisburg-Essen (unpublished).

## **Blended cements containing high volume of natural zeolites: Superplasticizer requirement and compressive strength of mortars**

**B. Uzal and L. Turanlı**

*Middle East Technical University; Ankara, Turkey; Email: uzal@metu.edu.tr*

### **Introduction**

Mineral additives are utilized in blended portland cements to save cost as well as to improve the properties of cementitious systems. However, most pozzolanic materials, especially natural pozzolans, tend to increase the mixing water requirement and lower the rate of strength development. Therefore, for structural applications, their proportion in blended Portland cements is generally limited to 30% or less.

The production of every tone of portland cement that is the binder component of the concrete releases approximately one tone of CO<sub>2</sub> to atmosphere for obtaining portland cement clinker. It is well known that CO<sub>2</sub> is a major contributor to the greenhouse gas emissions that is responsible for global warming. Considering the yearly portland cement production of 1.6 billion tons, the cement industry, itself, is responsible for 7% of total carbon dioxide emissions (Mehta, 2002).

Proportion of the mineral additives in blended cements should be as high as possible to reduce CO<sub>2</sub> emission associated with cement industry. The water requirement problem, which may arise when large amount of pozzolanic material is incorporated in blended cements, can be solved by modern chemical admixtures. Cementitious systems containing high-volume (50% or more) of pozzolanic materials seems to be an effective solution to reduce CO<sub>2</sub> emissions from cement industry.

### **Experimental Methods**

Clinoptilolite from Gordes deposits in west Anatolia with a zeolite content of about 80–85% was used in the study. Zeolite sample was ground so that the percent material finer than 45 µm is 80%. Blended portland cement mortars were prepared with replacement of portland cement by different amounts of natural zeolite, from 0% to 55% by weight. Since the zeolite replacement will decrease the flow value of fresh mortars with constant water/cement ratio, a naphthalene-based superplasticizer in a dry powder form was used to maintain the flow value constant despite the increasing zeolite content. Thus, superplasticizer requirements of zeolite blended mortars for a similar flow value to control portland cement mortar were determined. Compressive strength of hardened mortars was also determined at 3, 7, 28, and 91 days of age.

### **Results and Discussion**

Superplasticizer requirement of blended cement as weight percent of total binder (portland cement+zeolite) are given in Figure 1 as a function of zeolite content. Compressive strength of blended cement mortars containing zeolite is given in Figure 2 for 3, 7, 28, and 91 days of age.

Amount of superplasticizer required increased linearly with increasing zeolite content. Early strength values (3 and 7 days) decreased linearly with increasing pozzolan content, which is an expected result for the cements containing pozzolanic materials since the little or no pozzolanic reaction at early days. However, 28-days strength value of mortars increased with increasing zeolite content up to 35% replacement level. For 45% and 55% replacement levels, small reductions were observed in 28-day compressive strength of mortars, which are only 3% and 10% for 45% and 55% zeolite content, respectively, when compared to reference portland cement mortar.

The blended cement containing high-volume of natural zeolite showed a significantly better strength performance when compared to the ones containing non-zeolitic natural pozzolans which had been studied before (Uzal, Turanlı). 28-day compressive strength of mortars made with blended cements containing 55% non-zeolitic pozzolan was 25–30% lower than that of reference control mortar.

It can be concluded that compressive strength performance of high-volume natural pozzolan blended cements (containing 50% or more natural pozzolan) could be enhanced by using clinoptilolite type natural zeolites, and with the help of superplasticizing chemical admixtures.

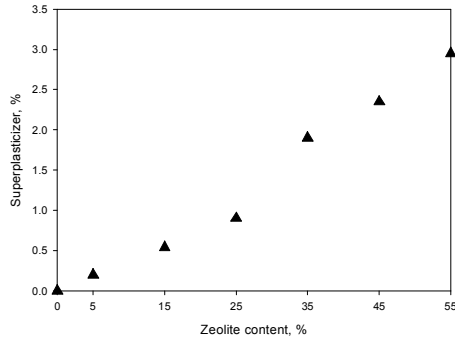


Figure 1. Effect of zeolite content on superplasticizer requirement

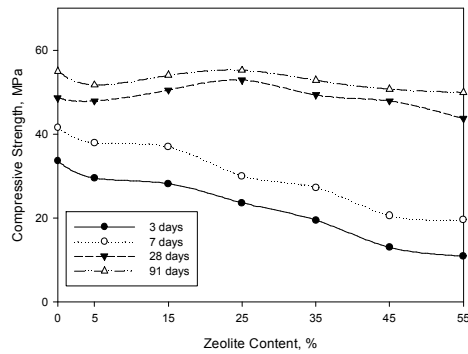


Figure 2. Effect of zeolite content of blended cement on compressive strength of mortars

## References

- Mehta, P.K. (2002) Greening of the concrete industry for sustainable development. *Concrete International*, **24**, 23–28.
- Uzal, B. and Turanli, L. (2003) Studies on blended cements containing a high volume of natural pozzolans. *Cement and Concrete Research*, **33**, 1777–1781.

## **Ion exchange reactions of natural zeolites: adsorption, exchange kinetics, and desorption**

**G. F. Vance<sup>1</sup>, G. K. Ganjegunte<sup>2</sup>, and M.A. Urynowicz<sup>1</sup>**

<sup>1</sup>*University of Wyoming; Laramie, Wyoming, USA; Email: gfv@uwyo.edu*

<sup>2</sup>*Texas A&M University System; El Paso, Texas, USA*

Calcium-rich, natural zeolites can be used for the removal of  $\text{Na}^+$  and other salts from saline-sodic water being produced from the coalbed natural gas (CBNG) industry that is active in many parts of the U.S., including the Powder River Basin (PRB) of Wyoming and Montana. The usefulness of natural zeolites as efficient ion exchangers depends on their cation exchange capacity (CEC), exchangeable cation content, adsorption reactions and rates, and recharging efficiency of spent zeolites. Batch studies examined the CEC and exchangeable cation concentrations in zeolites and the adsorption and exchange kinetics using NaCl solutions. In addition, zeolite materials saturated with  $\text{Na}^+$  were treated with  $\text{CaCl}_2$  and HCl to evaluate recharge. Results of these experiments indicate that Ca-rich zeolite material has a lower CEC (about  $110 \text{ cmol kg}^{-1}$ ) than many Na-rich zeolites, and that the exchange between  $\text{Na}^+$  by  $\text{Ca}^{2+}$  occurs within 5 min. Among the different adsorption isotherms, the Freundlich model provided a better fit for the smaller size zeolite materials (6x8, 6x14, and 14x40), while the Langmuir model provided a better fit for the larger size zeolites (4x6). The desorption studies indicated that a mixed solution of HCl acid and  $\text{CaCl}_2$  was more efficient in replacing  $\text{Na}^+$  adsorbed on zeolite, followed by HCl acid alone, and than  $\text{CaCl}_2$  alone. The results of these bench-scale experiments will be utilized in building a field-scale prototype to further examine the feasibility of natural zeolites for reducing the SAR of CBNG produced waters in the PRB.

### **Introduction**

Clinoptilolites are natural zeolites that occur in many parts of the western U.S. Their availability, high CEC, and low cost make them attractive ion exchangers for wastewater treatment processes. Clinoptilolites dominated by  $\text{Na}^+$  exchange cations are used to remove ammonium ( $\text{NH}_4^+$ ) from municipal wastewaters and  $\text{Cs}^+$  from nuclear power plant wastewaters in many parts of the world (Pansini, 1996; Cerri et al., 2002). In the PRB, poor-quality, saline-sodic water is being produced by the CBNG industry. CBNG water chemistry has pH values ranging from 7.0 to 9.9, SAR as high as 70 and EC from 0.4 to  $4.8 \text{ dS m}^{-1}$  (Rice et al., 2002). The cumulative production of CBNG-water over 15 years from PRB wells is estimated to be 366,000 ha-m. Not surprisingly, the use of CBNG waters for irrigating agricultural and rangeland ecosystems is becoming a popular management option. However, the application of CBNG waters with high  $\text{Na}^+$  and other salts can result in reduced water uptake and water stress to plants; reduced availability of plant nutrients; toxicity of chloride ( $\text{Cl}^-$ ), sodium ( $\text{Na}^+$ ), and boron (B); dispersion of soil clay particles and organic matter; surface crusting; reduced water infiltration; and reduced water movement in soils (Ganjegunte et al., 2005).

This study evaluated the utility of a Ca-rich zeolite for reducing  $\text{Na}^+$  and salts in poor-quality CBNG waters. Study objectives were to determine CEC and exchangeable cation contents of 4 zeolite size fractions, to evaluate the exchange kinetics between  $\text{Na}^+$ - $\text{Ca}^{2+}$  and  $\text{Na}^+$ - $\text{Mg}^{2+}$ , and to evaluate  $\text{Na}^+$  adsorption processes and desorption mechanisms involving HCL and  $\text{CaCl}_2$ .

### **Experimental Methods**

Four different size groups (4x6, 6x8, 6x14 and 14x40) of commercially-available, Ca-rich zeolite from the St. Cloud deposit in New Mexico were used for this laboratory experiment. The 4 sized zeolites were characterized using X-ray diffraction (XRD) and the effective CEC and exchangeable cations were determined using the ammonium acetate extraction method. Adsorption reactions and exchange kinetics were also studied using variable NaCl solutions and reaction time intervals ranging from 10 sec to 1 hour, respectively. Three solutions,  $\text{CaCl}_2$ , HCl and a combination of both, were used to evaluate  $\text{Na}^+$  desorption and zeolite recharge.

## Results and Discussion

XRD results indicated the zeolite materials were mainly clinoptilolite with inclusions of small amounts of potassium feldspars and quartz. The cation exchange capacity of the zeolite material was strongly related to its size and it ranged from 87 (4x6) to 111 cmol kg<sup>-1</sup> (14x40) zeolites. Different adsorption isotherms were fit to the data to evaluate the sorption mechanisms. The adsorption isotherm data followed the Langmuir model (Figure 1) for 4x6 sized zeolite, while the Freundlich model provided a better fit for finer sizes (6x8, 6x14, 14x40). Sorption kinetics followed a second order model, which resulted in an excellent fit of the desorption data (Figure 2). The second order sorption rate constants ( $k_2$ ) for Ca and Mg were 0.0076 and 0.0104 kg/cmol/s, respectively. Among the three solutions used for desorption of Na adsorbed on zeolite, a combination of HCl and CaCl<sub>2</sub> removed the maximum amount of Na<sup>+</sup>, followed by HCl alone, then CaCl<sub>2</sub> alone.

## References

- Cerri, G., Langella, A., Pansini, M. and Cappelletti, P. (2002) Methods of determining cation exchange capacities for clinoptilolite-rich rocks of the Logudoro region in Northern Sardinia, Italy. *Clays and Clay Minerals*, **50**, 127-135.
- Duong, T.D., Hoang, M., and Nguyen, K.L. (2005) Sorption of Na<sup>+</sup>, Ca<sup>2+</sup> ions from aqueous solution onto unbleached kraft fibers-kinetics and equilibrium studies. *Journal of Colloid and Interface Science* **287**, 438-443.
- Ganjugunte, G. K., Vance, G.F. and King, L.A. (2005) Soil chemical changes resulting from irrigation with water co-produced with coalbed natural gas. *Journal of Environmental Quality*, **34**, 2217-2227.
- Pansini, M. (1996) Natural zeolites as cation exchangers for environmental protection. *Mineralium Depsoita*, **31**, 563-575.
- Rice, C.A., Bartos, T.T., and Ellis, M.S. (2002) Chemical and isotopic composition of water in the PRB, WY & MT: Implications for CBM Development. Pp. 53-70 in: *CBM of North America II* (S.D Schwochow and V.F. Nuccio, Eds.). Rocky Mountain Association of Geologists.

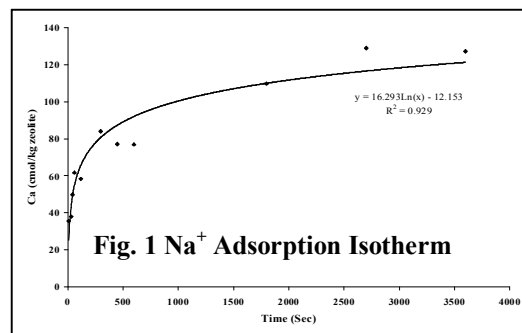


**Fig. 1 Na<sup>+</sup> Adsorption Isotherm**

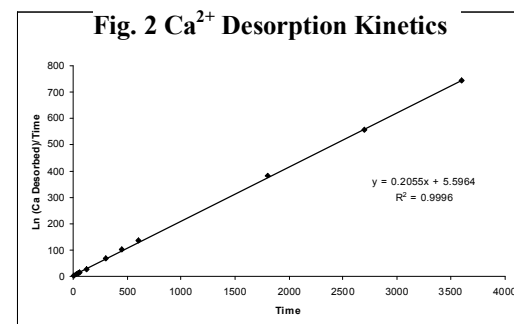


**Fig. 2 Ca<sup>2+</sup> Desorption Kinetics**

## Investigation of sorption processes for uranium, plutonium, and americium using tuffs in thin section

D. T. Vaniman, J. J. Kitten, and S. J. Chipera

*Los Alamos National Laboratory; Los Alamos, New Mexico, USA; Email: vaniman@lanl.gov*

### Introduction

Zeolite deposits provide attractive sites for isolation of radionuclides via natural barriers. The attraction stems from the high sorptive capacity of zeolites for alkali and alkaline-earth radionuclides, particularly  $^{137}\text{Cs}$  and  $^{90}\text{Sr}$ . For high-level nuclear waste dominated by actinide elements, the advantage gained from natural zeolite barriers is harder to define. While distribution coefficients with groundwater ( $K_d$ ) typically range from  $10^3$  to  $10^4$  ml/g for Cs, values are smaller for most actinide elements (e.g., Neymark et al. in this volume concerning site-scale sorption estimates for U in zeolitized tuff). There is a large literature on the quest for meaningful actinide  $K_d$  values in zeolitized rock, but most data are based on crushed samples in batch or column experiments where accumulation of the radionuclide is readily determined, but the mechanism of sorption is not revealed. This is important where natural rocks, rather than purified zeolites, are used because zeolitized lithologies often include other phases with strong radionuclide interactions, particularly clays and redox-active minerals such as Mn-oxides. Batch or column-flow experiments are better interpreted if parallel studies of sorption in thin section are conducted to determine which minerals accumulate the greatest amount of the radionuclide of concern. The standard method for this kind of analysis is microautoradiography.

Traditionally, microautoradiography is performed by preparing a thin section of the lithology being examined, exposing that section to a radionuclide-bearing solution, rinsing it to remove excess radionuclide-bearing solution, coating the rock slice on the section with a photoemulsion, and then developing and fixing the photoemulsion after an exposure time that allows  $\alpha$  or  $\beta$  decay tracks to be maximized without totally blackening the emulsion. The limitation to this method is <5% saturation of the photoemulsion. Saturation refers to the ratio of Ag crystals developed and fixed in the emulsion to the total possible amount of Ag possible; at 5% the dark Ag crystal abundance is so dense that individual tracks overlap and can not be counted. However, the photographic process provides a more quantitative method. Radiation generates a few Ag atoms in the AgBr crystals of the emulsion. On development, the “latent image” of a few Ag atoms has higher probability than “unhit” crystals of growing into ribbons of Ag metal. These are somewhat larger than the original AgBr crystal and represent a manyfold increase over the original latent signal. When the emulsion is fixed, all undeveloped AgBr crystals are dissolved and the only Ag left in the emulsion is that associated with radionuclide damage. With this high signal to background, electron microprobe (EMP) analysis of the emulsion (Benjamin et al., 1977; Vaniman et al, 1996) raises the practical analytical limit to ~60% saturation by directly measuring the Ag abundance.

### Experimental Methods

Six parallel thin sections were prepared from each of three tuff samples to accommodate experiments with three radionuclides and two water types. Splits of the same samples were crushed for batch sorption experiments using  $^{241}\text{Am}$ ,  $^{233}\text{U}$ , and  $^{239}\text{Pu}$  solutions in two different waters, one representing an aquifer in siliceous tuff (from well J-13 at Yucca Mountain) and one representing the deeper Paleozoic carbonate aquifer (simulated by filtering J-13 water through an  $\text{NaHCO}_3$  buffer to increase carbonate content). After sorption, splits were separated by centrifugation and counted in scintillation counters. Splits were also used to determine mineral abundances by quantitative X-ray diffraction (QXRD). In addition to zeolitized tuff (bedded Topopah Spring Tuff, drill hole SD-9 at 1465.9-1466.1 ft depth), the two other lithologies selected were: devitrified tuff composed mostly of feldspar and silica minerals (Prow Pass Tuff, drill hole SD-9 at 1638.7-1639.2 ft depth) and unaltered vitric nonwelded tuff (Topopah Spring Tuff, drill hole SD-12, 1388.0-1388.2 ft depth), all from the same locality (Yucca Mountain, Nevada, USA).



Table 1: wt% mineral abundances in three tuff samples

sample	smectite	clinoptilolite	opal-CT	quartz	cristobalite	feldspar	glass	biotite
zeolitized	2(1)	80(6)	9(2)	3(1)	-	7(2)	-	-
devitrified	7(2)	-	-	20(2)	15(1)	55(8)	-	1(1)
vitric	1(1)	3(1)	5(1)	4(1)	-	10(2)	78(2)	tr

Thin sections were exposed to the same radionuclide-bearing waters used for batch sorption experiments. Exposure was for at least 8 hours, with only the surface of the thin section in contact with the solution. Thin sections were then rinsed in deionized water for one minute and counted by a methane flow-proportional counter. After counting, the surfaces of the thin sections with sorbed radionuclides were coated with photoemulsion and exposed for times estimated from the count rate to only partially saturate the emulsion. The thin sections were then studied optically and relative Ag concentrations were counted by EMP in traverses across (1) background areas where the emulsion was over glass, (2) general areas of each section over the lithology exposed, and (3) across specific features within each lithology where optical inspection showed exceptionally strong radionuclide retention.

## Results and Discussion

Batch sorption results indicate a first-order difference between radionuclide species, with sorption increasing as  $\text{Am} > \text{Pu} > \text{U}$  with respective average  $K_d$  values  $10^3 > 10^2 > 1.5$ , regardless of water type or tuff lithology, except for higher Pu sorption in the zeolitic lithology ( $K_d 10^3$ ) with carbonate aquifer water, higher U sorption in the zeolitic lithology ( $K_d 10$ ) with volcanic aquifer water, and higher Am sorption in all samples exposed to carbonate aquifer water versus volcanic aquifer water. Microautoradiography results, in contrast, show little difference in U or Pu sorption between lithologies (all with cpm thin section/cpm thin starting solution  $< 1$ ) whereas Am has distinct lithologic preferences in the sequence zeolitic  $>$  vitric  $>$  devitrified ( $4.5 > 3 > 1.8$ ). These results indicate that batch sorption and thin section exposure do not yield directly comparable results; the former presents fresh broken surfaces with high area to solution and the latter presents limited polished areas to solution. However, optical and EMP microautoradiography reveal specific minor phases in all lithologies, particularly clays and Mn-oxides (rancieite and cryptomelane), and calcite in the carbonate aquifer water, that accumulate Pu to a much greater extent than do major phases, including zeolites. Such minor-phase preference was far less significant for Am and U.

## References

- Benjamin, T.M., Arndt, N.T., and Holloway, J.R. (1977) Instrumental techniques for  $\beta$ -track mapping. Annual Report of the Director, Geophysical Laboratory, Carnegie Institution, Washington, 1976-1977, 658-660.
- Vaniman, D., Furlano, A., Chipera, S., Thompson, J., and Triay, I. (1996) Microautoradiography in studies of Pu(V) sorption by trace and fracture minerals in tuff. Materials Research Society Symposium Proceedings, **412**, 639-646.

## **Chabazite, Ca-K-Na phillipsite, analcime, and natrolite: alkaline zeolites filling amygdaloids in tertiary basalts in Patagonia, Argentina, South America**

**M. E. Vattuone, C. I. Martínez Dopico, Y. Berbeglia, E. Gallegos, and S. Crosta**

*Universidad de Buenos Aires, Argentina; E-mail: elenavattuone@fibertel.com.ar*

Alkaline zeolites were found in tertiary amygdaloid basalts located in Junin de los Andes, Neuquén Patagonia (Vattuone et al., 2005a). The presence of alkaline zeolites in association with other secondary minerals has been confirmed in tertiary basalts in the Septentrional Patagonian Andes, Neuquén (Vattuone et al., 2001). Similarly, barrerite, tetranatrolite/gonnardite, and paranatrolite were found in Cretacic/Jurassic metamorphosed basalts in greenschist, actinolite-pumpellyite, and prehnite-pumpellyite facies of the NW of the Chubut province; a later alkaline event generated adularia and other very low-grade alkaline minerals such as barrerite and offretite (Vattuone & Latorre, 2002 and Vattuone et al., 2005b); analcime and natrolite infilling fractures were found in Rucachoroi (Latorre et al., 1990).

The outcrop is located in 39°54'57" south and 71°03'10" west. These volcanites show an amygdaloid (3 cm diameter) structure and hydraulic fractures infilled and successively cemented by zeolites. These zeolites were studied by means of petrographic and electronic microscopes (MEB), EDS and XRD.

These amygdaloids show a symmetrical zoning. Albite has been found in the edges together with chabazite and phillipsite sometimes in contact with smectite. In the center of the amygdaloids, the zeolites are acicular. The alkaline zeolites are found with some calcic zeolites.

Chabazite and phillipsite crystals are almost 1 mm in diameter; they are pink colored and have a vitreous luster. Chemical analyses of phillipsite twinned crystals have a wide compositional Ca, K and Na variation.

In the center of amygdaloids a needle-shaped zeolite is sometimes distinguished in a parallel/radiated arrangement of natrolite, together with thomsonite, mesolite, scolecite and very scarce yugawaralite. In some cases, shows idiomorphic icositetrahedral crystals of cubic and orthorhombic analcime of 5 mm length.

The alkaline assemblage of chabazite, analcime, natrolite, Ca-K-Na phillipsite with thomsonite, mesolite, and scolecite, are low silica minerals that seem to be formed with very low grade temperature (Deer et al., 2004). Besides, in the rock, their association with albite, interstratified chlorite/smectite, pumpellyite, and very scarce yugawaralite might indicate temperatures close to 200°C.

Natrolite is ordered and sometimes, are intergrowths with thomsonite. This is the typical association indicated by Passaglia and Sheppard (2001). The lack of gonnardite and paranatrolite implies low temperatures and low H<sub>2</sub>O pressures that allow the formation of ordered natrolite. We believe that this mineral originated from the analcime, according to textural evidence (in cases, natrolite grows above analcime faces) and crystallizes from late alkaline fluids interacting with analcime in a deuteric alteration process.

### **References**

- Deer, W., Howie, R., Zussman, J., and Wise, W. (2004) *Rock Forming Minerals. Vol. 4B. Framework Silicates*. The Geological Society. 2nd Edition, London, 982 pp.
- Latorre, C., Vattuone, M., Massafiero, G., Lagorio, S., and Viviani, R. (1990) Analcima, Thomsonita, Laumontita y Natrolita en basaltos de Rucachoroi: mineralogía y condiciones de formación. *Revista de Geólogos Economistas*, publicación especial: 18-26.
- Passaglia, E. And Sheppard, R. (2001) The crystal chemistry of zeolites. In: *Natural Zeolites* (Bish, D. and Ming, D., editors). *Reviews in Mineralogy and Geochemistry*, 45: Washington DC, USA, Mineralogical Society of America, 69-115 pp.
- Vattuone, M., Crosta, S., Martínez Dopico, C. I., Gallegos, E., Berbeglia, Y., Lagorio, S. and Latorre, C. (2005a) Zeolitas alcalinas en los basaltos amigdaloides de las cercanías de Junín de los Andes, Neuquén. XVI Congreso Geológico Argentino, La Plata.

- Vattuone, M. and Latorre, C. (2002) Na-Mg offretite from Futalaufquen, Patagonian Andes, Argentina. Zeolite 6<sup>th</sup> International Conference on the occurrence, properties and utilization of natural Zeolites. Thessaloniki, Greece. 1: 382-383.
- Vattuone, M., Latorre, C., and Leal, P. (2001) Procesos de formación de paragénisis ceolíticas en el metamorfismo de muy bajo grado de las volcanitas paleógenas al sur de Confluencia, Neuquén, República Argentina. *Revista Geológica de Chile*, **28**, N°2, 3-22.
- Vattuone, M., Latorre, C., and Leal, P. R. (2005b) Polimetamorfismo de muy bajo a bajo grado en rocas volcánicas jurásicas al sur de Cholila, Chubut. Patagonia Argentina. *Revista Mexicana de Ciencias Geológicas*, **23**, N°2, 315-328 .

## **Results of the application of organo-mineral products from natural zeolites as substitutes of chemical fertilizers**

**M. Velázquez Garrido, J. A. Febles González, C. J. Louis, L. Gómez, B. Villavicencio, and J. Estrada**

*Research Center for Mining and Metallurgy; Havana City, Cuba; Email: febles@cipimm.minbas.cu*

A series of organo-mineral fertilizers were developed from a combination of Cuban natural zeolites, other minerals, and different organic sources. The fertilizers were designed according to the conditions of the soils and crops to reduce and/or to substitute for the traditional chemical fertilizers used in agricultural cultivations. The technology used to develop this series of fertilizers does not produce any type of residue.

In a greenhouse, experiments under controlled conditions were carried out to determine the effect of seven formulations of the organo-mineral products with different nutritional levels and with twelve types of Ferrosols soils which had different levels of fertility.

After determining the best composition of the organo-mineral product for the different levels of fertility for each soil type, we conducted field experiments under production conditions for beet and lettuce crops in an organoponic system and for tomatoes in a technological system in a cultivation house. We were able to compare the agronomic effects of our products, CIPIMM, to that of a fertilizer irrigation based on a current fertilizer of high solubility from the Chilean agro-chemicals firm SQM.

In organoponic systems, the organo-mineral product was applied to stonemasons in doses of 3 and 6 ton/ha; the results were compared to the traditional fertilizing system which recommends the application of high doses of organic matter. This activity is carried out annually.

Similarly, the organo-mineral product was applied to the cultivation of tomatoes under a technological system in a cultivation house at a rate of 6 ton/ha. This dose was determined because the tomato crop is very poor in nutrition; the comparative variant was the fertilizer irrigation with a formulation recommended by the Chilean firm SQM.

The results from the application of the organo-mineral product to the different crops demonstrated that there is no reduction in agricultural yield and that the quality of the agricultural products obtained is notably improved.

The proposed objectives were reached: we wanted to replace the chemical fertilizers with an organo-mineral product that is friendly to the environment; we started with natural minerals and a minimum of chemicals; we applied the product in a way that supplied nutrients and at the same time contributed to the gradual improvement of the chemical and physical properties of the soils, which were deteriorated because of continuous use and in some cases because of the indiscriminant use of chemical fertilizers.

## Adsorption of arsenite and arsenate with pre-treated Chilean zeolites

C. Vidal Cruz, M. E. Torres, and M. A. Mardones

Fundación Chile; Santiago, Chile; Email: cvidal@fundacionchile.cl

### Introduction

The surface of zeolites can be modified by adsorption of different types of molecules depending on the uses we want for it. In this work, the objective was the adsorption of inorganic forms of arsenic, arsenite, and arsenate. For this, modified zeolites were prepared by addition of a cationic surfactant. The modified zeolites formed an organic/mineral complex with the cationic surfactant, octadecylammonium acetate (ODA).

In the north of Chile high concentrations of arsenic in natural waters are found, surpassing the limits established by the national regulation.

### Experimental Methods

Natural zeolites, mordenite, were obtained from a mineral deposit located in the central zone of Chile. The modification of Chilean zeolites is carried out in a two-step process: 1) activation process with hydrochloric acid, and 2) the zeolite was treated with an aqueous solution of ODA dissolved with acetic acid. Another surfactant, HDTMA (hexadecyl trimethylammonium bromide), was also tested for modification. Adsorptions tests were batch design, kinetics, and isotherms were obtained for adsorption of arsenite and arsenate from stock solutions.

### Results and Discussion

The arsenic adsorption capacity of modified zeolites depends on the type of cationic surfactants and the grain size of the natural zeolites used. In Figure 1a, SMZ modified with ODA showed a greater adsorption of arsenate than the SMZ modified with HDTMA. The size of the zeolite has two important effects on the adsorption of arsenate. First, it diminishes the time to reach equilibrium by 50% (Fig. 1b), and the adsorption capacity increases in modified zeolites with ODA (Fig. 1a). The maximum adsorption capacity was 10.3 mg of As/g SMZ when the cationic surfactant was ODA and size of zeolite was 1 mm.

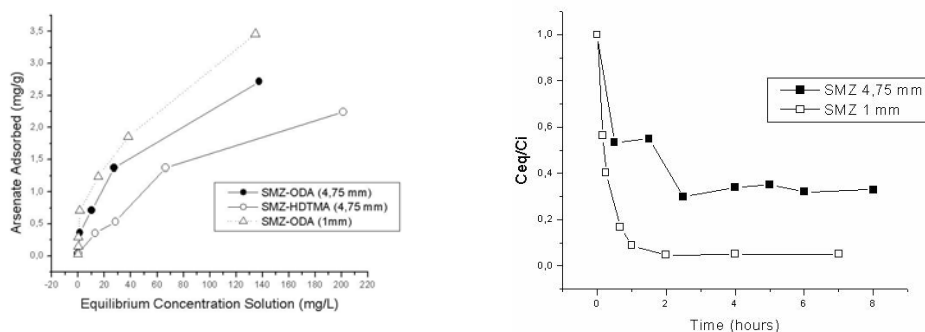


**Figure 1.** a) Isotherms of arsenate adsorption with SMZ-ODA and SMZ-HDTMA. b) Kinetics for arsenate adsorption with SMZ-ODA size 1 and 4.75 mm.

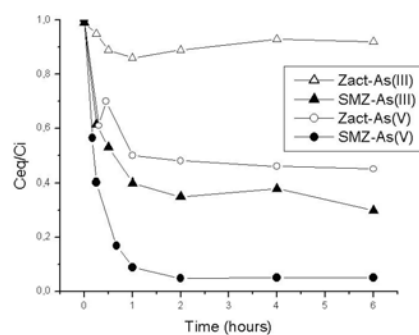
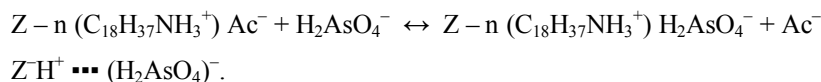


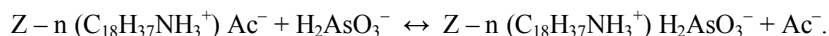
**Figure 2.** Adsorption of arsenate and arsenite in different pre-treated zeolites, activated zeolites (Zact) and modified zeolites (SMZ). Initial concentration was 10 mg/L, with a solid liquid ratio 1:30.

Results shown in Figure 2 demonstrated that the arsenate was adsorbed by both types of pre-treated zeolites, activated and modified ones. On the other hand, arsenite was only adsorbed by modified zeolites, SMZ-ODA.

The mechanisms proposed for adsorption of arsenic oxyanions are electrostatic attraction and ion exchange. The mechanism of arsenate adsorption in modified and activated zeolites is



The mechanism of arsenite adsorption in modified zeolites is



The results indicate that with increased relation  $Cl^-/As$ , arsenic adsorption decreased. The excess of chloride reduces the adsorption capacity of arsenic in SMZ. Even it is able to inhibit completely the arsenate adsorption when the chloride is 1500 times more concentrated, by competition effect.

**Table 1.** Effects of different ratio  $Cl^-/As$

Cl/As	mg As/g SMZ	Negative Effect (%)
0	10.31	
1	10.25	0.6
5	9.8	4.9
10	7.8	24.3
150	1.6	84.5
1500	0.016	99.8

## **Removal of lead ions by a fixed bed of clinoptilolite—the effect of the influent flow**

**N. Vukojević Medvidović, J. Perić, M. Trgo, and M. N. Mužek**

*University of Split; Split, Croatia; Email: nvukojev@ktf-split.hr*

### **Introduction**

The process of removal of lead ions from aqueous solutions by ion exchange is usually performed by the batch method or by the column method. This paper examines the performance in a column filled with natural zeolite clinoptilolite. It is becoming one of the most important natural inorganic cation exchangers, with high exchange capacity and selectivity for lead ions, and compatibility with the environment. The efficiency of the column method depends on dimensions of the glass column, particle size and depth of bed of clinoptilolite, and the flow and concentration of the aqueous solution of lead ions. This paper intends to optimise the flow of the influent solution with the time needed for exhaustion and with the capacity of the fixed bed of clinoptilolite.

### **Experimental Methods**

The natural zeolite sample originates from the Vranjska Banja deposit (Serbia and Montenegro) and contains more than 80% of clinoptilolite. The sample was analysed, milled, sieved to the particle size fraction of 0.6–0.8 mm, and dried at 60°C. The solution of lead ions with concentration of 212.15 mg/l was prepared by dissolving  $\text{Pb}(\text{NO}_3)_2$  in doubly distilled water. Experiments were carried out in a glass column with the inner diameter of 12 mm and a height of 500 cm, filled with 2.9 g (4.5 cm<sup>3</sup>) of the clinoptilolite sample to the bed height of 40 mm. Isothermal experiments were performed at the constant initial concentration and bed depth with changes of flows through the fixed bed of 1, 2, and 3 ml/min. After each service cycle, the regeneration was performed with the solution of  $\text{NaNO}_3$  at constant flow and concentration.

### **Results and Discussion**

The experimental results for the column method are shown by breakthrough curves, as concentration in the effluent versus bed volume (BV) (Fig. 1), or time (Fig. 2). In Figure 1 it is clear that for all flow rates through the fixed bed, the breakthrough points appear to have very close values of BV; i.e., volumes of treated solution. This means that the breakthrough capacities for the flow rates examined also have similar values. The time needed for reaching the breakthrough point decreases at higher flow rates, which is shown in Figure 2; moreover, the same volume of the lead ions solution can be treated in significantly shorter times. At higher flow rates the efficiency of the fixed-bed and empty-bed contact time (EBCT) decreases, while the mass transfer zone (MTZ) increases. These parameters are calculated from the breakthrough curves and represent main parameters for scaling up the process.

The application of empirical models to the experimental results helps define the mathematical dependence of process parameters and makes it possible to predict breakthrough curves for other experimental conditions without experimental performance. One of the empirical models used, for the column method, is the model by Yoon and Nelson which was not found in the literature for experiments with zeolite as an ion exchanger or adsorbent (Lin and Liu, 2003).

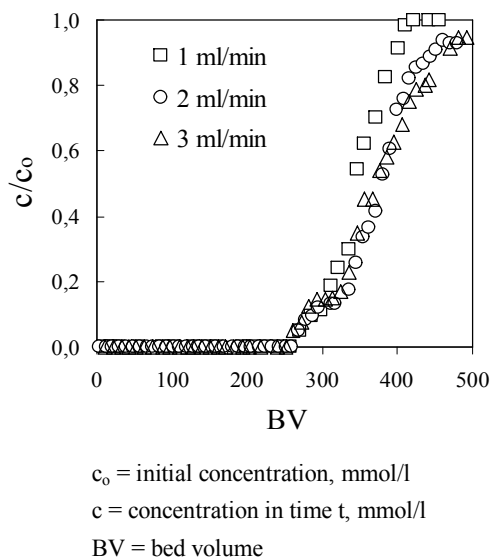


**Figure 1.** Breakthrough curves of lead removal for different flows expressed as  $c/c_0$  vs. BV.

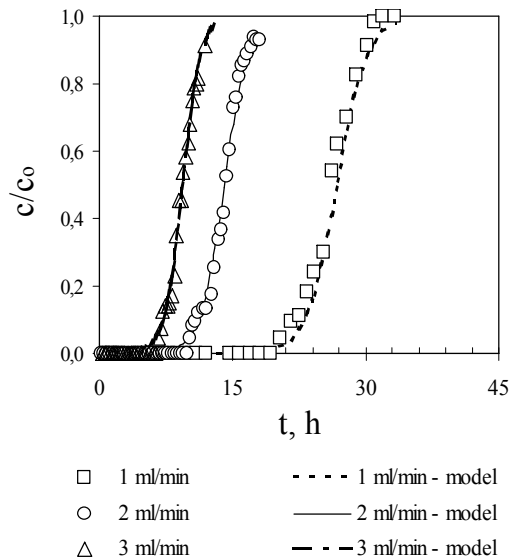


**Figure 2.** Breakthrough curves expressed as  $c/c_0$  vs. time. Fitting of experimental curves (points) with curves obtained from Yoon and Nelson model (lines).

The Yoon and Nelson model for a single component system is expressed by the equation

$$\ln [c/(c_0 - c)] = k_{YN}(t - \tau) \quad (1)$$

where  $k_{YN}$  = rate constant,  $\text{min}^{-1}$  and  $\tau$  = breakthrough time when  $c/c_0$  equals 0.5. The linear dependence of  $\ln[c/(c_0 - c)]$  versus time  $t$  indicates satisfactory fitting of experimental points to the model, and from these lines the parameters of the model ( $k_{YN}$  and  $\tau$ ) can be calculated. Insertion of calculated parameters into Equation 1 gives modelled breakthrough curves that are shown by lines in Figure 2. The excellent fit of experimental and modelled curves means that the equation of Yoon-Nelson can be used for predicting breakthrough curves for lead ion removal by fixed bed of clinoptilolite for different solution flows (Vukojević et al., in press 2006).

## References

- Lin, S.H. and Liu, J.M. (2003) Hydrofluoric acid recovery from waste semiconductor acid solution by ion exchange. *Journal of Environmental Engineering*, **129**, 472–478.  
 Vukojević Medvidović, N., Perić, J. and Trgo, M. (in press 2006) Column performance in lead removal from aqueous solutions by fixed bed of natural zeolite-clinoptilolite. *Separation and Purification Technology*.



## Dehydration/rehydration-induced structural phase transitions in natrolite

H.-W. Wang and D. L. Bish

*Indiana University; Bloomington, Indiana, USA; Email: hw7@indiana.edu*

In the 74 years since Hey (1932) studied natrolite dehydration, various authors have shown that natrolite converts to so-called  $\alpha$ -metanatrolite between 250°C and 350°C. However, dehydration involves both continuous and discontinuous processes, the structural details of which are still not completely understood. We have studied the dehydration process using temperature-controlled X-ray diffraction (XRD) with an Anton-Paar TTK-450 heating stage on a Bruker D8 diffractometer (Cu K $\alpha$  radiation) and a Vantec position-sensitive detector. Dehydration was also monitored with a TA Instruments simultaneous thermogravimetric analysis (TGA)/differential scanning calorimetric instrument using a dry N<sub>2</sub> gas flow. The temperature-induced response

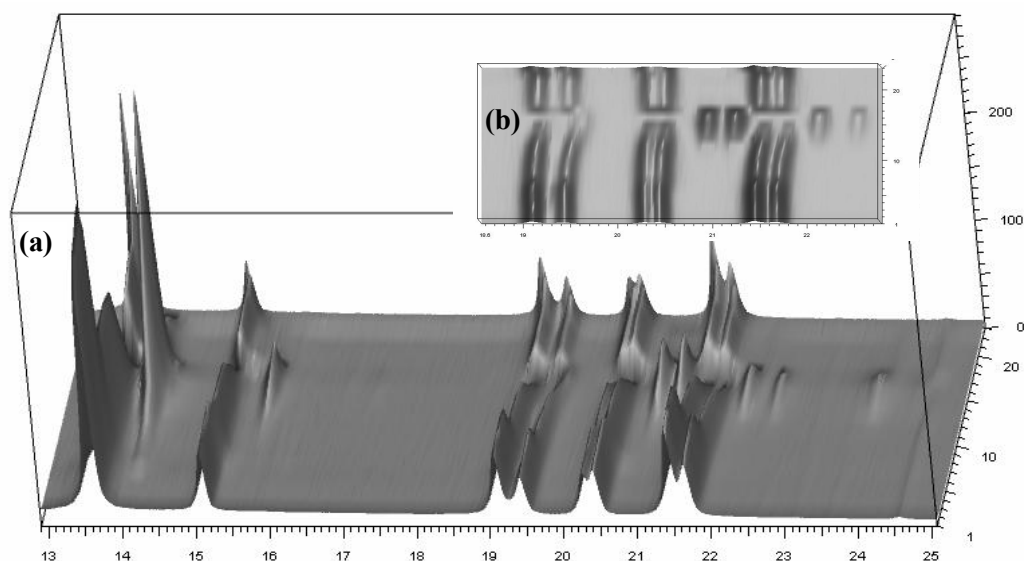


**Figure 1.** (a) 3D-XRD diffraction patterns for natrolite as a function of temperature:  $x$ ,  $y$ , and  $z$  axes represent  $\sim 13$ – $25^\circ 2\theta$ , intensity (cps), and temperature (23–350–23°C, #1–23), respectively. Patterns 1 and 23 represent 23°C, in air; #'s 2–22 represent 23–350–23°C in vacuum. (b) Expanded view of 3D-XRD patterns from  $\sim 18.5$ – $22.5^\circ 2\theta$ , showing peak position and intensity changes; dehydrated natrolite first appeared at  $\sim 275^\circ\text{C}$ , and dehydration was completed by  $350^\circ\text{C}$ .

of the crystal structure of natural natrolite (N. Ireland,  $a = 18.3122(5) \text{ \AA}$ ,  $b = 18.6286(4) \text{ \AA}$ ,  $c = 6.5932(2) \text{ \AA}$ , and  $V = 2249.16(1) \text{ \AA}^3$ —very similar to Neuhoff et al. (2002) NAT002, Marraat, W. Greenland) and the water adsorption capacity were investigated via X-ray powder diffraction and DSC/TGA thermal analyses during repeated dehydration/hydration excursions.

XRD data showed only gradual minor changes in peak positions and intensities with stepwise heating from 23°C to  $\sim 250^\circ\text{C}$ , reflecting a gradual decrease in unit-cell parameters (Fig. 1; under vacuum;  $25^\circ\text{C}$  or  $50^\circ\text{C}$  increment). At  $\sim 250^\circ\text{C}$ , XRD data showed a sudden decrease in peak intensities, at the temperature at which the TGA weight loss curve began an abrupt drop indicating the onset of rapid dehydration (Fig. 2). There is only one independent H<sub>2</sub>O site in the natrolite unit cell and only one abrupt weight loss. At  $275^\circ\text{C}$ , the XRD pattern showed discrete, discontinuous shifts in peak positions (Fig. 1b). Diffraction peaks were also broadened, likely due to structural strain caused by the loss of H<sub>2</sub>O molecules and the significant modification of the structure. By  $350^\circ\text{C}$ , the dehydrated phase, often referred to as  $\alpha$ -metanatrolite, had replaced the lower-temperature phase. As documented in the literature, this phase has different symmetry and unit-cell parameters considerably shortened in comparison with hydrated natrolite.

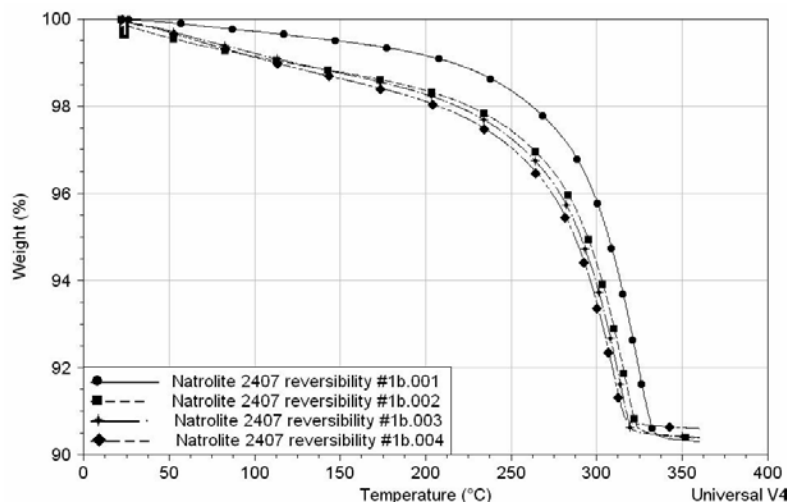


**Figure 2.** TGA curves for natrolite showing weight loss due to evolution of  $\text{H}_2\text{O}$  during repetitive heating (lines 001, 002, 003, and 004 represent the first through fourth measurements).

modified during each dehydration event. Although dehydration is accompanied by at least three phenomena, namely evolution of  $\text{H}_2\text{O}$  molecules from the framework, change in position of extraframework cations, and distortion of the tetrahedral Si/Al framework, the dehydration reaction appears to be largely reversible. Our diffraction results illustrate that natrolite dehydration involves *both* first- and second-order displacive phase transitions; the beginning of the dehydration process is second order, but dehydration above  $275^\circ\text{C}$  in vacuum is first order, giving rise to abrupt, discontinuous structural changes. Rietveld refinements with X-ray powder diffraction data collected at each temperature step are underway to provide a complete structural picture of the natrolite dehydration and rehydration processes.

## References

- Alberti, A. (1983) How the structure of natrolite is modified through the heating-induced dehydration. *Neues Jahrbuch für Mineralogie Monatshefte*, **3**, 135–144.
- Gottardi, G. and Galli, E. (1985) Natural Zeolites. Springer-Verlag, Berlin, p. 35–56.
- Neuhoff, P.S., Kroeker, S., Du, L.-S., Fridriksson, T. and Stebbins, J.F. (2002) Order/disorder in natrolite group zeolites: A  $^{29}\text{Si}$  and  $^{27}\text{Al}$  MAS NMR study. *American Mineralogist*, **87**, 1307–1320.
- Peacor, D.R. (1973) High-temperature, single-crystal X-ray study of natrolite. *American Mineralogist*, **58**, 676–680.

TGA data confirmed that natrolite that has been dehydrated at  $360^\circ\text{C}$  has a strong affinity for  $\text{H}_2\text{O}$  molecules. A single specimen was heated on the TGA instrument to  $360^\circ\text{C}$ , returned to room conditions and placed in 100% relative humidity atmosphere for 12 hours, and then reheated on the TGA instrument. This process was repeated four times to assess the degree of reversibility of the dehydration process. The weight loss for the first through the fourth heating experiments was 9.50%, 10.03%, 9.20%, and 9.37% respectively (Fig. 2). These results demonstrate that repeated dehydration/hydration did not greatly influence the total  $\text{H}_2\text{O}$  adsorption capacity even though the framework structure was significantly

## Temperature dependence of heat in hydration of natrolite and analcime

J. Wang and P. S. Neuhoff

University of Florida; Gainesville, Florida, USA; Email: jiewang@ufl.edu

Reversible dehydration of intracrystalline water in zeolites is an important consideration for assessing their stability, particularly at elevated temperatures and pressures. Derivation of thermodynamic properties of (de)hydration from phase equilibria requires prior knowledge of the heat capacity change across the hydration reaction ( $\Delta C_{p,\text{hyd}}$ ) in order to reduce the number of unknown variables (Bish and Carey, 2001). However, experimental determination of  $\Delta C_{p,\text{hyd}}$  is difficult because measurements at elevated temperatures often contain contributions from the enthalpy of dehydration (Carey, 1993). Statistical-mechanical reasoning is often used to suggest that  $\Delta C_{p,\text{hyd}}$  is independent of temperature (Barrer, 1978; Carey, 1993), permitting application of  $\Delta C_{p,\text{hyd}}$  determined at relatively low temperatures where dehydration is not an issue. In this study, we have explicitly tested this assumption through measurement of  $C_p$  for hydrated and dehydrated zeolites and for temperature dependence of the enthalpy of hydration.

We focused our study on natrolite ( $\text{Na}_2\text{Al}_2\text{Si}_3\text{O}_{10}\cdot 2\text{H}_2\text{O}$ ) and analcime ( $\text{NaAlSi}_2\text{O}_6\cdot \text{H}_2\text{O}$ ), two common rock-forming zeolites that are chemically and structurally less complex than other zeolites due to the presence of only one extraframework cation ( $\text{Na}^+$ ) and one crystallographically-distinct water site. Handpicked separates of natrolite and analcime were ground and sieved to a 20–40  $\mu\text{m}$  size fraction. The dehydration and rehydration experiments were conducted on a Netzsch STA 449C Jupiter simultaneous thermal analysis system at the University of Florida. This system simultaneously records differential scanning calorimetry (DSC) and thermogravimetric (TGA) signals, which allows the DSC signal to be interpreted directly in terms of water loss or gain to the sample as measured by TGA (Neuhoff, 2003).

Heat capacity measurements on homologous hydrated and dehydrated natrolite and analcime samples were obtained by scanning DSC measurements using synthetic sapphire as a  $C_p$  standard (Fig. 1a). Absence of discernable mass changes was taken as an indication that the DSC signal contained only contributions from the  $C_p$  and not enthalpies of dehydration. Figure 1b shows  $\Delta C_{p,\text{hyd}}$  for natrolite and analcime above 298.15 K. In analcime,  $\Delta C_{p,\text{hyd}}$  is nearly constant with temperature, whereas in natrolite a prominent glass-type transition (e.g., Hemingway and Robie, 1984) is present below 373.15 K. Above this transition,  $\Delta C_{p,\text{hyd}}$  is essentially constant until the onset of hydration at 403.15 K.

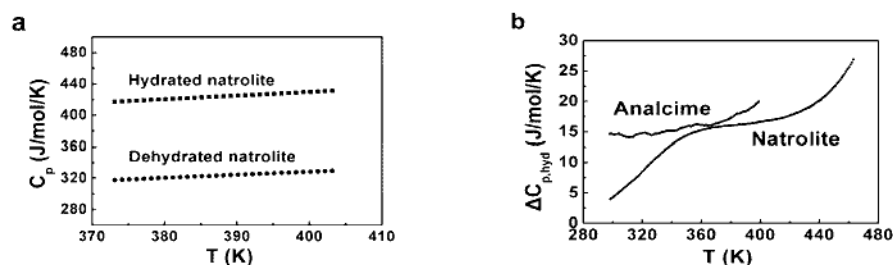


**Figure 1.** (a)  $C_p$  of hydrated and dehydrated natrolite between 373.15 and 403.15 K. (b)  $\Delta C_{p,\text{hyd}}$  of hydration of natrolite and analcime as a function of temperature

Determination of the enthalpy of hydration,  $\Delta H_{\text{hyd}}$ , over a range of temperatures permits an alternative means of assessing  $\Delta C_{p,\text{hyd}}$ . This was accomplished by performing isothermal heat of gas immersion experiments by DSC. The peak area of the DSC curve is proportional to  $\Delta H_{\text{hyd}}$ . Natrolite and analcime were rehydrated at constant water vapor pressure ( $\sim 1200$  Pa) at several temperatures between 373.15 and 473.15 K (Fig. 2). Natrolite fully rehydrated in 2–3 hours, permitting direct determination of the integral heat of hydration. Analcime rehydrated so slowly that it was impossible to measure the integral heat of hydration; consequently, the partial molar heat of hydration was calculated by comparing the variation of the DSC signal to the first derivative of the mass gain. Because a solid solution between hydrated and dehydrated analcime appears to be ideal (Ogorodova et al., 1996), these results were taken equal to the integral heat of hydration. Although measurements of  $\Delta H_{r,T,P}$  for analcime are accompanied by relatively large uncertainties (Fig. 2), the temperature dependence of our results is consistent with  $\Delta C_{p,\text{hyd}}$ , shown above, and  $\Delta H_{\text{hyd}}$  between 403.15 and 463.15 K of about  $-87.5$  kJ/mol- $\text{H}_2\text{O}$ . The temperature dependence of  $\Delta H_{r,T,P}$  in natrolite (Fig. 2) is consistent with  $\Delta C_{p,\text{hyd}}$  for hydration of  $72.4$  J/mol/K. This is about 4.5 times the value determined by direct measurement of  $C_p$  for the phases in the reaction, and it suggests a temperature-independent excess contribution to  $\Delta C_{p,\text{hyd}}$  arising from solvus behavior in natrolite. This behavior is not predicted by the statistical-mechanical model, and it indicates a need for direct measurements of heat capacities and enthalpies of hydration in zeolites.

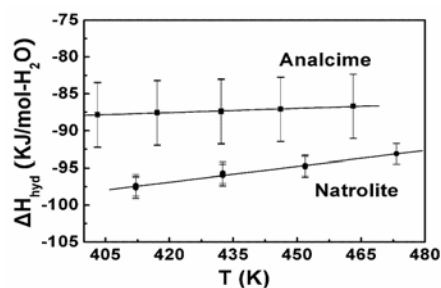


**Figure 2.**  $\Delta H_{\text{hyd}}$  of hydration of analcime and natrolite at constant water vapor pressure ( $\sim 1200$  Pa) as a function of temperature. The relationship between  $\Delta H_{\text{hyd}}$  and temperature is essentially linear, and the slopes calculated as  $\Delta C_{p,\text{hyd}}$  are  $19.1$  J/mol/K and  $72.4$  J/mol/K for analcime and natrolite, respectively.

## References

- Barrer, R.M. (1978) *Zeolites and clay minerals as sorbents and molecular sieves*. Academic Press, London, 497 pp.
- Bish, D.L. and Carey, J.W. (2001) Thermal behavior of natural zeolites. Pp. 403–452 in: *Natural Zeolites: Occurrence, Properties, Applications* (D.L. Bish and D.W. Ming, editors). Reviews in Mineralogy and Geochemistry **45**, Mineralogical Society of America, and Geochemical Society.
- Carey, J.W. (1993) The heat capacity of hydrous cordierite above 295 K. *Physics and Chemistry of Minerals*, **19**, 578–583.
- Hemingway, B.S. and Robie, R.A. (1984) Thermodynamic properties of zeolites: Low temperature heat capacities and thermodynamic functions of phillipsite and clinoptilolite. Estimates of the thermochemical properties of zeolitic water at low temperatures. *American Mineralogist*, **69**, 692–700.
- Neuhoff, P.S. (2003) Simultaneous thermal analysis techniques for determining the energetics of water in mineral hydrates. *Eos (Transactions, American Geophysical Union), Fall Meeting Supplement*, **84**, Abstract V51H-0384.
- Ogorodova, L.P., Kiseleva, I.A., Mel'chakova, L.V., Belitskii, I.A. and Fursenko, B.A. (1996) Enthalpies of formation and dehydration of natural analcime. *Geochemistry International*, **34**, 980–984.

## **Zeolites on fissures of crystalline basement rocks in the Swiss Alps**

**T. Weisenberger and K. Bucher**

*Albert-Ludwigs-University Freiburg; Freiburg, Germany; Email: tobias.weisenberger@minpet.uni-freiburg.de*

A number of zeolite species have been discovered from Alpine fissures in crystalline basement rocks of the Swiss Alps. The zeolites typically overgrow earlier minerals of the fissure assemblages, but zeolites also occur as single stage fissure deposits in gneiss and granite. A systematic study of zeolite samples in the collections of Swiss Natural History Museums showed that the majority of finds originate from three main areas. Two of them are located in gneiss and granite of the southern Aar Massif and one in granite-gneiss of the Pennine nappes of the Ticino area. In addition to these known localities from the surface, tunnel construction in the Alps provided excellent zeolite material from fissures in basement rocks. At present, a new 53-km-long Gotthard railroad base tunnel is being excavated and offers the unique opportunity to study the in situ formation of low-temperature minerals.

Reported zeolite species from Alpine fissures in gneiss and granite include chabazite, heulandite, laumontite, scolecite, stellerite, and stilbite. The zeolites often occur with other species in the fissures including quartz, apophyllite, and chlorite. Earlier minerals in zeolite-bearing fissures may include prehnite, adularia, fluorite, hematite, and others.

Particularly spectacular are the extensive occurrences of laumontite vein fillings in the new Gotthard rail tunnel. Laumontite covers fissure walls as dense mats. Up to 1 cm long, white needles of laumontite are the last minerals that precipitated from hot water in the fissures and cavities. It overgrows primary fissure quartz and chlorite coatings of the fissure walls. Locally, apophyllite overgrows laumontite as euhedral crystals, thus it is the last mineral formed in the fissures. Laumontite is the absolutely dominant zeolite of the tunnel fissures, but the mineral is rarely preserved in surface outcrops where chabazite and stilbite dominate. Laumontite in the tunnel forms by precipitation from alkaline hot water that acquired its chemical composition by reaction with primary plagioclase at temperatures of about 160°C. The present day rock temperature in the tunnel is < 44°C. Alpine cooling and exhumation rates for the Aar Massif suggest that fissure laumontite formed about 2–5 Ma ago.

## **Electro–physical and optical properties of natural zeolites (clinoptilolite) from Armenia and USA (preliminary results)**

**H. N. Yeritsyan, S. K. Nickoghosyan, A. A. Sahakyan, V. V. Harutunyan, E. A. Hakhverdyan, and N. E. Grigoryan**

*Yerevan Physics Institute; Yereva, Armenia; Email: grant@yerphi.am*

### **Introduction**

Among other physical parameters, the measurements of specific electric conductivity ( $\sigma$ ), dielectric, and optical properties of zeolites have a great interest. The frequency measurements of these parameters are carried out in a variable electric field to avoid various types of undesirable effects such as polarization, relaxation processes, etc.

### **Experimental Methods**

Measurements of electro-physical parameters were carried out on pressed samples. The samples are made of zeolite powder (with grain size of 50 micron). The zeolite powder was pressed into pellets at pressure of 150 kg/cm<sup>2</sup>. The pellets were then mechanically cut out into rectangular samples with an area of approximately 30 mm<sup>2</sup> and thickness of 2–3 mm. On both sides of the sample surfaces, silver contacts were made. The sample was stored at normal atmospheric pressure and contains about 11.2% water of its weight. The sample temperature was measured by germanium diode with accuracy of  $\pm 0.2$  K.

It should be mentioned that during the period of storage, the relative change of weight of samples (because of changing weather conditions) did not surpass 0.5%. Absolute accuracy of weight was 0.05 mg. The accuracy of measurement of  $\sigma$  is about 5%. An installation was developed for measurements of dielectric losses in the samples with various contents of clinoptilolite and molecules of water. The installation allows measuring of dielectric permittivity  $\epsilon = \epsilon' - i\epsilon''$  of samples in the frequency range from 200 Hz to 1 MHz, and amplitude of a sinusoidal voltage equal to 0.1 V on the sample contacts.

Pressed samples with different contents of clinoptilolite and KBr have been prepared for optical absorption measurements. The optimal thickness (350 mm), diameter (20 mm), and ratio of clinoptilolite to KBr (1:10) have been defined for obtaining more accurate results for measurements.

For luminescence measurements, an optical scheme on the basis of standard 1 kW Xenon lamp and SF-26 spectrophotometer (Russian production) was carried out. A bandwidth at 280–400 nm range was applied for excitation. Spectral registration was carried out by photomultipliers in the 300–1000 bandwidth range on the single photon accounting mode.

The tested measurements on zeolite samples give good accordance with literature data.

### **Results and Discussion**

It is known that zeolites have a large forbidden energy gap ( $\sim 7$  eV) and conductivity close to values for bad dielectrics. On the other hand, the prominent feature of conductivity for dielectric consists that after switching on a constant electric field, the current passing through dielectric in due course decreases. At the initial moment through a circuit, passes quickly falling current of displacement. This current disappears during near the constant of time RC that is very small (much smaller than one second). However, the current continues to fall with electrical frequency, continuing for several minutes to hours. The slowly varying component of current caused by redistribution of free charges in the volume of dielectric is known as absorption current. The absorption current is caused by absorption of free current carriers in the volume of dielectric: a part of them are trapped on defects of the crystal lattice that grasps and hold them. Eventually, when all traps are filled by current carriers, the absorption current disappears, leaving only a current independent of time which is caused by charge carriers moving from one electrode to another.

The conductivity of sample at temperature 24°C in electric field strength of  $(1 \div 2)$  V/cm is measured after high temperature annealing (for preparing of ohmic contacts). In order to study the influence of humidity on conductivity, the samples are located a closed vessel containing saturated water vapors at temperature 24°C and

are stored there up to 4–5 days to achieve full saturation. Further, samples are removed, and in a dynamic mode in air, the conductivity is measured depending on time.

The measurement results show that both samples during 3 hours come to an equilibrium condition when conductivity does not depend on time. In other words, dehydration takes place and is accompanied by reduction of conductivity from  $1.2 \cdot 10^{-5} \text{ Ohm}^{-1} \text{ cm}^{-1}$  up to  $6.77 \cdot 10^{-9} \text{ Ohm}^{-1} \text{ cm}^{-1}$  for the Armenian sample, and from  $2.27 \cdot 10^{-6} \text{ Ohm}^{-1} \text{ cm}^{-1}$  up to  $3.96 \cdot 10^{-9} \text{ Ohm}^{-1} \text{ cm}^{-1}$  for the American sample.

Values of conductivity of both samples with various degrees of dehydration are given in Table 1. It is typical that the American sample is less sensitive to water content in comparison to the Armenian sample. Besides, the conductivity for the American sample is much lower, and with increase of a degree of dehydration, this difference decreases. On the other hand, growth of a degree of dehydration results in reduction of conductivity, i.e., presence of water in zeolite increases its instability. However, the more stable character of the American sample in comparison with the Armenian sample is caused not only by a lower content of water, but also due to another cation structure with more stable positions in an elementary cell. The rather high stability of the American sample is also probably caused by larger molar ratio Si/Al in comparison with the Armenian one; that also determines its conductivity. It is known that with the increase of this ratio that the conductivity of the sample decreases, which also takes place in our case.

One can conclude from the given results that all features for Armenian and American samples are typical for zeolites—only the rates of corresponding dependences are different. For example: the intensity of luminescence bands for Armenian zeolites differs from American samples concerning the spectral range, the increased water content decreases optical transmission and luminescence abilities of the samples, while the increasing of water concentration increases conductivity and dielectric parameters.

In all cases these results are considered as preliminary and further detailed investigations are necessary for precise conclusions.

Some values of specific electric conductivity at  $T = 24^\circ\text{C}$  for Armenian ( $A_{11}$ ) and American ( $A_{21}$ ) natural zeolites with different degrees of dehydration  $d_h = (m_0 - m)100\%/m_0$ , where  $m_0$  is mass of the sample with maximal water content, are presented in Table 1.

**Table 1.** Some values of zeolites' specific conductivity

Samples	$\sigma$ (in $\text{Ohm}^{-1} \text{ cm}^{-1}$ ) for corresponding degree of dehydration (in %)		
$A_{11}$	$1.2 \cdot 10^{-5}$ for $d_h = 0$	$6.77 \cdot 10^{-9}$ for $d_h = 9.22$	$1.5 \cdot 10^{-11}$ for $d_h = 14.8$
$A_{21}$	$2.275 \cdot 10^{-6}$ for $d_h = 0$	$3.96 \cdot 10^{-9}$ for $d_h = 7.47$	$1.21 \cdot 10^{-11}$ for $d_h = 13.3$

## **Clinoptilolite in volcanic neck structure near Kralevo deposit, Haskovo region (Bulgaria)**

**A. Yoleva<sup>1</sup>, O. Petrov<sup>2</sup>, S. Djambazov<sup>1</sup>, O. Malinov<sup>3</sup>, and D. Stoycheva<sup>1</sup>**

<sup>1</sup>*University of Chemical Technology and Metallurgy; Sofia, Bulgaria; Email: djam@uctm.edu*

<sup>2</sup>*Bulgarian Academy of Sciences; Sofia, Bulgaria*

<sup>3</sup>*GRAVELITA Ltd.; Sofia, Bulgaria*

### **Introduction**

The studied clinoptilolite rock is from a deposit at the northernmost part of the area of zeolitized tuffs in Eastern Rhodopes (southeast of the village of Kralevo, Haskovo district). The zeolitic rocks are composed mainly of clinoptilolite and are an altered product in the newly mapped polyphase neck structure in rhyolitic vitroclastic sediments related to the second acidic Paleogene volcanism (O<sub>3</sub>). Studying a typical section of O<sub>3</sub> in this region, are two clinoptilolite varieties: less stable (< 550°C) Ca-clinoptilolite and a more stable (up to 700°C) high-silica K-Ca clinoptilolite.

The zeolitic raw material near Kralevo village is of economic value and, thus, the aim of this work is to qualitatively and quantitatively study the clinoptilolite there using XRD, DTA, TG and DTG, IR-spectroscopy, and a polarizing microscope, as well as to establish the structural behavior of the natural zeolite under thermal treatment and examine its ion exchanged forms.

### **Experimental Methods**

The clinoptilolite sample is studied by AES-ICP, DTA/TG analysis on an STA 409C apparatus from 20–1000°C with a step of 10°C/min, and by IR-spectroscopy using a “Perkin-Elmer Spectrum 1000” in the range 4000–400 cm<sup>-1</sup>. The texture and mineral composition of the zeolitic rock are observed under a polarizing microscope in thin section. The content and structure of clinoptilolite is studied by quantitative and qualitative powder XRD performed on a DRON 3M diffractometer (horizontal Bragg-Brentano goniometer; Fe-filtered Co-K<sub>α</sub> radiation). After sedimentation of the ground zeolitic rock, the fine fraction from 10–60 μm is thermally treated at temperatures of 200, 350, 400, 500, 600, and 700°C for 4 h at each step and studied by XRD. A step-scan technique was applied with a step of 0.02 °2θ and 3 s per step in the range 8–40 °2θ. The ion exchange procedures are performed with 1N solutions of NH<sub>4</sub>Cl, Pb(OCOCH<sub>3</sub>)<sub>2</sub> and SrCl<sub>2</sub>, for 72 h at room temperature and for 4 h at 100°C. Then the samples were washed and dried.

### **Results and Discussion**

A detailed geological mapping in the volcanogenic-sedimentary complex near Kralevo village revealed for the first time a series of volcanic neck tuffaceous buildings, one of which is the studied object. The rock is built by clasts of quartz, sanidine, and plagioclase, and the zeolitization is mainly on the volcanic glass shards.

The XRD pattern of the studied zeolite sample reveals clinoptilolite as the major phase with some plagioclase and opal-C phase. The quantitative analysis using a standard from Beli plast deposit (Kurdjali district) showed that the clinoptilolite content is about 75 wt%. Analysis of isolated fractions showed that the 10–60 μm fraction is richest in zeolite component. This fraction was subjected to thermal treatment (200, 300, 350, 400, 500, 600, and 700°C) in order specify the clinoptilolite variety. As seen from Figure 1, a major part of the studied clinoptilolite is stable up to 700°C. Checking the chemical analysis of a representative zeolite sample (Table 1) we come to the conclusion that the zeolitic phase is high silica K-Ca clinoptilolite. However, a gradual slight amorphization occurs with temperature, indicated by an increase in the intensity of the broad peak near 4.06 Å, which is characteristic for opal-C.

DTA/TG analysis from room temperature up to 1000°C shows that at around 135°C a significant endothermal effect is registered which is related to the release of almost all of the H-bonded water molecules. The total TG loss is about 11.5 wt%.



**Table 1.** Chemical analysis of clinoptilolite rock from Kralevo deposit, NE Rodopes (Bulgaria)

Oxides	SiO <sub>2</sub>	Al <sub>2</sub> O <sub>3</sub>	TiO <sub>2</sub>	Fe <sub>2</sub> O <sub>3</sub>	MgO	CaO	Na <sub>2</sub> O	K <sub>2</sub> O	ΣH <sub>2</sub> O
wt%	71.35	12.72	0.20	0.90	0.94	2.20	0.94	3.94	12.79

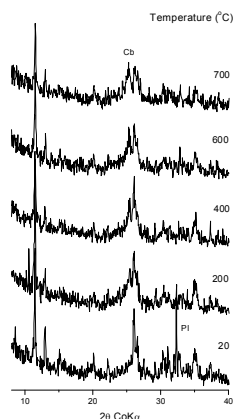


**Figure 1.** XRD patterns of the initial and heated clinoptilolite from Kralevo deposit (Bulgaria)

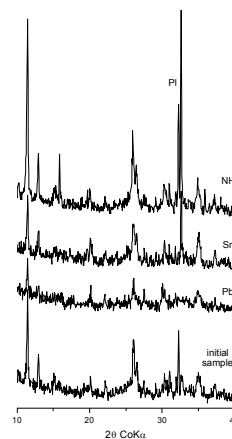


**Figure 2.** XRD patterns of the initial and ion-exchanged forms of the studied clinoptilolite

The IR data shows peaks of H-bonded H<sub>2</sub>O (3645 cm<sup>-1</sup> and 1660 cm<sup>-1</sup>). Other vibrations recorded are the Si-O-Si asymmetric stretch at 1000–1100 cm<sup>-1</sup>, the Si-O-Si symmetric stretch at 800 cm<sup>-1</sup>, and the O-Si-O band at 475 cm<sup>-1</sup>.

The XRD patterns of NH<sub>4</sub>, Sr, and Pb exchanged forms of Kralevo clinoptilolite are presented in Figure 2. Profound intensity changes are apparently connected with eager cation exchange. This material is useful as a sorbent.

The studied polyphase neck structure is characterized by K-Ca clinoptilolite (~ 75 wt%) rocks, which preceded the postvolcanic hydrothermal acts described by Djourova and Aleksiev (1988).

## The determination of immersion heats and investigation of amphoteric effect of some natural zeolites (Turkey)

E. Yörükoğulları, M. Sakızcı, and H. Özçelik

*Anadolu University; Eskisehir, Turkey; Email: eyorukog@anadolu.edu.tr*

### Introduction

Immersion calorimetry is a powerful technique for the characterization of microporous solids. When a solid is immersed into a liquid, it gives some amount of heat. This measured heat is called immersion heat,  $Q$  (J/g). Zeolites are minerals that give relatively high immersion heat. As a result of this property, zeolites can find applications in areas such as solar energy storage and agriculture. In addition, the zeolite tendency to neutralize an acidic or basic aqueous medium is known as amphoteric effect. Based on their amphoteric character, zeolites can also be used in medical applications, etc.

The aim of this study is to determine the immersion heats of some natural zeolites and investigate the amphoteric effect of their behavior in salt solutions.

### Experimental Methods

Clinoptilolite tuffs, obtained from Gördes, Bigadic, and Sivas regions, Turkey, containing about 90% clinoptilolite, were used in this study. The tuffs were finely ground and sieved to  $<100\ \mu\text{m}$ . These clinoptilolite samples, after being cleaned with 1 N HCl solution, were characterized using XRD, XRF, DTA-TGA, and DSC standard methods. Then, they were dehydrated at  $110^\circ\text{C}$  for 16 h and at  $180^\circ\text{C}$  for 1 h. The heats of immersion (in water) of dehydrated clinoptilolite tuffs were determined with a Calvet-type C-80 calorimeter. In addition, the amphoteric effects of those zeolites were investigated by measuring the pH values in 4% NaCl solution after a period of 15 days. The experimental values are listed in Table 1.

**Table 1.** The immersion heats and pH values measured in salt solution of natural zeolites

Samples (washed with 1 N HCl solution)	T ( $^\circ\text{C}$ ) – dehydration period (h)	Q (J/g)	pH (initial-after 15 days)
Gördes clinoptilolite	$110^\circ\text{C}$ (16 h)	55.5062	8.00–6.50
	$180^\circ\text{C}$ (1 h)	562.7808	
Bigadic clinoptilolite	$110^\circ\text{C}$ (16 h)	45.8812	8.00–7.30
	$180^\circ\text{C}$ (1 h)	403.6190	
Sivas clinoptilolite	$110^\circ\text{C}$ (16 h)	42.4264	8.00–6.60
	$180^\circ\text{C}$ (1h)	305.3503	

Q: Immersion heat

### Results and Discussion

As shown in Table 1, the immersion heats of clinoptilolite samples dehydrated at  $180^\circ\text{C}$  for 1 h were too high in comparison to those obtained for clinoptilolite samples dehydrated at  $110^\circ\text{C}$  for 16 h. The pH of the salt solutions changed from basic to neutral after addition of the zeolite. In conclusion, clinoptilolite samples dehydrated at  $180^\circ\text{C}$  can be proposed as heat exchanger, and, due to their amphoteric effects, natural zeolites can be used for many applications.

## Using natural zeolites as deicers on highways

E. Yörükoğulları and M. Sakızcı

Anadolu University; Eskisehir, Turkey; Email: eyorukog@anadolu.edu.tr

### Introduction

In winter freezing occurs especially on highways causing many fatal traffic accidents and high cost damages. The cheapest and the easiest way to prevent freezing is to use salt (NaCl). Salt can be spread on roads easily by several vehicles and can melt the ice but the harmful effect of salt to roads and bridges is corrosion.

The aim of this study is using natural zeolites that have wide beds in Turkey as deicers on highways in winter. As a result, the harmful effect of salt to underground water, vehicles, roads, and planted fields can be reduced.

### Experimental Methods

Natural zeolite (clinoptilolite) samples were obtained from the Gördes, Bigadic, and Sivas regions in Turkey. The samples correspond to approximately 1–2 mm size fraction. Properties of those zeolites were previously studied. The immersion heat values and cation exchange capacity values of different ionic forms of natural zeolites, prepared by Batch method, were determined.

Freezing-points and the time of melting values of the solution were prepared by using several salts (NaCl, CaCl<sub>2</sub>, MgCl<sub>2</sub>, Na<sub>2</sub>SO<sub>4</sub>, etc.). Natural and modified zeolites were determined by the system that we designed. In addition, pH values of those solutions were also measured. The aim of these experiments was to determine whether the solutions are harmful to roads and vehicles.

### Results and Discussion

Convenient mixtures prepared by adding certain amount of the zeolites into the aqueous solutions of salts such as NaCl and CaCl<sub>2</sub> depend on temperature of the region. Two graphs obtained from the experimental results of freezing-points and pH values are given in Figures 1 and 2. As shown in the graphs, both of the solutions can be used as the deicers at about –10°C.

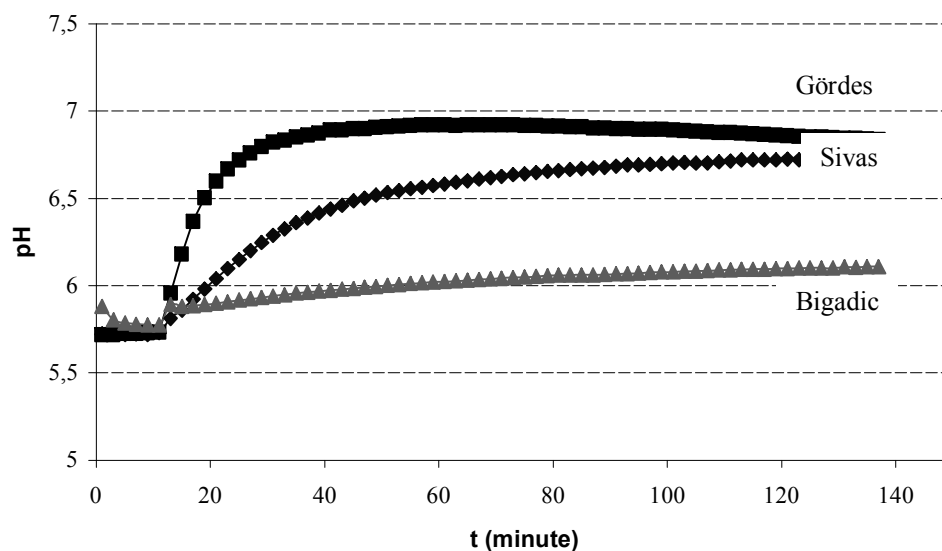
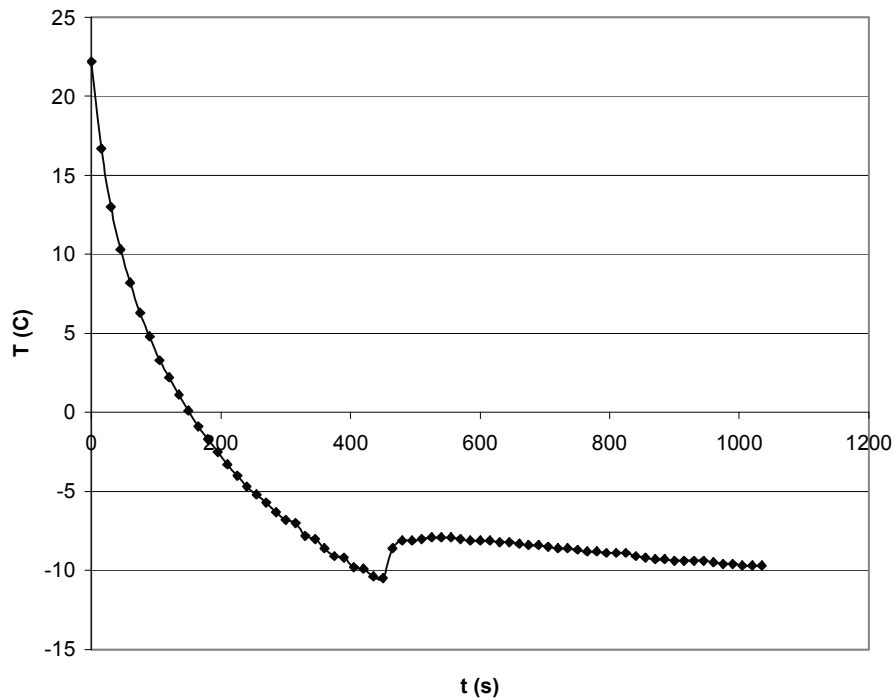


Figure 1. pH values of Gördes, Sivas, and Bigadic zeolites



**Figure 2.** Freezing point values of 0.3 g NaCl solution + 0.7 g zeolite + 9 ml water mixture

## Adsorption of ethylene on natural and modified natural zeolites from Bigadic and Gördes, Turkey

**E. Yörükoğulları and B. Erdoğan**

*Anadolu University; Eskisehir, Turkey; Email: eyorukog@anadolu.edu.tr*

### Introduction

Ethylene ( $C_2H_4$ ) is a simple naturally occurring organic molecule that is a colorless gas at biological temperatures. Most plants synthesize small amounts of  $C_2H_4$  that appear to coordinate growth and development. Moreover, increased rates of  $C_2H_4$  production are especially pronounced during the ripening of climacteric fruits such as apples, avocados, bananas, pears, and tomatoes. Once internal  $C_2H_4$  exceeds a level characteristic for the species, the further production of  $C_2H_4$  is simulated by the presence of previously produced  $C_2H_4$ . Excessive amounts of ethylene simulate further softening and decaying of the fruit and vegetables.

The aim of this study was the adsorption of the ethylene on the natural and modified natural zeolites from Bigadic and Gördes, Turkey.

### Experimental Methods

In this study,  $K^+$ ,  $Na^+$  and  $Ca^{+2}$  ionic forms of the natural zeolites (clinoptilolite) from Bigadic, Balıkesir and Gördes, Manisa regions were prepared by the Batch method, using 2M metal solutions. The natural zeolites and those of cationic forms were dehydrated at  $110^\circ C$  during 16 hours.

Experiments of the ethylene adsorption on natural and modified natural zeolites were carried out by using ethylene analyzer which is a battery powered portable instrument for measuring ethylene and is particularly suited to fruit and vegetable storage, ripening, and curing applications. Experimental results were also tested by GC (gas chromatography). Table 1 shows the results of ethylene adsorption on  $Ca^{+2}$  modified natural zeolites. In addition, the ethylene adsorption on natural zeolites was investigated by IR spectroscopy.

**Table1.** Varied concentration amount of ethylene versus time at about  $+4^\circ C$

Time (Day)	1	2	3	4	5	6	7	8	9	10	11	12	13	14
Bigadic	41.5	31.9	21.4	16.0	12.2	8.5	6.1	4.4	3.3	2.3	1.6	1.2	0.9	0.4
Gördes	27.2	16.3	10.4	7.0	4.8	3.3	2.3	1.6	1.3	0.8	0.8	0.5	0.5	0.5
Ethylene	ppm													

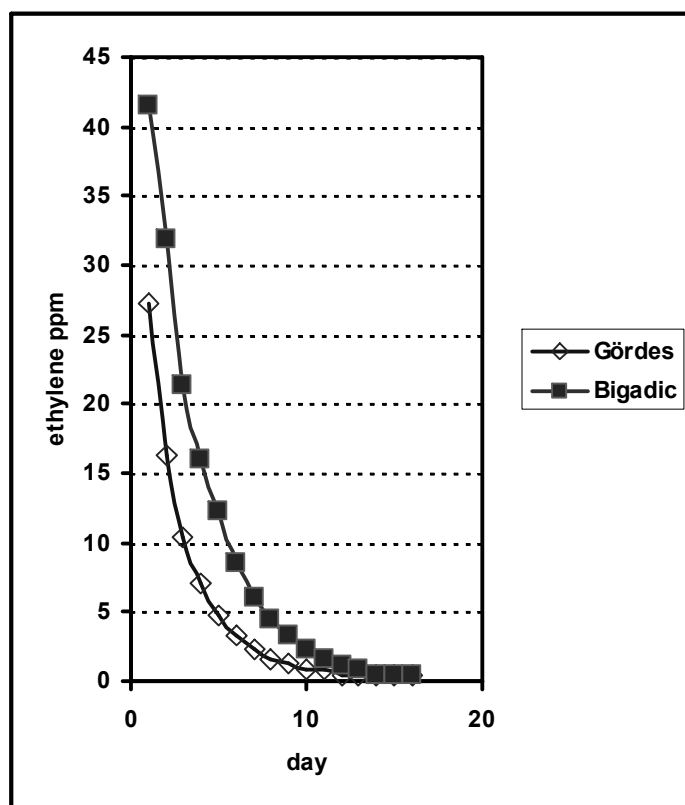


**Figure 1.** Ethylene adsorption on  $\text{Ca}^{+2}$  modified natural zeolites from Bigadic and Gördes regions at about  $+4^{\circ}\text{C}$

### Results and Discussion

At the end of the experiments, it was determined that  $\text{K}^{+}$ ,  $\text{Na}^{+}$ , and  $\text{Ca}^{+2}$  ionic forms of the natural zeolite belonging to Bigadic adsorbed the ethylene better than those of the natural zeolite from Gördes, as shown in Figure 1.

## **Perchlorate removal using surfactant-modified zeolite**

**P. Zhang, D. M. Avudzega, and G. Zikalala**

*City College of New York; New York, New York, USA; Email: pzhang@sci.ccny.cuny.edu*

Batch and column experiments were conducted to evaluate the performance of surfactant-modified zeolite (SMZ) as an inexpensive sorbent material for perchlorate removal from contaminated waters. The effects of pH and competing anions (chloride, sulfate, and nitrate) on perchlorate removal were examined.

In batch experiments, when 12 mL of perchlorate solution of various concentrations (up to 2 mM or 200 mg/L, pH 7) were mixed with 1 g of 8–14 mesh SMZ, over 98% of the perchlorate was removed from the solution after overnight shaking. Perchlorate removal efficiency did not change when the solution pH was raised to 12, or when 10 mM of sulfate or chloride was present in the solution. The addition of 10 mM nitrate lowered the removal efficiency slightly (~ 5%). Batch perchlorate sorption data were well described by the Langmuir sorption isotherm, and the maximum sorption capacities obtained from the Langmuir fits were about 40 mmol perchlorate per kilogram of SMZ in all cases.

In column transport experiments, perchlorate solution (0.1 mM, or 10 mg/L, with 3 mM of NaHCO<sub>3</sub>, 1.0 mM of CaCl<sub>2</sub>, and 0.5 mM each of MgCl<sub>2</sub>, Na<sub>2</sub>SO<sub>4</sub>, and KNO<sub>3</sub>) was pumped through columns packed with 8–14 mesh SMZ (78 g each) at a linear velocity of 2 m/d (residence time of 1.8 hrs). Chloride broke through the columns first, followed by sulfate, nitrate, and then perchlorate, indicating that the SMZ preferentially sorbed perchlorate. The SMZ columns were able to retard the breakthrough of perchlorate for at least 400 pore volumes, and each column removed about 2.7 mmol of perchlorate (corresponding to a loading of 34 mmol/kg). This loading was very close to the maximum sorption capacity of about 40 mmol/kg determined from the batch experiments.





# AUTHOR INDEX

## A

Adamović, M. · 159  
 Akhalbedashvili, L. · 41, 43  
 Alapishvili, M. · 43  
 Alcántara, D. · 88  
 Aleksanyan, G. M. · 114  
 Al-Haddad, A. · 45  
 Al-Salem, M. · 45  
 Al-Sewaillem, M. · 221  
 Altare, C. R. · 46  
 Amirbekyan, Y. · 48  
 Archipova, N. · 150  
 Arcon, I. · 168  
 Armbruster, T. · 11  
 Artioli, G. · 124  
 Atalan, G. S. · 50  
 Avudzege, D. M. · 263

## B

Baur, W. H. · 109  
 Bechtel, R. · 29  
 Berbeglia, Y. · 242  
 Bertetti, F. P. · 202  
 Bhattacharyya, S. · 52  
 Biagioli, M. · 73  
 Bian, J. · 152, 153, 155  
 Bish, D. L. · 13, 53, 249  
 Boak, J. · 13  
 Bogdanchikova, N. · 88  
 Bokich, J. · 55  
 Bonferoni, M. C. · 75  
 Borisova, L. I. · 226  
 Borsatto, F. · 107  
 Bosch, P. · 214  
 Bowman, R. S. · 46, 56, 172, 216  
 Brathwaite, R. L. · 25, 60  
 Breus, I. · 150, 178  
 Breus, V. · 150, 178  
 Brotzu, P. · 92  
 Brundu, A. · 73  
 Bucher, K. · 253  
 Bulbulian, S. · 214  
 Buondonno, A. · 58

## C

Çağın, V. · 62, 182, 184  
 Campbell, L. · 81  
 Campos Reales, E. · 132  
 Cano-Aguilera, I. · 128  
 Capasso, S. · 64

Cappelletti, P. · 66, 69, 94, 96  
 Caputo, D. · 27, 71, 86  
 Caramella, C. · 75  
 Carretero, M. I. · 210  
 Casas, J. · 210  
 Catlow, C. R. A. · 224  
 Cerjan-Stefanovic, S. · 168  
 Cerri, G. · 69, 73, 75, 94, 96  
 Chaikovski, I. · 77  
 Chakalov, K. · 78  
 Chen, J. · 152, 153  
 Chimedtsogzol, A. · 80, 81  
 Chipera, S. J. · 82, 84, 190, 240  
 Chmielewska, E. · 86  
 Chung, Y. C. · 146  
 Colella, A. · 58, 69  
 Colella, C. · 3, 15, 58, 64  
 Concepción-Rosabal, B. · 88  
 Coppola, E. · 58, 64  
 Counce, D. · 84  
 Crosta, S. · 242  
 Cygan, R. T. · 195

## D

Daemen, L. L. · 195  
 Daković, A. · 90, 144  
 Damjanović, L. · 144  
 Dave, G. · 113  
 De Fazio, A. · 92  
 de Gennaro, B. · 58  
 de Gennaro, M. · 66, 69, 75, 94, 96  
 de Gennaro, R. · 94, 96  
 De la Rosa, L. · 88  
 de las Pozas, C. · 174  
 De Rita, D. · 119  
 Demberel, N. · 186  
 Demberel, S. · 186  
 Deng, S. · 98  
 Diego Gatta, G. · 31  
 Dikmen, Z. · 100, 198  
 Djambazov, S. · 256  
 Donahoe, R. J. · 52  
 Dondi, M. · 94, 96  
 Dondur, V. · 144  
 Donmez, Z. · 101  
 Drăg, E. B. · 102, 103, 104  
 Dyer, A. · 80, 81

## E

Ehler, D. · 84  
 Elsen, J. · 166  
 Emerich, H. · 161  
 Eng, K. S. · 29

Erdoğan, B. · 261  
 Estrada, J. · 244  
 Ewing, R. C. · 37

## F

Faghihian, H. · 105  
 Falatah, A. M. · 221  
 Farias, F. · 107  
 Febles González, J. A. · 108, 244  
 Febles, J. A. · 107  
 Fercia, L. M. · 92  
 Ferdov, S. · 148  
 Filcheva, E. · 78  
 Fischer, R. X. · 109  
 Fittipaldo, M. · 82

## G

Galindo, Jr., C. · 122  
 Gallegos, E. · 242  
 Ganjegunte, G. K. · 111, 238  
 Ganrot, Z. · 113  
 Gáplovská, K. · 86  
 Gardea-Torresdey, J. L. · 128  
 Gasparyan, T. A. · 114  
 Gedik, K. · 115, 117  
 Georgescu, V. · 206  
 Ghiara, M. R. · 92  
 Giampaolo, C. · 119, 121  
 Gier, S. · 136  
 Giordano, G. · 119  
 Goff, C. J. · 82  
 Goff, F. · 82  
 Gómez, L. · 244  
 Graham E. Y. · 52  
 Graziano, S. F. · 94  
 Green, M. A. · 161  
 Gregory, R. W. · 111  
 Grigoryan, N. E. · 254  
 Gruener, J. E. · 122  
 Gualtieri, A. F. · 3  
 Guarini, G. · 96  
 Guastoni, A. · 124  
 Gubulin, J. C. · 228

## H

Hakhverdyan, E. A. · 254  
 Hale III, E. C. · 126  
 Haque, M. N. · 128  
 Hartl, M. T. · 195  
 Harutunyan, V. V. · 254  
 Hauri, F. · 130  
 Henderson, K. E. · 122  
 Hernández, M. A. · 132

Hill, D. · 60  
 Hovhannisyan, D. · 48  
 Hovis, G. I. · 134  
 Hutcheson, D. · 29

## I

Ibrahim, K. M. · 140  
 Ilangovan, K. · 174  
 Iliev, Tz. · 208  
 Imamoglu, I. · 115, 117  
 İmamoglu, I. · 182, 184  
 İmamoglu, İ. · 62  
 Iovino, P. · 64  
 Isakov, A. · 48  
 Ivanova, R. · 136

## J

Jablonski, J. M. · 138  
 Jbara, H. A. · 140  
 Jiménez Cedillo, M. J. · 142  
 Johnston, C. T. · 53  
 Jordanov, G. · 144  
 Jovanović, V. · 144  
 Juliano, C. · 75  
 Jung, J. Y. · 146

## K

Karamyan, G. G. · 114  
 Katz, L. E. · 46  
 Kaucic, V. · 168  
 Keheyan, Y. · 43  
 Kekelidze, N. · 43  
 Kelly D. J. A. · 153  
 Kelly, D. J. A. · 152  
 Khaidarova, G. · 150  
 Kinney, K. A. · 46  
 Kitten, J. J. · 240  
 Kobayashi, T. · 196  
 Koczka, B. · 212  
 Koenig, A. · 153, 155  
 Kostov-Kytin, V. · 148  
 Krason, J. · 138  
 Krasoň, J. · 102, 103, 104  
 Krivosheeva, A. · 150, 178  
 Kropacheva, O. · 77  
 Kułazyński, M. · 103, 104  
 Kuznicki, S. M. · 153, 155  
 Kuznicki, S. M. · 152

**L**

Langella, A. · 58, 69, 73, 94, 96  
 Larentzos, J. P. · 157  
 Ledésert, B. · 158  
 Leggo, P. J. · 158  
 Lemić, J. · 159  
 Letizia, A. · 58  
 Lewis, D. W. · 161, 224  
 Li, Z. · 163  
 Lin, C. · 152, 153  
 Liu, Y. · 152, 153  
 Lkhagvajav, R. · 201  
 Llanes Monter, M. M. · 180  
 Lo Mastro, S. · 119  
 Lombardo, M. · 64  
 Longmire, P. · 84  
 Lonis, R. · 92  
 Louis, C. J. · 244  
 Lueth, V. W. · 165

**M**

Machiels, L. · 166  
 Maginn, E. J. · 33, 157  
 Maisuradze, G. · 43  
 Malinov, O. · 256  
 Mardones, M. A. · 245  
 Margeta, K. · 168  
 Marthi, K. · 212  
 Martín Rubí, J. A. · 210  
 Martínez Dopico, C. I. · 242  
 Martynova, T. · 170  
 Matijašević, S. · 90  
 Maver, K. · 168  
 McCaffrey, W. C. · 155  
 Medina, J. A. · 210  
 Medvidović, N. V. · 247  
 Meier, D. · 172  
 Mengarelli, L. · 121  
 Miecznikowski, A. · 138  
 Mihailova, B. · 148  
 Milán, Z. · 174  
 Miles, W. J. · 176, 177  
 Milićević, S. · 159  
 Milliken, R. · 53  
 Milošević, S. · 159  
 Minato, H. · 34  
 Ming, D. W. · 17, 122  
 Mishchenko, A. · 178  
 Mitchell, M. C. · 36  
 Mitlin, D. · 152  
 Mitov, K. · 78  
 Monroy, O. · 174  
 Mora-Fonz, M. · 224  
 Morali, N. · 62, 182, 184  
 Morante, F. · 166  
 Morimoto, T. · 34

Morozova, T. A. · 226  
 Morrison, G. M. · 128  
 Mousazadeh, M. H. · 105  
 Mužek, M. N. · 247

**N**

Neckludov, S. · 178  
 Nenoff, T. M. · 195  
 Neuhoﬀ, P. S. · 50, 134, 188, 251  
 Neymark, L. A. · 190  
 Nickoghosyan, S. K. · 254  
 Nikashina, V. A. · 19, 192, 194  
 Novak Tusar, N. · 168

**O**

Ockwig, N. W. · 195  
 Okamoto, M. · 196  
 Olguín Gutiérrez, M. · 230  
 Olguín Gutiérrez, M. T. · 142, 180  
 Olguín, M. T. · 88  
 Orhun, O. · 100, 101  
 Orhun, Ö. · 198  
 Ostrooumov, M. · 199  
 Ostrooumova, I. · 199  
 Oyuntseteg, J. · 201  
 Özçelik, H. · 258

**P**

Pabalan, R. T. · 5, 202  
 Paces, J. B. · 190  
 Paredes, C. · 166  
 Parlato, L. · 96  
 Pavel, C. C. · 109  
 Pawełczyk, A. · 203  
 Pepe, F. · 86  
 Perić, J. · 232, 247  
 Perrotta, A. · 69  
 Petranoskii, V. · 132  
 Petrov, O. · 78, 148, 256  
 Petrov, P. I. · 205  
 Pode, R. · 206  
 Pode, V. · 206  
 Poellmann, H. · 80, 81  
 Pokol, G. · 212  
 Popov, N. · 208  
 Popova, T. · 78, 208  
 Popovici, E. · 206  
 Popowicz, A. · 203  
 Portillo, R. · 132  
 Pozo, M. · 210  
 Prasad, P. S. R. · 218, 222  
 Princy, P. · 212

**R**

Ramana Murthy, S. · 218  
 Reiersen, D. · 98  
 Revazyan, L. R. · 114  
 Rodríguez-Fuentes, G. · 88  
 Rodríguez-Trejo, R. · 214  
 Rojas, F. · 132  
 Rolandi, G. · 66  
 Rottinghaus, G. E. · 90  
 Rueda, G. · 132  
 Ruiz-Salvador, A. R. · 161  
 Rust, C. · 216

**S**

Sabová, L. · 86  
 Sadhana, K. · 218  
 Sahakyan, A. A. · 254  
 Sakamoto, E. · 196  
 Sakızci, M. · 258, 259  
 Salih, D. · 161, 224  
 Salvestrini, S. · 64  
 Sau, A. · 92  
 Scarpati, C. · 69  
 Schmidt, W. · 109  
 Schulze-Makuch, D. · 216  
 Selbekk, R. S. · 220  
 Serova, T. V. · 226  
 Sheta, A. S. · 221  
 Shiva Prasad, K. · 218, 222  
 Slater, B. · 224  
 Smith, M. E. · 84  
 Smith, S. E. · 212  
 Snellings, R. · 166  
 Solache Ríos, M. · 230  
 Solache Ríos, M. J. · 142, 180  
 Son, D. H. · 146  
 Spencer, C. · 121  
 Stoycheva, D. · 256  
 Sukharenko, V. I. · 226  
 Sullivan, E. J. · 46  
 Surdam, R. C. · 111

**T**

Taylor, T. · 84  
 Tchernev, D. · 6, 20  
 Tomašević-Čanović, M. · 90  
 Tomašević-Čanović, M. · 159  
 Torosyan, G. · 48  
 Torracca, E. · 121  
 Torres Pérez, J. · 230  
 Torres, J. C. · 228  
 Torres, M. E. · 245  
 Trgo, M. · 232, 247  
 Turanli, L. · 236

**U**

Upmeier, M. · 234  
 Urynowicz, M. A. · 238  
 Usenko, S. I. · 226  
 Uzal, B. · 236

**V**

van Beek, W. · 161  
 Vance, G. F. · 111, 238  
 Vaniman, D. T. · 190, 240  
 Vattuone, M. E. · 242  
 Velázquez Garrido, M. · 244  
 Velázquez, M. · 107, 108  
 Vidal Cruz, C. · 245  
 Villavicencio, B. · 244  
 Viswanathan, V. · 98  
 Vukojević Medvidović, N. · 232

**W**

Wang, H. W. · 249  
 Wang, J. · 188, 251  
 Wang, L. M. · 37  
 Wangen, E. · 155  
 Weisenberger, T. · 220, 253  
 White, C. L. I. M. · 161  
 Williams, C. D. · 80, 81  
 Wise, W. S. · 8  
 Wu, A. · 86

**X**

Xu, Z. · 152, 153

**Y**

Yanev, Y. · 208  
 Yeom, L. T. · 146  
 Yeritsyan, H. N. · 254  
 Yertsyan, G. · 43  
 Yoleva, A. · 256  
 Yörükoğulları, E. · 258, 259, 261

**Z**

Zabukovec Logar, N. · 168  
 Zanelli, C. · 96  
 Zhang, P. · 263  
 Zikalala, G. · 263  
 Zolzaya, M. · 186